

**ISTANBUL TECHNICAL UNIVERSITY ★ GRADUATE SCHOOL OF SCIENCE**  
**ENGINEERING AND TECHNOLOGY**

**MULTITEMPORAL CHANGE DETECTION ON URMIA LAKE AND ITS  
CATCHMENT AREA USING REMOTE SENSING AND GEOGRAPHICAL  
INFORMATION SYSTEMS**

**M.Sc. THESIS**

**YUSUF ALIZADE GOVARCHIN GHALE**

**Department of Civil Engineering**

**Geomatics Engineering Program**

**JUNE 2014**



**ISTANBUL TECHNICAL UNIVERSITY ★ GRADUATE SCHOOL OF SCIENCE**  
**ENGINEERING AND TECHNOLOGY**

**MULTITEMPORAL CHANGE DETECTION ON URMIA LAKE AND ITS  
CATCHMENT AREA USING REMOTE SENSING AND GEOGRAPHICAL  
INFORMATION SYSTEMS**

**M.Sc. THESIS**

**YUSUF ALIZADE GOVARCHIN GHALE  
(501101616)**

**Department of Civil Engineering**

**Geomatics Engineering Program**

**Thesis Advisor: Assoc. Prof. Dr. Elif SERTEL**

**JUNE 2014**



**İSTANBUL TEKNİK ÜNİVERSİTESİ ★ FEN BİLİMLERİ ENSTİTÜSÜ**

**URMİYE GÖLÜNDEKİ ZAMANSAL DEĞİŞİMLERİN UZAKTAN  
ALGILAMA VE CBS KULLANILARAK BELİRLENMESİ**

**YÜKSEK LİSANS TEZİ**

**YUSUF ALIZADE GOVARCHIN GHALE  
(501101616)**

**İnşaat Mühendisliği Anabilim Dalı**

**Geomatik Mühendisliği Programı**

**Tez Danışmanı: Doç. Dr. Elif SERTEL**

**HAZİRAN 2014**



**Yusuf Alizade Govarchin Ghale**, a **M.Sc.** student of ITU **Institute of / Graduate School of Engineering and Technology** student ID **501101616**, successfully defended the **thesis** entitled “**MULTITEMPORAL CHANGE DETECTION ON URMIA LAKE AND ITS CATCHMENT AREA USING REMOTE SENSING AND GEOGRAPHICAL INFORMATION SYSTEMS**”, which he prepared after fulfilling the requirements specified in the associated legislations, before the jury whose signatures are below.

**Thesis Advisor :**      **Assoc. Prof. Dr. Elif SERTEL**      .....

İstanbul Technical University

**Co-advisor :**      **Assist. Prof. Dr. Barat MOJARADI**      .....

Iran University of Science and Technology

**Jury Members :**      **Assoc. Prof. Dr. Şinasi KAYA**      .....

İstanbul Technical University

**Assist. Prof. Dr. Ahmet ÖZGÜR DOĞRU** .....

İstanbul Technical University

**Assist. Prof. Dr. Beyza USTAOĞLU** .....

Sakarya University

**Date of Submission : 05 May 2014**

**Date of Defense : 30 June 2014**





*To my family and Urmian people*



## **FOREWORD**

I want to record my sincere thanks to all contributors whose cooperation and assistance helped me through my M.Sc. study reported herein. First of all, thanks to my supervisors Assoc. Prof. Dr. Elif Sertel, and Assist. Prof. Dr. Barat Mojaradi for inspiring me and for providing such an interesting project for me to work on. Thank you for your direction and your help in the development of my mind. Thank you for teaching me. I am honored to have worked with you and I have learned more from you than you know.

I want to record my special thanks to Ahmad Alizade Govarching Ghale, Muhittin Karaman and Emre Ozelkan who always helped and encouraged me. I also wish to thank Istanbul Technical University (BAP), Turkey National Cultural Institution, Mr. Sharafattin Yilmaz and Mr. Ali Polat for their financial and emotional helps.

I would also thank to the West Azerbaijan Environmental Protection Office, West Azerbaijan and East Azerbaijan Meteorological Offices and Artemia Research Center of Urmia University for their help.

I would also to thank the Department of Geomatics Engineering and Research and Application Center for Satellite Communications and Remote Sensing (ITU-CSCRS) at the Istanbul Technical University for giving me the opportunity to come here and for providing an exciting and dynamic environment for me to mature as a scientist.

Finally, I want to convey my thanks to my family for their support and encourage and understanding.

June 2014

Yusuf Alizade Govarchin Ghale



## TABLE OF CONTENTS

	Page
<b>FOREWORD</b> .....	<b>ix</b>
<b>TABLE OF CONTENTS</b> .....	<b>xi</b>
<b>ABBREVIATIONS</b> .....	<b>xiii</b>
<b>LIST OF TABLES</b> .....	<b>xv</b>
<b>LIST OF FIGURES</b> .....	<b>xvii</b>
<b>SUMMARY</b> .....	<b>xxi</b>
<b>ÖZET</b> .....	<b>xxv</b>
<b>1. INTRODUCTION</b> .....	<b>1</b>
1.1 Coastline Change Detection Methods .....	2
1.2 Objective Of Thesis.....	7
<b>2. PRINCIPLES OF REMOTE SENSING AND GIS</b> .....	<b>9</b>
2.1 Introduction To Remote Sensing.....	9
2.2 Energy Interaction With The Earth Surface Features .....	10
2.2.1 Spectral reflectance of vegetation .....	11
2.2.2 Spectral reflectance of water bodies.....	13
2.2.3 Spectral reflectance of soils.....	15
2.3 Geographical Information Systems (GIS).....	15
2.3.1 GIS data sources.....	16
2.3.2 Geodatabase .....	17
<b>3. STUDY AREA AND DATA USED</b> .....	<b>19</b>
3.1 Study Area.....	19
3.2 Satellite Images .....	23
3.2.1 Landsat-5 TM.....	23
3.2.2 UK-DMC (United Kingdom-Disaster Monitoring Constellation).....	25
3.2.3 Landsat-8.....	26
3.3 Meteorological Data.....	27
3.4 Landuse Maps .....	30
3.5 Water Surface Elevation.....	30
3.6 HYDROWEB Database .....	31
3.7 Dams.....	33
3.8 Underground Water Sources .....	36
3.9 Population.....	38
<b>4. IMAGE PROCESSING TECHNIQUES AND DATA ANALYSIS</b> .....	<b>39</b>
4.1 Preprocessing .....	39
4.1.1 Radiometric calibration.....	40
4.1.2 Atmospheric correction.....	41
4.1.3 Topographic correction .....	42
4.1.4 Geometric correction.....	42
4.1.5 Classification.....	43

4.2 Normalized Difference Vegetation Index (NDVI).....	43
4.3 Normalized Difference Water Index (NDWI).....	44
4.4 Normalized Differential Salinity Index (NDSI) And Salinity Index (SI) .....	45
4.5 Normalized Difference Drought Index (NDDI).....	46
4.6 Geostatistics Analysis .....	48
4.6.1 Interpolation and kriging.....	48
4.6.2 Kinds of kriging .....	49
4.6.3 Ordinary kriging.....	51
4.7 Standardized Precipitation Index (SPI) .....	52
<b>5. CHANGE DETECTION ON URMIA LAKE AND ITS CATCHMENT</b>	
<b>AREA USING REMOTE SENSING AND GIS.....</b>	<b>57</b>
5.1 Preprocessing of Satellite Images .....	57
5.2 Mosaic And Classification .....	61
5.2.1 Unsupervised classification.....	62
5.2.2 Supervised classification.....	80
5.2.3 Comparing the results of unsupervised and supervised classification.....	95
5.3 Analyzing The Results Of NDVI, NDWI, NDDI, NDSI, And SI .....	108
5.3.1 Normalized Difference Vegetation Index (NDVI) .....	108
5.3.2 Calculation water surface area using NDVI and unsupervised classification.....	117
5.3.3 Normalized Difference Water Index (NDWI) .....	120
5.3.4 Normalized Difference Drought Index (NDDI).....	125
5.3.5 Normalized Differential Salinity Index (NDSI) and Salinity Index (SI)	129
5.4 Analyzing Meteorological Data .....	141
5.4.1 Geostatistical analysis .....	142
5.4.1.1 Kriging to temperature data .....	142
5.4.1.2 Kriging to precipitation data .....	147
5.4.2 Standardized Precipitation Index (SPI).....	152
5.4.2.1 Spatio-temporal analysis of different SPIs.....	154
5.4.3 Analyzing meteorological data of 5 close stations to Urmia Lake .....	159
5.4.3.1 Analyzing temperature data .....	160
5.4.3.2 Analyzing precipitation data .....	161
5.4.3.3 Analyzing humidity data.....	162
<b>6. CONCLUSIONS AND RECOMENDATIONS.....</b>	<b>165</b>
<b>REFERENCES .....</b>	<b>177</b>
<b>APPENDICES .....</b>	<b>183</b>
APPENDIX A .....	184
APPENDIX B .....	197
<b>CURRICULUM VITAE.....</b>	<b>227</b>

## **ABBREVIATIONS**

<b>GPS</b>	:Global Positioning System
<b>TM</b>	: Thematic Map
<b>GIS</b>	: Geographical Information Systems
<b>UV</b>	: Ultraviolet
<b>SWIR</b>	: Short Wave Infrared
<b>Landsat</b>	: Land Satellite
<b>DEM</b>	: Digital Elevation Model
<b>VI</b>	: Vegetation Indices
<b>UTM</b>	: Universal Transverse Mercator
<b>DMC</b>	: Disaster Monitoring Constellation
<b>EMR</b>	: Electromagnetic Radiation
<b>NDVI</b>	: Normalized Difference Vegetation Index
<b>NDWI</b>	: Normalized Difference Water Index
<b>SI</b>	: Salinity Index
<b>NDSI</b>	: Normalized Differential Salinity Index
<b>NDDI</b>	: Normalized Difference Drought Index
<b>NIR</b>	: Near Infrared
<b>SPI</b>	: Standardized Precipitation Index





## LIST OF TABLES

	<u>Page</u>
<b>Table 3.1</b> : Spectral and spatial information about Landsat TM.....	24
<b>Table 3.2</b> : Spectral and spatial information about DMC. ....	25
<b>Table 3.3</b> : Spectral and spatial information about Landsat-8 Operational Land Imager (OLI) and Thermal Infrared Sensor (TIRS).....	27
<b>Table 3.4</b> : Meteorological stations .....	29
<b>Table 3.5</b> : Water consumption of dams .....	35
<b>Table 3.6</b> : Cultivation area using dams .....	36
<b>Table 3.7</b> : Population (million) of both West Azerbaijan and East Azerbaijan.....	38
<b>Table 4.1</b> : SPI and cumulative probability.....	55
<b>Table 5.1</b> : Unsupervised classification results (km <sup>2</sup> ) in spring and winter times .....	79
<b>Table 5.2</b> : Unsupervised classification results (km <sup>2</sup> ) in summer time .....	80
<b>Table 5.3</b> : Supervised classification results (km <sup>2</sup> ) in spring and winter times.....	94
<b>Table 5.4</b> : Supervised classification results (km <sup>2</sup> ) in summer time .....	95
<b>Table 5.5</b> : Error matrix of ISODATA – 2010 - Summer .....	101
<b>Table 5.6</b> : Accuracy totals and Kappa statistics of ISODATA – 2010 - Summer..	101
<b>Table 5.7</b> : Error matrix of Maximum Likelihood – 2010 - Summer .....	101
<b>Table 5.8</b> : Accuracy totals and Kappa statistics of Maximum Likelihood – 2010 - Summer .....	101
<b>Table 5.9</b> : Error matrix of ISODATA – 2011 - Summer.....	102
<b>Table 5.10</b> : Accuracy totals and Kappa statistics of ISODATA – 2011 - Summer	102
<b>Table 5.11</b> : Error matrix of Maximum Likelihood – 2011 - Summer .....	102
<b>Table 5.12</b> : Accuracy totals and Kappa statistics of Maximum Likelihood – 2011 - Summer .....	103
<b>Table 5.13</b> : Error matrix of ISODATA – 2013 - Summer .....	103
<b>Table 5.14</b> : Accuracy totals and Kappa statistics of ISODATA – 2013 - Summer	103
<b>Table 5.15</b> : Error matrix of Maximum Likelihood – 2013 - Summer .....	104
<b>Table 5.16</b> : Accuracy totals and Kappa statistics of Maximum Likelihood – 2013 - Summer .....	104
<b>Table 5.17</b> : Error matrix of ISODATA – 2014 - February .....	104
<b>Table 5.18</b> : Accuracy totals and Kappa statistics of ISODATA – 2014 - February	105
<b>Table 5.19</b> : Error matrix of Maximum Likelihood – 2014 - February .....	105
<b>Table 5.20</b> : Accuracy totals and Kappa statistics of Maximum Likelihood – 2014 - February .....	105
<b>Table 5.21</b> : NDVI results (km <sup>2</sup> ) in summer time .....	117
<b>Table 5.22</b> : Water surface area (km <sup>2</sup> ) of Urmia Lake using 4 methods – Summer time.....	118
<b>Table 5.23</b> : Error matrix of NDVI-Unsupervised – 2010 - Summer .....	118
<b>Table 5.24</b> : Accuracy totals and Kappa statistics of NDVI-Unsupervised – 2010 - Summer .....	118

<b>Table 5.25:</b> Error matrix of NDVI-Unsupervised – 2011 - Summer .....	119
<b>Table 5.26:</b> Accuracy totals and Kappa statistics of NDVI-Unsupervised – 2011-Summer .....	119
<b>Table 5.27:</b> Error matrix of NDVI-Unsupervised – 20113-Summer .....	119
<b>Table 5.28:</b> Accuracy totals and Kappa statistics of NDVI-Unsupervised – 2013-Summer .....	119
<b>Table 5.29:</b> NDWI results (km <sup>2</sup> ) in summer time .....	124
<b>Table 5.30:</b> SI results (km <sup>2</sup> ) in summer time .....	136
<b>Table 5.31:</b> Mean temperature values (°C) in August month .....	143
<b>Table 5.32:</b> Annually precipitation values (mm) .....	148
<b>Table 5.33:</b> Meteorological stations, which were used to calculate SPI.....	153
<b>Table 5.34:</b> SPI values and drought intensity.....	154
<b>Table 6.1:</b> Unsupervised classification results .....	166
<b>Table 6.2:</b> Supervised classification results .....	167
<b>Table 6.3:</b> Water surface area changes of Urmia Lake from 1984 to 2013 in summer time.....	168
<b>Table 6.4:</b> Established dams between 1970 and 2000.....	170
<b>Table 6.5:</b> Some of dams established between 2000 and 214.....	171
<b>Table 6.6:</b> Minimum and maximum area (km <sup>2</sup> ) of Indexes .....	174

## LIST OF FIGURES

	<u>Page</u>
<b>Figure 1.1</b> : Area of Urmia Lake according to S. Sima et al (2012). .....	5
<b>Figure 1.2</b> : Area of Urmia Lake according to Keivan Kabiri et al (2012).....	6
<b>Figure 2.1</b> : Electromagnetic spectrum. ....	10
<b>Figure 2.2</b> : Spectral reflectance curves for various features types .....	11
<b>Figure 2.3</b> : Processes acting upon solar radiant energy in the visible region of the spectrum over an area of shallow water.....	13
<b>Figure 2.4</b> : Spectral reflectance of water. Graph developed for Prospect (2002 and 2003) using Aster Spectral Library.....	14
<b>Figure 3.1</b> : Female Artemia Urmiana (Left) – Male Artemia Urmiana (Right) – Photo from Artemia Research Center of Urmia University. ....	20
<b>Figure 3.2</b> : Shahid Kalantari causeway on Urmia Lake – Photo taker is unknow – 1990 decade .....	20
<b>Figure 3.3</b> : Bridge on Urmia Lake that allows a little water exchange between 2 parts of Urmia Lake – Photo taken by Yusuf Alizade Govarchin Ghale – 2014 - February.....	21
<b>Figure 3.4</b> : Shahid kalantari causway on Urmia Lake – Photo taker and date are unknown.....	21
<b>Figure 3.5</b> : Urmia Lake’s catchment area with rivers and streams (Left) – Study area – Landsat-8 – 2013 – Mosaic of 6 frames (Right) .....	23
<b>Figure 3.6</b> : Meteorological stations around Urmia Lake – Landsat-8 – Mosaic of 6 frames – 2013-Summer.....	28
<b>Figure 3.7</b> : Water surface elevation of Urmia Lake – November.....	31
<b>Figure 3.8</b> : Water level variations of Urmia Lake. ....	31
<b>Figure 3.9</b> : Comparing water level variations of HYDROWEB database by water surface elevation variations of Energy Ministry of Iran in November..	32
<b>Figure 3.10</b> : Water surface variations of Urmia Lake. ....	32
<b>Figure 3.11</b> : Volume variations of Urmia Lake .....	33
<b>Figure 3.12</b> : Total inflow from rivers and other sources to Urmia Lake. Other soruces include flood water, precipitation, and underground water .....	34
<b>Figure 3.13</b> : Urmia Lake’s position in Iran. ....	35
<b>Figure 3.14</b> : Total discharge water from underground resources. ....	37
<b>Figure 3.15</b> : Discharge water from deep wells .....	37
<b>Figure 3.16</b> : Discharge water from semi deep wells.....	37
<b>Figure 3.17</b> : Discharge water from aqueduct.....	38
<b>Figure 3.18</b> : Discharge water from water fountains. ....	38
<b>Figure 4.1</b> : One spatial dimension ordinary kriging. ....	52
<b>Figure 5.1</b> : Mosaic of 6 frames – Landsat-8 – 2013 – Summer .....	61

<b>Figure 5.2</b> : Changes in color and quality of water – Urmia Lake – 2005-spring and 2010-summer – Photos taken by Yusuf Alizade Govarchin Ghale .....	63
<b>Figure 5.3</b> : Salt area of Urmia Lake in 2013 and 2014 years – Photos taken by Yusuf Alizade Govarchin Ghale.....	63
<b>Figure 5.4</b> : Extraction salt from Urmia Lake by local people – Photo taken by Yusuf Alizade Govarchin Ghale – 2013 year.....	64
<b>Figure 5.5</b> : Border of water, salt, and salty soil in the study area – Photo taken by Yusuf Alizade Govarchin Ghale – 2012 year .....	65
<b>Figure 5.6</b> : Soil and salty soil – Photo taken by Yusuf Alizade Govarchin Ghale – 2012 year.....	65
<b>Figure 5.7</b> : Border of water (blue and white arrow), salt (red arrow), salty soil (yellwo arrow), soil (black arrow), and farming (green arrow) in the study area – 2010 year (same area was full of water in 2005) – Photos taken by Yusuf Alizade Govarchin Ghale in land study .....	66
<b>Figure 5.8</b> : Unsupervised classification maps from 1984 to 1990.....	67
<b>Figure 5.9</b> : Unsupervised classification maps from 1995 to 2006.....	68
<b>Figure 5.10</b> : Unsupervised classification maps from 2007 to 2010.....	69
<b>Figure 5.11</b> : Unsupervised classification maps from 2011 to 2013.....	70
<b>Figure 5.12</b> : Unsupervised classification maps of 2013-summer and 2014-February. ....	71
<b>Figure 5.13</b> : Water surface area in summer time – Unsupervised classification. ....	72
<b>Figure 5.14</b> : Water surface area in spring and winter times – Unsupervised classification. ....	72
<b>Figure 5.15</b> : Comparing the results of water surface area in spring and summer times – Unsupervised classification.....	73
<b>Figure 5.16</b> : Salt area in summer time – Unsupervised classification. ....	73
<b>Figure 5.17</b> : Salt area in spring and winter times – Unsupervised Classification. ..	74
<b>Figure 5.18</b> : Comparing the results of salt area in spring and summer times – Unsupervised classification. ....	74
<b>Figure 5.19</b> : Salty soil area in summer time – Unsupervised classification. ....	75
<b>Figure 5.20</b> : Salty soil area in spring and winter times – Unsupervised classification. ....	75
<b>Figure 5.21</b> : Comparing the results of salty soil class in spring and summer times – Unsupervised classification. ....	76
<b>Figure 5.22</b> : Soil area in summer time – Unsupervised classification.....	76
<b>Figure 5.23</b> : Soil area in spring and winter times – Unsupervised classification. ...	77
<b>Figure 5.24</b> : Comparing the results of soil area in spring and summer times – Unsupervised classification. ....	77
<b>Figure 5.25</b> : Farming area in summer time – Unsupervised classification.....	78
<b>Figure 5.26</b> : Farming area in spring time – Unsupervised classification.....	78
<b>Figure 5.27</b> : Comparing the results of farming area in spring and summer times – Unsupervised classification. ....	79
<b>Figure 5.28</b> : Supervised classification maps from 1984 to 1990.....	82
<b>Figure 5.29</b> : Supervised classification maps from 1995 to 2006.....	83
<b>Figure 5.30</b> : Supervised classification maps from 2007 to 2010.....	84
<b>Figure 5.31</b> : Supervised classification maps from 2011 to 2013.....	85
<b>Figure 5.32</b> : Supervised classification maps of 2013-summer and 2014-February. ....	86
<b>Figure 5.33</b> : Water surface area in summer time –Supervised classification. ....	87
<b>Figure 5.34</b> : Water surface area in spring and winter times –Supervised classification. ....	87

<b>Figure 5.35</b> : Comparing the results of water surface area in spring and summer times –Supervised classification.....	88
<b>Figure 5.36</b> : Salt area in summer time – Supervised classification. ....	88
<b>Figure 5.37</b> : Salt area in spring and winter times – Supervised classification.....	89
<b>Figure 5.38</b> : Comparing the results of salt area in spring and summer times – Supervised classification.....	89
<b>Figure 5.39</b> : Salty soil area in summer times – Supervised classification. ....	90
<b>Figure 5.40</b> : Salty soil area in spring and winter times – Supervised classification.....	90
<b>Figure 5.41</b> : Comparing the results of salty soil area in spring and summer times – Supervised classification.....	91
<b>Figure 5.42</b> : Soil area in summer time – Supervised classification. ....	91
<b>Figure 5.43</b> : Soil area in spring and winter times – Supervised classification. ....	92
<b>Figure 5.44</b> : Comparing the results of soil area in spring and summer times – Supervised classification.....	92
<b>Figure 5.45</b> : Farming area in summer time – Supervised classification. ....	93
<b>Figure 5.46</b> : Farming area in spring time – Supervised classification.....	93
<b>Figure 5.47</b> : Comparing the results of farming class in spring and summer times – Supervised classification.....	94
<b>Figure 5.48</b> : Comparing the results of water area in summer time.....	96
<b>Figure 5.49</b> : Comparing the results of salt area in summer time. ....	96
<b>Figure 5.50</b> : Comparing the results of salty soil area in summer time. ....	96
<b>Figure 5.51</b> : Comparing the results of soil class in summer time.....	97
<b>Figure 5.52</b> : Comparing the results of farming class in summer time. ....	97
<b>Figure 5.53</b> : Comparing the results of water class in spring and winter times.....	97
<b>Figure 5.54</b> : Comparing the results of salt class in spring and winter times. ....	97
<b>Figure 5.55</b> : Comparing the results of salty soil class in spring and winter times. .	98
<b>Figure 5.56</b> : Comparing the results of soil class in spring and winter times. ....	98
<b>Figure 5.57</b> : Comparing the results of farming class in spring times. ....	98
<b>Figure 5.58</b> : Correlation between water surface area and water surface elevation changes in summer time. ....	107
<b>Figure 5.59</b> : Correlation between water surface area (summer) and water surface elevation (November) changes. ....	108
<b>Figure 5.60</b> : Some kinds of water bodies in the study area – Photos taken by Yusuf Alizade Govarchin Ghale in land study .....	110
<b>Figure 5.61</b> : Extracted areas using MNDWI – Landsat-5 TM – 1987-spring .....	111
<b>Figure 5.62</b> : NDVI maps in summer time of 1984, 1987, 2000, and 2006 . ....	113
<b>Figure 5.63</b> : NDVI maps in summer time of 1990, 2010, 2011, and 2013 . ....	114
<b>Figure 5.64</b> : NDVI values between 0 and 0.1 .....	115
<b>Figure 5.65</b> : NDVI values between 0.1 and 0.5.....	115
<b>Figure 5.66</b> : NDVI values between 0.5 and 1 .....	116
<b>Figure 5.67</b> : NDWI maps in summer time of 1984, 1987, 2000, and 2006 .....	121
<b>Figure 5.68</b> : NDWI maps in summer time of 1990, 2010, 2011, and 2013 .....	122
<b>Figure 5.69</b> : NDWI values between -1 and 0 .....	123
<b>Figure 5.70</b> : NDWI values between 0 and 0.5 .....	123
<b>Figure 5.71</b> : NDWI values between 0.5 and 1 .....	124
<b>Figure 5.72</b> : NDDI maps in summer time of 1984, 1987, 2000, and 2006 . ....	126
<b>Figure 5.73</b> : NDDI maps in summer time of 1990, 2010, 2011, and 2013 . ....	127
<b>Figure 5.74</b> : NDDI values between 0 and 2 .....	128
<b>Figure 5.75</b> : NDDI values between 2 and 10 .....	128
<b>Figure 5.76</b> : NDDI values between 10 and 100 .....	129

<b>Figure 5.77</b> : NDSI maps in summer time of 1984, 1987, 2000, and 2006 .....	130
<b>Figure 5.78</b> : NDSI maps in summer time of 1990, 2010, 2011, and 2013 .....	131
<b>Figure 5.79</b> : SI maps in summer time of 1984 and 2000 .....	132
<b>Figure 5.80</b> : SI maps in summer time of 1987, 1990, 2006, 2010 .....	133
<b>Figure 5.81</b> : SI maps in summer time of 2011 and 2013 .....	134
<b>Figure 5.82</b> : SI values between 0 and 0.2 .....	134
<b>Figure 5.83</b> : SI values between 0.2 and 0.4 .....	135
<b>Figure 5.84</b> : SI values between 0.4 and 1 .....	135
<b>Figure 5.85</b> : Unsupervised classification results in 1984-summer (Left) and 2013-summer (Right). .....	137
<b>Figure 5.86</b> : SI maps of Urmia Lake in summer time of 1984, 1987, 2000, and 2006 .....	138
<b>Figure 5.87</b> : SI maps of Urmia Lake in summer time of 1990, 2010, 2011, and 2013 .....	139
<b>Figure 5.88</b> : Comparing SI and unsupervised classification maps of Urmia Lake .....	140
<b>Figure 5.89</b> : Climate zones of Iran .....	141
<b>Figure 5.90</b> : Prediction maps of air temperature in August month from 2000 to 2009 .....	144
<b>Figure 5.91</b> : Prediction maps of air temperature in August month from 2010 to 2011 .....	145
<b>Figure 5.92</b> : Prediction standard error maps of air temperature in August month from 2000 to 2009 .....	146
<b>Figure 5.93</b> : Prediction standard error maps of air temperature in August month of 2010 to 2011 .....	147
<b>Figure 5.94</b> : Prediction maps of annual precipitation from 2000 to 2009 .....	149
<b>Figure 5.95</b> : Prediction maps of annual precipitation in 2010 and 2011 .....	150
<b>Figure 5.96</b> : Prediction standard error maps of annual precipitation from 2000 to 2009 .....	151
<b>Figure 5.97</b> : Prediction standard error maps of annual precipitation in 2010 and 2011 .....	152
<b>Figure 5.98</b> : Location of synoptic stations which were used to calculate SPI .....	153
<b>Figure 5.99</b> : SPI values and ranges .....	158
<b>Figure 5.100</b> : Location of synoptic stations which are close to Urmia lake .....	159
<b>Figure 6.1</b> : Location of some dams in Urmia Lake's catchment area – Landsat-8 – 2013-summer – Mosaic of 9 frames .....	170
<b>Figure 6.2</b> : Trends in hydro-climatic stations of Urmia Lake basin .....	173

# MULTITEMPORAL CHANGE DETECTION ON URMIA LAKE AND ITS CATCHMENT AREA USING REMOTE SENSING AND GEOGRAPHICAL INFORMATION SYSTEMS

## SUMMARY

Different types of environmental sources, especially water bodies play a crucial role in human life and economy. Nowadays, the significance of water bodies, especially fresh water sources like lakes is increasing since these sources are being threatened due to global warming, drought and human needs. In addition to serving as supply for human needs such as irrigation and drinking water, a water reserve in a lake and its catchment area can also be important source contributing to country's economy and policy like the case of Urmia Lake in Iran.

Urmia Lake is located in the northwest of Iran between West Azerbaijan and East Azerbaijan provinces (N 37.5° E 45.5°). Its catchment area is about 51876 km<sup>2</sup> and it is the largest inland lake of Iran and the second largest hypersaline lake in the world after Dead Sea and the habitat of *Artemia Urmiana* which is a unique bisexual *Artemia* Species. The brine shrimp *Artemia* is a zooplanktonic organism found in hypersaline habitats such as inland salt lakes, coastal salt pans and manmade saltworks worldwide.

Urmia Lake is divided into 2 parts including north and south parts separated by a causeway which has about 1500 m bridge allows a little water exchange between 2 parts. Due to the establishment of different dams on contrary rivers which supply Urmia Lake's water, establishment of more than 80,000 wells in Urmia Lake's catchment area, increased demands for irrigation in the Lake's basin, temperature and precipitation changes, and drought, the salinity of the lake has risen remarkable during recent years, and about 70% of the lake's area is drought. There are two important points that should be emphasized for the temperature and precipitation changes impacts on Urmia Lake and its vicinity.

Firstly, the annual amount of water the lake receives has significantly decreased as a result of establishment of dams, wells, and drought. This in turn has increased the salinity of the lake's water, lowering the lake viability as home to thousands of migratory birds including the large flamingo populations and diminishing other assets especially *Artemia Urmiana*.

Secondly, it is also important to consider the results of drying Urmia Lake and its risks on human life and ecosystem in Iran and neighbor countries of Urmia Lake. Drying of Urmia Lake will impact the local and regional climate of the area and this will have severe impacts on human and environment. Hotter temperature values and water shortage as a result of complete drying of Urmia Lake may even cause diseases and migration of local people. A similar example to Urmia Lake case is Aral Sea and its vicinity, therefore lessons learned from the Aral Sea case should be taken into account for the protection of Urmia Lake.

This study focuses mainly on multi-temporal change detection on Urmia Lake and its catchment area by integration of remote sensing and geographical information systems for a thirty year period from 1984 to 2014. In addition to satellite images,

meteorological data, GPS measurements, landuse maps and ground photographs were analyzed to investigate the changes on Urmia Lake and understand the causes of this environmental problem including the role and effects of human and global warming.

A total number of 95 Landsat-5 TM, Landsat-8, and DMC images obtained between 1984 and 2014 were used in this study. Also, different meteorological variables like temperature, precipitation, humidity which has been measured at 20 synoptic stations around Urmia Lake were used to interpret meteorological impacts during last years. Moreover, data collected from different sources like Landuse maps of West Azerbaijan and East Azerbaijan provinces, control points, population, dams, underground water resources were used in this study to analyze the human and climate induced impacts on drying of Urmia Lake.

After preprocessing steps, 6 frames, which have taken between 1984 and 2014 are mosaiced to output study area including Urmia Lake and its catchment area. Then, Unsupervised classification and supervised classifications were done on output information and compare the changes which have been occurring during the last 30 years. According to the results of the accuracy assessment process, the overall classification accuracy and overall Kappa statistics using the supervised classification method were shown to be better than the unsupervised classification for every time period except the summer of 2011. Therefore, to analyze the water surface area of Urmia Lake using supervised classification was determined to be better than unsupervised classification. The minimum and maximum water surface areas are about 1852 (2013) and 5982 (1995) km<sup>2</sup>. The water surface area of Urmia Lake decreased nearly 2000 km<sup>2</sup> from 5982 km<sup>2</sup> in 1995 to 4058 km<sup>2</sup> in 2006. In other words, 32% of Urmia Lake dried up during the period of 1995 until 2006. It then decreased another 2000 km<sup>2</sup> from 4058 km<sup>2</sup> in 2006 to 1852 km<sup>2</sup> in 2013.

To analyze Urmia Lake's catchment area and change detection in Urmia Lake's vicinity, Normalized Difference Vegetation Index (NDVI), Normalized Difference Water Index (NDWI), Normalized Differential Salinity Index (NDSI), Salinity Index (SI), and Normalized Difference Drought Index (NDDI) are used. According to the results of these indexes, 2006 can be considered as a year with the highest soil salinity value, least NDVI, least NDWI, and most severe drought conditions. 1987 can be considered as the year with the lowest soil salinity value, highest NDVI, highest NDWI, and least drought condition. The salinity of soil and water bodies has been increased in all parts of the study area during recent years especially in south and east parts of Urmia Lake.

The air temperatures in 2006 and 2010 were the warmest while following years cooled down. In 2006 and 2010 the high temperatures were also years of increased precipitation compared to other years. By considering the results of geostatistical analysis and Standard Precipitation Index (SPI), the meteorological analysis showed changes toward a dry climatic condition from 1999 to 2010 but these changes were not regular and some years like 2003, 2004 and 2007 had normal climatic condition.

There are, in total, 103 dams in the West Azerbaijan and East Azerbaijan provinces. Of these dams 56 are located in Urmia Lake's catchment area. 14 dams were established between 1970 and 1990, and 10 dams were made from 1990 to 2000, and 32 dams were built from 2000 to 2014. Moreover, there are additional dams which are under construction or in the study stage. These dams play a critical role in developing agriculture areas in Urmia Lake's catchment area, but it also means an



increase in irrigation and water usage. The total cultivation area using dams supplied water was about 102966 Hectare in 1999 and it increased to 192648 Hectare in 2013. Annual adjustable water volumes of all dams in Urmia lake's catchment area was about 2060.30 million m<sup>3</sup> in 2013 while the annual agricultural water consumption was about 1320.28 million m<sup>3</sup>. According to these statistics, cultivation areas using water supplied from dams doubled from the periods of 1970-1999 until 1999-2013.

Underground water sources which include deep wells, semi deep wells, aqueducts, and water fountains are another source that provides needed water for irrigation and agricultural developing. Discharge water from underground water sources was 1534 million m<sup>3</sup> during 1984 to 1985 with an increase to 2156 million m<sup>3</sup> during 2011 to 2012. Moreover, discharge water from underground water sources increased by 400 million m<sup>3</sup> alone from 1998 to 1999. According to the available statistics from underground water sources between 1972 and 2012, there are totally 74336 semi deep wells and 8047 deep wells in Urmia Lake's catchment area in 2012.

By considering that rivers Jighati (Zarrinerood), Tatau (Siminerood), Soyugh Bulagh chay (Mahabad), Gadar chay, Baranduz chay, Shahar chay, Roze chay, Nazlu chay, Zola chay, Tasuj chay, Aji chay, and Sufi Chay rivers provide 75% of the inflow water to Urmia Lake while underground water sources, precipitation, and flood water provide 25% of the water inflow. When comparing this climate and nature controlled inflow sources to population and agricultural activities during recent years, it seems more probable that the primary reason of the drying of Urmia Lake must be human activities such as improper water and agricultural management in the catchment area.

A good water and agricultural monitoring and management program should be designed for Urmia Lake's catchment area to rescue and recover the Urmia Lake. Remotely sensed data in conjunction with field survey would be a valuable asset for such monitoring program. In addition, GIS technology could be effectively used to conduct spatial and temporal analysis within the lake and its catchment in order to support the decision making process.

The DMC satellite images used in this study were provided by Istanbul Technical University (ITU, BAP: 37016) and Landsat images were downloaded from United States Geological Survey website. Meteorological data were also provided by West Azerbaijan Meteorological and East Azerbaijan Meteorological Offices. Landuse maps are provided by National Cartographic Center of Iran. ERDAS IMAGINE 2011, ERDAS IMAGINE 2013, ArcGIS10, ArcGIS 10.1, Envi 5, and SPI\_SL\_6.exe programs were used in this study.



## URMİYE GÖLÜNDEKİ ZAMANSAL DEĞİŞİMLERİN UZAKTAN ALGILAMA VE CBS KULLANILARAK BELİRLENMESİ

### ÖZET

Göllerde ve barajlarda bulunan su rezervleri ve bu rezervlerin izlenmesi uzun yıllardır, yerel ve küresel ölçekte en önemli çevresel konulardan biri olmuştur. Su kaynakları ve havzalarındaki değişimlerin izlenmesi, bu kaynakların yönetimi ve doğru kullanımı açısından gereklidir. Su kaynakları ve özellikle göller, küresel ısınma, kuraklık ve artan dünya nüfusunun beraberinde getirdiği insan gereksinimleri nedeniyle önem kazanmaktadır. İnsan gereksinimleri için (içme suyu gibi) kaynak sağlaması dışında, bir göldeki su rezervi, Urmıye Gölü örneğinde olduğu gibi, bir ülkenin ekonomisine katkı sağlayan önemli bir kaynak da olabilmektedir.

Klasik yöntemler kullanılarak göllerde yapılan ölçümler genellikle noktasal bazlı olup, küçük çalışma alanları ile sınırlı kalmaktadır. Bu durum göz önünde bulundurulduğunda, uzaktan algılama teknikleri özellikle geniş alanlara yönelik farklı parametreler ile bilgi ve haritalar üretilmesine imkan sağladığı için su kaynaklarının izlenmesi gibi pek çok farklı çalışmada kullanılmaktadır. Bu projenin amacı; uydu görüntüleri, saha ölçümleri ve meteorolojik verileri kullanarak Uzaktan Algılama ve CBS yöntemleriyle Urmıye Gölü ve civarında olan zamansal değişimleri analiz etmektir. Buna ek olarak göldeki değişimlerin olası nedenlerini incelemek, meteorolojik parametrelerin zamansal analizlerini yapmak ve gölün kurumasını engellemeye yönelik bilimsel öneriler ortaya koymaktır.

Urmıye Gölü, İran'ın kuzey batısında, Batı Azerbaycan ve Doğu Azerbaycan arasında yer almaktadır (N 37.5° E 45.5°). İran'ın en büyük içgölü olan Urmıye Gölü dünyada Lut Gölü'nden sonra aşırı tuzluluk oranına sahip ikinci göldür. Aynı zamanda bu göl özel bir canlı türü olan Urmıye Artemia'ya da ev sahipliği yapmaktadır. Artemia dünya çapında bilinen ve tuz göllerinde bulunan bir zooplanktonik organizmadır.

Bu çalışmada yapılan analizlere göre, Urmıye gölü, 1995 yılında yaklaşık 5982 km<sup>2</sup> yüzey alana sahipken 2013 yılında yaklaşık 1852 km<sup>2</sup> yüzey alana kadar düşen göl, deniz seviyesinden 1250 m yükseklikte ve en fazla 16-20 m derinliğe sahip olup ortalama derinliği ise 6 m'dir. 1995 yılında eni max. 60 km., boyu ise max. 150 km. olarak ölçülmüştür. Göl 15 km uzunluğunda toprak yol ile kuzey ve güney olmak üzere iki parçaya ayrılmıştır. Bu yolun ortası 1500 m uzunluğunda bir köprü ile bağlanmış, köprü altından, bu iki bölüm arasındaki su geçişi sağlanmıştır.

Urmıye Gölü havzası 51876 km<sup>2</sup> alana sahiptir. Havzada 80.000 adetten fazla kuyunun bulunması, birçok barajın kurulmuş olması, sıcaklık ve yağmur değişimleri, ve kuraklık gibi nedenlerden dolayı tuzluluk oranı, son yıllarda göl havzasını tehdit edecek şekilde artmıştır. Yapılan bu çalışmada son otuz yıl içerisinde gölün yaklaşık

%70'inin kurumuş olduđu tespit edilmiştir. Göl ve havzasında meydana gelen doğal ve yapay deęişikliklerin etkilerini iki önemli nokta ile açıklamak mümkündür.

İlk olarak, gölü besleyen akarsular üzerinde özellikle 2000 yılı sonrasında kurulmuş olan çok sayıda baraj, göle akarsular tarafından taşınan su miktarını azaltmıştır. Ayrıca, göl havzasında bulunan çok sayıda kuyu ve bu kuyulardan özellikle tarımsal sulama amaçlı çekilen sular, yeraltı su seviyesinde deęişimlere neden olmuştur. Göl çevresindeki istasyonlardan elde edilen meteorolojik veriler incelendiğinde ise sıcaklık artışı ve yağış azalması gözlemlenmiştir. Bazı araştırmalarda bu deęişimlerin küresel ısınmadan kaynaklı olduđu belirtilmiş olmasına rağmen, göl ve çevresindeki insan kaynaklı müdahalelerin de bu deęişimler üzerinde etkisi olduđu gözardı edilmemelidir. Belirtilen nedenler dolayısıyla göldeki su seviyesi ve yüzey alanı azalmaktadır. Bu durum göl suyunun tuzluluk oranının artmasına neden olmaktadır. Deęişen koşullar nedeni ile Urmiye gölü flamingo gibi binlerce göçmen kuşa ve Urmiye Artemia'si gibi özel türlere artık ev sahiplięi yapamaz hale gelmektedir.

İkinci olarak, Urmiye Gölü'nde oluşan kuraklık, İran başta olmak üzere göl çevresinde yer alan ülkelerde ekosistem ve insan hayatı için tehlike yaratmaktadır. Urmiye Gölü'nün kuruması ile oluşan iklim deęişiklikleri, insan ve doğal hayat üzerinde hastalık ve göç gibi olumsuz olaylara neden olmaktadır. Benzer problem ile Aral Denizi de karşı karşıya kalmış olup bu göl için gerekli tedbirlerin alınmamış olması nedeniyle gölün büyük kısmı artık kullanılamaz haldedir. Bu durum Aral Deniz'i ve çevresindeki ülkeler için önemli bir çevresel sorun haline gelmiştir. Aral Denizi örneęi dikkate alınarak benzer problemlerin yaşanmaması adına Urmiye Gölünün koruma altına alınması son derece önemlidir.

Bu çalışma esas olarak Uzaktan Algılama ve Coęrafî Bilgi Sistemlerinin (CBS) entegrasyonu ile Urmiye Gölü'ndeki 1984 ve 2014 yılları arasındaki otuz yıl içerisinde zamansal deęişimleri belirlemeyi hedeflemektedir. Uydu görüntüleri, meteorolojik veriler, GPS ölçümleri, barajlar, yeraltı su kaynakları, nüfus deęişikliği ve arazi kullanım haritaları Urmiye Gölü'ndeki deęişimleri tespit etmek amacı ile kullanılmıştır.

Çalışmada 1984 yılı ve 2014 yılı arasında elde edilen toplam 95 uydu görüntüsüyle Urmiye Gölü yakınlarında kurulmuş olan 20 sinoptik meteorolojik istasyonun kaydettięi sıcaklık, yağış, ve nem gibi farklı meteorolojik veriler temin edilerek kullanılmıştır. Bu verilere ek olarak, Batı Azerbaycan ve Doęu Azerbaycan bölgelerine ait arazi kullanım haritaları aracılığıyla, nüfus, yeraltı su kaynakları ve barajlar gölün durumunun genel deęerlendirilmesi için kullanılmıştır.

Çalışmanın ilk aşamasında uydu görüntüsü olarak kullanılan veri seti oluşturulmuştur. USGS arşivindeki Landsat-4, -5 TM ve Landsat-8 uydularına ait farklı yılların aynı aylarında ve mevsimlerinde elde edilmiş, düşük bulut etkisi gözlenen en iyi verilerin olduđu görüntüler seçilmiştir. Daha sonra 1984-yaz, 1987-bahar, 1987-yaz, 1990-yaz, 1995-yaz, 1998-bahar, 1998-yaz, 2000-yaz, 2006-yaz, 2007-bahar, 2007-yaz, 2009-yaz, 2010-yaz, ve 2011-yaz görüntülerini içeren Landsat-5 TM uydu verileri ile 2013-bahar, 2013-yaz, ve 2014-kış Landsat-8 verileri ve 2011-bahar, ve 2012-yaz mevsimlerini içeren DMC verileri seçilerek veri seti oluşturulmuştur. Sonuç olarak, toplamda 1984-2014 yılları arasında 95 adet uydu görüntüsü ile çalışılmıştır.

Görüntü ön işlemenin ilk aşamasında Landsat-5 TM uydusunun 1, 2, 3, 4, 5, 7 bantları ve Landsat-8 uydusunun 1, 2, 3, 4, 5, 6, 7 bantları birleştirilerek görüntü oluşturulmuştur. İkinci aşamada görüntülerde piksellerin parlaklık deęerlerinde

meydana gelen hatalar ve atmosferik kořullardan meydana gelen bulut etkisini dűřürmek için radyometrik ve atmosferik düzeltmeler yapılmıřtır.

Görüntü ön iřlemesi bittikten sonra, alıřma alanını kapsamak için 6 görüntü mozaiklenmiř ve alanı kapsayan tek bir görüntü oluřturulmuřtur. Bu alıřmadaki amalardan bir tanesi Urmiye gölünün yüzey alanında meydana gelen deęiřikliklerin belirlenmesi için en uygun ve en doęru yöntemi ortaya koymaktır. Bu amala, görüntüler kontrollü ve kontrolsüz sınıflandırma yöntemleri kullanılarak sınıflandırılmıř ve son 30 yıllık periyotta göl ve evresinde meydana gelen deęiřimler karřılařtırılmıřtır.

Yapılan Doğruluk analizlerine göre kontrollü sınıflandırma ile daha iyi sonuçlar elde edilmiřtir. Bu nedenle gölün yüzeyinde meydana gelen deęiřimlerin tespiti için kontrollü sınıflandırma sonuçları kullanılmıřtır. Bu sonuçlara göre gölün su yüzey alanı 1995 yılında yaklaşık 5982 km<sup>2</sup> iken 2013 yılında yaklaşık 1852 km<sup>2</sup> olarak hesaplanmıřtır. Aynı zamanda bu alıřmada su yüzey alanını, kıyı boyunca su kütlelerini ve sulu olmayan kütleleri ayırmak için NDVI (Normalized Difference Vegetation Index) ve MNDWI (Modified Normalized Difference Water Index) kullanılmıřtır ve bu indislerden elde edilen sonuçlar kıyaslanmıřtır.

Gölün su yüzey alanı 1995 ve 2006 yıllar arasında yaklaşık 2000 km<sup>2</sup> azalmıřtır, bu %32 oranında bir kurumunun meydana geldiđini göstermektedir. Bu tarihten sonra, 2006 ve 2013 yıllar arasında da gölün su yüzey alanı 2000 km<sup>2</sup> azalmıřtır ve kontrollü sınıflandırma sonuçlarına göre gölün su yüzey alanı 2013 yılında 1853 km<sup>2</sup> bulunmuřtur.

Urmiye gölünün havzasında olan deęiřimleri tespit etmek için NDVI (Normalize Difference Vegetation Index), NDWI (Normalized Difference Water Index), NDSI (Normalized Differential Salinity Index), SI (Salinity Index) ve NDDI (Normalized Difference Drought Index) kullanılmıřtır. Bulunan Sonuçlara göre 2006 yılı, 30 yıllık periyotta yüksek toprak tuzluluęu, en az NDVI, en az NDWI ve en řiddetli kuraklıęa sahip olan yıldır. 2006 yılının tersine 1987 yılı düşük toprak tuzluluęu, yüksek NDVI, yüksek NDWI ve az kuraklıęa sahip bir yıl olmuřtur.

Meteorolojik verilerin analizine göre 2006 ve 2010 yılları, son yılların en sıcak yılları olmasına raęmen, bu yıllara ait olan yaęıř grafiklerine bakıldıđında, son yıllara göre yüksek miktarda yaęıř artıřı gözükmemektedir. Jeostatistik analizi ve SPI (Standard Precipitation Index) sonuçlarını dikkate alındıđında 1999 ve 2010 yılları arasında kuraklık gözlemlenmekte fakat bu kuraklık yılların hepsini kapsamamaktadır. Örnek olarak 2003, 2004 ve 2007 yıllarında kuraklık tespit edilmemiřtir.

Gölün havzasında bulunan su kaynaklarına göre , Kuzey ve Güney Azerbaycan da toplam 103 tane baraj bulunmaktadır. Bu barajlardan 56 tanesi Urmiye Gölü havzasında yer almaktadır. Bu barajların 14 tanesi 1970-1990, ve 10 tanesi 1990-2000 ve 32 tanesi ise 2000-2014 yılları arasında inřa edilmiřtir. Bu barajlar, Urmiye gölü havzasında tarım alanlarının geliřtirilmesinde önemli bir rol oynamaktadır. 1999 yılında 102966 hektar tarım alanı varken 2013 yılında tarım alanları 192648 hektara kadar ulařmıřtır. 2013 istatistiklerine göre Urmiye Gölü havzasındaki barajların yıllık tařıdıđı toplam su miktarı 2060.30 milyon metreküp olup bunların 1320.28 milyon metreküpü yalnızca tarım faaliyetleri için kullanılmaktadır. 2013 yılında ime suyu tüketimi ise 389.04 milyon metreküptür. Bölgede 1985 yılından 2010'a yılına kadar nüfus 1.800.000 artıř göstermiř ve buna baęlı olarak İrandaki su tüketimi dünya standartlarına oranla 2 kat artmıřtır.

Yeraltı suları, tarım arazileri için diğer temel su kaynağıdır. Yer altı sularının çekilme miktarı, 1984-1985 yılları arasında 1534 milyon metreküpken, 2011-2012 yılları arasında 2156 milyon metreküptür. Örnek olarak yalnızca 1998-1999 yılları arasında yer altı suları çekilmesi 400 milyon metreküp artmıştır. Ulaşılabilir kaynaklar doğrultusunda 2012 yılında Urmiye Gölü havzasında toplam 74336 adet orta-derin kuyu ve 8047 adet derin kuyu bulunmaktadır.

Sonuç olarak, gölün giriş suyunu temin eden kaynaklara baktığımızda, gölün havzasında olan Cığatı (Zarrinerood), Tatau (Siminerood), Soyuk Bulak Çay (Mahabad), Gadar Çay, Baranduz Çay, Şehir Çay, Roze Çay, Nazlı Çay, Zola Çay, Tesuc Çay, Acı Çay, ve Sufi Çay Urmiye Gölü'nün yaklaşık %75 giriş suyunu sağlamaktadır. Kalan %25 giriş suyu yağış, yeraltı suları ve diğer kaynaklara bağlıdır. Urmiye Gölü havzasında nüfusun artması, çok sayıda barajın yapılması, yeraltı sularının çekilmesi ve tarımsal arazinin çoğalması göz önüne alındığında bölgede meydana gelen değişikliklerde iklim etkisinden daha çok insan etkisi olduğu tespit edilmiştir. Urmiye Gölü ve havzasında değişimlerin takibi için başarılı bir izleme sistemi kurulması noktasında Uzaktan algılama ve CBS entegrasyonu büyük bir önem taşımaktadır.

Bu çalışmada DMC uydu görüntüleri, İstanbul Teknik Üniversitesi (İTÜ BAP: 37016) tarafından sağlanmıştır. Landsat görüntüleri Amerika Birleşik Devletleri Jeolojik Araştırmalar sitesinin veritabanından indirilmiştir. Ayrıca meteorolojik veriler Batı Azerbaycan Meteoroloji Dairesi ve Doğu Azerbaycan Meteoroloji Dairesi'nden temin edilirken arazi haritaları da Ulusal Kartoğrafya Merkezi'nden alınmıştır. Bu çalışmada ERDAS IMAGINE 2011 ve 2013, Arcgis 10 ve 10.1, Envi 5 ve SPI\_SL\_6.exe programları kullanılmıştır.

## 1. INTRODUCTION

Different types of environmental sources, especially water bodies play a crucial role in human life and economy. Nowadays, the significance of water bodies, especially fresh water sources like lakes is increasing since these sources are being threatened due to global warming, drought and human needs. In addition to serving as supply for human needs such as irrigation and drinking water, a water reserve in a lake and its catchment area can also be important sources contributing to country's economy and policy like the case of Urmia Lake in Iran[1].

Remote sensing systems measure the reflected or emitted energy from the earth's surface using a sensor mounted on an aircraft or spacecraft platform. GIS is used to capture, store, retrieve, analyze, and display spatial data. Remote Sensing and Geographic Information System (GIS) in conjunction with field survey provide valuable spatial information to evaluate environmental changes on water bodies and their vicinity all around the world in from local to global scales[2,3].

Urmia Lake is located in the northwest of Iran between West Azerbaijan and East Azerbaijan provinces. It is the largest inland lake of Iran and the second largest hypersaline lake in the world after Dead Sea and the habitat of *Artemia Urmiana* which is a unique bisexual *Artemia* Species. The brine shrimp *Artemia* is a zooplanktonic organism found in hypersaline habitats such as inland salt lakes, coastal salt pans and manmade saltworks worldwide. Urmia Lake is an oligotrophic lake of thalassohaline origin at an altitude of 1250 m above sea level with average depth of 6 m and a maximum depth between 16-20 m. Urmia Lake is divided into 2 parts including north and south parts separated by a causeway which has about 1500 m bridge, allowing a little water exchange between 2 parts[4,5,6].

Based on the results obtained from this research, the total surface area of Urmia Lake is about 1900 km<sup>2</sup> in 2013 and 6000 km<sup>2</sup> in 1995 and the maximum length and width of the lake are about 150 km and 60 km, respectively, in the year of 1995. During the last 20 years, human activities around the lake such as agricultural practices,

irrigation, construction of dams and wells and temperature and precipitation changes have significantly decreased the amount of water that the lake receives annually. The salinity has particularly increased in all parts of the lake and about 70% of the lake's area was dried during this period. It is possible that the most part of the northwest of Iran and neighbor countries (Turkey, Azerbaijan, Iraq, and Armenia) be affected by the impacts of drying Urmia Lake at future years.

### 1.1 Coastline Change Detection Methods

Coastline evaluation of different kinds of water bodies is one of the most important points in analyzing water bodies and their surrounds to have a good management in environmental protection. Different image processing techniques could be applied to various remotely sensed data to detect coastline changes. Statistical classification methods (unsupervised classification and supervised classification), different indices like Normalized Difference Vegetation Index (NDVI), Normalized Difference Water Index (NDWI), Modified Normalized Difference Water Index (MNDWI), and band ratios are used to calculate the area of water bodies. Moreover, some researchers have used a combination of different methods to improve the accuracy of results. Most of these methods are based on multispectral optical remote sensing[7].

Lei Ji et al (2009) used normalized difference water index (NDWI) to identify water surface. NDWI obtained from different band combinations (visible, near-infrared, or shortwave-infrared) can generate different results. It should also be considered that NDWI thresholds vary depend on the proportions of subpixel water/non water components. They used the spectral data obtained from a spectral library to simulate the satellite sensors Landsat ETM+, SPOT-5, ASTER, and MODIS, and calculated the simulated NDWI in different forms. They found that the NDWI calculated from Eq.(1.1)[8]:

$$NDWI = \frac{(Green - SWIR)}{(Green + SWIR)} \quad (1.1)$$

Where *SWIR* is the shorter wavelength region (1.2 to 1.8 mm), had the most stable threshold. They recommended this NDWI be employed in mapping water, but adjustment of the threshold based on actual situation was necessary in this method.

McFeeters (1996) proposed the Normalized Difference Water Index (NDWI) to describe open water features, which is expressed as follows in Eq.(1.2):



$$NDWI = \frac{(\rho_{Green} - \rho_{NIR})}{(\rho_{Green} + \rho_{NIR})} \quad (1.2)$$

Where  $\rho_{Green}$  and  $\rho_{NIR}$  are the reflectance of green and NIR bands, respectively. The NDWI values are between -1 to 1. McFeeters (1996) set zero as the threshold. That is the water body if  $NDWI > 0$  and it is non-water if  $NDWI \leq 0$ .

Gao (1996) developed a different NDWI to be used for estimating water content of vegetation canopy. Although McFeeters' and Gao's NDWIs have the same terminology, the concepts of the two NDWIs are completely different. Gao's NDWI is calculated as the normalized difference of NIR and SWIR bands.

Rogers and Kearney (2004) used red and SWIR bands (bands 3 and 5 in Landsat TM) to produce NDWI, given by Eq.(1.3) [8]:

$$NDWI = \frac{(\rho_{Red} - \rho_{SWIR})}{(\rho_{Red} + \rho_{SWIR})} \quad (1.3)$$

Where  $\rho_{Red}$  is the reflectance of the red band, and  $\rho_{SWIR}$  is the reflectance of the SWIR band. Xu (2005) modified the NDWI by using a middle infrared (MIR) band such as TM5 to substitute the NIR band in the NDWI. The modified NDWI (MNDWI) is expressed as follows:

$$MNDWI = \frac{\rho_{Green} - \rho_{MIR}}{\rho_{Green} + \rho_{MIR}} \quad (1.4)$$

Xu (2006) found that McFeeters' NDWI was unable to completely separate built-up features from water features. NDWI showed positive values in built-up features which were similar to water because the NIR reflectance was lower than the green reflectance. To compensate the drawbacks of McFeeters' NDWI, Xu (2006) proposed the modified NDWI (MNDWI), in which the SWIR band (Landsat TM band 5) was used to replace the NIR band in McFeeters' NDWI equation[8]:

$$MNDWI = \frac{(\rho_{Green} - \rho_{SWIR})}{(\rho_{Green} + \rho_{SWIR})} \quad (1.5)$$

Like McFeeters' NDWI, the threshold value for MNDWI was set to zero (Xu, 2006). However, Xu (2006) found a manual adjustment of the threshold which could achieve a more accurate result in the water delineation. As an independent study, Lacaux et al. (2007) developed a Normalized Difference Pond Index (NDPI) to

classify ponds in West Africa. The NDPI is expressed as the normalized difference of green and SWIR reflectances (SPOT-5 bands 1 and 4, respectively) [8]:

$$NDPI = \frac{(\rho_{SWIR} - \rho_{Green})}{(\rho_{SWIR} + \rho_{Green})} \quad (1.6)$$

The equations of MNDWI and NDPI are almost identical, except that the orders of  $\rho_{SWIR}$  and  $\rho_{Green}$  are different in the two equations. Lacaux et al. (2007) used these criteria for detecting ponds: If  $NDPI < \text{Threshold 1}$  and  $\rho_{SWIR} < \text{Threshold 2}$ , then cover is pond; otherwise, cover is not pond.

Taheri Shahriani et al (2005) applied processing methods to investigate of Hirmand, Sabury and Poozak lakes in the southeast of Iran. They used threshold of NDVI map with visual interpretation of False Color Composite (FCC) image as a reference to evaluate other processing methods. Moreover, it concluded that in all of the processing methods using different multispectral images, estimation can be improved through the combination with NDVI map [9].

S. Sima et al (2012) investigated the seasonal and annual variations of Urmia lake area from 2000 to 2011 using remote sensing data. Normalized Differential Vegetation Index (NDVI) image obtained from MODIS data were used to extract the water surface area of the lake. This study confirms the successful application of MODIS NDVI products for retrieving the variation of the large lakes area with an acceptable spatial and temporal resolution. They applied HYDROWEB database to validate the extracted area from MODIS-NDVI products. HYDROWEB database contains satellite altimetry data for around 150 large lakes and reservoirs worldwide (Cretaux et al., 2011). They selected NDVI thresholding method in their study because of the availability of MODIS-NDVI satellite images with an appropriate temporal resolution (16 days) and a satisfactory spatial resolution (nominal 250×250 m) to monitor both seasonal and within year variations of Urmia Lake surface area. Figure 1.1 shows their results[9].

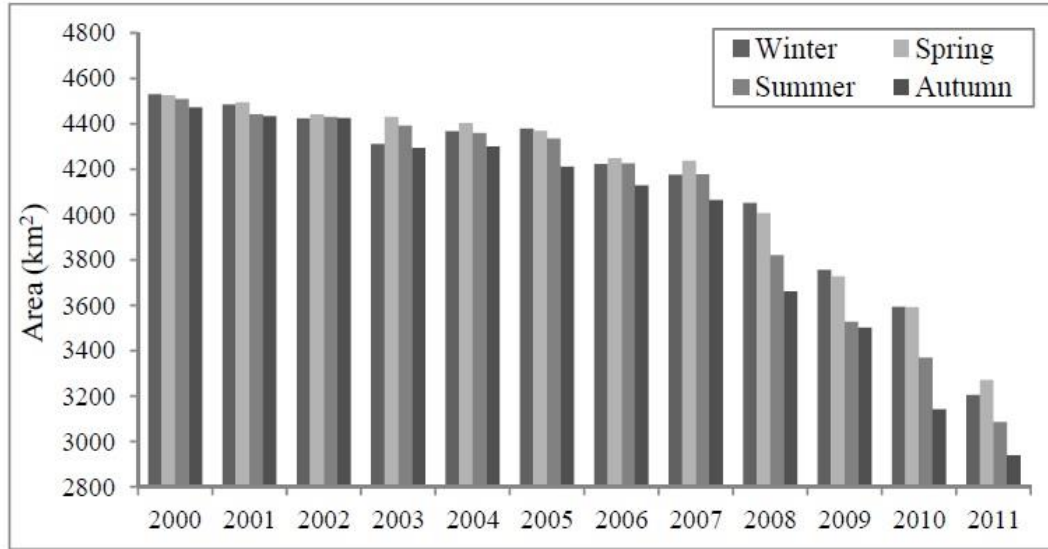


**Figure 1.1** : Area of Urmia Lake according to S. Sima et al (2012).

A. Alesheikh et al (2007) developed a new procedure for coastline change detection of Urmia Lake using combination of histogram thresholding and band ratio techniques. They applied the ratio in Landsat-7 ETM and Landsat-5 TM images according to Eq.(1.7):

$$\text{Band ratio} = \frac{\text{band2}}{\text{band5}} \quad (1.7)$$

Which is greater than one for water and less than one for land in the study area. This law includes high accuracy in coastal zones covered by soil rather than in land with vegetative cover. Actually, this law mistakenly considers some of the vegetative lands as water body. They combined two ratios to solve this problem. Applying this method, the coastline can be extracted with higher accuracy. But the problem occurs in some of the coastal zones (i.e. In some areas, the coastline moves toward the water). If the aim is to rapidly calculate coastline, then it can be a supreme method. Two techniques exist for calculating an accurate coastline. In the first technique, a color composite can be used for editing the coastline map. The best color composite for this technique in Landsat-7 ETM and Landsat-5 TM images is RGB (Red Green Blue) 5-4-3 band combination. This color composite nicely depicts water-land interface. Furthermore, it is very similar to the true-color composite of earth's surface. Moreover, it includes the bands that have low correlation coefficient, and therefore, it contains higher information in comparison to other color composites

(Moore, 2000). However, this technique is time-consuming and needs a lot of editing. In the second technique, the histogram thresholding method is used on band 5 of Landsat-7 ETM and Landsat-5 TM for separating land from water. The threshold values have been chosen such that all water pixels are classified as water, and most of land pixels have been classified as land. In this case, few land pixels have mistakenly been assigned to water pixels. The image obtained from band ratio technique, also labels water pixels to one and land pixels to zero. This second image is named “image No. 2”. Then the two images are multiplied. The final obtained binary image represents the coastline accurately. The area of Urmia Lake in 1998 and 2001 were calculated 5650 and 4610 square kilometers, respectively. According to their results, the area of Urmia lake decreased approximately 1040 square kilometers from August 1998 to August 2001 in a three year period[10].

Keivan Kabiri et al (2012) used Landsat images to calculate the area of Urmia Lake. They applied unsupervised classification method to determine the area of Urmia Lake from 1984 to 2011. They used unsupervised classifier to distinct water and land bodies on all satellite images. They selected images from June to September (Summer time in studying area). Figure 1.2 shows their results [11].

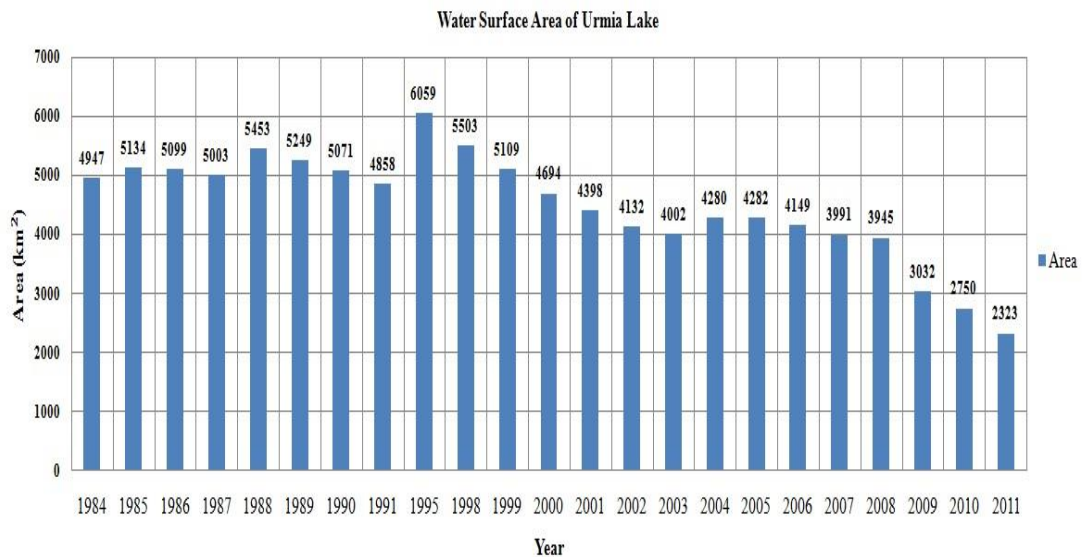


**Figure 1.2 :** Area of Urmia Lake according to Keivan Kabiri et al (2012).

## **1.2 Objectives Of Thesis**

This study focuses mainly on multi-temporal change detection on Urmia Lake and its catchment area by integration of remote sensing and geographical information systems for a thirty-year period from 1984-August to 2014-February. In addition to satellite images, meteorological data, GPS measurements, landuse maps and ground photographs were analyzed to investigate the changes on Urmia Lake and to understand the role and effects of human and global warming on drying of Urmia lake.

This thesis aims to:

- 1)** Integrate Remote Sensing (RS) and Geographical Information Systems (GIS) to analyze changes in Urmia Lake and its vicinity during the last thirty years using Normalized Difference Vegetation Index (NDVI), Normalized Difference Water Index (NDWI), Normalized Difference Drought Index (NDDI), Normalized Differential Salinity Index (NDSI), and Salinity Index (SI).
- 2)** Compare different methods to accurately map the water surface area of Urmia Lake including unsupervised classification, supervised classification, MNDWI, NDVI.
- 3)** Analyze the reasons of drying Urmia Lake using satellite images, Standardized Precipitation Index (SPI), geostatistical maps of meteorological variables and related information about Dams, underground water resources and population.



## **2. PRINCIPLES OF REMOTE SENSING**

### **2.1 Introduction To Remote Sensing**

Integration of sensing technology and GIS techniques are used in a variety of applications to derive valuable information by conducting spatial analysis to solve environmental problems and aid decision making. It is difficult, expensive and time-consuming to use traditional surveying methods to investigate and monitor large regions like water bodies, forest, agriculture, and urban. On the other hand, remotely sensed data is an alternative source of environmental monitoring that provides economic, fast and accurate information.

*“Remote sensing is the science and art of obtaining information about an object, area or phenomenon through the analysis of data acquired by a device that is not in contact with the object, area, or phenomenon under investigation”*[12].

There are 2 kinds of remote sensing systems; passive and active. In passive systems, remote sensing systems do not have their own energy source and the natural energy source like the sun is used as an energy source. But in an active system the sensor provides its own energy like synthetic aperture radar (SAR) system. Also active sensors include the ability to measure targets anytime, regardless of the time of day or season. The energy recorded by the remote sensing system is the electromagnetic radiation. Electromagnetic radiation consists of an electrical field and a magnetic field; these fields are oriented at right angles to each other. Both of these fields travel at the speed of light. Wavelength and frequency are two characteristics of electromagnetic radiation. Wavelength is the distance between continuous wave crests. It is measured in meters or some factors of meters. Frequency is the number of cycles of a wave passing a fixed point per second. It is measured in hertz. Wavelength and frequency are inversely related to each other [12,13].

The sun's light is the form of EMR that is most familiar to human beings. Sunlight that is reflected by physical objects travels in most situations in a straight line to the observer's eye. On reaching the retina, it generates electrical signals that are

transmitted to the brain by the optic nerve. The brain uses these signals to construct an image of the viewer's surrounding. This is the process of remote sensing; indeed, the vision is a form-perhaps the basic form of remote sensing. The electromagnetic spectrum ranges from the shorter wavelengths to the longer ones (Figure 2.1). The shortest are gamma and x-rays. The longest are microwave and broadcast radio waves. Most parts of the electromagnetic spectrum are used in science for spectroscopic and other probing interactions, as ways to study and characterize matter. In addition, radiation from various parts of the spectrum has found many other uses for communications and manufacturing. The ultraviolet or UV portion of the spectrum which has the shortest wavelength practical for remote sensing can be used for some purposes too [12,13].

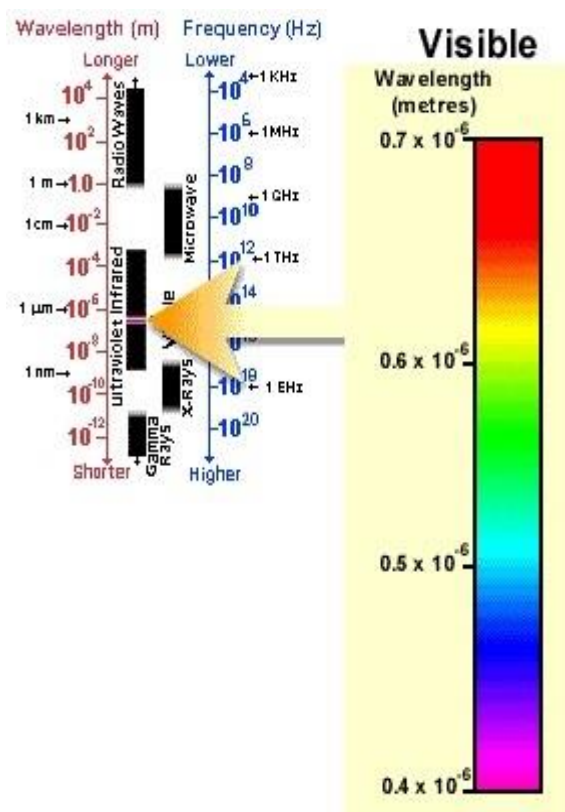


**Figure 2.1:** Electromagnetic spectrum[13].

## 2.2 Energy Interaction with the Earth Surface Features

When electromagnetic energy reaches the Earth's surface from the Sun is reflected, transmitted or absorbed. Reflected energy travels upwards through and interacts with the atmosphere; that part of it which enters the field of view of the sensor is detected and converted into a numerical value that is transmitted to a ground receiving station



on the Earth. The amount and spectral distribution of the reflected energy is used in remote sensing to infer the nature of the reflecting surface. A basic assumption made in remote sensing is that specific targets (soils, water, vegetation and etc) have an individual and characteristic manner of interaction with incident radiation that is described by the spectral response of that target (Figure 2.2). In some instances, the nature of the interaction between incident radiation and Earth surface material will vary from time to time during the year, such as might be expected in the case of vegetation as it develops from the leafing stage, through growth to maturity and, finally, to senescence[12,13].

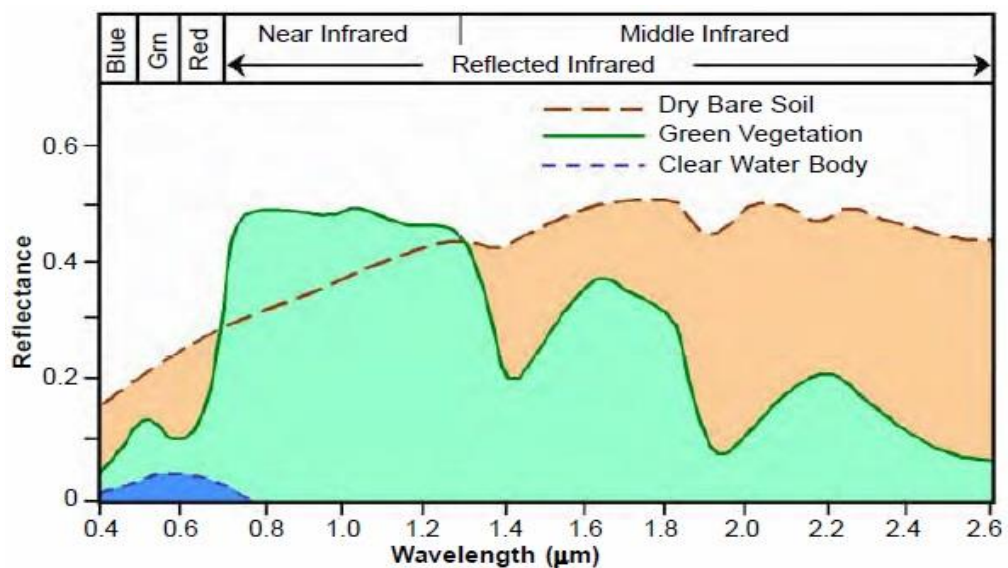


**Figure 2.2:** Spectral reflectance curves for various features types[66].

### 2.2.1 Spectral Reflectance Of Vegetation

To analyze vegetation using remotely sensed data, knowledge of the function and structure of vegetation and its reflectance properties need to be known. This enables researchers to link the reflectance behavior of vegetation and their structure and ecological system. Vegetation reflectance properties are used to derive vegetation indices (VIs). The VIs are used to analyze various ecologies. VIs are constructed from reflectance measurements in two or more wavelengths to analyze specific characteristics of vegetation, such as total leaf area and water content.

A VI is a simple measure of some vegetation property calculated from reflected solar radiation measurements made across the optical spectrum. The solar-reflected optical spectrum spans a wavelength range of 400 nm to 3000 nm. Of this range, the 400 nm

to 2500 nm region is routinely measured using a variety of optical sensors ranging from multispectral (for example, Landsat TM, SPOT MSS, QuickBird) to hyperspectral (for example, AVIRIS, HyMap, Hyperion). The interaction of vegetation with EMR differs from those of soil and water. The absorption and reflection of solar radiation are the result of many interactions with different plant materials, varying considerably with wavelength. Water, pigments, nutrients, and carbon are each expressed in the reflected optical spectrum from 400 nm to 2500 nm, with often overlapping, but spectrally distinct reflectance behaviors. These are known signatures allow scientists to combine reflectance measurements at different wavelengths to enhance specific vegetation characteristics by defining VIs.

The optical spectrum is partitioned into four distinct wavelength ranges:

- Visible: 400 nm to 700 nm
- Near-infrared: 700 nm to 1300 nm
- Shortwave infrared 1 (SWIR-1): 1300 nm to 1900 nm
- Shortwave infrared 2 (SWIR-2): 1900 nm to 2500 nm

The transition from near-infrared to SWIR-1 is marked by the 1400 nm atmospheric water absorption region in which satellites and aircraft cannot acquire measurements. Similarly, the SWIR-1 and SWIR-2 transition is marked by the 1900 nm atmospheric water absorption region.

Spectral reflectance curves for healthy green vegetation almost always manifest the peak-and-valley configuration illustrated by green grass. The valleys in the visible portion of the spectrum are dictated by the pigments in plant leaves. Chlorophyll strongly absorbs energy in the wavelength bands centered at about 0.45 and 0.67  $\mu\text{m}$ . Hence, our eyes perceive healthy vegetation as green in color because of the very high absorption of blue and red energy by plant leaves and the relatively high reflection of green energy. If a plant is subject to some form of stress that interrupts its normal growth and productivity, it may decrease or cease chlorophyll production. The results are less chlorophyll absorption in the blue and red bands. Often the red reflectance increase of the point that we see the plant turn yellow (a combination of green and red) [12,13].

### 2.2.2 Spectral Reflectance Of Water Bodies

The characteristic spectral reflectance curve for water shows a general reduction in reflectance with increasing wavelength, so that in the near infrared the reflectance of deep, clear water is virtually zero. However, the spectral reflectance of water is affected by the presence and concentration of dissolved and suspended organic and inorganic material, and by the depth of the water body. Thus, the intensity and distribution of the radiance upwelling from a water body are indicative of the nature of the dissolved and suspended matter in the water, and of the water depth. Figure 2.3 shows how the information that oceanographers and hydrologists require is only a part of the total signal received at the sensor[2].

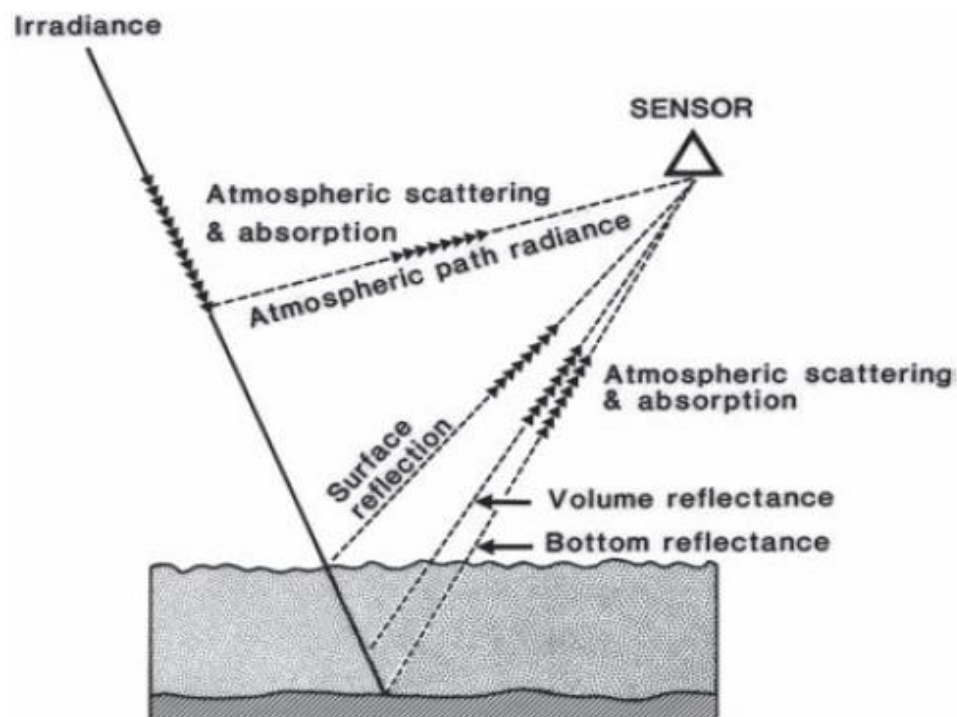


**Figure 2.3:** Processes acting upon solar radiant energy in the visible region of the spectrum over an area of shallow water[2].

Once within the water body, EMR may be absorbed by the water (the degree of absorption being strongly wavelength-dependent) or selectively absorbed by dissolved substances, or backscattered by suspended particles. This latter component is termed the volume reflectance. At a depth of 20 m only visible light (mainly in the blue region) is present, as the near-infrared component has been completely absorbed. Particulate matter, or suspended solids, scatters the down-welling

radiation, the degree of scatter being proportional to the concentration of particulates, although other factors such as the particle size distribution and the color of the sediment are significant[2].

The spectral absorption characteristics of water body in visible and infrared bands differ very much from the other ground objects. They depend only on the used spectral bands and can be considered as invariant and sensor independent. Considering the spectral reflectance of water, probably the most distinctive characteristics are the energy absorption at near-IR wavelengths and beyond. In short, water absorbs energy in these wavelengths whether we are talking about water features or water contained in vegetation or soil. Clear water absorbs relatively little energy having wavelengths less than about 0.6  $\mu\text{m}$ . High transmittance typifies these wavelengths with a maximum in the blue-green portion of the spectrum [12,13].

Spectral reflectance of clear water (Figure 2.4) is low in all portions the spectrum. Reflectance increases in the visible portion when materials are suspended in the water. Turbid water has a high reflectance in the visible region than clear water. This is also true for waters containing high chlorophyll concentrations. These reflectance patterns are used to detect algae colonies as well as contaminations such as oil spills or industrial waste water[14].

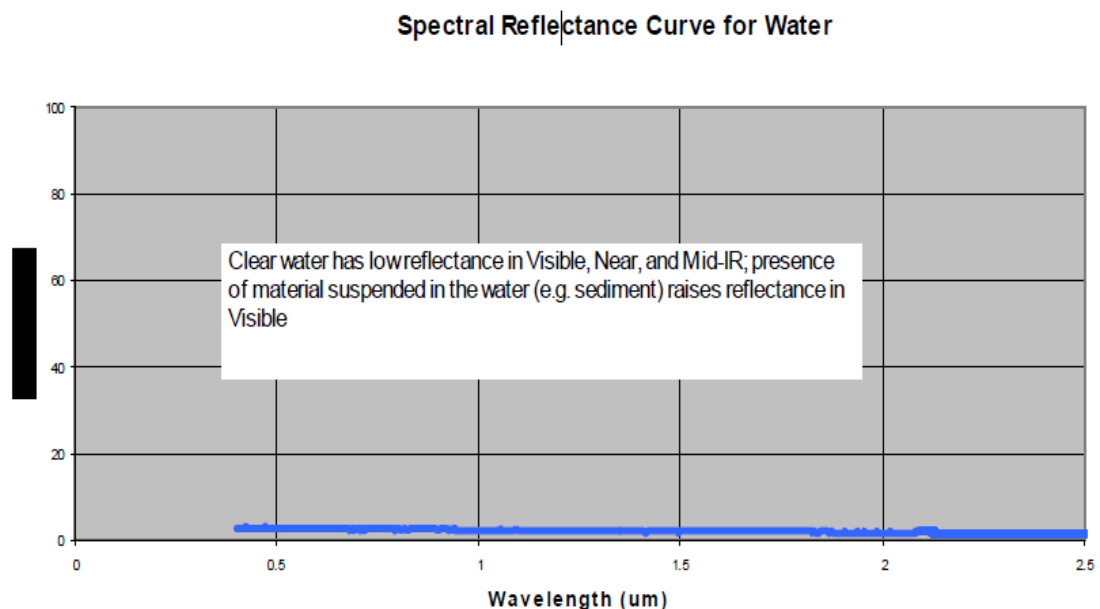


**Figure 2.4 :** Spectral reflectance of water. Graph developed for Prospect (2002 and 2003) using Aster Spectral Library[14].

### 2.2.3 Spectral Reflectance Of Soils

The soil curve shows a considerably less peak-and-valley variation in reflectance. That is, the factors that influence soil reflectance act over less specific spectral bands. Some of the factors affecting soil reflectance are moisture content, organic matter content, soil texture, surface roughness, and presence of moisture in the soil will decrease its reflectance. As with vegetation, this effect is greatest in the water absorption bands at about 1.4, 1.9, and 2.7  $\mu\text{m}$ . Soil moisture content is strongly related to the soil texture. Coarse, sandy soils are usually well drained, resulting in low moisture content and relatively high reflectance; poorly drained fine-textured soils will generally have lower reflectance [12, 13].

### 2.3 Geographical Information Systems (GIS)

*GIS is many simultaneous technological revolutions. Geographic information science merges skills and theory across geography, cartography, geodesy, database theory, computer science and mathematics. GIS is sequenced by location, and so can organize almost any other information type, because everything exists or happens somewhere. A GIS is any information system capable of integration, storing, editing, analyzing, sharing, and displaying geographically referenced information. GIS's are automated systems to the capture, storage, retrieval, analysis, and display of spatial data [3].*

In the early decades of GIS, professionals focused mainly on data compilation and application projects and spent most of their time creating GIS databases and authoring geographic knowledge. GIS professionals then started employing these knowledge collections in different GIS applications and settings. Users applied comprehensive GIS workstations to compile geographic datasets, build work flows for data compilation and quality control, author maps and analytical models, and document their work and methods[3].

A geographic information system supports multiple views for working with geographic information; they are as follows:

1. The Geodatabase view: A GIS is a spatial database containing datasets that represent geographic information in terms of a generic GIS data model (features, rasters, topologies, networks, and so forth).

2. The Geovisualization view: A GIS is a set of intelligent maps and other views that show features and feature relationships on the earth's surface. Various map views of the underlying geographic information can be constructed and used as windows into the database to support queries, analysis, and editing of the information.

3. The Geoprocessing view: A GIS is a set of information transformation tools that derive new geographic datasets from existing datasets. These geoprocessing functions take information from existing datasets, apply analytic functions, and write results into new derived datasets[15,16].

### **2.3.1 GIS DATA Sources**

A GIS database stores descriptive information about map features as attributes. For example, a water system database includes attributes for pipes, valves, meters, hydrants, and so on; and a sewer system database contains attributes for pipes, manholes, catch basins, outfalls, and so on. The creation of an appropriate GIS database is the most difficult and expensive part of developing GIS applications. Successful GIS applications require a database that provides appropriate information in a useful and accessible form. The design of the database is, therefore, driven by application needs[3].

The word data refer to groups of information that represent the qualitative or quantitative attributes of a variable or set of variables. Data is typically the results of measurements and can be the basis of graphs, images, or observations of a set of variables. Data is often viewed as the lowest level of abstraction from which information and knowledge are derived. There are different types of sources of information on GIS such as[3]:

- The internet and the world wide web
- Books, Journals, and Magazines
- Professional Societies
- Conferences
- Educational Organizations and Universities

### 2.3.2 Geodatabase

A geographic information system (GIS) handles geospatial data. Geospatial data is data that describes both the location and characteristics of spatial features such as roads, land parcels, and vegetation stands on the Earth's surface. The locations of spatial features are measured in geographic coordinates (i.e., longitude and latitude values) or projected coordinates (for example, Universal Transverse Mercator or UTM coordinates). The term geographic data is used to describe data that include the locations of spatial features, and the term nongeographic data is used to describe data that include only the attributes of spatial features. There are different types of data, including both geographic and nongeographic data as follows, which can be stored in a geodatabase[17]:

- Vector Data

The geodatabase data model represents vector-based spatial features as points, polylines, and polygons. A point feature may be a simple point feature or a multipoint feature with a set of points. A polyline feature is a set of line segments, which may or may not be connected. A polygon feature may be made of one or many rings. A ring is a set of connected, closed, nonintersecting line segments.

- Raster Data

The geodatabase data model represents raster data as a two-dimensional array of equally spaced cells. The use of arrays and cells for raster data is the same as the ESRI grid model. A large variety of raster data are available in GIS. They include satellite imagery, Digital Elevation Models (DEMs), digital orthophotos, scanned files, graphic files and software-specific raster data such as ESRI grids.

- Triangulated Irregular Networks (TINs)

The geodatabase data model uses a TIN dataset to store a set of nonoverlapping triangles that approximate a surface. Elevation values along with x,y coordinates are stored at nodes that make up the triangles. In many instances, a TIN dataset is an alternative to a raster dataset for surface mapping and analysis.

- Location Data

The term location data refers to data that can be converted to point features. Common examples of location data are tables that contain x,y coordinates or street addresses.

A table with x-, y coordinates can directly be converted into a point feature class, with each feature corresponding to a pair of x and y coordinates. Using a street network as a reference, a list of street addresses can be geocoded into a set of point features.

- Nongeographic Data

A table that stores nongeographic data does not have a geometry field. The geodatabase data model defines such a table as an object class. Examples of object classes include comma-delimited text files and dBASE files. These files or tables contain attributes of spatial features and have keys (i.e., relate fields) to link to geographic data in a relational database environment.



### **3. STUDY AREA AND DATA USED**

This research was conducted for Urmia Lake, located in the northwest part of Iran. A total number of 95 satellite images obtained from Landsat-5 TM, Landsat-8, and DMC images from August 1984 to February-2014 were used in this study. Different meteorological variables such as temperature, precipitation, and humidity which have been measured at 20 synoptic stations around Urmia Lake were also used to interpret meteorological changes during the last 60 years. Results of 5 stations close to Urmia Lake were presented. Moreover, data collected from Landuse maps of West Azerbaijan and East Azerbaijan provinces, the population of these provinces, information on dams, underground water resources, and water surface elevation were used in this study to analyze the human and climate induced impacts on drying of Urmia Lake.

#### **3.1 Study Area**

Urmia Lake is located in the northwest of Iran between West Azerbaijan and East Azerbaijan provinces (N 37.5° E 45.5°). It is the largest inland lake of Iran and the second largest hypersaline lake in the world after Dead Sea and the habitat of *Artemia Urmiana* which is a unique bisexual *Artemia* Species. The brine shrimp *Artemia* is a zooplanktonic organism found in hypersaline habitats such as inland salt lakes, coastal salt pans and manmade saltworks worldwide [4, 5, 6].

Urmia Lake is very similar to Great Salt Lake in the Utah state of USA in many aspects of chemistry, sediments, and morphology. There are 102 islands in Urmia Lake. Among these 102 islands, Islamic island (Shahi Island) is the largest one and it is the only island having human population. The smallest island is known as Osman Yumrughu. Urmia Lake is an oligotrophic Lake of thalassohaline origin at an altitude of 1250 m above the sea level with an average depth of 6 m and a maximum depth of 16 m. Urmia Lake is divided into two parts including north and south parts separated by a causeway which has 1500 m bridge allows a little water exchange between two parts [4, 5, 6]. Figure 3.2 and 3.4 show the causeway.

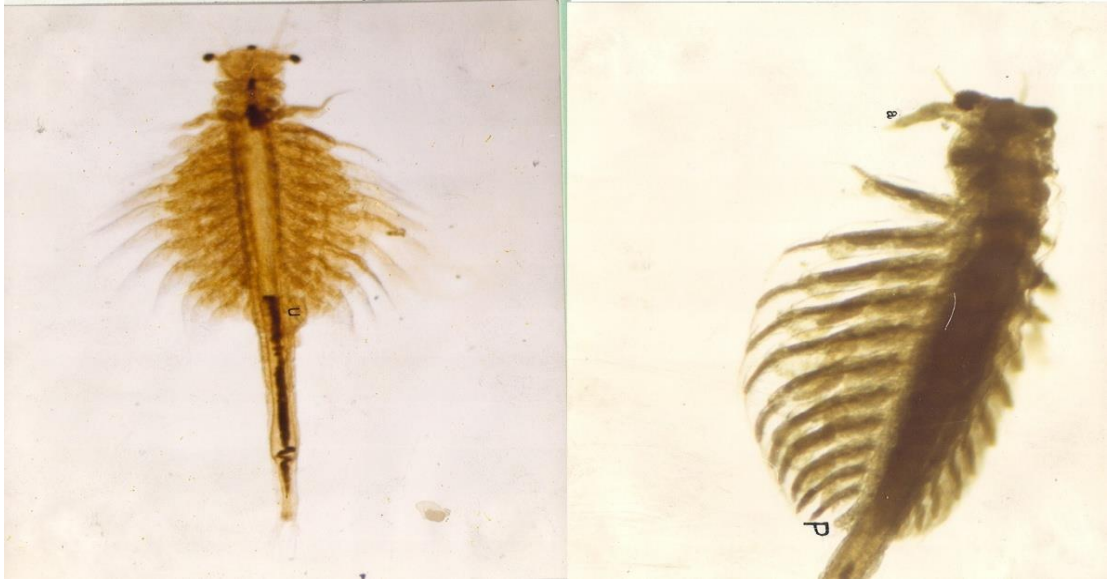


**Figure 3.1:** Female *Artemia Urmiana* (Left) – Male *Artemia Urmiana* (Right) –  
Photo from Artemia Research Center of Urmia University.



**Figure 3.2 :** Shahid Kalantari causeway on Urmia Lake – Photo taker is unknown –  
1990 decade.



**Figure 3.3** : Bridge that allows a little water exchange between 2 parts of Urmia Lake - Photo taken by Yusuf Alizade in land study – 2014-February.



**Figure 3.4** : Shahid Kalantari causeway on Urmia Lake - Photo taker and date are Unknown.

Urmia Lake's catchment area covers about 51876 km<sup>2</sup> including West Azerbaijan, East Azerbaijan and Kurdistan provinces of Iran. Total study area investigated in this research is about 90,000 km<sup>2</sup> including Urmia Lake's catchment area, and some parts of Turkey and Iraq. Figure 3.5 shows the interested study area. The catchment area contains 21 permanent and ephemeral streams together with 39 episodic rivers. Urmia Lake is home to some 212 species of birds, 41 reptiles, 7 amphibians, and 27 species of mammals, including the Iranina yellow deer. It is an internationally registered protected area as both a UNESCO Biosphere Reserve and a Ramsar site. The Iranian Department of Environment has designated most of the lake as a "National Park" [4, 7, 18].

Due to the establishment of different dams on contrary rivers which supply Urmia Lake's water, the establishment of more than 80,000 wells in Urmia Lake's catchment area, increased demands for irrigation in the Lake's basin, temperature and precipitation changes, and drought, the salinity of the lake has risen remarkably during recent years and as a result, the large areas of the lake bed have been desecrated. There are two important points that should be emphasized for the temperature and precipitation change impacts on Urmia Lake and its vicinity. Firstly, the annual amount of water the lake receives has significantly decreased as a result of establishment of dams, wells, and drought. This in turn has increased the salinity of the lake's water and led to lowering the lake viability as home to thousands of migratory birds including the large flamingo populations and diminishing other assets especially *Artemia Urmiana*. Secondly, it is also important to consider the results of drying Urmia Lake and its risks on human life and ecosystem in Iran and neighbor countries of Urmia Lake. Drying of Urmia Lake will impact the local and regional climate of the area and this will have severe impacts on human and environment. Hotter temperature values and water shortage as a result of complete drying of Urmia Lake may even cause diseases and migration of local people. A similar example to Urmia Lake case is Aral Sea and its vicinity, therefore lessons learned from the Aral Sea case should be taken into account for the protection of Urmia Lake [6, 11, 19].

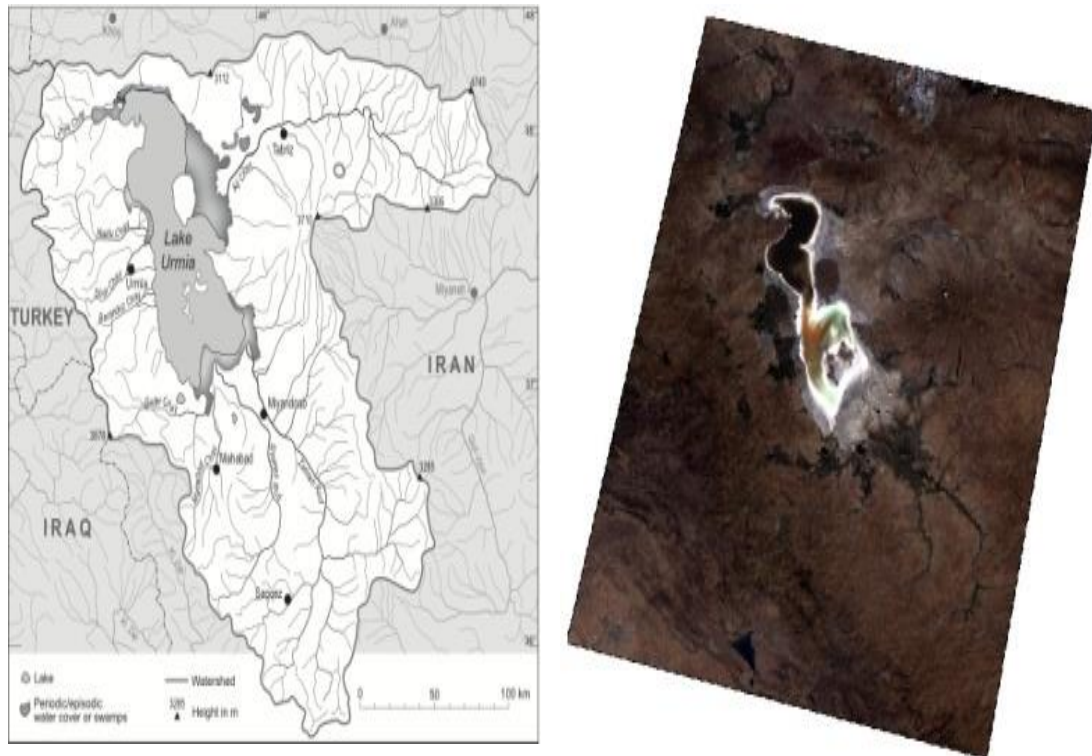


**Figure 3.5 :** Urmia Lake’s catchment area with rivers and streams (Left). Study area Landsat-8 – 2013-Summer – Mosaic of 6 frames (Right).

### 3.2 Satellite Images

#### 3.2.1 Landsat-5 Thematic Mapper (TM)

Landsat-5 is the American earth land resource satellite and launched in 1984.03.01. Landsat-5 was launched into repetitive, circular, sun-synchronous, near-polar orbits. However, these orbits were lowered on 705 km. Landsat-5 orbits have an inclination angle of  $98.2^\circ$  ( $8.2^\circ$  from normal) with respect to the equator. The satellite crosses the equator on the north-to-south portion of each orbit at 9:45 A.M. local sun time. Each orbit takes approximately 99 min, with just over 14.5 orbits being completed in a day. There is in a 16-day repeat cycle for each satellite[12, 20].

Landsat-5 includes both the Multi Spectral Scanner (MSS) and the TM (Thematic Mapper). The MSS onboard Landsat-5 is essentially identical to the MSS sensors on the previous Landsat satellites. The across track swath of 185 km has been maintained at the lower orbit altitude by increasing the total field of view to  $14.92^\circ$  (from  $11.56^\circ$  on previous systems). The optics of the MSS approximates the 79-m-ground-resolution cell of the previous systems. The same four spectral bands are

used for data collection, but they have been renumbered. That is, bands 1 to 4 of the Landsat-4 and -5 MSS correspond directly to bands 4 to 7 of the previous MSS systems [12,20].

The TM is a highly advanced sensor incorporating a number of spectral, radiometric and geometric design improvements relative to the MSS. Spectral improvements include the acquisition of data in seven bands instead of four, with new bands in the visible (blue), mid-IR, and thermal portions of the spectrum based on experience with MSS data and extensive field radiometer research results, the wavelength range and location of the TM bands have also been chosen to improve the spectral differentiability of major earth surface features. Radiometrically, the TM performs its onboard A-to-D signal conversion over a quantization range of 256 digital numbers (8 bits). Geometrically, TM data are collected using a 30-m-ground-resolution cell (for all but the thermal band, which has 120 m resolution). The scene size of Landsat-TM5 is 170 km \* 185 km. Normal operations for the Landsat 5 Thematic Mapper (TM) ceased in November 2011[12, 20, 53].

**Table 3.1** : Spectral and spatial information about Landsat TM.

Landsat 4-5	Wavelength (micrometers)	Resolution (meters)
Band1-Blue	0.45-0.52	30
Band2-Green	0.52-0.60	30
Band 3- Red	0.63-0.69	30
Band 4- NIR	0.76-0.90	30
Band 5- SWIR 1	1.55-1.75	30
Band 6- Thermal	10.40-12.50	120*(30)
Band 7- SWIR 2	2.08-2.35	30

\*TM Band 6 was acquired at 120-meter resolution, but products processed before February 25, 2010 are resampled to 60-meter pixels. Products processed after February 25, 2010 are resampled to 30 meter pixels.

At the beginning of the study, all available Landsat-4 and -5 TM data acquired between 1984 and 2011 was analyzed to choose the most appropriate data set for

this research. Finally, 80 Landsat-5 TM level-1 frames were chosen to be used in this study in order to investigate changes on Urmia Lake and its catchment area. Landsat frames acquired in summer time of (June, July, August) 1984, 1987, 1990, 1995, 1998, 2000, 2006, 2007, 2009, 2010, and 2011 and spring time of (April, and May) 1987, 1998, 2007 were used. At least 3 Landsat-5 frames are needed to cover Urmia Lake surface area and at least 6 Landsat-5 frames are needed to cover the Lake's catchment area. All Landsat-5 TM data used were georeferenced into UTM projection.

### 3.2.2 UK-DMC (United Kingdom-Disaster Monitoring Constellation)

The Disaster Monitoring Constellation (DMC) is an international program initially proposed in 1996 and led by SSTL (Surrey Satellite Technology Ltd), Surrey, UK, to construct a network of five affordable Low Earth Orbit (LEO) microsattellites. The objective is to provide a daily global imaging capability at medium resolution in 3-4 spectral bands, for rapid-response disaster monitoring and mitigation. The DMC provides emergency Earth imaging for disaster relief under the International Charter for Space and Major Disasters, which the DMC formally joined in November 2005. DMC provides wide-swath multispectral imagery at higher resolutions (660 km swath with 22 m pixel size at nadir) and the maximum image size is about 444,000 km<sup>2</sup>. DMC has 3 bands including NIR (band 1), Red (band 2), and Green (band 3). Two DMC images of 2011- April, and 2012-July were used in this research to investigate up to date surface conditions in Urmia Lake and its catchment area [21,50,56,57].

**Table 3.2 :** Spectral and spatial information about DMC.

DMC	Wavelength (micrometers)	Resolution (meters)
Green	0.52-0.60	22
Red	0.63-0.69	22
NIR	0.77-0.90	22

### **3.2.3 Landsat-8**

Landsat-8 is the American satellite launched on 2013.02.11 by NASA. Landsat-8 was launched into repetitive, circular, sun-synchronous, near-polar orbits. However, these orbits were lowered on 705 km. Landsat-8 orbits have an inclination angle of 98.2° (slightly retrograde) with respect to the equator. The satellite crosses the equator on the north-to-south portion of each orbit at 10:00 a.m. +/- 15 minutes local sun time. Each orbit takes 98.9 minutes [53].

Landsat-8 has 2 sensors, including Operational Land Imager (OLI) and Thermal Infrared Sensor (TIRS). OLI sensor has 9 spectral bands, including a pan band and TIRS sensor has 2 spectral bands. The scene size of Landsat-8 is 170 km\*185 km. Geometrically, OLI data are collected using a 30-m-ground-resolution cell (for all but the panchromatic band, which has 15 m resolution). TIRS data also are collected using a 100-m-ground-resolution cell. The scene size of Landsat-TM5 is 170 km \* 185 km. Normal operations for the Landsat 5 Thematic Mapper (TM) ceased in November 2011[53].

All Landsat-8 data have been investigated and finally, 13 Landsat-8 level-1 frames were chosen for this study to conduct change detection on Urmia Lake and its catchment area. 12 frames were collected in spring and summer 2013 and one frame was collected in February 2014.



**Table 3.3 :** Spectral and spatial information about Landsat 8 Operational Land Imager (OLI) and Thermal Infrared Sensor (TIRS).

Landsat 4-5	Wavelength (micrometers)	Resolution (meters)
Band1-Coastal	0.43-0.45	30
Band2-Blue	0.45-0.51	30
Band 3-Green	0.53-0.59	30
Band 4-Red	0.64-0.67	30
Band 5-NIR	0.85-0.88	30
Band 6-SWIR 1	1.57-1.65	30
Band 7-SWIR 2	2.11-2.29	30
Band 8-Panchromatic	0.50-0.68	15
Band 9- Cirrus	1.36-1.38	30
Band 10-TIRS 1	10.60-11.19	100*(30)
Band 11-TIRS 2	11.50-12.51	100*(30)

\*TIRS bands are acquired at 100 meter resolution, but are resampled to 30 meter in delivered data product.

### 3.3 Meteorological Data

The meteorological data (temperature, precipitation, and humidity,) contain measurements at 20 synoptic weather stations located around Urmia Lake in both West Azerbaijan and East Azerbaijan provinces of Iran cover a time which satellite images were taken (Figure 3.6). Exact collection dates vary by weather stations. These data were used to find out meteorological changes around Urmia Lake. The graphs of 5 near synoptic stations to Urmia Lake are available in this study and geostatistics analyze were done for all stations between 2000 and 2011 considering the total number of data collected from these stations. Before 2000, it was not

possible to collect continuous data for all stations. Tale 3.4 summarizes location and names of meteorological stations in the catchment area.

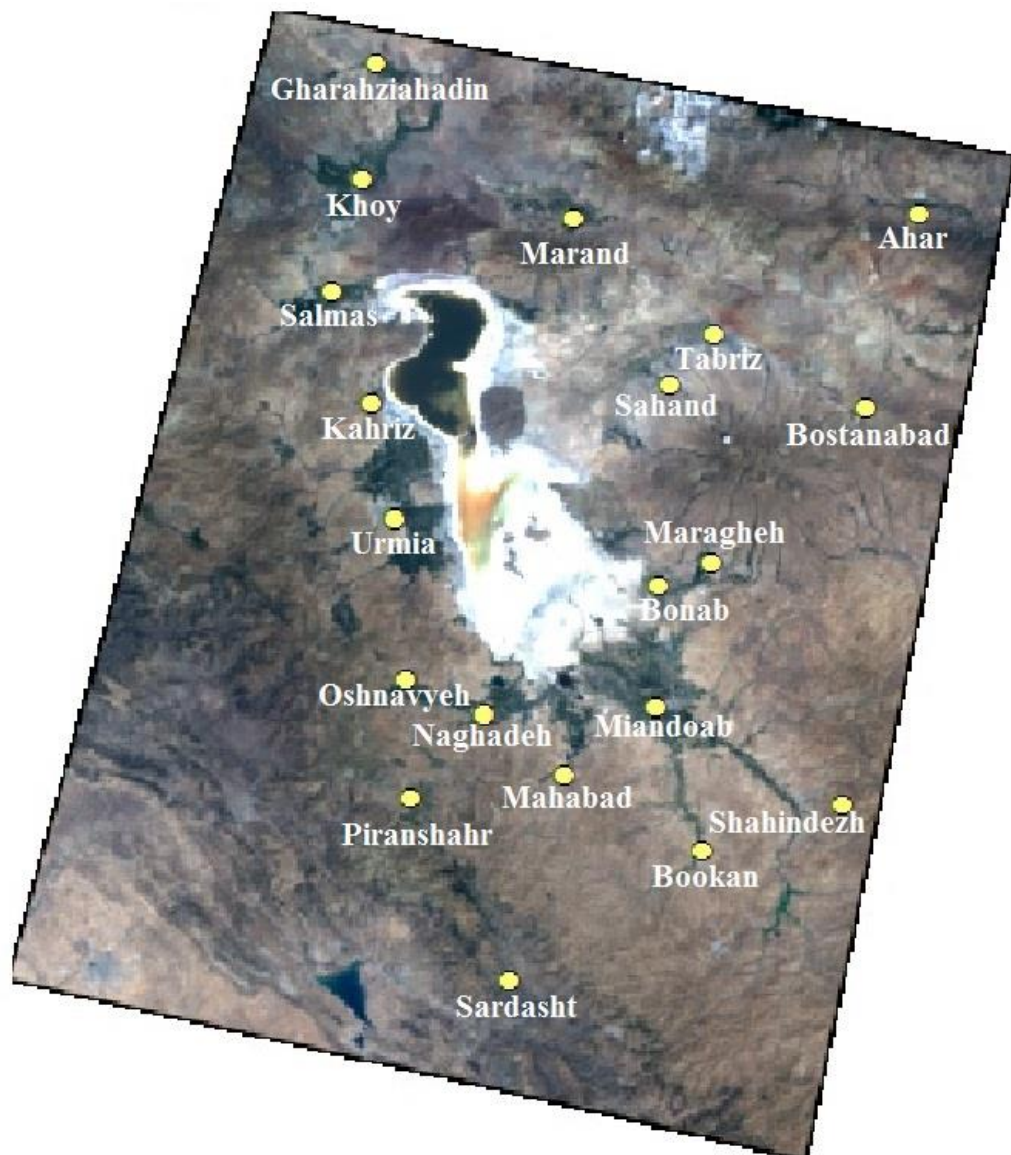


**Figure 3.6 :** Meteorological Stations around Urmia Lake – Landsat-8 – mosaic of 6 frames – 2013-summer.

**Table 3.4 : Meteorological Stations.**

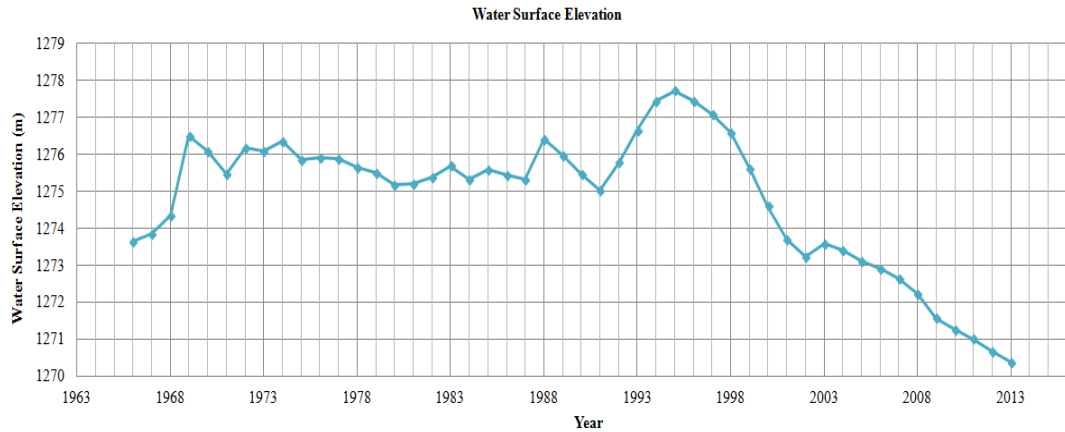
Name	Longitude	Latitude	Elevation (m)
Gharaziyaadin	45° 01'	38° 54'	1108
Khoy	44° 58'	38° 33'	1103
Salmas	44° 51'	38° 13'	1337
Kahriz	45° 10'	37° 53'	1325
Urmia	45° 03'	37° 40'	1315.9
Oshnaviyeh	45° 08'	37° 03'	1415.9
Naghadeh	45° 25'	36° 57'	1338
Piranshahr	45° 09'	36° 42'	1443.5
Sardasht	45° 30'	36° 09'	1670
Mahabad	45° 43'	36° 46'	1385
Bookan	46° 13'	36° 32'	1386.1
Shahindej	46° 44'	36° 40'	1395
Miyandoab	46° 03'	36° 58'	1300
Maragheh	46° 16'	37° 24'	1344
Bonab	46° 04'	37° 20'	1290
Bostanabad	46° 51'	37° 51'	1750
Sahand	46° 07'	37° 56'	1641
Tabriz	46° 17'	38° 05'	1364
Marand	45° 46'	38° 26'	1550
Ahar	47° 04'	38° 26'	1391

### **3.4 Landuse Maps**

Landuse maps provide information about the application of different kinds of Earth's terrestrial according to its use. There are a number of different applications for such maps, and in many nations, land use maps are prepared by several government agencies. Individual groups and organizations can also generate maps with land use information. There are different methods to create land-use maps like remote sensing and Land survey. Landuse maps are applied for different aims like marking out areas designated for specific types of land use or how land is being used. Therefore, people developing land know which kinds of uses will be allowed and it can be determined whether or not zoning changes need to be made[61]. Land-use maps of West Azerbaijan and East Azerbaijan provinces which were prepared between the years 2000-2003 were used in this study to conduct spatial analysis in GIS for Urmia Lake's catchment area. Landuse maps which were used in this study include 9 classes; range, irrigated farming, dry farming, forest, no suitable range, urban, Urmia Lake, saline soil, and scattered dry farming. Water surface area of Urmia Lake is also about 4595 km<sup>2</sup> according to these maps.

### **3.5 Water Surface Elevation**

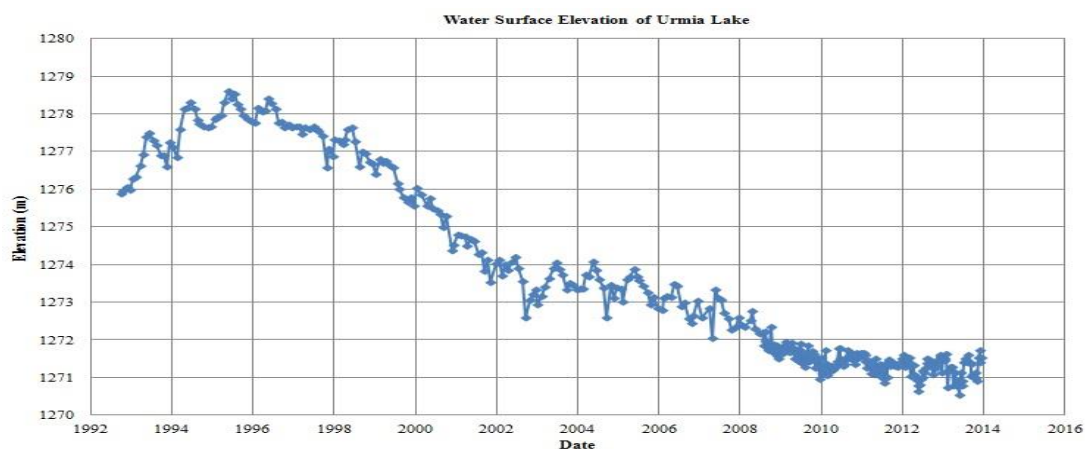
Water surface elevation of Urmia Lake is available from 1966 to 2013 and it was measured in 15<sup>th</sup> November of each year. This data were provided by the Energy Ministry of Iran during last 47 years. Environmental Protection Office of West Azerbaijan offered this data to researcher to analyze changes in Urmia Lake. According to figure 3.7 water surface elevation of Urmia lake was about 1273.64 m in 1966 and this year had the minimum amount of water surface elevation between 1966 to 2000. Then, it increased during 1966 to 1969 and there were no considerable changes in water surface elevation of Urmia Lake until 1988. Water surface elevation of Urmia Lake decreased from 1988 to 1991 and then it increased to its highest value in 1995 about 1277.71 m. Water surface elevation of Urmia Lake decreased from 1995 to 2013 to its lowest value in 2013 about 1270.37 m. In other words, the difference between maximum and minimum value of water surface elevation in 1995 and 2013 was 7.34 m during the last 20 years.



**Figure 3.7 :** Water surface elevation of Urmia Lake – November.

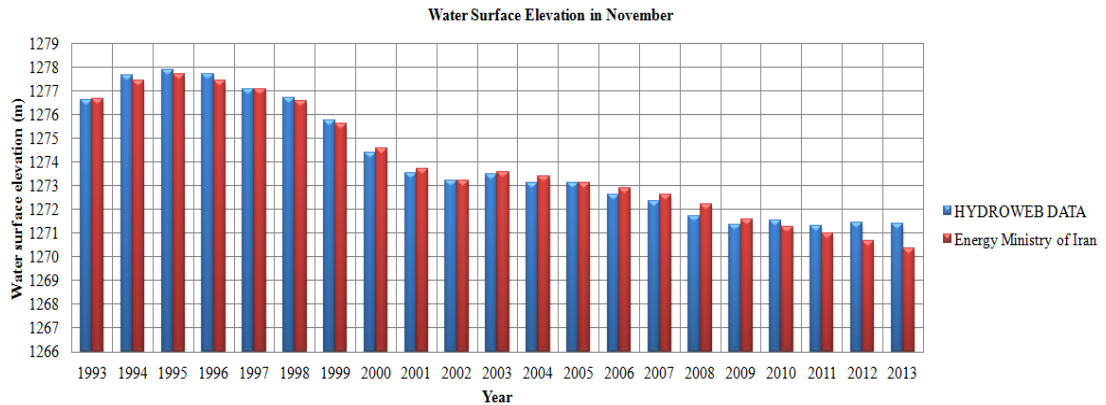
### 3.6 HYDROWEB Data

HYDROWEB provides useful information about water bodies such as rivers and lakes around the world using satellite imagery. Water level variation, surface variation, and volume variation of Urmia Lake were provided from HYDROWEB and direct contact with Jean-Francois, who is the head of the research team about Urmia Lake[60]. Figure 3.8 shows the water level variation of Urmia Lake from 1993 to 2013 in different seasons of each year. According to this figure water level of Urmia Lake decreased from winter to summer of each year. Water surface elevation of Urmia Lake increased from 1993 to 1995 to its highest value in 1995-May about 1278.60 m and then it decreased from 1995 to 2013 to its lowest value 1270.53 m in 2013-May. In other words, the difference between maximum and minimum value of water surface elevation was 8.07 m during the last 20 years.



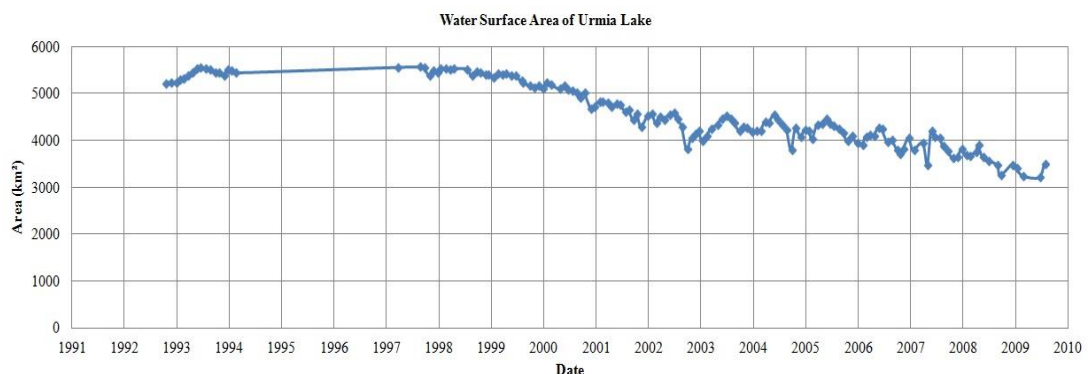
**Figure 3.8 :** Water level variation of Urmia Lake.

Figure 3.9 shows the results of water surface elevation changes calculated by Energy Ministry of Iran in November from 1993 to 2013 and water surface elevation variations of HYDROWEB database in November from 1993 to 2013. According to this figure the results of both references are very close to each other. The minimum difference is about 1 cm in 1997 and the maximum difference is 102 cm in 2013.



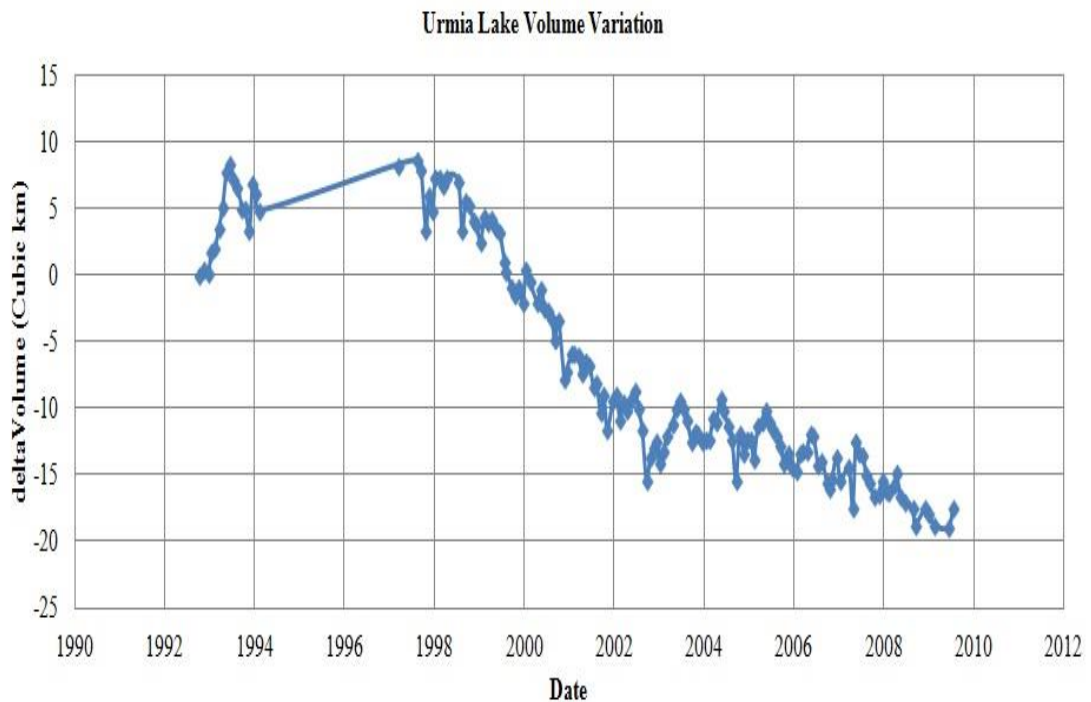
**Figure 3.9 :** Comparing water level variations of HYDROWEB database and water surface elevation variations of Energy Ministry of Iran in November.

Figure 3.10 shows water surface variation of Urmia Lake using HYDROWEB database in different seasons from 1993 to 2009 which is observed with optical and radar imagery. There were missing data in 1995 and 1996 years and the water surface area of Urmia Lake didn't calculate between 1995 and 1996. According to this figure water surface area of Urmia Lake increased from 1993 to 1998 and then it decreased from 1998 to 2013. The maximum area was about 5572 km<sup>2</sup> in 1997-Summer and the minimum area was about 3359 km<sup>2</sup> in 2009-Summer.



**Figure 3.10 :** Water surface variation of Urmia Lake.

Figure 3.11 shows volume variation of Urmia Lake using HYDROWEB database in different seasons between 1993 and 2009. Water level and surface variations are combined to estimate the total volume variation. There were no data during 1995 and 1996 and the volume variation of Urmia Lake didn't calculated during these years. The volume of Urmia Lake increased from 1993 to 1998 and then it decreased from 1998 to 2009.



**Figure 3.11 :** Volume variation of Urmia Lake.

### 3.7 Dams

Urmia Lake's catchment area contains together 21 permanent and ephemeral streams together with 39 episodic rivers. There are thirteen main rivers in the lake basin named; Jighati (Zarrinerood), Tatau (Siminerood), Soyugh Bulagh chay (Mahabad), Gadar chay, Baranduz chay, Shahar chay, Roze chay, Nazlu chay, Zola chay, Tasuj chay, Aji chay, and Sufi chay. Jighati, Tatau, and Aji Chay all together provide about 42% of Urmia Lake's entrance water. Jighati and Tatau are located in the south part of Urmia Lake and Aji Chay is located in the northeast part of Urmia Lake. Aji Chay brings salty solute along its way to Urmia Lake and it is one of the reasons that the water of Urmia Lake is salty. Among mentioned rivers Jighati is the largest river with a total annual discharge value of about  $2 \times 10^9$  m<sup>3</sup>. Annual inflow into the lake is

6900\*10<sup>6</sup> m<sup>3</sup> provided from 4 sources including rivers, flood water (through rainfall), precipitation, and underground water. 4900\*10<sup>6</sup> m<sup>3</sup> is from rivers, and 2000\*10<sup>6</sup> m<sup>3</sup> from other resources like flood water, precipitation, and underground water. The exact volume of underground springs is not known but underground water sources play an important role in developing irrigation in Urmia Lake's catchment area as dams[4,5,22].

Figure 3.12 shows the total inflow into the lake from different sources. According to this figure, rivers account for nearly 75% of the total inflow to the lake and other sources, including flood water, precipitation, and underground water account for the remaining 25%. Rivers situation can be divided into 4 parts (East, West, Southwets, and South-southeast) by considering the position of Urmia Lake. Aji Chay, Azarshahr Chay, Ghale Chay, and Sufi Chay inflow into lake from east part. Jighati Chay and Leylan inflow to Lake from south-southeast parts. Tatau, Godar Chay, and Mahabad Chay inflow to the lake from southwets part and Nazlu Chay, Roze Chay, Shahr Chay, Baranduz Chay, and Zola Chay inflow to the lake from west part[4,5,22].

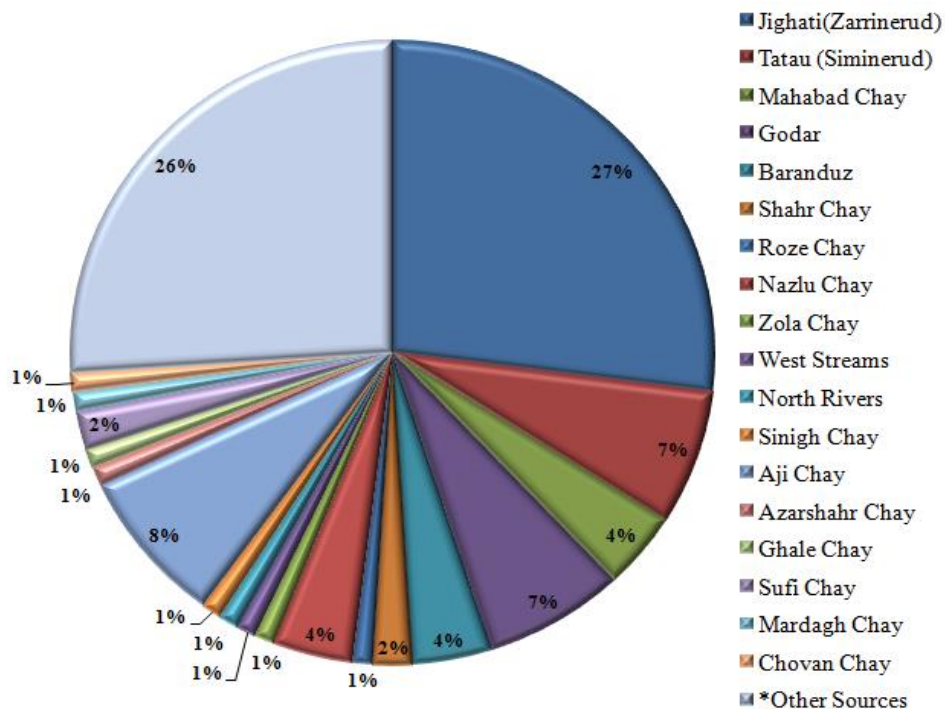


**Figure 3.12 :** Total inflow from rivers and other sources to Urmia Lake. \*Other sources include flood water, precipitation, and underground water.



There are totally 103 dams in both West Azerbaijan and East Azerbaijan provinces. 56 of these dams are located in the Urmia lake's catchment area. 14 dams were established until 1990, and 10 dams were constructed between 1990 and 2000, finally 32 dams were built up from 2000 to 2014. Moreover, there are many dams in the region, which are under construction or study stage. Many of these dams were established for agricultural aims and these dams play a critical role in developing agriculture areas in Urmia Lake's catchment area[58].

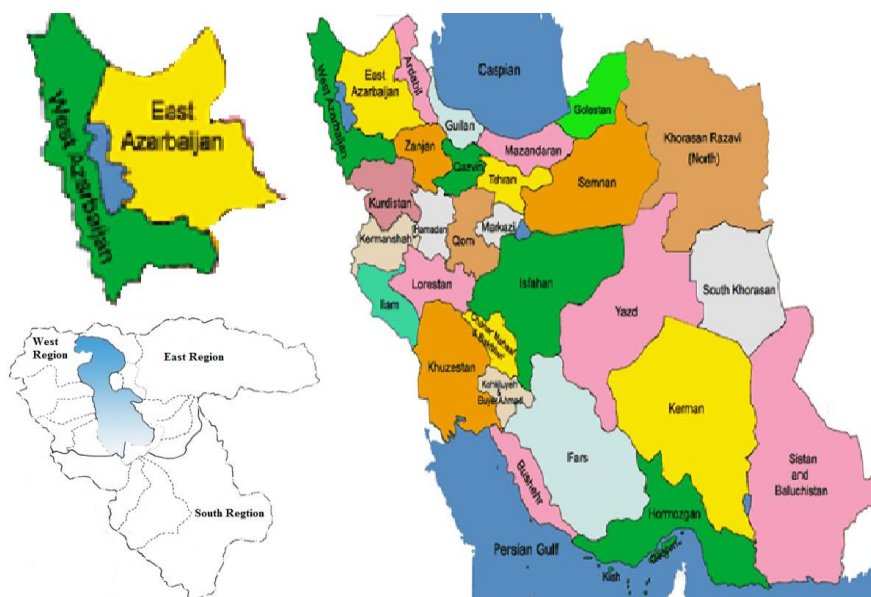


**Figure 3.13 :** Urmia Lake's position in Iran.

Table 3.5 shows the amount of annual adjustable water, agricultural water consumption and drinking water consumption in West Azerbaijan, East Azerbaijan, and Urmia Lake's catchment area[58].

**Table 3.5 :** Water consumption (million m<sup>3</sup>) of dams.

Number of Dams	Annual Adjustable Water (million m <sup>3</sup> )	Agriculture water consumption (million m <sup>3</sup> )	Drinking water consumption (million m <sup>3</sup> )
*84	627.96	405.13	38
**19	1766.22	1237.68	357.04
***56	2060.30	1320.28	389.04

\*East Azerbaijan, \*\*West Azerbaijan, \*\*\*Urmia Lake's catchment area

Table 3.6 shows the cultivation area and annual power generation from dams which are located in West Azerbaijan, East Azerbaijan, and Urmia Lake's catchment area[58].

**Table 3.6 : Cultivation area using Dams.**

Number of Dams	Cultivation area (Hectare)	Annual power generation (gigawatt-hour)
*84	70319	-
**19	157690	80.20
***56	192648	80.20

\*East Azerbaijan, \*\*West Azerbaijan, \*\*\*Urmia Lake's catchment area

### 3.8 Underground Water Resources

There are many irrigation areas in Urmia Lake's catchment area and the need for irrigating these areas is provided from two important sources including dams and underground water sources. Underground water sources are divided into four parts including deep wells, semi deep wells, aqueduct, and water fountains. Discharge water from underground water sources is available for 40 years from 1972 to 2012[61]. Total discharge of underground water sources is according to figure 3.14. Figures 3.15 and figure 3.16 show total discharge water from deep wells and semi deep wells. Figure 3.17 and 3.18 show total discharge water from aqueduct and water fountains. Total discharge water from deep wells is more that other types of underground water sources.

According to figure 3.14 discharge water from underground water sources was 1534 million m<sup>3</sup> from 1984 to 1985 with an increase to 2156 during 2011 to 2012. Moreover, discharge water from underground water sources increased by 400 million m<sup>3</sup> alone from 1998 to 1999. According to the available statistics from underground water sources between 1972 and 2012, there were totally 74336 semi deep wells and 8047 deep wells in Urmia Lake's catchment area in 2012.

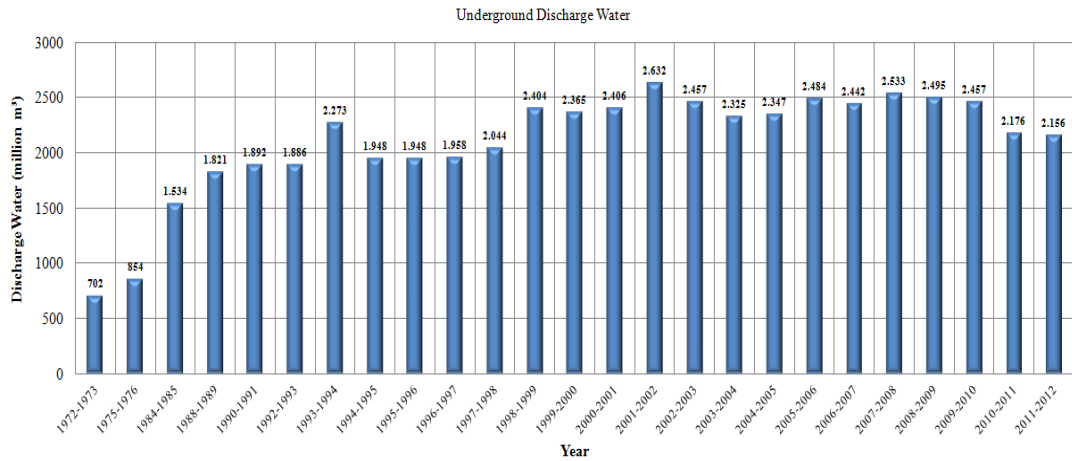


**Figure 3.14 :** Total discharge water from underground resources.

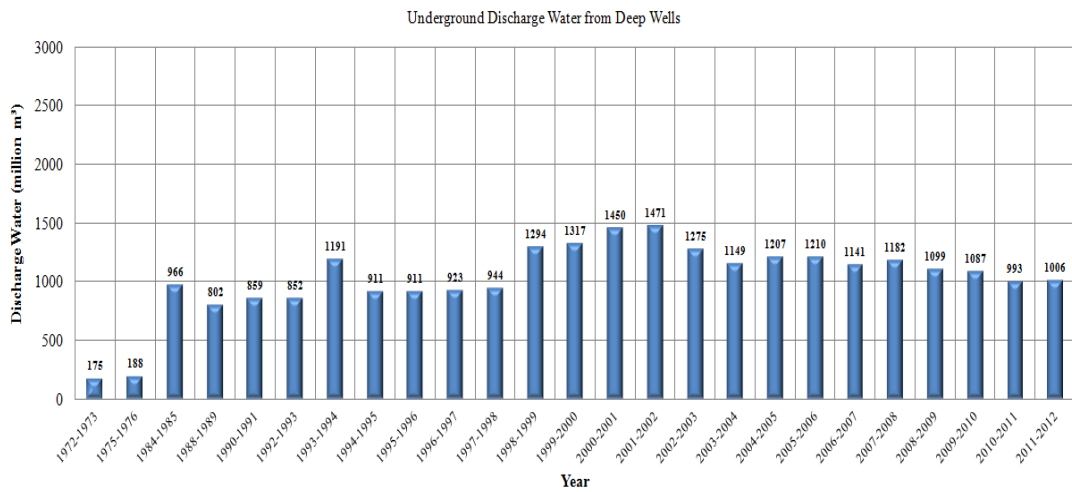


**Figure 3.15 :** Discharge water from deep wells.

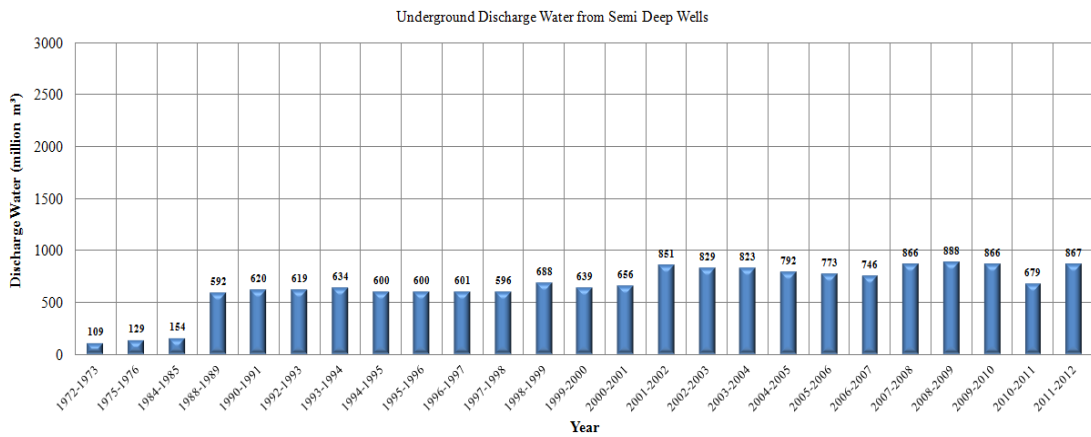


**Figure 3.16 :** Discharge water from semi deep wells.

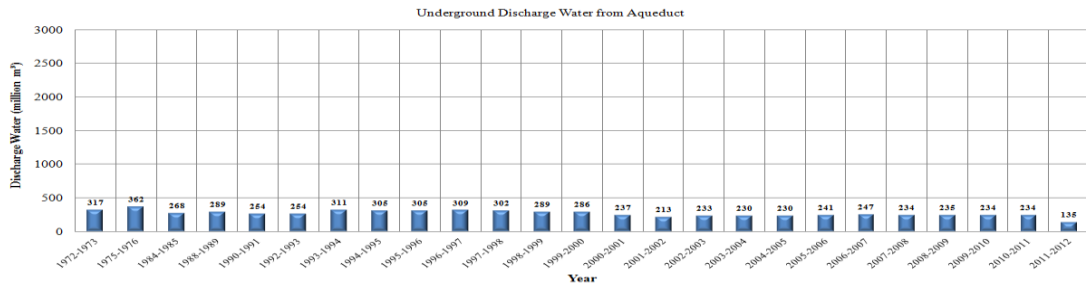


**Figure 3.17 :** Discharge water from aqueduct.

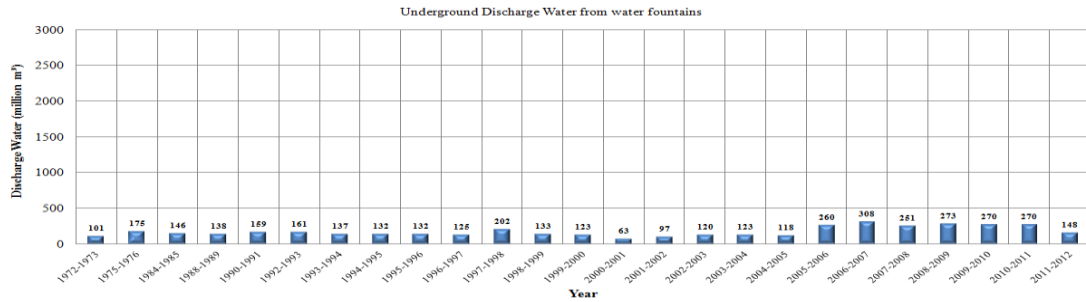


**Figure 3.18 :** Discharge water from water fountains.

### 3.9 Population

According to table 3.7, the population of both West Azerbaijan and East Azerbaijan provinces has been available for the last 25 years from 1985 to 2010[62]. Rural population increased about 112.085 from 1985 to 1990 and urban population increased about 401282 during this time. Then, rural population decreased about 378982 from 1990 to 2010 and urban population increased about 1,621,252 during this time. In total, rural and urban population of both West Azerbaijan, and East Azerbaijan increased about 1,755,637 from 1985 to 2010 by considering that urban population has increased 2,022,534 during this time and rural population decreased about 266,897 during this time.

**Table 3.7 :** Population (million) of both West Azerbaijan and East Azerbaijan.

Year	Urban Population	Rural Population	Total Population
1985	2489188	2560371	5049559
1990	2890470	2672456	5562926
1995	3319645	2502215	5821860
2005	4127493	2349422	6376915
2010	4511722	2293474	6805196

## **4. IMAGE PROCESSING TECHNIQUES AND DATA ANALYSIS**

Remotely sensed data usually contains geometric, radiometric and other distortions due to the sensor instabilities, topography, sensor viewing geometry, etc. Therefore, it is crucial to conduct corrections and preprocessing on remotely sensed data.

Most of the common image processing functions available in image interpretation systems include the following four categories:

- 1) Preprocessing
- 2) Image Enhancement
- 3) Image Transformation
- 4) Image Classification and Interpretation

The pre-processing techniques means removing or minimizing of data errors or unwanted or distracting elements of the image. It is noticeable data errors such as missing scan lines cannot be removed because the data in error are simply replaced with some other data that are felt to be better estimates of the true but unknown values.

### **4.1 Preprocessing**

Preprocessing step includes radiometric calibration, Atmospheric corrections, topographic corrections, geometric corrections (Rectification and orthorectification). Calibration and instrument characterization which are usually available in Metadata are essential for any satellite or airborne remote sensing device. The main fundamental aspects that need to be calibrated are the sensor system's response to electromagnetic radiation as a function of

- Wavelength and/or spectral band (spectral response).
- The intensity of the input signals (radiometric response).

- Different locations across the instantaneous field of view and/or the overall scene (spatial response or uniformity).
- Different integration times and lens or aperture settings.
- Unwanted signals such as stray light and leakage from other spectral bands[23,24].

#### 4.1.1 Radiometric Calibration

Radiometric calibration is a process that converts recorded sensor voltages or digitized counts to an absolute scale of radiance that is independent of the image forming characteristics of the sensor. In this process data for sensor irregularities and unwanted sensor or atmospheric noise be corrected and data be converted so they accurately represent the reflected or emitted radiation measured by the sensor. There are two kinds of radiometric calibration, Absolute and Relative. Absolute calibration, is performed by use of standard equations to convert DNs to at-satellite reflectance. Relative calibration is determined by normalizing the outputs of the detectors to a given, often average, output from all the detectors in the band[23,25].

In this process first of all images are converted to at-satellite radiance using Eq. (4.1)

$$L_{Sat} = \frac{DN-B}{G} \quad (4.1)$$

Where  $L_{Sat}$  is at-satellite spectral radiance ( $w m^{-2} sr^{-1} \mu m^{-1}$ ), DN is digital number, B is bias in DN, and G is band specific gain ( $m^2 sr \mu m w^{-1}$ )

In Landsat-5 images DNs can be converted to radiance values using Eq. (4.2)

$$L_{Sat} = \left[ \frac{LMAX_{Sat}-LMIN_{Sat}}{DNMAX-DNMIN} \right] * (DN - DNMIN) + LMIN_{Sat} \quad (4.2)$$

Where  $LMAX_{Sat}$  is radiance scaled to  $DNMAX$  ( $w m^{-2} sr^{-1} \mu m^{-1}$ ),  $LMIN_{Sat}$  is radiance scaled to  $DNMIN$  ( $w m^{-2} sr^{-1} \mu m^{-1}$ ),  $DNMAX$  is maximum quantized calibrated digital number, and  $DNMIN$  is minimum-quantized calibrated digital number. After conversion DNs to at-satellite radiance, to further correct for scene-to-scene differences in solar illumination, it is useful to convert each image to at-satellite reflectance (assuming a uniform Lambertian surface under cloudless

conditions) Using Eq. (4.3). The term “at-satellite” refers to the fact that this conversion does not account for atmospheric influences.

$$\rho_{ASR} = \frac{((\pi * L_{Sat}) * d^2)}{(E_0 * \cos(\theta))} \quad (4.3)$$

Where  $\rho_{ASR}$  is at-satellite reflectance,  $E_0$  is exoatmospheric solar constant ( $W m^{-2} \mu m^{-1}$ ) (corrected for solar distance), and  $\theta$  is solar zenith angle, and  $d$  is Earth-sun distance in astronomical units, ranges from approx. 0.9832 to 1.0167 (earth-sun distance for the imagery acquisition date). It should be considered that by definition, at-satellite reflectance does not remove atmospheric effects [23, 24, 25].

#### 4.1.2 Atmospheric Correction

Atmospheric correction consists of two major steps: atmospheric parameter estimation and surface reflectance retrieval. Atmospheric effects include molecular and aerosol scattering and absorption by gases, such as water vapor, ozone, oxygen, and aerosols. There are 2 atmospheric correction techniques, absolute and relative. At-satellite reflectance is converted to surface reflectance in full absolute correction. For full absolute correction, at-satellite reflectance is converted to surface reflectance using Eq. (4.4) :

$$\rho = \frac{\pi(L_{Sat} - L_P)}{T_v(E_0 * \cos(\theta) * T_z + E_{down})} \quad (4.4)$$

Where  $\rho$  is estimated surface reflectance,  $L_P$  is path radiance ( $W m^{-2} sr^{-1} \mu m^{-1}$ ),  $T_v$  is atmospheric transmittance from the target toward the sensor,  $T_z$  is atmospheric transmittance in the illumination direction, and  $E_{down}$  is downwelling diffuse irradiance ( $W m^{-2} \mu m^{-1}$ ).

Absolute removal of all atmospheric influences is difficult and requires a number of assumptions, additional ground and/or meteorological reference data and sophisticated software. Relative correction takes one band and/or image as a baseline and transforms the other bands and/or images to match. Absolute Techniques include Radiative Transfer Based Models (ACORN, ATCOR2, ATCOR3, ATREM, and FLAASH) and empirical line calibration. Relative Techniques include Dark Object Subtraction (DOS), modified dense dark vegetation (MDDV), and second simulation of the satellite signal in the solar spectrum. These methods range in complexity from

a simple image-based correction procedure (DOS) to a detailed, theoretical model based on radiative transfer theory [23, 24, 25]. ATCOR2 method was used in this study to obtain surface reflectance values.

#### **4.1.3 Topographic Correction**

Topographic correction or topographic normalization refers to the compensation of the different solar illuminations due to the irregular shape of the different solar illuminations due to the irregular shape of the terrain. This effect causes shaded areas show less than expected reflectance, whereas in sunny areas the effect is the opposite. Therefore, the topographic correction may be critical in areas of rough terrain, as a preliminary step of the multispectral and for multitemporal digital classification of vegetation types. Topographic correction over mountain regions or areas of rough terrain is at least as important as atmospheric correction. The aim of this correction is to remove all topographically induced illumination variation so that two objects having the same reflectance properties show the same brightness value in the image despite their different orientation to the sun's position. Topographic correction requires high-resolution, and accurate digital elevation model (DEM) data, which are not available globally [23, 26].

#### **4.1.4 Geometric Correction**

All remotely sensed data have different types of geometric distortions. These distortions may be due to several factors, including the motion of the scanning system, the motion of the platform, the platform altitude, attitude, and velocity, the terrain relief, and the curvature and rotation of the Earth, and the perspective of the sensor optics. The sources of distortion can be grouped into two broad categories: the observer or the acquisition system (platform, imaging sensor and other measuring instruments, such as gyroscopes, stellar sensors, etc.) and the observed (atmosphere and Earth). Geometric corrections are intended to compensate for these distortions and due to these corrections geometric representation of the imagery will be as close as possible to the real world. Different models and mathematical functions like 2D/3D empirical models (such as 2D/3D polynomial or 3D rational functions, RFs) or with rigorous 2D/3D physical and deterministic models are required to perform geometric corrections of imagery. The 2D/3D empirical models do not require a



priori information of any component of the total system and they do not reflect the source of distortions. When the parameters of the acquisition systems or a rigorous 3D physical model are not available, the 2D/3D empirical models have been used. 2D models do not use elevation information, and the accuracy of the results is depended on the image viewing angle and the terrain relief. 3D models are used to account the elevation distortion; therefore a DEM is needed to create precise orthorectified images [23, 24, 27].

#### **4.1.5 Classification**

In pixel based image classification step spectral information represented by the digital numbers in one or more bands are used to classify each individual pixel based on the spectral information. Depending on the type of information needed to extract from the original data, classes may be associated with known features on the ground or may simply represent areas that look different to the references.

An example of a classified image is a land cover map, showing vegetation, bare land, pasture, urban, etc. There are two classification methods, supervised classification and unsupervised classification. Supervised classification is closely controlled by the analyst. In this process, the analyst select training areas represent different patterns or land cover features to be input for the supervised classification algorithm. Aerial photos, ground truth data or maps could be used for the selecting of training areas. Unsupervised classification is more computer-automated. This method enables the analyst to specify some features to be used for the clustering algorithm based on statistical patterns included in the data. Unsupervised classification is dependent on the data itself for the definition of classes. This method requires less knowledge about the study area since there is not a training area selection step[20,24].

#### **4.2 Normalized Difference Vegetation Index (NDVI)**

Normalized Difference Vegetation Index (NDVI) is an index derived from red and infrared bands of remotely sensed images, giving information about the spatial distribution and condition of vegetated areas. The formula for NDVI is according to Eq. (4.5) [28, 29] :

$$NDVI = \frac{\rho_{IR} - \rho_{Red}}{\rho_{IR} + \rho_{Red}} \quad (4.5)$$

Where  $\rho_{IR}$  stands for the reflectance value of infrared band and  $\rho_R$  stands for the reflectance value of the red band of the remote sensing system. NDVI values can be used to identify vegetated and non-vegetated areas in an image with respect to their values ranging from 1 to -1. Normalized Difference Vegetation Index (NDVIs) images were produced to monitor and analyze vegetation changes within the study area. NDVI values were different for water, salt, vegetation, and some other land cover types which provided useful land cover information about the lake and its surrounding. Water, snow, and ice typically have NDVI value less than 0, bare soils between 0 and 0.1, sparse vegetation such as shrubs and grasslands or senescing crops between 0.2 and 0.5 and dense vegetation such as that found in temperate and tropical forests or crops at their peak growth stage between 0.6 and 1. The pigment in plant leaves, chlorophyll, strongly absorbs radiation in the red and blue wavelengths, but reflects green wavelengths resulting in green leaves for healthy vegetation. The cell structure of the leaves, on the other hand, strongly reflects in near-infrared wavelengths (from 0.7 to 1.1  $\mu\text{m}$ ). High absorbance of energy by water in the leaves impact the spectral reflectance of vegetation at 1.45-1.55  $\mu\text{m}$  and 1.90-1.95  $\mu\text{m}$  wavelengths. Leaf structure, maturation, water content and mesophyll arrangement impact the amount of spectral reflectance from different wavelengths for a selected vegetation type[28, 29,31].

### 4.3 Normalized Difference Water Index (NDWI)

Remote sensing of vegetation liquid water has important applications in agriculture and forestry. Normalized Difference Water Index (NDWI) is used for determination of vegetation water content (VWC) based on physical principles. The formula of this index for Landsat thematic mapper is according to Eq(4.6)

$$NDWI = \frac{\rho_{NIR} - \rho_{SWIR}}{\rho_{NIR} + \rho_{SWIR}} \quad (4.6)$$

Where  $\rho_{SWIR}$  is the reflectance or radiance in a short wave infrared wavelength band and  $\rho_{NIR}$  is the reflectance or radiance in a near infrared wavelength band. For landsat-5 TM, NIR and SWIR correspond to bands 4 and 5 respectively, and for landsat-8, NIR and SWIR correspond to bands 5 and 6 respectively. NDWI does not

remove completely the background soil reflectance effects, similar to NDVI. NDWI values are between -1 and 1, minus values indicate dry vegetation types and positive values indicate green vegetation types. Higher NDWI value means higher percent of water in vegetation types [8, 30, 31].

By considering different formulas for NDWI, this index can also be used to identify water body's surface. Lei Ji et al (2009) used normalized difference water index (NDWI) according to Eq.(4.7) to distinct water body's surface.

$$NDWI = \frac{(Green - SWIR)}{(Green + SWIR)} \quad (4.7)$$

Spectral data obtained from a spectral library to simulate the satellite sensors Landsat ETM+, SPOT-5, ASTER, and MODIS, was used to calculate the simulated NDWI in this study.

Eq.(4.8) was used by McFeeters (1996) proposed to describe open water features.

$$NDWI = \frac{(\rho_{Green} - \rho_{NIR})}{(\rho_{Green} + \rho_{NIR})} \quad (4.8)$$

Where  $\rho_{Green}$  and  $\rho_{NIR}$  are the reflectance of green and NIR bands, respectively. McFeeters (1996) set zero as the threshold. That is, the cover type is water if  $NDWI > 0$  and it is non-water if  $NDWI \leq 0$ [8].

#### **4.4 Normalized Differential Salinity Index (NDSI) and Salinity Index (SI)**

Remote sensing is used as a valuable tool to analyze relevant data on soil salinity in the irrigated area. Salinity changes at the terrain surface can be detected from remotely sensed data either directly on bare soil, with salt specialized and crust, or indirectly through the biophysical characteristics of vegetation as there are affected by salinity. Soil Salinity refers to the state of accumulation of the soluble salts in the soil. It can be determined by measuring the electrical conductivity of a solution extracted from a water-saturated soil paste. The electric conductivity as E (Electrical Conductivity of the extract) with units of decismens per meter (dS.) or millimhos per centimeter (mmhos/cm) is an expression for the anions and cations in the soil. From the agricultural point of view, saline soils are those, which contain sufficient neutral soluble salt in the root zone to adversely affect the growth of most crops. By

considering the definition, saline soils have an electrical conductivity of saturation extracts of more than 4 dS. at 25 °C[32].

Salt-affected soils can be determined using Normalized Difference Vegetation Index (NDVI), Normalized Differential Salinity Index (NDSI), Salinity Index-1 (SI-1), and Salinity Index-2 (SI-2).NDSI and SI-1 proposed by Tripathi et al (1997) for Landsat images applied to identify the salt-affected soils.

$$NDSI = \frac{\rho_{Red} - \rho_{NIR}}{\rho_{Red} + \rho_{NIR}} \quad (4.7)$$

Where  $\rho_{Red}$  is the reflectance or radiance in a red wavelength band and  $\rho_{NIR}$  is the reflectance or radiance in a near infrared wavelength band. NDSI values are between -1 and 1, less values show less salt-affected areas and high values show high salt-affected areas.

$$SI = \sqrt{\rho_{Blue} * \rho_{Red}} \quad (4.8)$$

Where  $\rho_{Blue}$  is the reflectance or radiance in a blue wavelength band and  $\rho_{Red}$  is the reflectance or radiance in a red wavelength band.

Abbas et al (2007) used another Salinity Index (SI) in Landsat images to show salty affected areas. They used green and red bands to to detect salinity soil. The higher reflection means high saline soil. SI values are between 0 and 1, less values show less salt-affected areas and high values show high salt-affected areas[32, 33, 34, 35].

$$SI = \frac{\rho_{Green} + \rho_{Red}}{2} \quad (4.9)$$

#### 4.5 Normalized Difference Drought Index (NDDI)

The aridity and drought are two types of natural phenomena related to variables such as rainfall, soil moisture, and groundwater. The conceptions of aridity and drought aren't same and they are different from each other. Drought is a temporary aberration and aridity is a permanent feature of climate. Although there is not a precise and universally accepted definition of drought, since this phenomenon responds to the particular characteristics of a region and its effects can vary greatly from region to region, a common definition can be found in: "Drought is an insidious natural hazard characterized by lower than expected or lower than normal precipitation that, when

extended over a season or longer period of time, is insufficient to meet the demands of human activities and the environment"[36].

The phenomenon of drought occurs in most countries, both dry and wet regions. The impacts are complex, involving many people, varying in spatial and temporal scales that can cause land degradation and, if unchecked, a progression of dry land or an increase in desertification. Drought by itself is not a disaster. Whether it becomes a disaster depends on its impact on local people, economies and the environment and their ability to cope with and recover from it. The use of remote sensing data has a number of advantages to examine the effects of drought on vegetation. The information covers the entire territory, the repetition of images provides multitemporal measurements and vegetation indices derived from satellite data allow to identify areas affected by drought and take into account different types of vegetation and environmental conditions. For the calculation of these indices, low spatial resolution data from different sensors like the Moderate Resolution Imaging Spectroradiometer (MODIS) or Advanced Very High Resolution Radiometer (AVHRR), carried by a series of the (NOAA) satellites can be used but with these low spatial resolution sensors it is difficult to study specific target types, because the pixel size is often greater than the size of forest stands. For a local analysis higher spatial resolution data should be used like Landsat. In this case we have the necessary bands in the red and infrared spectrum to facilitate the calculation of indices [30, 36].

Normalized Difference Drought Index (NDDI), can offer an appropriate measure of the dryness of a particular area, because it combines information on both vegetation and water. Diego Renza, et al (2010) used Drought Estimation Maps by Means of Multidate Landsat Fused Images from the NDVI and NDWI data. NDDI had a stronger response to summer drought conditions than a simple difference between NDVI and NDWI, and is therefore a more sensitive indicator of drought in grasslands than NDVI alone"[30, 36].

$$NDDI = \frac{NDVI - NDWI}{NDVI + NDWI} \quad (4.10)$$

## **4.6 Geostatistics Analysis**

Exploring about meteorological data is a very important part of environmental science. Geostatistics expresses this intuitive knowledge quantitatively and then uses it for prediction. Geostatistics is an appropriate scientific approach study about meteorological properties of different location. Geostatistics studies spatial variability of regionalized variables. Regionalized variables are variables that have an attribute value and a location in a two or three dimensional space. “Geostatistics can be regarded as a collection of numerical techniques that deal with the characterization of spatial attributes, employing primarily random models in a manner similar to the way in which time series analysis characterizes temporal data[37,38].”

Geostatistics are also described sometimes as a set of techniques and tools used to analyze and predict values of a variable distributed in space and in time. With geostatistics we can explore our sample data, construct variogram models and produce interpolated surfaces. “Geostatistics offers a way of describing the spatial continuity of natural phenomena and provides adaptations of classical regression techniques to take advantage of this continuity[37,38].”

### **4.6.1 Interpolation And kriging**

A point interpolation (also known as gridding) performs an interpolation on randomly distributed point values and returns regularly distributed point values. The input for point interpolation is mostly a point map with the domain type value or a point map with domain type class or identifier that is linked to an attribute table, in which the attribute values are stored in a column with domain type value. The output of a point interpolation is a raster map in which each pixel has a value calculated by an interpolation on the input point values. The interpolation methods include of Nearest Point, Moving Average, Trend Surface and Moving Surface. An alternative to the above mentioned straightforward deterministic methods is kriging. Kriging is a statistical method based on the theory of regionalized variables. Kriging provides a solution to the problem of estimation based on a continuous model of stochastic spatial variation. It makes the best use of existing knowledge by taking account of the way that a property varies in space through the variogram model. In its original

formulation a kriged estimate at a place was simply a linear sum or weighted average of the data in its neighborhood. Since then kriging has been elaborated to tackle increasingly complex problems in mining, petroleum engineering, pollution control and abatement, and public health[38, 39, 40].

Kriging was developed in mining originally to estimate the amounts of metal blocks of rock, and it is still used in this way. In these circumstances every block of rock is potentially of interest, and its metal content will be estimated. The miner may then decide whether the rock contains sufficient metal to be mined and sent for processing. Environmental scientists, and pedologists in particular, have used kriging in a rather different way, namely optimal interpolation at many places for mapping. Some examples are those by Burgess and Webster (1980a, 1980b) and Burgess et al. (1981), who used ordinary kriging. There have been many since, for example Mulla (1997), Frogbrook (1999) and Frogbrook et al (1999) in precision agriculture. To map a variable the values are kriged at the nodes of a fine grid. Isarithms are then threaded through this grid, and there are now many programs and packages, such as Surfer (Golden Software, 2002) and Gsharp, and Geographical Information Systems (GIS), such as Arc/Info, that will do this with excellent graphics. Computing the isarithms involves another interpolation which is rarely optimal in the kriging sense, but if the kriged grid is fine enough this lack of optimality is immaterial. In most instances kriging at intervals of 2mm on the finished map will be adequate. The kriging variances and their square roots, the kriging errors, can be mapped similarly, and these maps give an idea of the reliability of the maps of estimates. A standard version of kriging is called ordinary kriging (OK)[38, 39, 40].

#### **4.6.2 Kinds of Kriging**

Kriging covers a range of least-squares methods of spatial prediction.

- Ordinary kriging of a single variable is the most robust method and the one most used.
- Simple kriging is rather little used as it stands because we usually do not know the meaning. It finds application in other forms such as indicators and disjunctive kriging in which the data are transformed to have known means.

- Lognormal kriging is ordinary kriging of the logarithms of the measured values. It is used for strongly positively skewed data that approximate a lognormal distribution.
- Kriging with drift, also known as universal kriging, recognizes both non-stationary deterministic and random components in a variable, estimates the trend in the former and the variogram of the latter, and recombines the two for prediction. This introduces residual maximum likelihood into the kriging procedure.
- Factorial kriging or kriging analysis is of particular value where the variation is nested, i.e. more than one scale of variation is present. Factorial kriging estimates the individual components of variation separately, but in a single analysis.
- Ordinary cokriging is the extension of ordinary kriging of a single variable to two or more variables. There must be some coregionalization among the variables for it to be profitable. It is particularly useful if some property that can be measured cheaply at many sites is spatially correlated with one or more others that are expensive to measure and are measured at many fewer sites. It enables us to estimate the more sparsely sampled property with more precision by cokriging using the spatial information from the more intensely measured one.
- Indicator kriging is a non-linear, non-parametric form of kriging in which continuous variables are converted to binary ones (indicators). It is becoming popular because it can handle distributions of almost any kind, and empirical cumulative distributions of estimates can be computed and thereby provides confidence limits on them. It can also accommodate 'soft' qualitative information to improve prediction.
- Disjunctive kriging is also a non-linear method of kriging, but it is strictly parametric. It is valuable for decision-making because the probabilities of exceeding or not exceeding a predefined threshold are determined in addition to the kriged estimates.
- Probability kriging was proposed by Sullivan (1984) because indicator kriging does not take into account the proximity of a value to the threshold,



but only its position. It uses the rank order for each value,  $z(x)$ , normalized to 1 as the secondary variable to estimate the indicator by cokriging. Chile`s and Delfiner (1999) and Goovaerts (1997) describe the method briefly.

- Bayesian kriging was introduced by More (1987) for situations I which there is some prior knowledge about the drift. It is intermediate between simple kriging, used when there is no drift, and universal kriging where there is known to be drifting. The kriging equations are those of simple kriging, but with non-stationary covariances (Chile`s and Delfiner, 1999) [38].

Before using kriging, it is necessary to make a semi-variogram model, which will determine the interpolation function and following steps needed for kriging[38,40]:

Step 1: Examining the input data

Step 2: Calculating experimental variograms

Step 3: Modelling variograms

Step 4: Kriging interpolation

### **4.6.3 Ordinary Kriging**

Ordinary kriging is the simplest form of kriging. It uses dimensionless points to estimate other dimensionless points, e.g. elevation contour plots. The aim of kriging is to estimate the value of a random variable,  $Z$ , at one or more unsampled points or over larger blocks, from more or less sparse sample data on a given support, say  $z(X_1), z(X_2), \dots, z(X_N)$  at points  $X_1; X_2; \dots; X_N$ . The data may be distributed in one, two or three dimensions, though applications in the environmental sciences are usually two-dimensional.

Ordinary kriging is by far the most common type of kriging in practice. Ordinary kriging assumes an unknown constant mean. The data points need to be sampled from a phenomenon that is continuous in space. Important parameters include an appropriate transformation, a possible detrending surface, covariance/semivariogram models, and search neighborhoods. The predictions are based on the model according to Eq.(4.11):

$$Z(X) = \mu + \epsilon'(X) \quad (4.11)$$

Where  $\mu$  is the constant stationary function (global mean) and  $\epsilon'(X)$  is the spatially correlated stochastic part of variation. The predictions are made as in Eq.(4.12):

$$\hat{Z}(X_0) = \sum_{i=1}^N \lambda_i(X_0) \cdot z(X_i) \quad (4.12)$$

Where  $\lambda_i$  are the weights for neighbor  $i$ . The sum of weights needs to equal one to ensure an unbiased interpolator. To ensure that the estimate is unbiased the weights are made to sum to 1 according to Eq.(4.13) [38, 39, 40] :

$$\sum_{i=1}^N \lambda_i = 1 \quad (4.13)$$

One of the main issues concerning ordinary kriging is whether the assumption of a constant mean is reasonable. Sometimes there are good scientific reasons to reject this assumption. However, as a simple prediction method, it has remarkable flexibility. The Figure 4.1 is an example in one spatial dimension[63]:

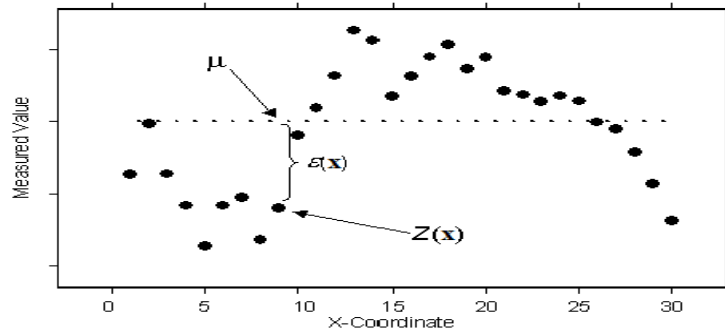


**Figure 4.1:** One spatial dimension ordinary kriging[63]

#### 4.7 Standardized Precipitation Index (SPI)

Meteorological drought is the most common and accurate event in the process of drought conditions and rainfall is the primary driver of meteorological drought. Drought is an insidious natural hazard that results from lower levels of precipitations than what is considered normal. When this phenomenon extends over a season or a longer period of time, precipitation is insufficient to meet the demands of human activities and the environment. The drought must be considered a relative, rather than absolute, condition. There are also many different methodologies for monitoring drought. Droughts are regional in extent and each region has specific climatic

characteristics. Droughts that occur in the North American Great Plains will differ from those that occur in northeast Brazil, southern Africa, western Europe, eastern Australia, or the North China Plain. The amount, seasonality and form of precipitation differ widely between each of these locations. Temperature, wind and relative humidity are also important factors to include in characterizing drought. Drought monitoring also needs to be application-specific because drought impacts will vary between sectors. Drought means different things to different users such as water managers, agricultural producers, hydroelectric power plant operators and wildlife biologists. Even within sectors, there are many different perspectives of drought because impacts may differ markedly. Droughts are commonly classified by type as meteorological, agricultural and hydrological, and differ from one another in intensity, duration and spatial coverage. There are numerous indicators based on precipitation that are used for drought monitoring. The deviation of rainfall from normal i.e. long term mean, is the most commonly used indicator for drought monitoring[42].

The Standardized Precipitation Index (SPI) is a tool which was developed primarily for defining and monitoring drought. It allows an analyst to determine the rarity of a drought at a given time scale (temporal resolution) of interest for any rainfall station with historic data. It can also be used to determine periods of anomalously wet events. The SPI is not a drought prediction tool. The standardize precipitation Index (SPI) was developed by American scientists McKee, Doesken and Kleist in 1993. The SPI (McKee and others, 1993, 1995) is a powerful and flexible index that is simple to calculate and precipitation is the only required input parameter. McKee and others (1993) used the classification system to define drought intensities resulting from the SPI. They also defined the criteria for a drought event for any of the timescales. Mathematically, the SPI is based on the cumulative probability of a given rainfall event occurring at a station. The historic rainfall data of the station are fitted to a gamma distribution, as the gamma distribution has been found to fit the precipitation distribution quite well. This is done through a process of maximum likelihood estimation of the gamma distribution parameters,  $\alpha$  and  $\beta$ . In simple terms, the process described above allows the rainfall distribution at the station to be effectively represented by a mathematical cumulative probability function. Therefore, based on the historic rainfall data, an analyst can then tell what is the

probability of the rainfall being less than or equal to a certain amount. Thus, the probability of rainfall being less than or equal to the average rainfall for that area will be about 0.5, while the probability of rainfall being less than or equal to an amount much smaller than the average will be also be lower (0.2, 0.1, 0.01 etc, depending on the amount). Therefore, if a particular rainfall event gives a low probability on the cumulative probability function, then this is indicative of a likely drought event. Alternatively, a rainfall event which gives a high probability on the cumulative probability function is an anomalously wet event. The SPI is a representation of the number of standard deviations from the mean at which an event occurs, often called a “z-score”. The unit of the SPI can thus be considered to be “standard deviations”. Standard deviation is often described as the value along a distribution at which the cumulative probability of an event occurring is 0.1587. In a like manner, the cumulative probability of any SPI value can be found, and this will be equal to the cumulative probability of the corresponding rainfall event. A drought event occurs any time the SPI is continuously negative and reaches an intensity of -1.0 or less. The event ends when the SPI becomes positive. Each drought event, therefore, has a duration defined by its beginning and end, and an intensity for each month that the event continues. The positive sum of the SPI for all the months within a drought event can be termed the drought’s “magnitude”. To calculate SPI, difference of significant precipitation ( $X_i$  monthly) from average precipitation ( $X_i^{mean}$  monthly) is obtained, then the difference is divided by standard deviation ( $\sigma$ ) of the selected study time period. The Eq. (4.14) is used to obtain SPI[42,43,44,65].

$$SPI = \frac{(X_i - X_i^{mean})}{\sigma} \quad (4.14)$$

Where  $X_i$  is significant precipitation and  $X_i^{mean}$  is average precipitation, and finally  $\sigma$  is standard deviation of the selected study time period. Table 4.1 gives the cumulative probabilities for various SPI values[64] :

**Table 4.1: SPI and cumulative probability.**

SPI	Cumulative Probability	Interpretation
-3.0	0.0014	Extremely dry
-2.5	0.0062	Extremely dry
-2.0	0.0228	Extremely dry (SPI < -2.0)
-1.5	0.0668	Severely dry (-2.0 < SPI < -1.5)
-1.0	0.1587	Moderately dry (-1.5 < SPI < -1.0)
-0.5	0.3085	Near normal
0.0	0.5000	Near normal
0.5	0.6915	Near normal
1.0	0.8413	Moderately wet (1.0 < SPI < 1.5)
1.5	0.9332	Very wet (1.5 < SPI < 2.0)
2.0	0.9772	Extremely wet (2.0 < SPI)
2.5	0.9938	Extremely wet
3.0	0.9986	Extremely wet



## **5. CHANGE DETECTION ON URMIA LAKE AND ITS CATCHMENT AREA USING REMOTE SENSING AND GIS**

### **5.1 Preprocessing of Satellite Images**

The main purpose of this study is to conduct multi-temporal change detection on Urmia Lake and its catchment area by integration of remote sensing and geographical information systems (GIS) for the last 30 years from 1984 to 2014. At the first step, all Landsat-4, -5 TM, and Landsat-8 data archive were skimmed to choose the best data having a low cloud percentage which obtained in the same seasons and/or months of different years. Secondly, 80 Landsat-5 TM, 12 Landsat-8 frames and 2 DMC images collected during summer and spring of the years 1984 to 2013 were chosen for analysis. A Landsat-8 frame also was selected in 2014-February to understand the current conditions of Urmia Lake in 2014. Landsat-5 TM data include 1984-Summer, 1987-Spring, 1987-Summer, 1990-Summer, 1995-Summer, 1998-Spring, 1998-Summer, 2000-Summer, 2006-Summer, 2007-Spring, 2007-Summer, 2009-Summer, 2010-Summer, and 2011-Summer images. In 1995-Summer there were just 2 Landsat frames and because of missing data in the Landsat archive from 1991 to 1994, a frame of 1998-May was used to fully cover Urmia Lake in 1995 year. The cloud cover percentage in 1998-Spring was very high; however the area of Urmia Lake was calculated at this time using classification. Landsat-8 data include 2013-Spring, 2013-Summer and 2014-February. A frame was used to cover water surface area of Urmia Lake in 2014-February. DMC data in 2011-April, and 2012-July were used in this study to have the further analysis in 2011-Spring and 2012-Summer when there were no Landsat data.

The methodology of this study was based on using different spectral bands of images for classification or creation of different indices to find out spatial changes in the study area; therefore the application of Landsat images in this study had some advantages rather than DMC images due to its better spectral resolution. Spatial

resolution, temporal resolution and spectral resolution are very important parts of different remote sensing systems and analyzing and extracting information from images depend on them.

In the first step of image preprocessing, bands 1, 2, 3, 4, 5, and 7 of Landsat-5 TM and bands 1, 2, 3, 4, 5, 6, and 7 of Landsat-8 satellite were stacked in ENVI to create new output images. In the second step, radiometric calibration was performed for all satellite data in ENVI to minimize the radiometric effects. In radiometric correction process, all remotely sensed Digital Numbers (DNs) were converted to Top Of Atmospheric (TOA) reflectance values in ENVI. Since DNs are scaled mathematical quantities, it is important to convert them into physical quantity like radiance or reflectance. To convert DNs to TOA reflectance, they should be converted to the absolute scale of radiance which is independent of the images forming characteristics of the sensor. Then radiance values can be converted to reflectance values which are between 0 and 1. Reflectance values indicate reflected energy from the phenomenon. Eq.(5.1) shows the related formula to convert DNs to radiance values in Landsat-5 TM images.

$$L_{Sat} = \left[ \frac{LMAX_{Sat} - LMIN_{Sat}}{DNMAX - DNMIN} \right] * (DN - DNMIN) + LMIN_{Sat} \quad (5.1)$$

Where  $LMAX_{Sat}$  is radiance scaled to  $DNMAX$  ( $w m^{-2} sr^{-1} \mu m^{-1}$ ),  $LMIN_{Sat}$  is radiance scaled to  $DNMIN$  ( $w m^{-2} sr^{-1} \mu m^{-1}$ ),  $DNMAX$  is maximum quantized calibrated digital number, and  $DNMIN$  is minimum-quantized calibrated digital number. Data which were used to convert DNs to radiance value were available in the metadata file. After conversion DNs to at-satellite radiance values, they were converted to at-satellite or TOA reflectance using Eq.(5.2) :

$$\rho_{ASR} = \frac{((\pi * L_{Sat}) * d^2)}{(E_0 * \cos(\theta))} \quad (5.2)$$

Where  $\rho_{ASR}$  is at-satellite reflectance,  $E_0$  is exoatmospheric solar constant ( $w m^{-2} \mu m^{-1}$ ) (corrected for solar distance), and  $\theta$  is the solar zenith angle, and  $d$  is Earth-sun distance in astronomical units, ranges from approx. 0.9832 to 1.0167 (earth-sun distance for the imagery acquisition date) [23,25].

Landsat-8 data were converted to TOA spectral radiance using the radiance rescaling factors provided in the metadata file according to Eq.(5.3):



$$L_{\lambda} = (M_L * Q_{cal}) + A_L \quad (5.3)$$

Where  $L_{\lambda}$  is at-satellite spectral radiance ( $w m^{-2}sr^{-1}\mu m^{-1}$ ),  $M_L$  is band-specific multiplicative rescaling factor from the metadata, and  $A_L$  is band-specific additive rescaling factor from the metadata and  $Q_{cal}$  is Quantized and calibrated standard product pixel values (DN). Landsat-8 data can also be converted to TOA planetary reflectance using reflectance rescaling coefficients provided in the product metadata file. The Eq.(5.4) was used to convert DN values to TOA reflectance for Landsat-8 data :

$$\rho\lambda' = M_{\rho}Q_{cal} + A_{\rho} \quad (5.4)$$

Where  $\rho\lambda'$  is TOA planetary reflectance, without correction for solar angle. Note that  $\rho\lambda'$  does not contain a correction for the sun angle.  $M_{\rho}$  is band-specific multiplicative rescaling factor from the metadata, and  $A_{\rho}$  is band-specific additive rescaling factor from the metadata, and  $Q_{cal}$  is quantized and calibrated standard product pixel values (DN). TOA reflectance with a correction for the sun angle is then :

$$\rho\lambda = \frac{\rho\lambda'}{\cos(\theta_{sz})} = \frac{\rho\lambda'}{\sin(\theta_{se})} \quad (5.5)$$

Where  $\rho\lambda$  is TOA planetary reflectance, and  $\theta_{sz}$  is the Local sun elevation angle. The scene center sun elevation angle in degrees is provided in the metadata and  $\theta_{sz}$  is Local solar zenith angle;

$$\theta_{SZ} = 90^{\circ} - \theta_{SE} \quad (5.6)$$

For more accurate reflectance calculations, per pixel solar angles could be used instead of the scene center solar angle, but per pixel solar zenith angles are not currently provided with the Landsat-8 products [53].

DMC data can be converted to TOA spectral radiance using the Eq.(5.7) [21].

$$Radiance = [DN * RESCALE GAIN] + RESCALE BIAS \quad (5.7)$$

The TOA reflectance of DMC images were calculated using Eq.(5.8), regardless of the product level.

$$\rho_{ASR} = \frac{((\pi * L_{Sat}) * d^2)}{(E_0 * \cos(\theta))} \quad (5.8)$$

At-satellite reflectance values mean that the study area is considered as a uniform Lambertian surface under cloudless condition. Therefore, atmospheric correction is necessary to obtain surface reflectance values. In the third step of the satellite image preprocessing, atmospheric condition of all frames and images, were conducted in ERDAS IMAGINE using ATCOR to decrease aerosols, clouds, their shadows, and other atmospheric effects from imagery. At-satellite reflectance values were converted to surface reflectance values in full absolute correction using ATCOR algorithm according to Eq.(5.9) [23,25]:

$$\rho = \frac{\pi(L_{Sat} - L_P)}{T_v(E_0 * \cos(\theta) * T_z + E_{down})} \quad (5.9)$$

Where  $\rho$  is estimated surface reflectance,  $L_P$  is path radiance ( $w m^{-2} sr^{-1} \mu m^{-1}$ ),  $T_v$  is atmospheric transmittance from the target toward the sensor,  $T_z$  is atmospheric transmittance in the illumination direction, and  $E_{down}$  is downwelling diffuse irradiance ( $w m^{-2} \mu m^{-1}$ ).

In the fourth step, geometric accuracy of satellite images was checked to identify images requiring geometric corrections. Since the images of Landsat-5 TM and Landsat-8 used in this study were level-1 Geo TIFF products, and the geometric correction process had been applied earlier, further rectification procedure was not conducted for these images. Level-1 Geo TIFF products were suitable for this study and geometric correction process was not necessary for them. For more information about Level-1 products, United States Geological Survey (USGS) website could be used. Landsat standard data products are processed using the Level-1 Product Generation System (LPGS) with the following parameters applied:

- GeoTIFF output format
- Cubic Convolution (CC) resampling method
- 30-meter (TM, ETM+) and 60-meter (MSS) pixel size (reflective bands)
- Universal Transverse Mercator (UTM) map projection (Polar Stereographic projection for scenes with a center latitude greater than or equal to -63.0 degrees)

- World Geodetic System (WGS) 84 datum
- MAP (North-up) image orientation

## 5.2 Mosaic and Classification

After preprocessing steps, 6 frames of Landsat images covering the study area were mosaiced and complete images covering Urmia Lake and its catchment area were formed for each summer and spring time mentioned in the previous section. Figure 5.1 shows an example of mosaiced images in 2013-summer. Then, unsupervised classification and supervised classifications were conducted on mosaiced images and spatio-temporal changes over the Urmia Lake were determined for the last 30-year period using classification methods. Different indices were also used to understand spatio-temporal changes over Urmia Lake's catchment area and some parts of Iran, Turkey, and Iraq which were near to Urmia Lake and it is possible they be affected by drying Urmia Lake at next future years.

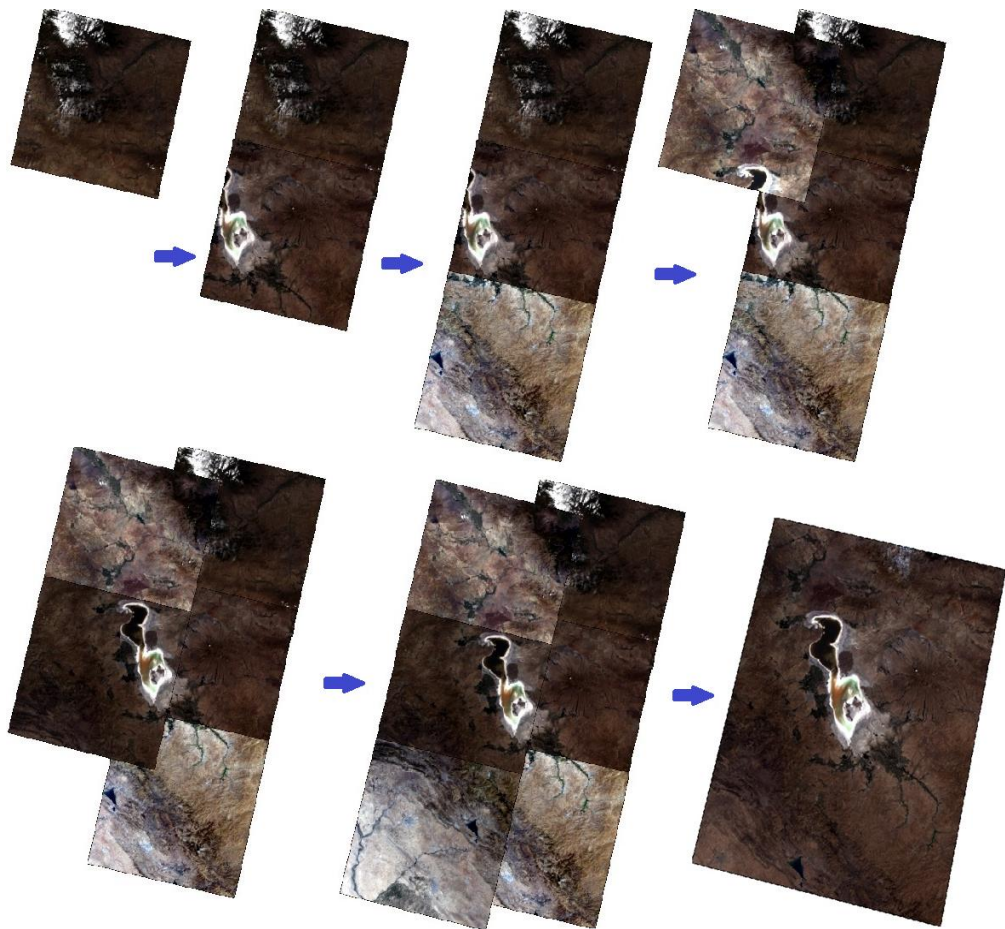


**Figure 5.1 :** Mosaic of 6 frames – Landsat-8 – 2013 - Summer.

### 5.2.1 Unsupervised Classification

Unsupervised classification is more computer-automated. This method enables the analyst to specify features to be used for the clustering algorithm based on statistical patterns included in the data. Unsupervised classification depends on the data for the definition of classes. This method requires less knowledge about the study area since there is not a training area selection step. Unsupervised classification is also called clustering, because it is based on the natural groupings of pixels in image data when they are plotted in feature space. The Iterative Self-Organizing Data Analysis Technique (ISODATA) method was used as an unsupervised classification method in this study. According to the specified parameters, these groups can later be merged, disregarded; otherwise the ISODATA method uses minimum spectral distance to assign a cluster for each candidate pixel. The process begins with a specified number of arbitrary cluster means or the means of existing signatures, and then it processes repetitively, so those means shift to the means of the clusters in the data [4, 13].

In this research, unsupervised classification-ISODATA was fulfilled with 150 clusters in ERDAS IMAGINE, then an Area Of Interest (AOI) was chosen around Urmia Lake by consideration the maximum area of Urmia Lake in 1995. This AOI was used in all studied dates to analyze changes in Urmia Lake. These clusters were reduced into 5 classes, including Water, Salt, Salty Soil (Badland), Soil, and Farming classes during the labeling, procedure. Finally, the area of each class was extracted and compared for different dates in ArcGIS and all of classified images were prepared as comparable maps to understand changes in the study area. Water class includes different kinds of water bodies like; deep water, shallow water, less saline water, saturated water, dirty water, rivers, streams, and clean water. Physical and chemical features of Urmia Lake don't have the same properties in different places and dates. The salinity of water has been increased extremely during recent years(). Therefore, all kinds of water bodies classified into one class which was named: water class. Figure 5.2 shows changes in color and quality of Urmia Lake's water in 2005-spring and 2010-summer.



**Figure 5.2:** Changes in color and quality of water - Urmia Lake - 2005-spring and 2010-summer - Photos taken by Yusuf Alizade Govarchin Ghale.

Salt class is another class used in this study to understand salinity changes in Urmia Lake. Salt areas, fully covered with salt and these areas are absolutely different from salty soil areas which are covered by different salty soil types that have a high percentage of salinity. It is not possible to conduct agricultural activities in both salt and salty soil areas. Figure 5.3 shows two sample areas of salt areas in Urmia Lake. These bodies were covered by water in 2012 and they were converted to salt as a result of drying Urmia Lake in recent years.

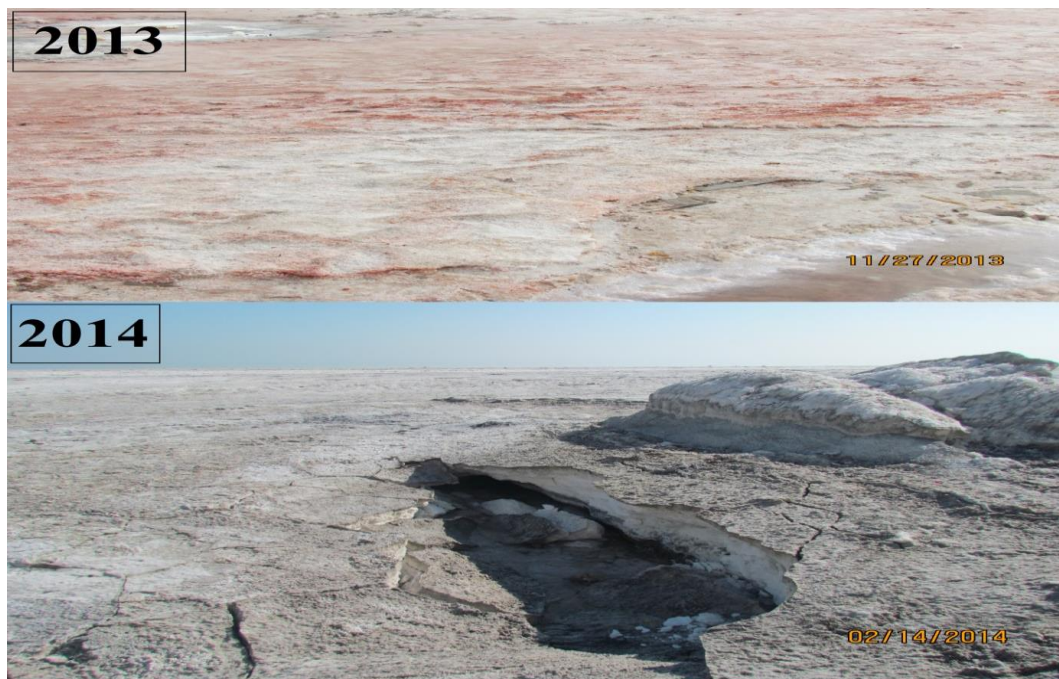


**Figure 5.3:** Salt area of Urmia Lake in 2013 and 2014 years – Photos taken by Yusuf Alizade Govarchin Ghale.

Extracting salt from Urmia Lake is also a common economical activity in Urmia Lake which has been done by Iran's government and local people using different methods. Figure 5.4 shows extracting salt from Urmia Lake by local people.



**Figure 5.4:** Extracting salt from Urmia Lake by local people - Photo taken by Yusuf Alizade Govarchin Ghale – 2013 year.

Salty soil is another class used in this study. These areas include high salinity percentage rather than normal soil and farming is not possible for most of the crop types in these areas due to the high level of salinity. However, some vegetations could survive in salty conditions like unique species of grasses, which are flowering plants found only in shallow intertidal areas. These plants are highly specialized and able to live in salt water and salty soil, and are therefore referred to as halophytes. They are also able to survive submerged in water part of the time, and are thus classified as hydrophytes[68].



**Figure 5.5:** Border of water, salt, and salty soil in the study area - Photo taken by Yusuf Alizade Govarchin Ghale - 2012 year.

Soil is another class which includes normal soil with low salinity percentage. Farming is possible in this class and vegetation kinds can grow up in soil areas. Farming class includes irrigated areas and agricultural areas that have different types of crops. Farming areas also can include some dense vegetation types in the study area. Figure 5.6 shows a sample of soil body and salty soil body beside each other.

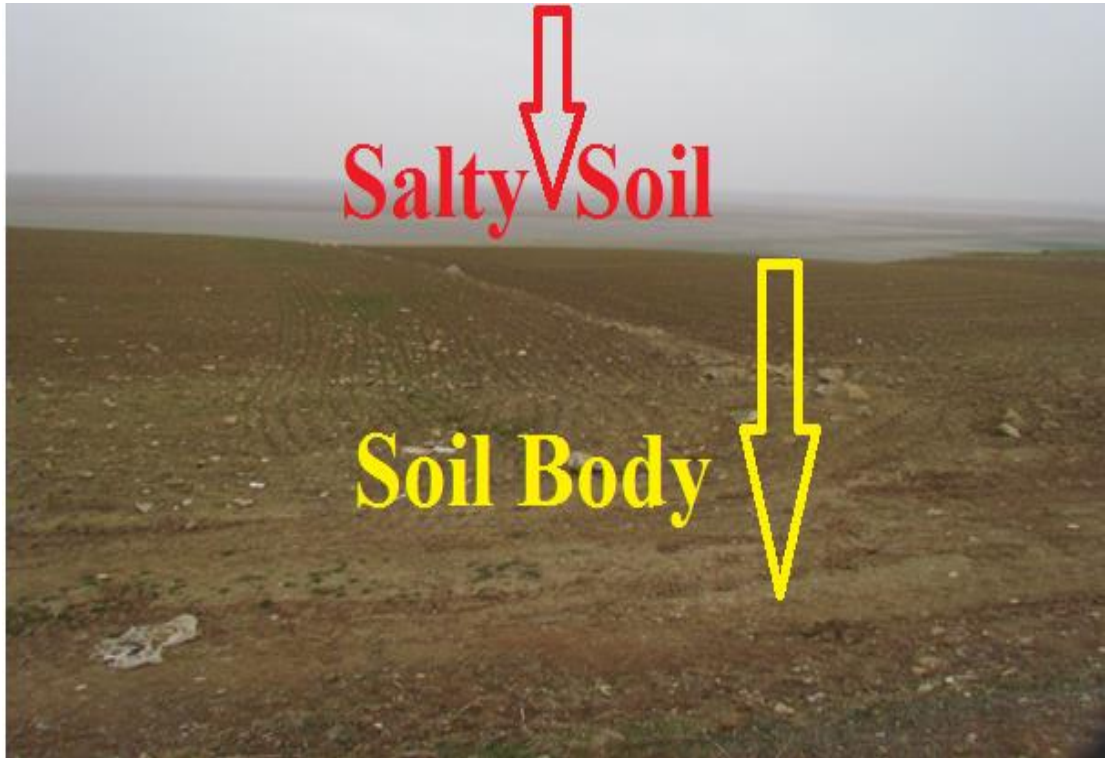


**Figure 5.6:** Soil and salty soil – Photo taken by Yusuf Alizade Govarchin Ghale – 2012 year.

Figure 5.7 shows all classes beside each other in the northwest part of Urmia Lake. According to this figure, water area in 2005 converted to salty soil and salt areas in 2010 due to drying Urmia Lake from 2005 to 2010. In spring and winter time, some classes such as soil and salty soil bodies mix to each other and distinction between them can be difficult because of precipitation and inflow water to Urmia Lake. In other words, salinity percentage of some salty soil areas decreases in level of normal soil due to precipitation and inflow water to Urmia Lake. In order to conduct an accurate classification, it is important to conduct field survey and collect ground truth data. To this aim, field survey was conducted at different times to collect ground truth data. GPS coordinates of sample locations were collected and photographs were taken during the field study.

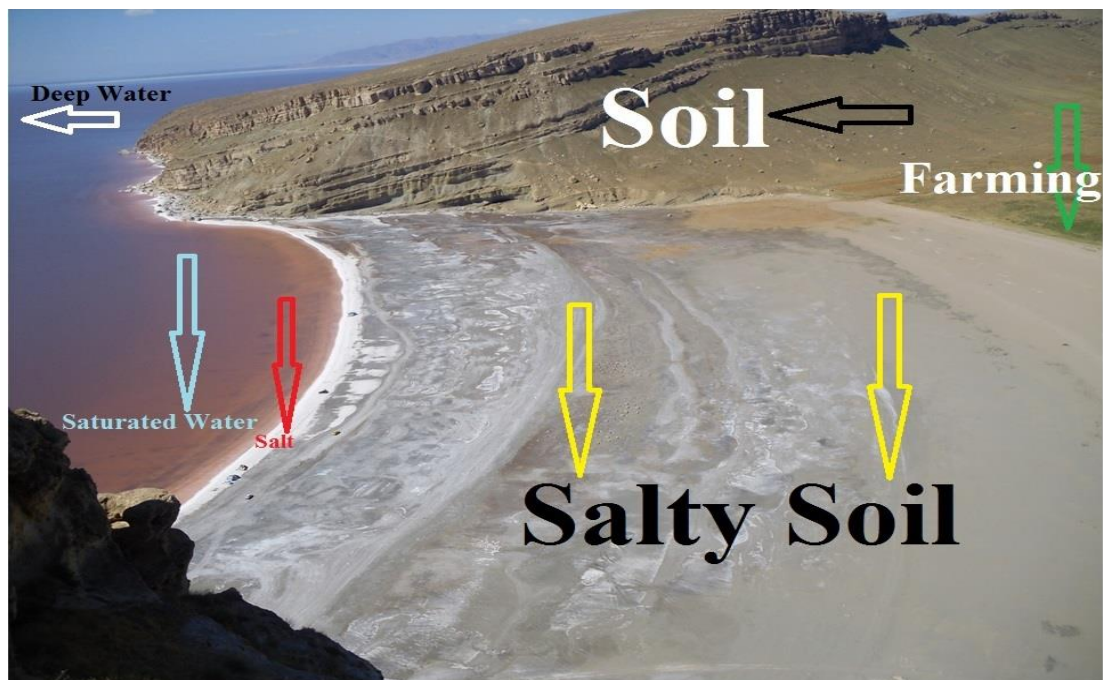


**Figure 5.7:** Border of water (blue and white arrow), salt (red arrow), salty soil (yellow arrow), soil (black arrow), and farming (green arrow) in the study area - 2010 year (same area was full of water in 2005) – Photos taken by Yusuf Alizade Govarchin Ghale in land study.

Figure 5.8 to 5.12 show the maps of unsupervised classification from 1984 to 2014. Blue color shows water areas, red color shows salt areas, yellow color shows salty soil areas, brown color shows soil body and green color shows farming class.



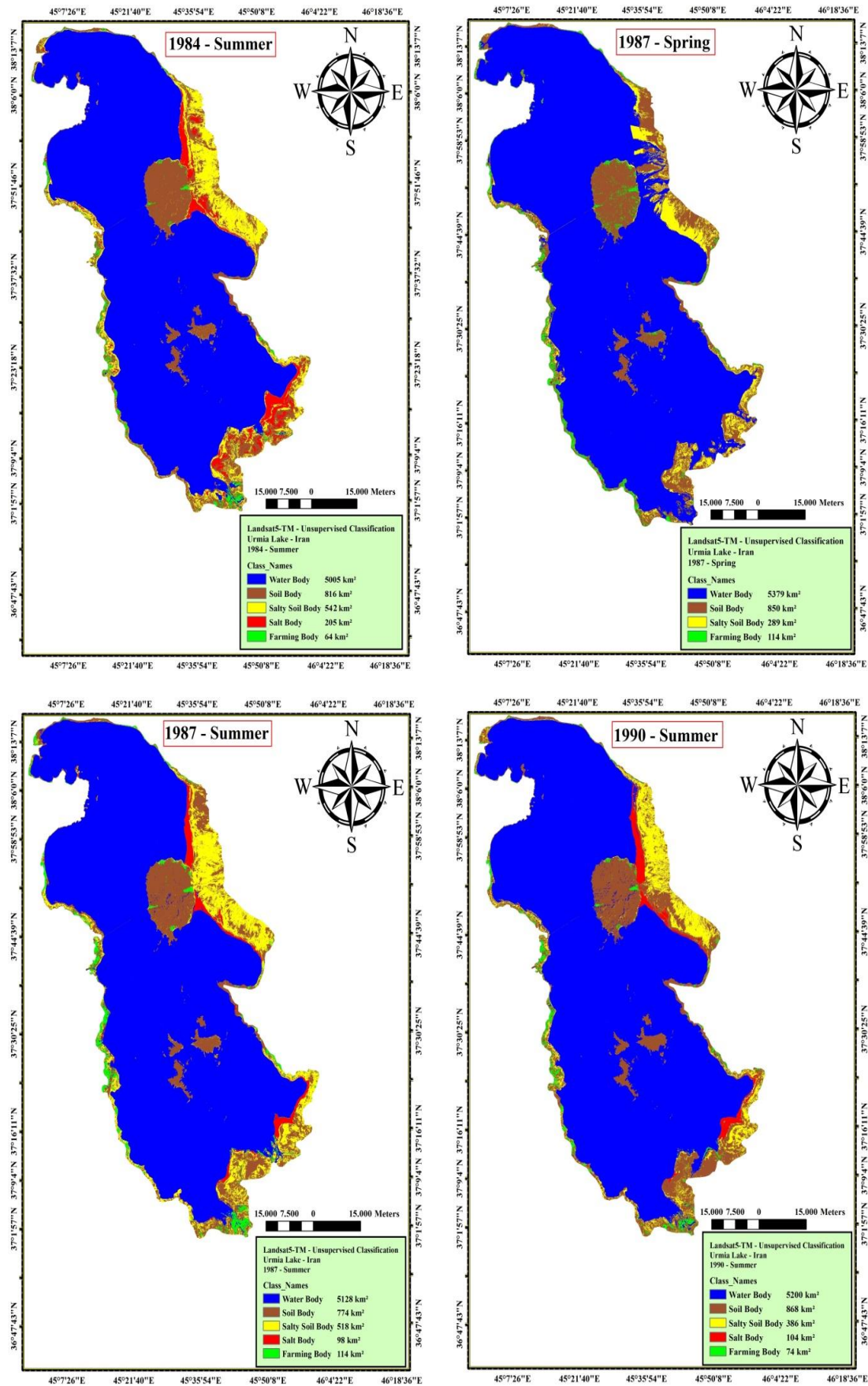


Figure 5.8: Unsupervised classification maps from 1984 to 1990.

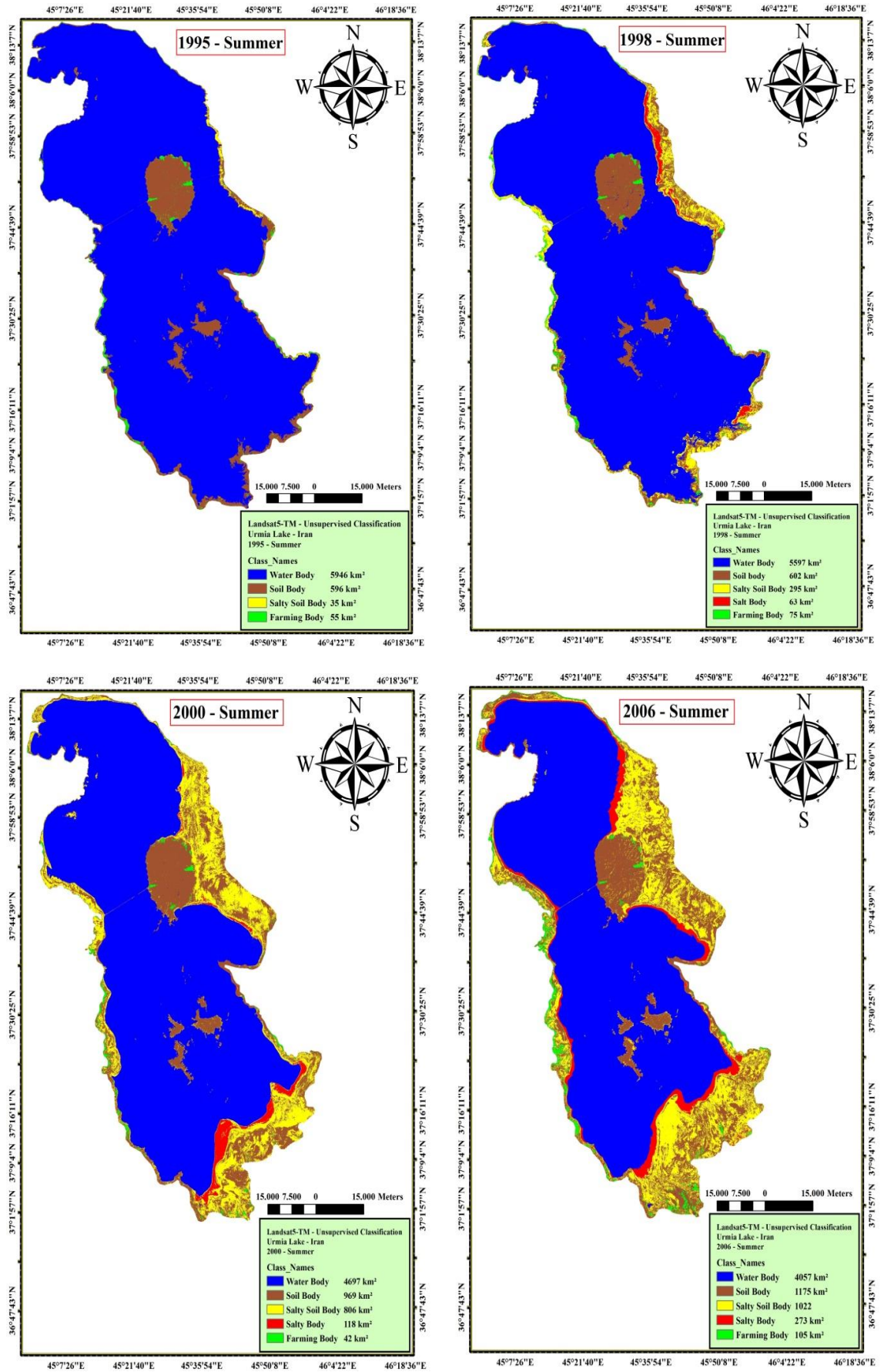


Figure 5.9: Unsupervised classification maps from 1995 to 2006.

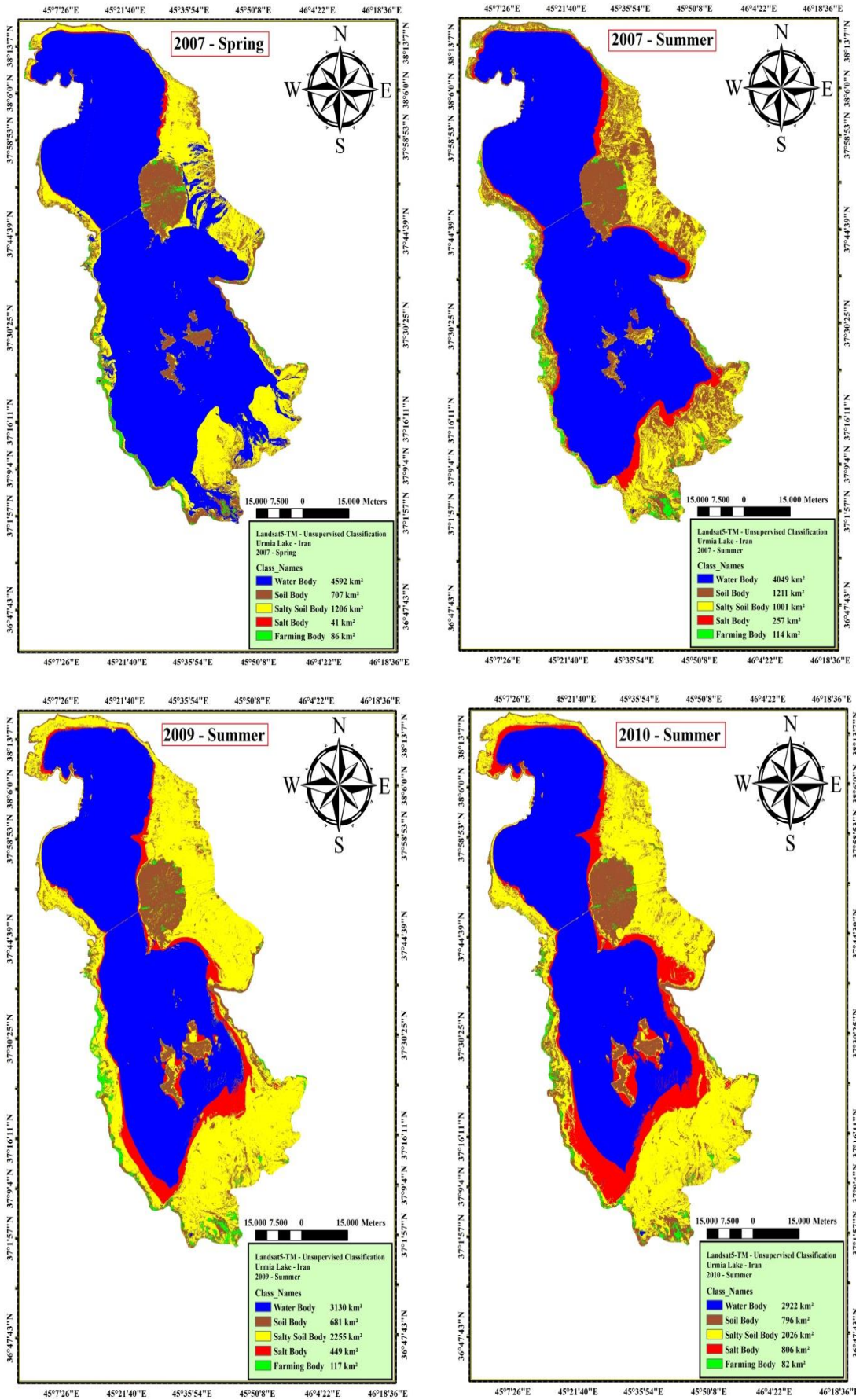


Figure 5.10: Unsupervised classification maps from 2007 to 2010.

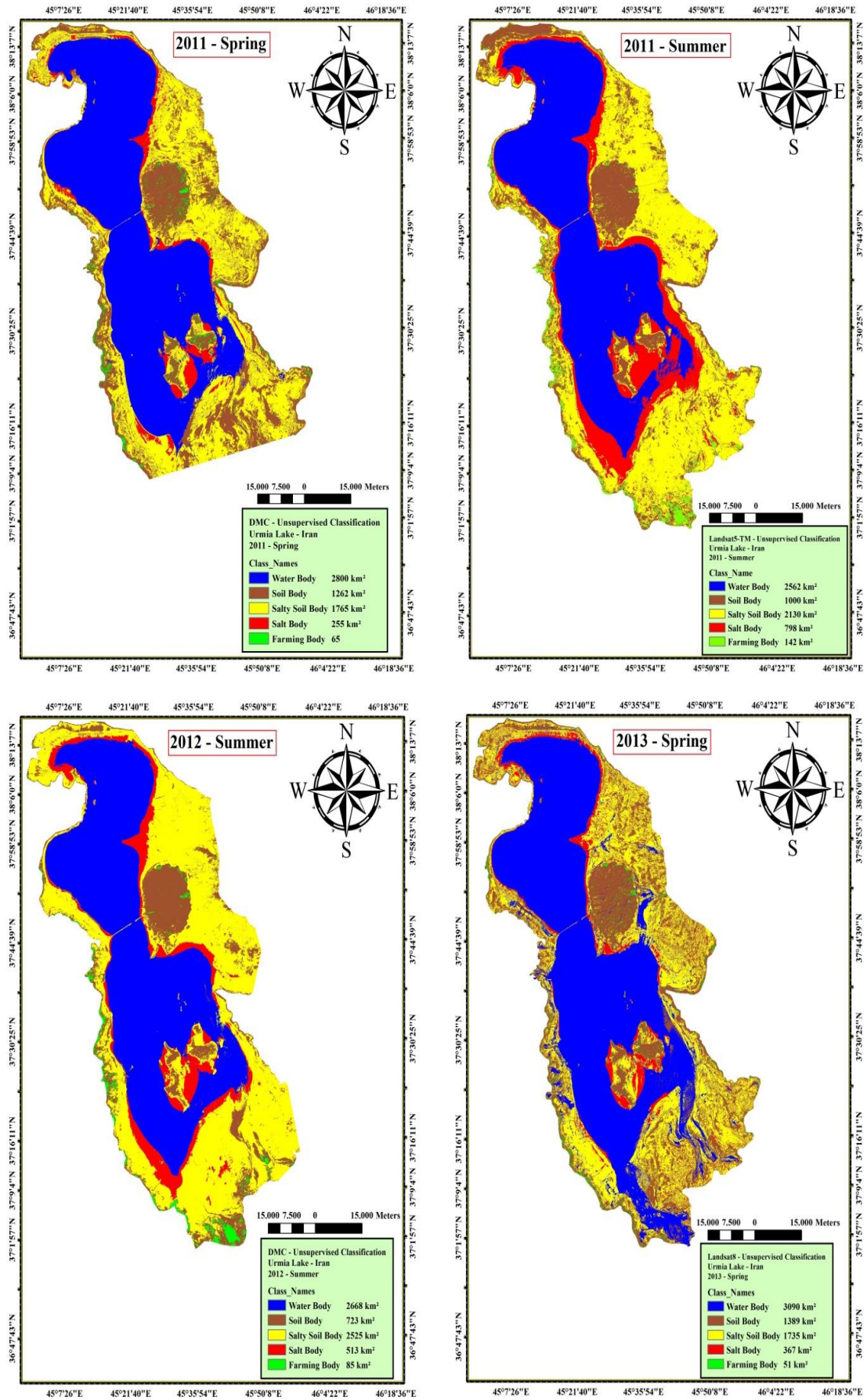
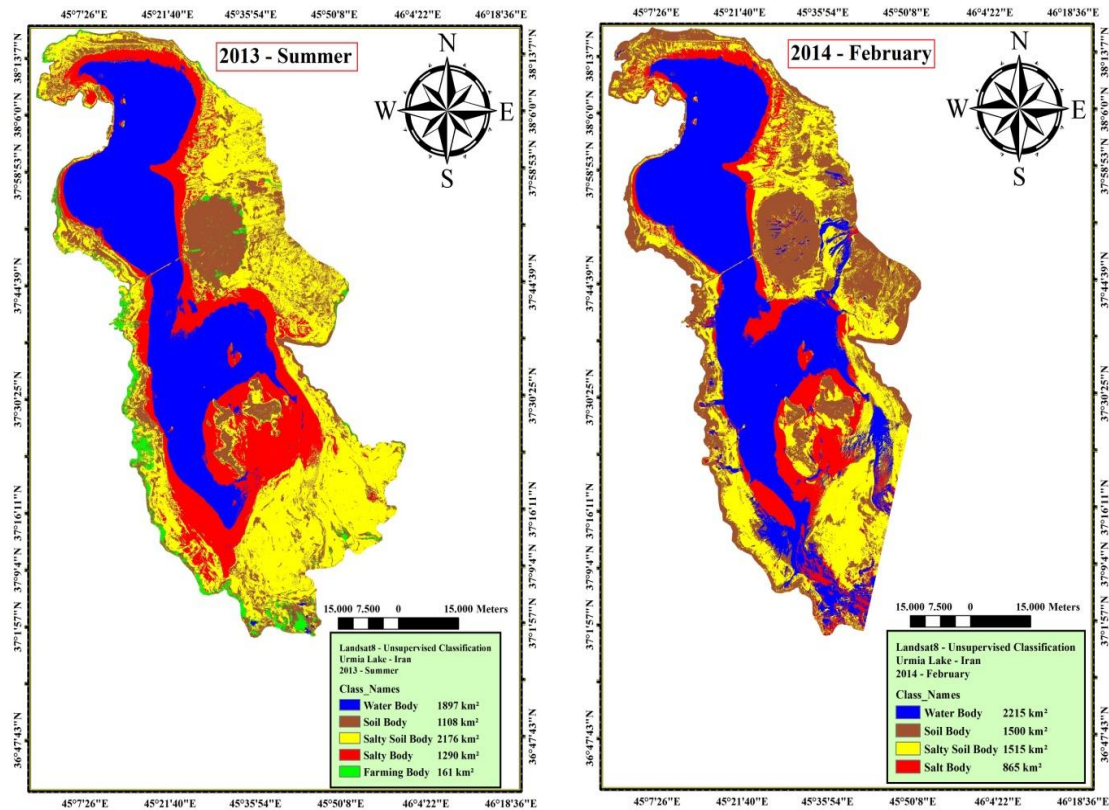


Figure 5.11: Unsupervised classification maps from 2011 to 2013.

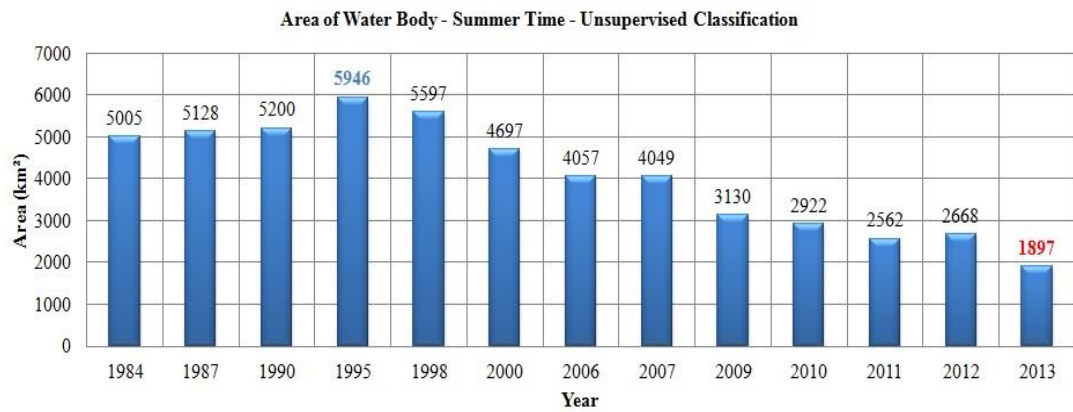


**Figure 5.12:** Unsupervised classification maps of 2013-summer and 2014-February.

Inflow water bodies from rivers and streams to Urmia Lake during spring time of 1987, 2007, 2013 and 2014-February are visible in south and east parts of Lake in Figures (5.8), (5.10), (5.11) and (5.12). These bodies were classified as water body in this study. The study area was classified into 4 classes in 2014-February and it didn't include farming class because it is so difficult to recognize farming bodies in winter time. In other words, there is no agricultural activity during winter and farming areas seem soil areas during this season.

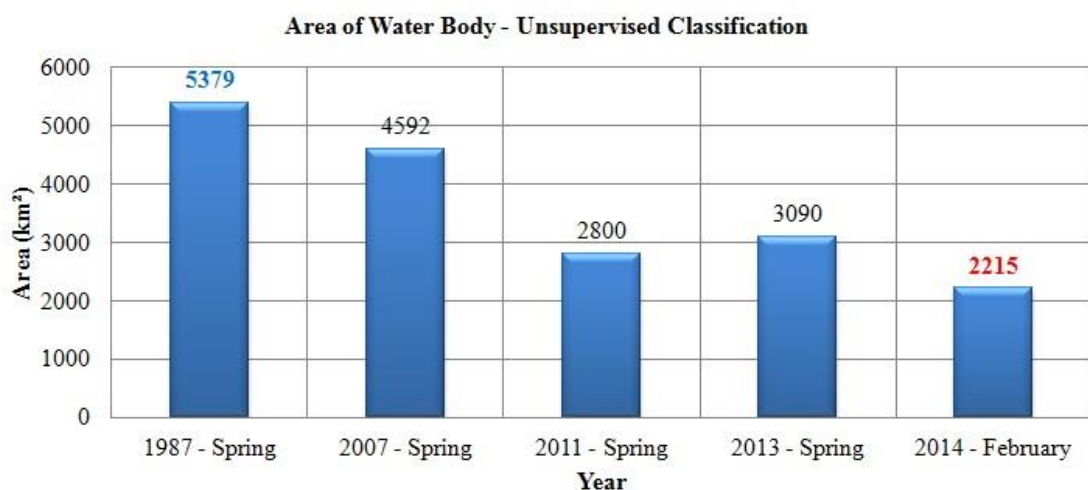
Figure 5.13 shows the total area of water class at summer time between 1984 and 2013. According to this figure water surface area of Urmia Lake increased from 1984 to 1995, then there was a decreasing trend in water surface area between 1995 and 2013. Decreasing water surface area was also considerable between 1998-2000 and 2007-2009. The water surface area difference between 1998 and 2000 was 900 km<sup>2</sup> and the difference between 2007 and 2009 was 919 km<sup>2</sup>. The maximum area of Urmia Lake was 5946 km<sup>2</sup> in 1995 and the minimum area was 1897 km<sup>2</sup> in 2013. There were two exceptions in water surface area changes from 1998 to 2013. In all studied years, the area was decreased compared to previous years but the area of Urmia Lake was very close to each other in 2006 and 2007 and there was not

significant difference in water surface area of Urmia Lake in the summer time of these years. The second exception was clear between 2011 to 2012. Water surface area of Urmia Lake in 2012 year was more than 2011 year about 106 km<sup>2</sup> and after this time the area has been decreased abruptly in 2013 about 771 km<sup>2</sup>.



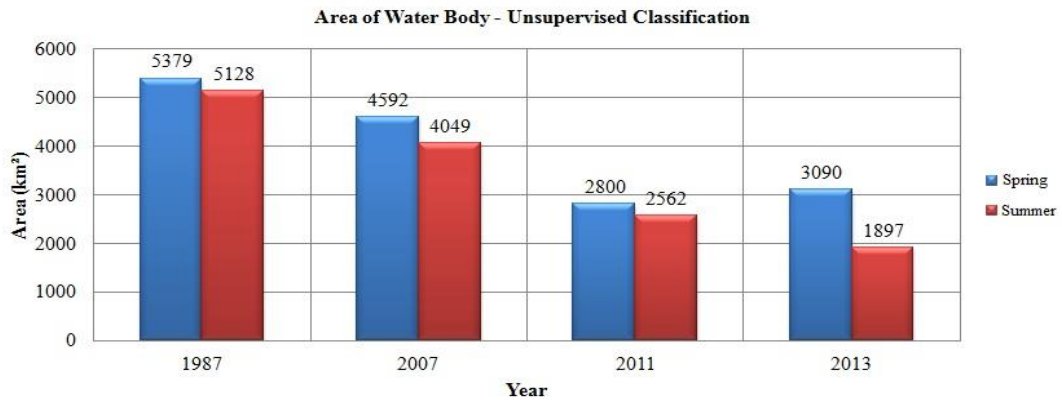
**Figure 5.13:** Water surface area in summer time – Unsupervised classification.

Spring time changes were also analyzed and compared in addition to summer time to interpret the seasonal impact on water surface area. Figure 5.14 shows water surface area changes in spring and winter times. Water surface area decreased between 1987 and 2014 but there was an exception during this time. The area of Urmia Lake in 2013-spring was more than 2011-spring about 290 km<sup>2</sup>. Water surface area in 1998-spring also calculated as 5678 km<sup>2</sup> using unsupervised classification and recoding clusters into two classes including water body and non water body.



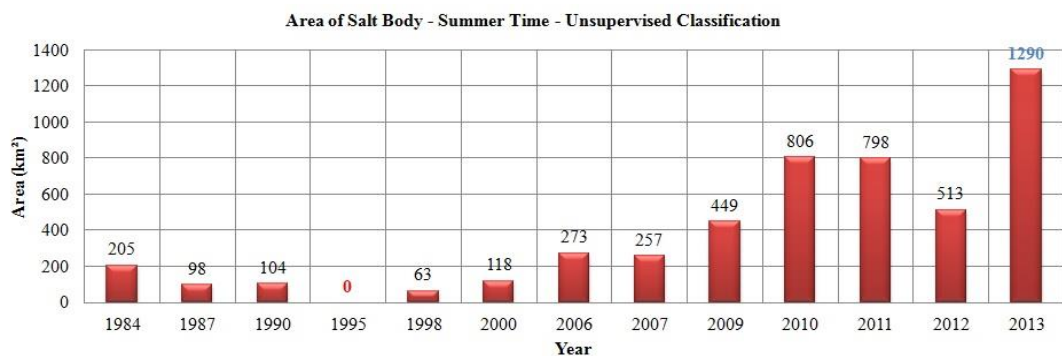
**Figure 5.14:** Water surface area in spring and winter times – Unsupervised classification.

By comparing water surface area results in summer and spring times of same years, it could be understood that the area of Urmia Lake in spring time was more than summer time. Moreover, the area of Urmia Lake decreased extremely during spring and summer of 2013. Figure 5.15 shows that the area decreased about 1193 km<sup>2</sup> during this time.



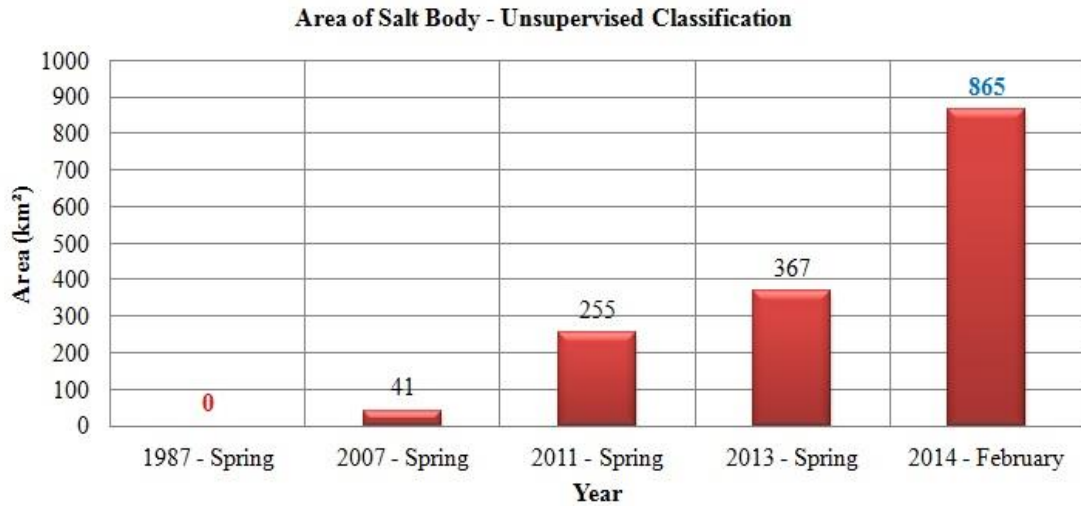
**Figure 5.15:** Comparing the results of water surface area in spring and summer times – Unsupervised classification.

Figure 5.16 shows the total area of salt class in summer time from 1984 to 2013. The minimum area was about zero km<sup>2</sup> in 1995 and the maximum area was 1290 km<sup>2</sup> in 2013. Salt area decreased from 1984 to 1995 and then it increased from 1995 to 2013. The area decreased about 285 km<sup>2</sup> between 2011 and 2012. The correlation coefficient value between area of water class and area of salt class in summer time was -0.915254967 denoting that there is a reverse correlation between the area of water class and the area of salt class at summer time. By decreasing the area of water class, the area of salt class is increasing.



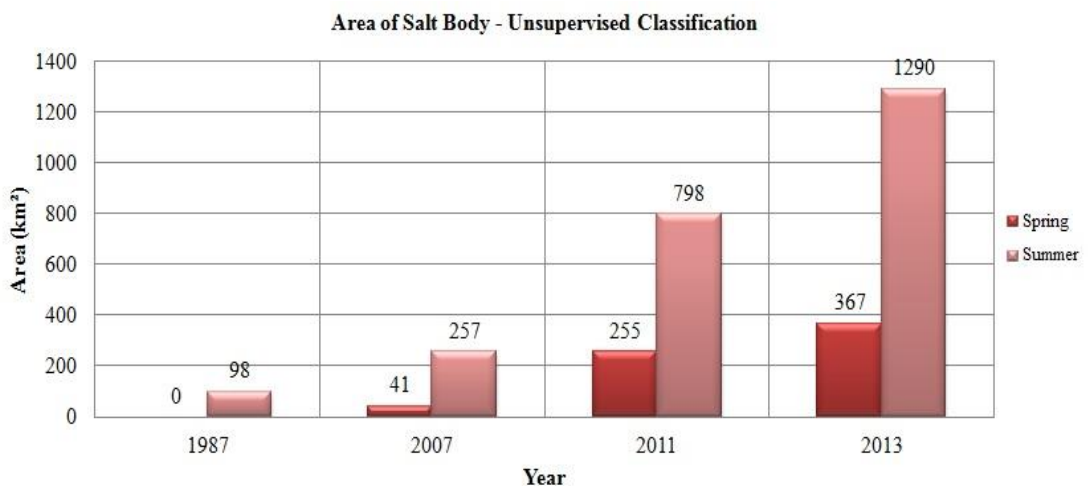
**Figure 5.16:** Salt area in summer time – Unsupervised classification.

Figure 5.17 shows the area of salt class in spring and winter times between 1987 and 2014. According to this figure, the area of salt class increased from 1987 to 2014. The minimum area was zero km<sup>2</sup> in 1987-spring and the maximum area was 865 km<sup>2</sup> in 2014-February. The correlation coefficient value between water and salt in spring and winter times was -0.857169918.



**Figure 5.17:** Salt area in spring and winter times – Unsupervised classification.

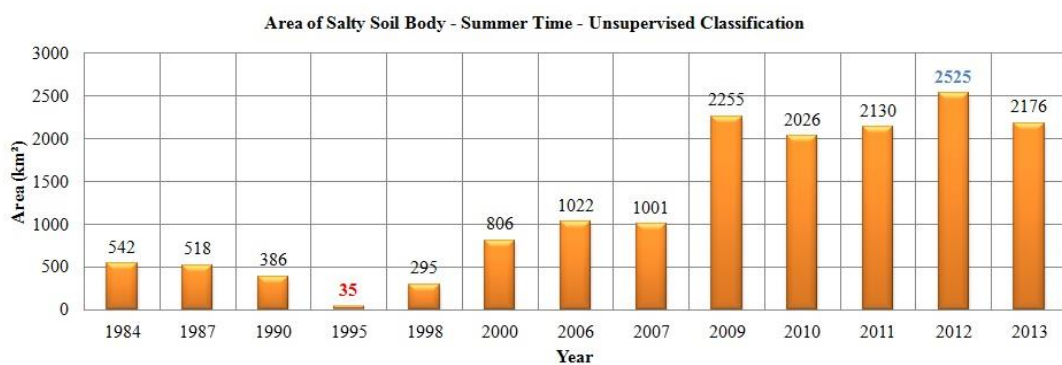
Comparing salt area results in summer and spring times of same years shows the total area of salt class in spring time was less than summer time. Moreover, the area of salt class increased significantly between spring and summer of 2013. Figure 5.18 shows the area increased about 923 km<sup>2</sup> during this time.



**Figure 5.18:** Comparing the results of salt area in spring and summer times – Unsupervised classification.

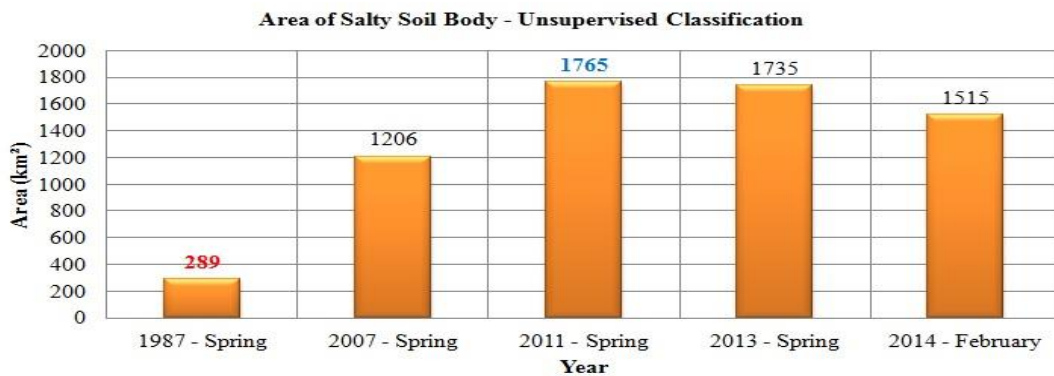


Figure 5.19 shows the total area of salty soil class in summer time from 1984 to 2013. The minimum area was about 35 km<sup>2</sup> in 1995 and the maximum area was 2525 km<sup>2</sup> in 2012. Salty soil area decreased from 1984 to 1995 and then it increased between 1995 and 2013. There was an abrupt increase in salty soil class from 2007 to 2009. The area has increased about 1254 km<sup>2</sup> during this time. The correlation coefficient value between area of water class and area of salty soil class in summer time was -0.963615176 denoting that there is a reverse correlation between the area of water and the area of salty soil at summer time. By decreasing the area of water class, the area of salty soil class is increasing.



**Figure 5.19:** Salty soil area in summer time – Unsupervised classification.

Figure 5.20 shows the area of salty soil in spring and winter times from 1987 to 2014. According to this figure, the area increased between 1987 and 2014. The minimum area was 289 km<sup>2</sup> in 1987-spring and the maximum area was 1765 km<sup>2</sup> in 2011-spring. The correlation coefficient value between water and salt body in spring time was -0.866159892.



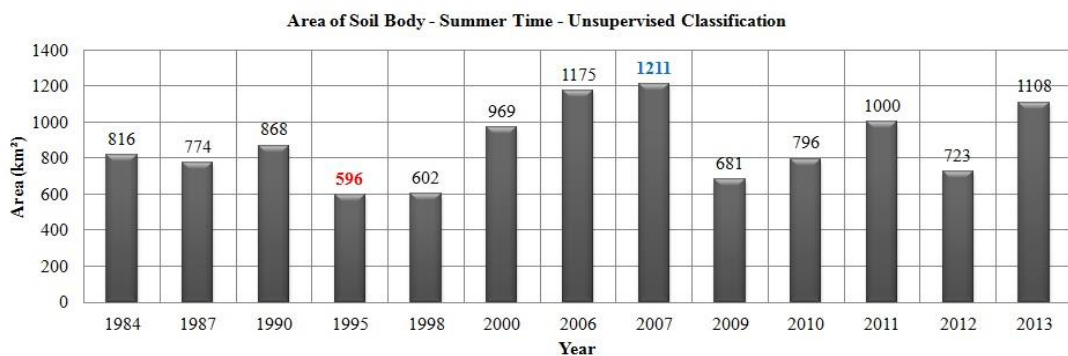
**Figure 5.20:** Salty soil area in spring and winter times – Unsupervised classification.

By comparing salty soil results in spring and summer times of same years, it could be understood that the area of salty soil class in spring time was less than summer time, but there was an exception in 2007 year and the area of salty soil class in spring was more than summer about 205 km<sup>2</sup> but it should be considered that the area of salt class in spring time of 2007 was less than summer time of 2007 about 216 km<sup>2</sup>. Figure 5.21 shows that the maximum change in increasing area is about 441 km<sup>2</sup> during spring and summer time of 2013.



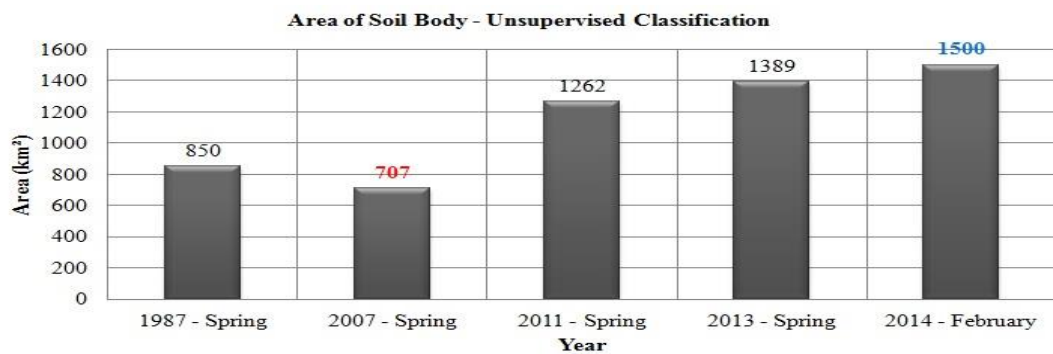
**Figure 5.21:** Comparing the results of salty soil class in spring and summer times – Unsupervised classification.

Figure 5.22 shows the total area of soil class at summer time between 1984 and 2013. The minimum area was about 596 km<sup>2</sup> in 1995 and the maximum area was 1211 km<sup>2</sup> in 2007. Soil area changes didn't show especial behavior like last classes. The correlation coefficient value between area of water class and area of soil class in summer time is -0.389705917. This value means that there was less correlation between these bodies because soil class included areas which weren't in related to water surface area changes.



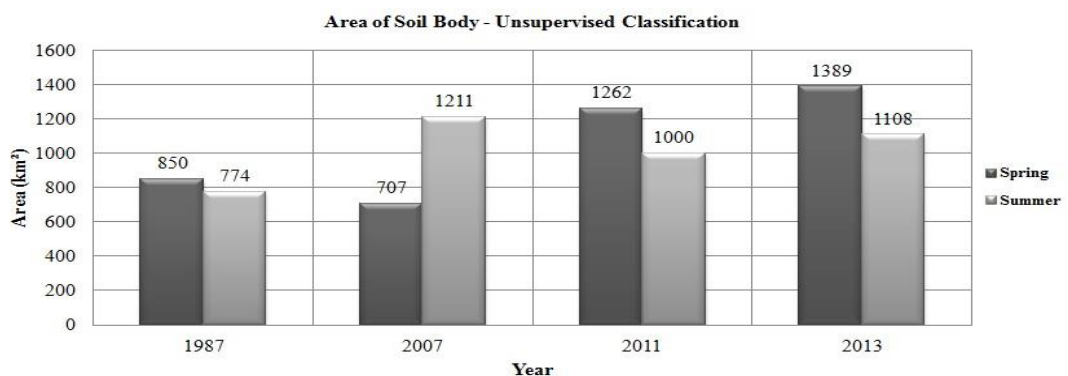
**Figure 5.22:** Soil area in summer time – Unsupervised classification.

Figure 5.23 shows the total area of soil class in spring and winter times from 1987 to 2014. According to this figure, the area increased between 2007 and 2014. The minimum area was 707 km<sup>2</sup> in 2007-spring and the maximum area was 1500 km<sup>2</sup> in 2014-February. The correlation coefficient values between water class and soil class in spring and winter times was -0.914444688 denoting that there is a reverse correlation between the area of water class and the area of soil class at spring and winter times. By decreasing the area of water class, the area of soil class is increasing.



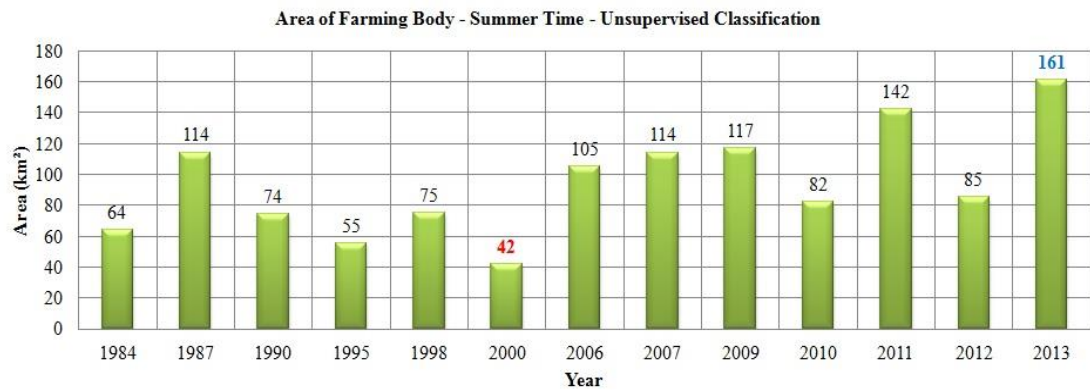
**Figure 5.23:** Soil area in spring and winter times – Unsupervised classification.

By comparing soil body area results in spring and summer times of same years, it could be understood that the area of soil class in spring time was more than summer time but there was an exception in 2007 year and the area of soil class in spring was less than summer time about 500 km<sup>2</sup>. Figure 5.24 shows that the maximum change in area was about 500 km<sup>2</sup> between spring and summer time of 2007.



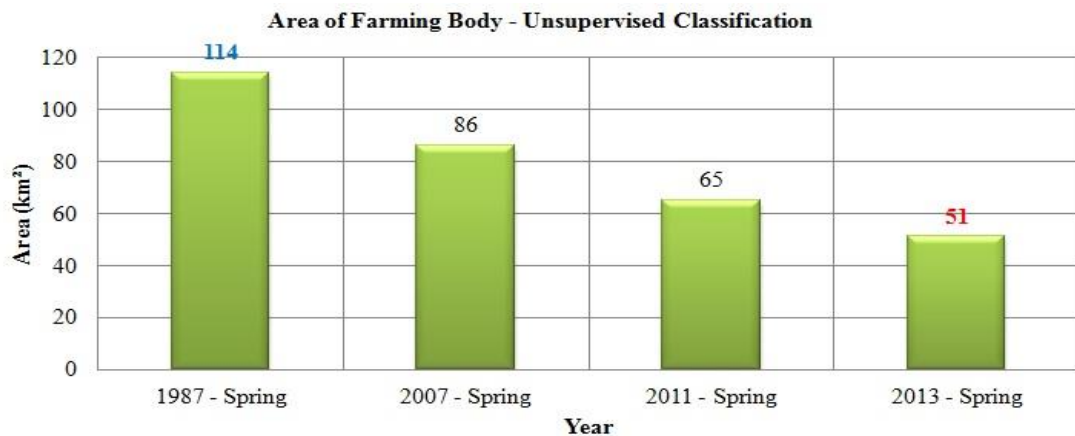
**Figure 5.24:** Comparing the results of soil area in spring and summer times – Unsupervised classification.

Figure 5.25 shows the total area of farming class in summer time from 1984 to 2013. The minimum area was about 42 km<sup>2</sup> in 2000 and the maximum area was 161 km<sup>2</sup> in 2013. The main focus of this research was to investigate the multi-temporal changes of water area, therefore farming class was not investigated in detail. The farming area changes aren't the aim of this study because this body has less area between classified bodies.



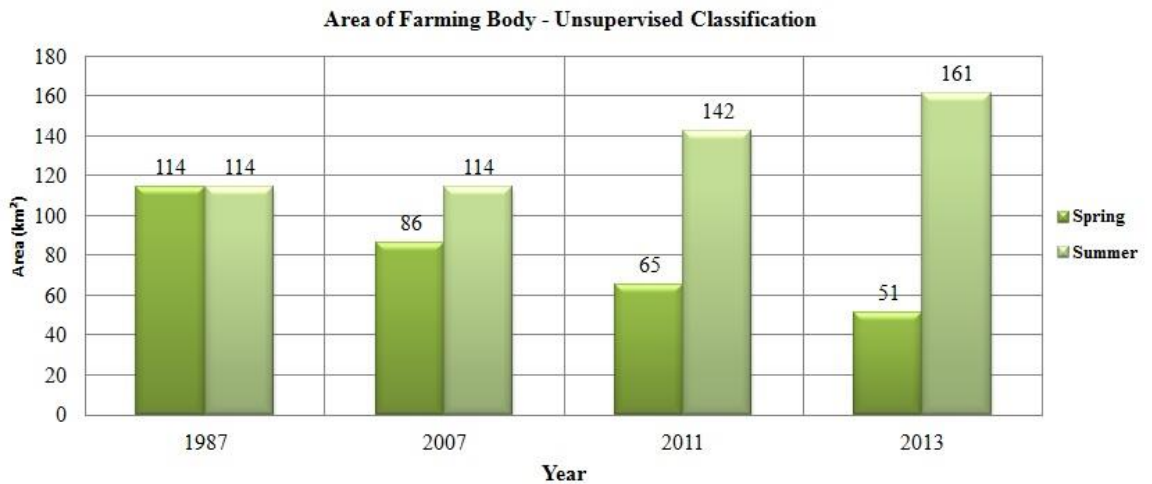
**Figure 5.25:** Farming area in summer time – Unsupervised classification.

Figure 5.26 shows the area of farming class in spring time from 1987 to 2013. According to this figure, the area increased between 1987 and 2014. The minimum area was 51 km<sup>2</sup> in 2013-spring and the maximum area was 114 km<sup>2</sup> in 2013-spring.



**Figure 5.26** Farming area in spring time – Unsupervised classification.

By comparing farming results in spring and summer times of same years, it could be understood that the area of farming class in spring time was less than summer time. Figure 5.27 shows that the maximum change was about 110 km<sup>2</sup> between spring and summer time of 2013.



**Figure 5.27:** Comparing the results of farming area in spring and summer times – Unsupervised classification.

The areas of different classes obtained from unsupervised classification in spring and winter times from 1987 to 2014 show decreases for water class and increases for salt and salt soil classes. Table 5.1 shows the results of all classes in spring and winter times.

**Table 5.1:** Unsupervised classification results (km<sup>2</sup>) in spring and winter times.

Year	Water	Salt	Salty soil	Soil	Farming	Total area
1987	5379	0	289	850	114	6632
2007	4592	41	1206	707	86	6632
2011 <sup>1</sup>	2800	255	1765	1262	65	6147
2013	3090	367	1735	1389	51	6632
2014 <sup>2</sup>	2215	865	1515	1500	-	6095

<sup>1</sup> Classified results of DMC image. The classified area was 6147 km<sup>2</sup> in 2011 year.

<sup>2</sup> Classified results of 2014-February. The total classified area was 6095.

According to the results of unsupervised classification in table 5.1, the total classified area was 6632 km<sup>2</sup> in all years but there were two exceptions in 2011-spring and 2014-February. In 2011 year, DMC satellite was used and the study area covered by this image was smaller compared to the area covered by Landsat data. Also, the study area covered in 2014-February was smaller than other dates because a frame was enough to analyze water body changes in Urmia Lake. There was also no farming class in 2014-February because of the especial condition in winter time that it made difficult to analyze farming bodies. In other words, there was no agricultural activity during winter and farming bodies seemed soil during this season.

Table 5.2 shows the results of all classes in summer time. The results of unsupervised classification in summer time show that there were increases in the area of water class and decreases in the area of salt and salty soil classes from 1984 to 1995. It also shows decreasing trend in the area of water class and increasing trend in the area of salt and salty soil classes between 1995 and 2013.

**Table 5.2:** Unsupervised Classification results (km<sup>2</sup>) in Summer Time.

Year	Water	Salt	Salty soil	Soil	Farming	Total area
1984	5005	205	542	816	64	6632
1987	5128	98	518	774	114	6632
1990	5200	104	386	868	74	6632
1995	5946	0	35	596	55	6632
1998	5597	63	295	602	75	6632
2000	4697	118	806	969	42	6632
2006	4057	273	1022	1175	105	6632
2007	4049	257	1001	1211	114	6632
2009	3130	449	2255	681	117	6632
2010	2922	806	2026	796	82	6632
2011	2562	798	2130	1000	142	6632
2012 <sup>1</sup>	2668	513	2525	723	85	6514
2013	1897	1290	2176	1108	161	6632

<sup>1</sup> Classified results of DMC satellite. The classified area was 6514 km<sup>2</sup> in 2012 year.

According to the results of unsupervised classification in table 5.2 the total classified area was 6632 km<sup>2</sup> in all years but there was an exception in 2012. In 2012 year, DMC satellite was used and the study area was smaller compared to the area covered by Landsat data. Water surface area of Urmia Lake increased from 1984 to 1995 and then it decreased from 1995 to 2013. The area of salt and salty soil classes increased during this time.

### 5.2.2 Supervised Classification

In supervised classification process, the analyst selects training areas representing different patterns or land cover features to be input for the supervised classification algorithm. Supervised classification is closely controlled by the analyst. Aerial photos, ground truth data or maps could be used for the selecting of training areas. In supervised training, the analyst relies on his/her own pattern recognition skills and a priori knowledge of the data to help the system determine the statistical criteria (signatures) for data classification. The location of a specific characteristic, such as a

land cover type, may be known through ground truthing. Ground truth data refer to the acquisition of information about the study area from field work, analysis of aerial photography, personal experience, etc. Ground truth data have been considered as reference (assumed as correct) data available for the study area. Ground truth and remotely sensed data should be collected simultaneously avoid any misunderstanding or mismatching [4,12,13].

The maximum likelihood method was used in this research. This rule is based on the probability that a pixel belongs to a particular class. The basic equation assumes that these probabilities are equal for all classes, and that the input bands have normal distributions. It means maximum likelihood algorithm assumes that the histograms of the bands of data have normal distributions.

To compare the results of supervised classification with unsupervised classification, the study area was classified into 5 classes such as unsupervised classification. In the first step of supervised classification at least 10 training areas were selected as Area Of Interests (AOI) for each class and finally signatures were merged to extract 5 classes, including Water, Salt, Salty Soil (Badland), Soil, and Farming classes in ERDAS IMAGINE. Finally, the area of all classes were extracted and compared in different dates in ArcGIS and the results were prepared as comparable maps. To obtain good supervised classification results, it was necessary to select enough AOIs and this was the most important part of a supervised classification requiring useful information about study area. The analyst should have knowledge about the study area to identify different classes from each other.

Figure 5.28 to 5.32 show the maps of supervised classification between 1984 and 2014. Blue color shows water areas, red color shows salt areas, yellow color shows salty soil areas, brown color shows soil body and green color shows farming areas.

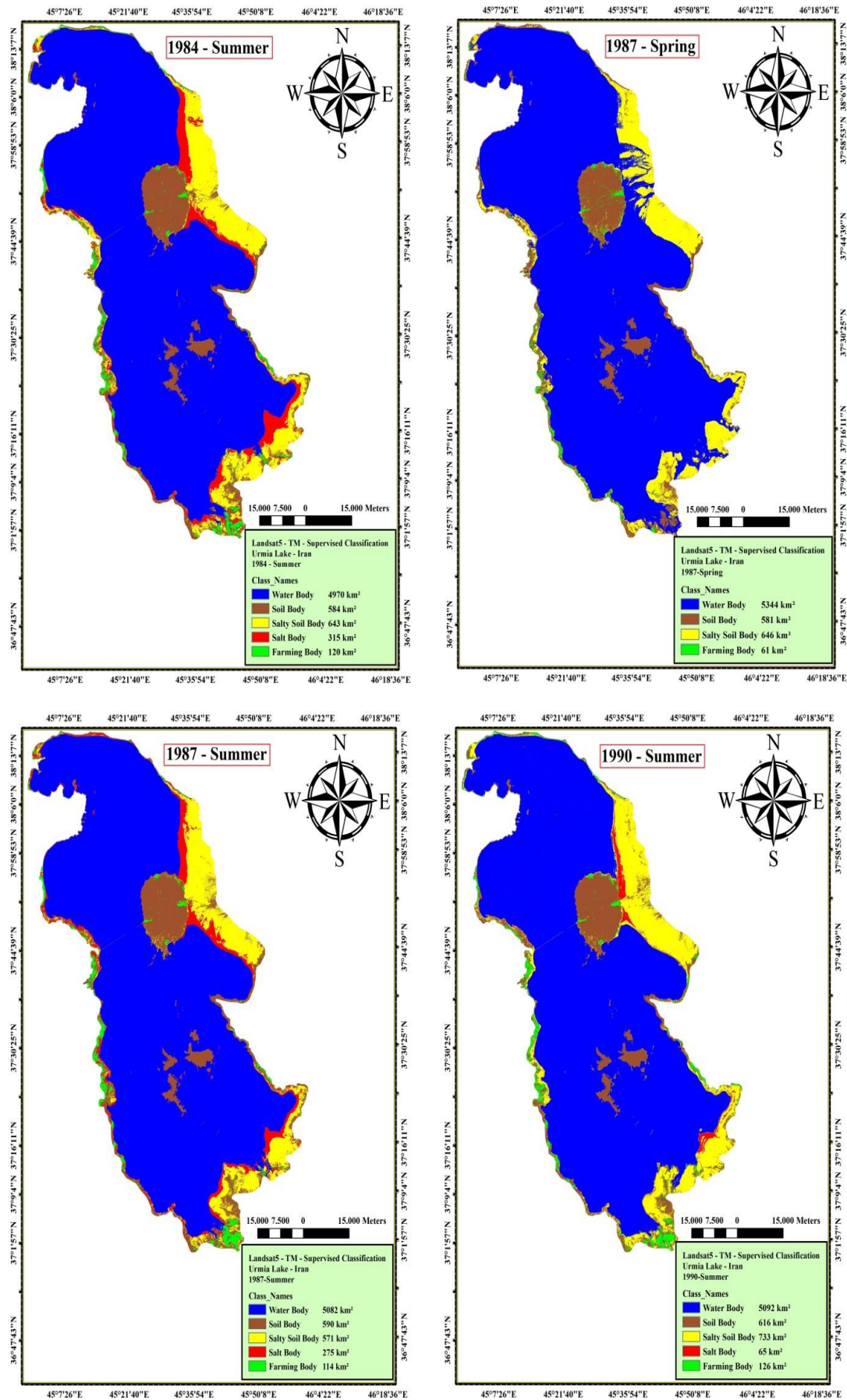


Figure 5.28: Supervised classification maps from 1984 to 1990.



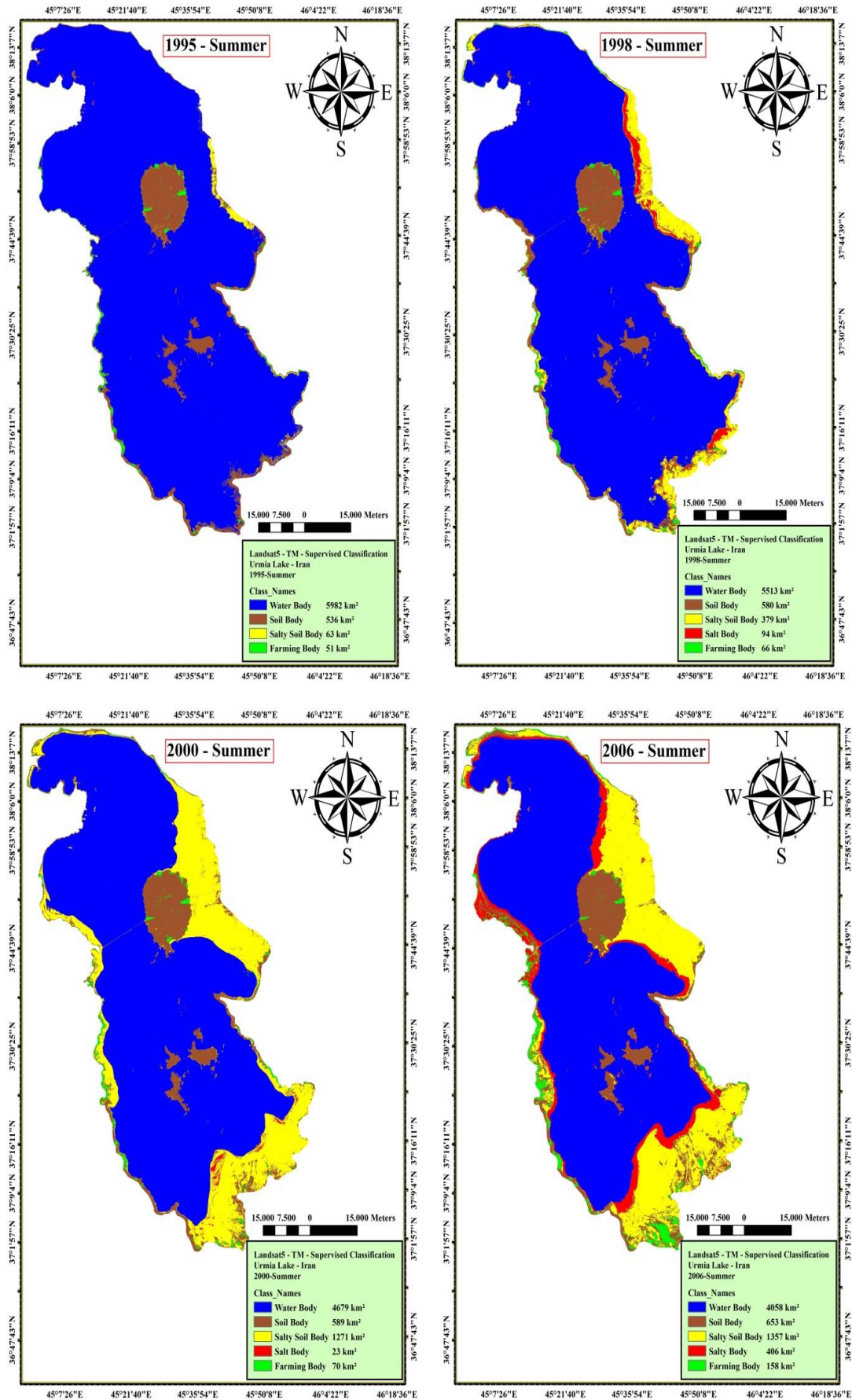


Figure 5.29: Supervised classification maps from 1995 to 2006.

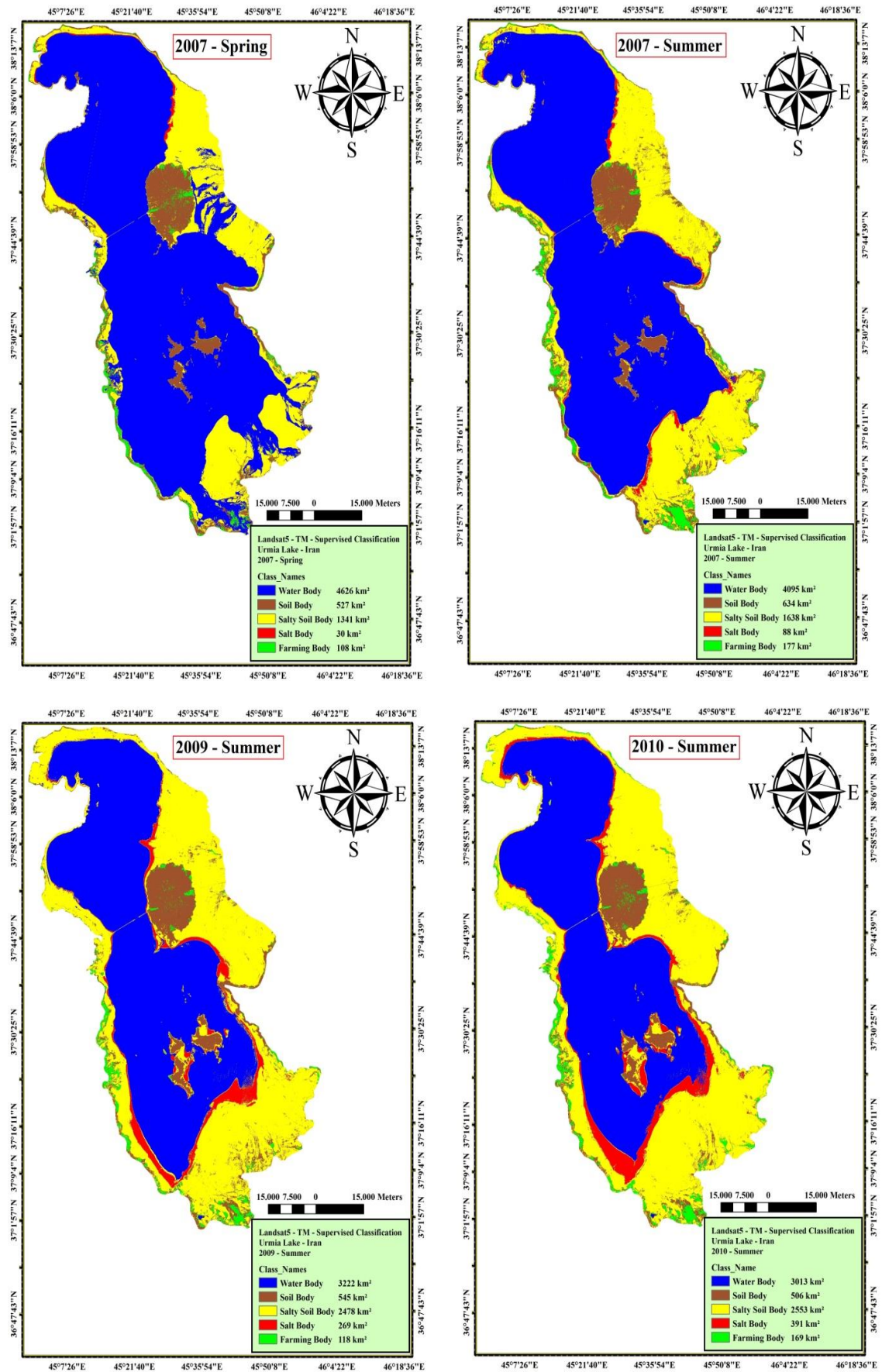


Figure 5.30: Supervised classification maps from 2007 to 2010.

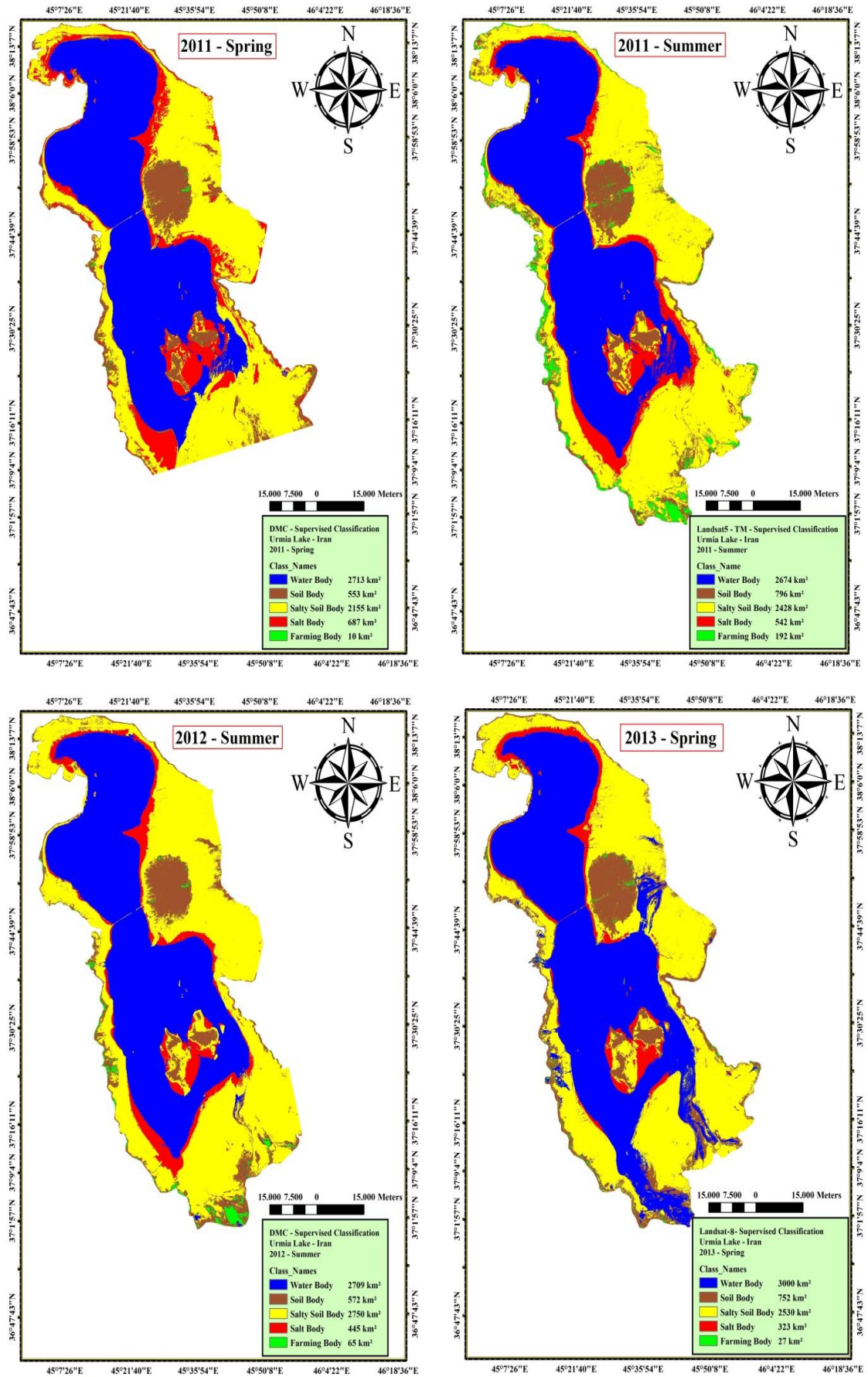
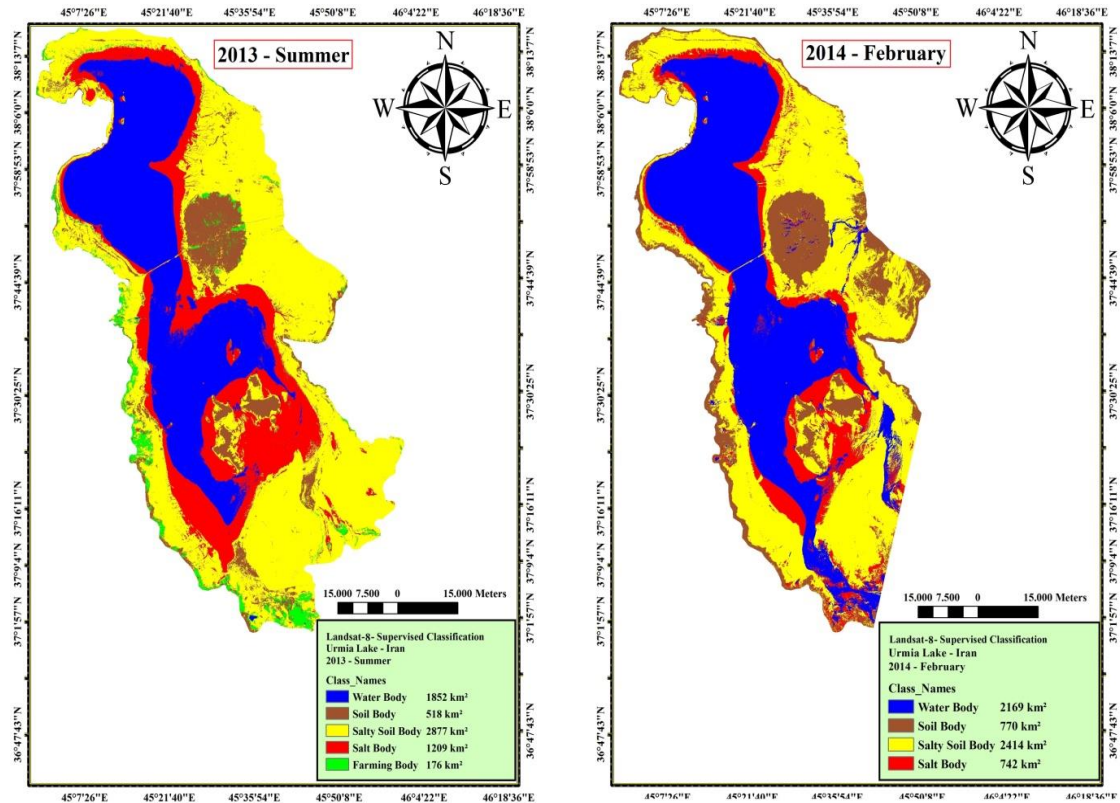
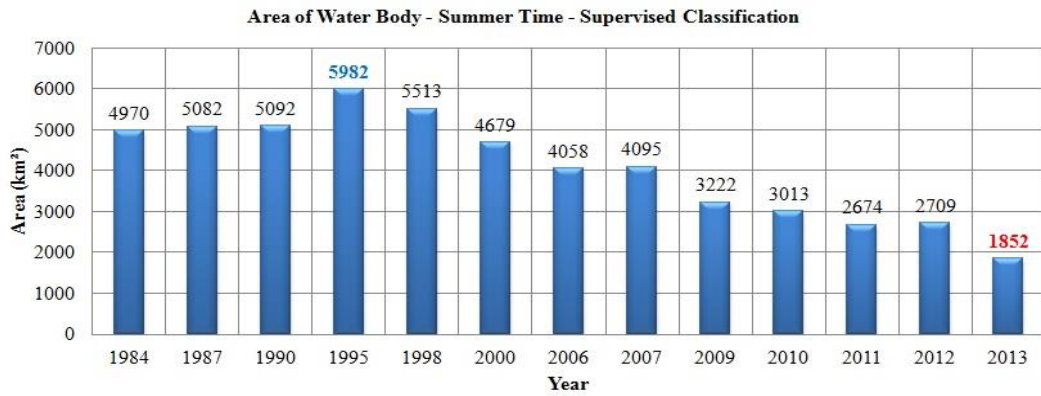


Figure 5.31: Supervised classification maps from 2011 to 2013.



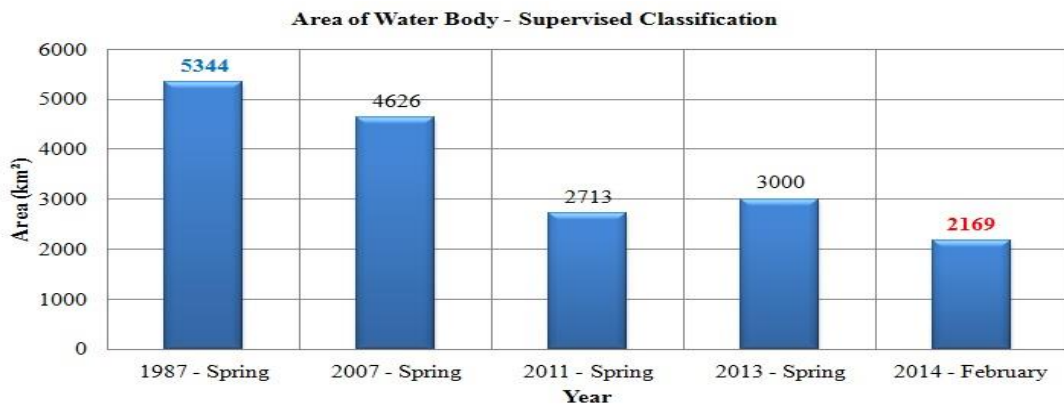
**Figure 5.32:** Supervised classification maps of 2013-summer and 2014 February.

Figure 5.33 shows the total area of water class in summer time from 1984 to 2013. According to this figure, water surface area of Urmia Lake increased from 1984 to 1995, then there was a decreasing trend in water surface area between 1995 and 2013. Decreasing water surface area was also considerable between 1998-2000 and 2007-2009. The water surface area difference between 1998 and 2000 was 834 km<sup>2</sup> and its difference between 2007 and 2009 was 873 km<sup>2</sup>. The maximum area of Urmia Lake was 5982 km<sup>2</sup> in 1995 and the minimum area was 1852 km<sup>2</sup> in 2013. There were two exceptions in water surface area changes between 1998 and 2013. In all studied years, the area was decreased compared to previous years, but the area of Urmia Lake was very close to each other in 2006 and 2007. There was not significant difference in water surface area of Urmia Lake in the summer time of these years. The area of Urmia Lake in 2007 was more than 2006 about 37 km<sup>2</sup>. The second exception was obvious between 2011 and 2012. Water surface area of Urmia Lake in 2012 was more than 2011 about 35 km<sup>2</sup> and after this time the area has been decreased abruptly in 2013 about 857 km<sup>2</sup>.



**Figure 5.33:** Water surface area in summer time - Supervised classification.

Spring time changes were also analyzed and compared in addition to summer time to interpret seasonal impact on water surface area. Figure 5.34 shows water surface area changes in spring and winter times from 1987 to 2014. The area of Urmia Lake in 2013-spring was more than 2011-spring about 287 km<sup>2</sup>. Water surface area in 1998-spring also calculated about 5808 km<sup>2</sup> using supervised classification by considering training area selection from water body and non water body.



**Figure 5.34:** Water surface area in spring and winter times – Supervised classification.

By comparing water surface area results in summer and spring times of same years, it could be understood that the area of Urmia Lake in spring time was more than summer time. Moreover, the area of Urmia Lake decreased considerably between spring and summer of 2013. Figure 5.35 shows the area decreased about 1148 km<sup>2</sup> during this time.

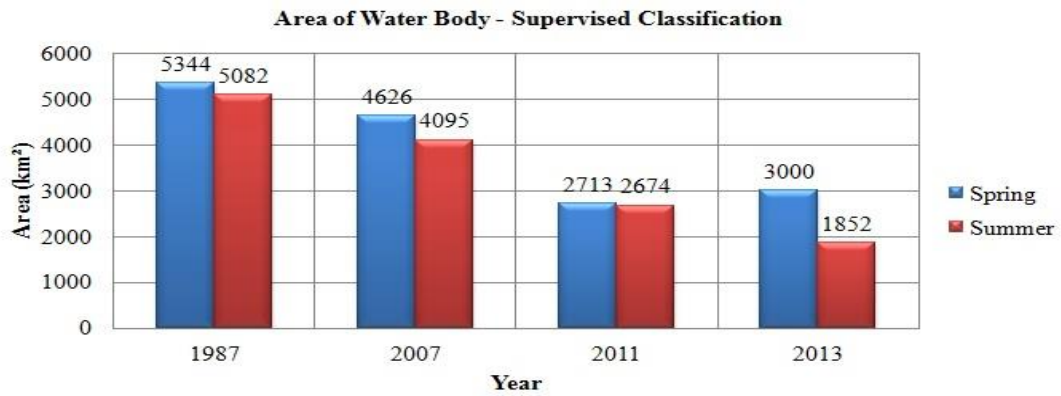


**Figure 5.35:** Comparing the results of water surface area in spring and summer times – Supervised classification.

Figure 5.36 shows the total area of salt class in summer time from 1984 to 2013. The minimum area was about zero km<sup>2</sup> in 1995 and the maximum area was 1209 km<sup>2</sup> in 2013. Whereas salt area decreased between 1984 and 1995, these areas increased from 1995 to 2013. Total salt area decreased about 97 km<sup>2</sup> from 2011 to 2012. The correlation coefficient value between area of water class and area of salt class in summer time was -0.798572793. This value corresponded to a reverse correlation between the area of water class and the area of salt class in summer time. By decreasing the area of water, the area of salt is increasing. Most of the salty areas were mixed with water class (salty water), whenever there was change in water class due to extensive evaporation, temperature increases or other reasons, remaining part became salt. Therefore, water changes impacts the amount of salt within the area. This is the case when working on saline lakes and we do not interpret this reverse relationship as a global approach but a specific condition for our region of interest.

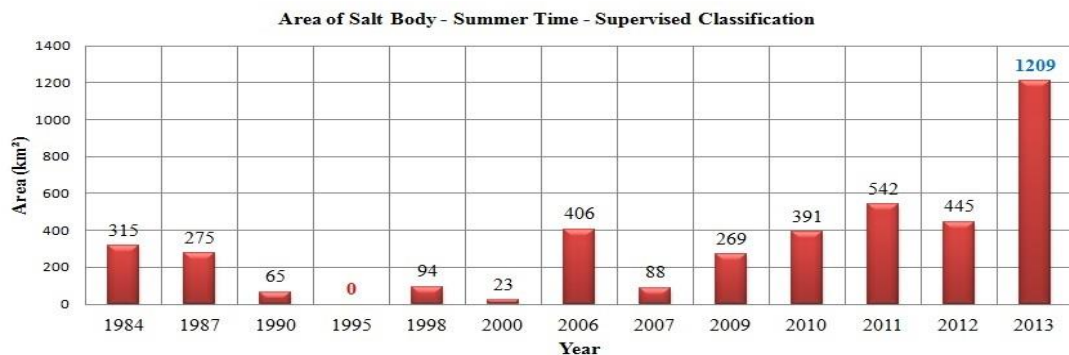


**Figure 5.36:** Salt area in summer time - Supervised classification.

Figure 5.37 shows the area of salt class in spring and winter times from 1987 to 2014. According to this figure, there was an increasing trend between 1987 and 2014. The minimum area was about zero km<sup>2</sup> in 1987-spring and the maximum area was 742 km<sup>2</sup> in 2014-February. The correlation coefficient values between water and salt classes in spring was -0.940381275 denoting that there was a reverse correlation between the area of water and the area of salt in summer time. By decreasing the area of water, the area of salt is increasing similar to the previous explanation.



**Figure 5.37:** Salt area in spring and winter times - Supervised classification.

By comparing salt area results in summer and spring times of same years, it could be understood that the area of salt in spring time was less than summer time. Moreover, the area of salt increased significantly between spring and summer of 2013 considering that 2013 was a drought year. There was an exception in 2011 and the area of salt in spring was more than summer in this year. Moreover, the area of salt increased considerably between spring and summer of 2013. Figure 5.38 shows the area increased about 886 km<sup>2</sup> during this time.



**Figure 5.38:** Comparing the results of salt area in spring and summer times – Supervised classification.

Figure 5.39 shows the results of salty soil in summer time from 1984 to 2013. The minimum area was about 63 km<sup>2</sup> in 1995 and the maximum area was 2877 km<sup>2</sup> in 2013. Salty soil area decreased from 1984 to 1995 and then it increased between 1995 and 2013. There was an abrupt increase in salty soil class from 2007 to 2009. The area increased about 840 km<sup>2</sup> during this time. The correlation coefficient value between area of water and area of salty soil in summer time was -0.979521523 denoting that there was a reverse correlation between the area of water and the area of salty soil in summer time. By decreasing the area of water, the area of salty soil is increasing.

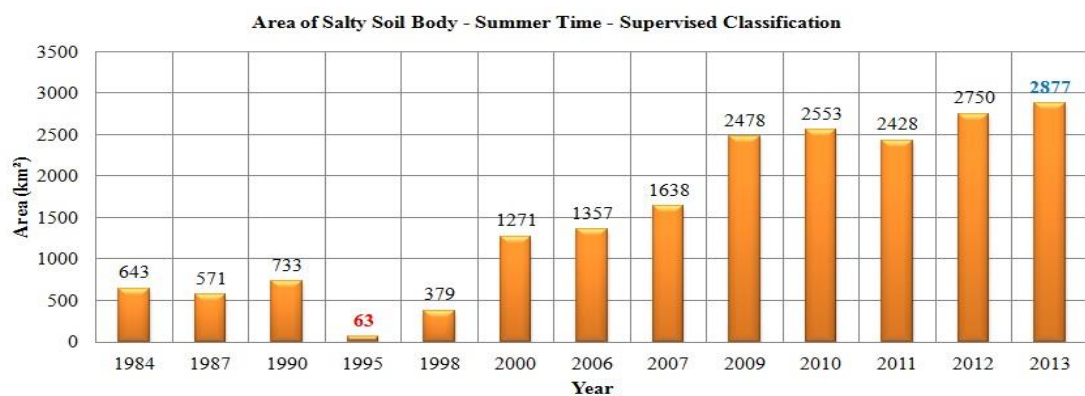


**Figure 5.39:** Salty soil area in summer time – Supervised classification.

Figure 5.40 shows the area of salty soil in spring and winter times from 1987 to 2014. According to this figure, the area increased between 1987 and 2014. The minimum area was about 646 km<sup>2</sup> in 1987-spring and the maximum area was 2530 km<sup>2</sup> in 2011-spring. The correlation coefficient value between water and salty soil body in spring was -0.949215445.



**Figure 5.40:** Salty soil area in spring and winter times – Supervised classification.

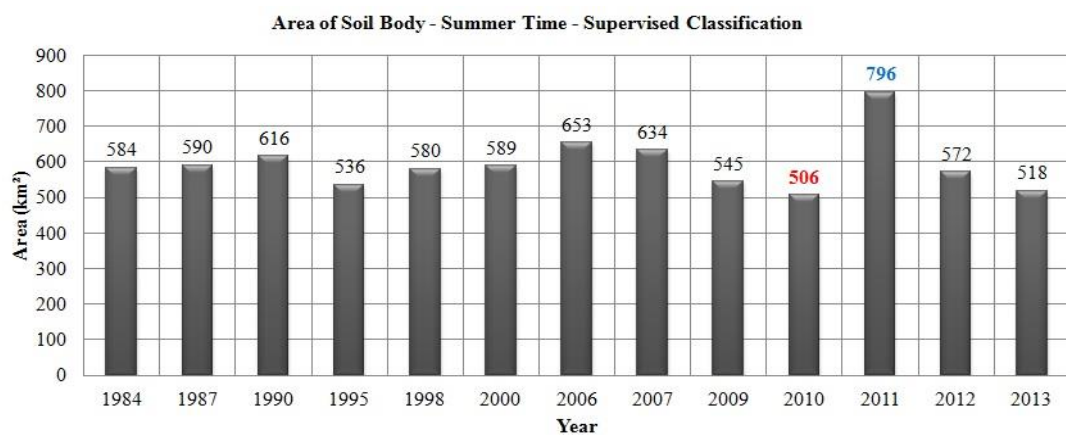


By comparing salty soil body results in spring and summer times of same years, it could be understood that the area of salty soil in spring time was less than summer time, but there was an exception in 1987 year and the area of salty soil body in spring was more than summer about 75 km<sup>2</sup>.



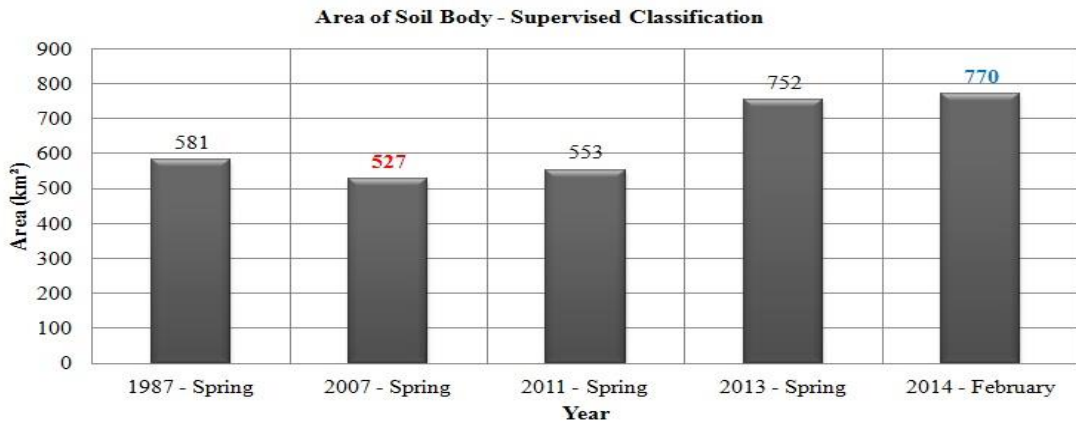
**Figure 5.41:** Comparing the results of salty soil in spring and summer times – Supervised classification.

Figure 5.42 shows the total area of soil in summer time between 1984 and 2013. The minimum area was about 506 km<sup>2</sup> in 2010 and the maximum area was 796 km<sup>2</sup> in 2011. Soil class changes didn't show especial behavior like other classes. The correlation coefficient value between area of water and area of soil in summer time was -0.064325963. This value means that there was no correlation between these classes.



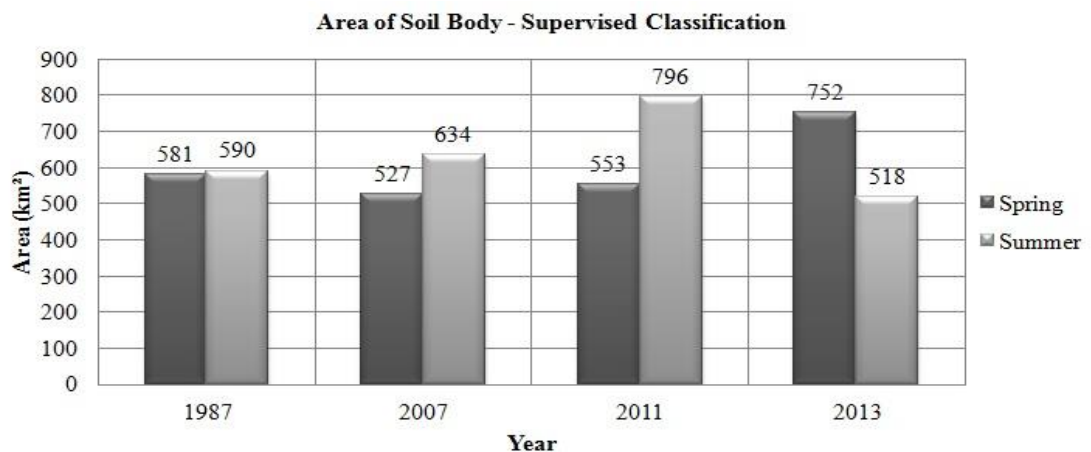
**Figure 5.42:** Soil area in summer time – Supervised classification.

Figure 5.43 shows the area of soil in spring and winter times from 1987 to 2014. According to this figure, the area increased from 2007 to 2014. The minimum area was 527 km<sup>2</sup> in 2007-spring and the maximum area was 770 km<sup>2</sup> in 2014-February. The correlation coefficient value between water and soil in spring was -0.635128954.



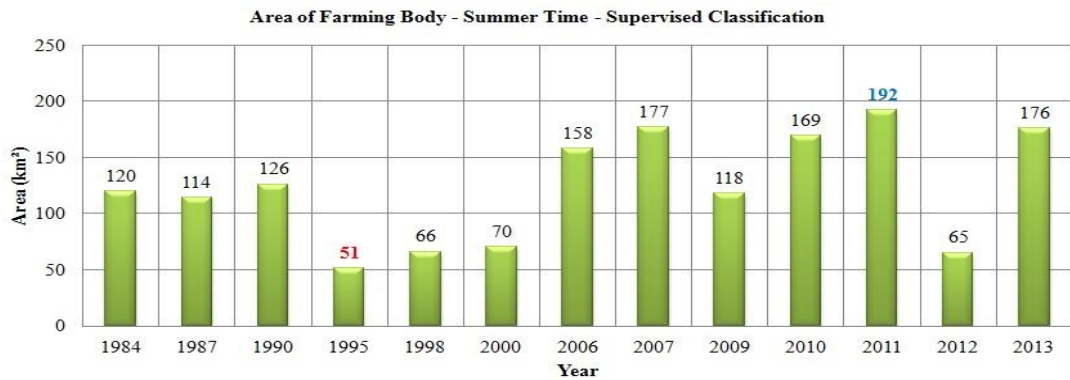
**Figure 5.43:** Soil area in spring and winter times – Supervised classification.

By comparing soil area results in spring and summer times of same years, it could be understood that the area of soil in spring time was less than summer time, but there was an exception in 2013 year and the area of soil body in spring was more than summer time about 234 km<sup>2</sup>. Figure 5.44 shows that the maximum change was between spring and summer times of 2011 and 2013.



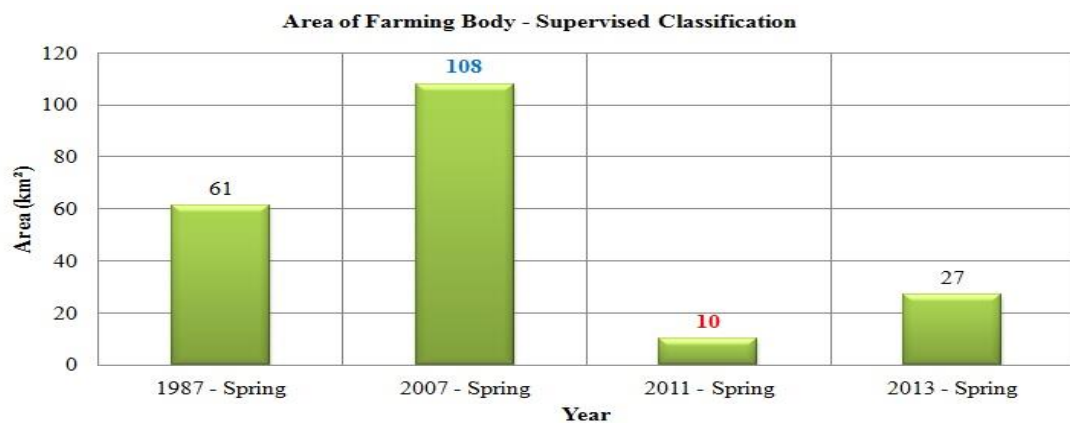
**Figure 5.44:** Comparing the results of soil in spring and summer times – Supervised classification.

Figure 5.45 shows the results of farming in summer time from 1984 to 2013. The minimum area was about 51 km<sup>2</sup> in 1995 and the maximum area was 192 km<sup>2</sup> in 2011.



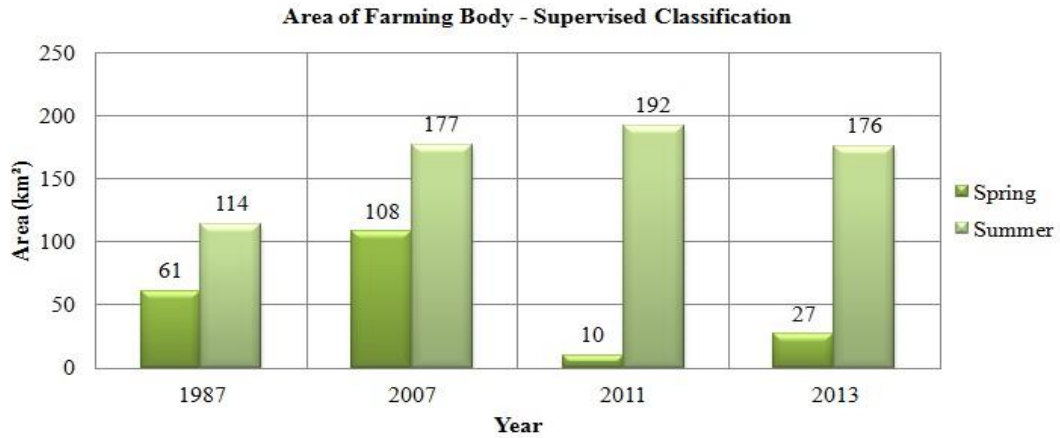
**Figure 5.45:** Farming area in summer time– Supervised classification.

Figure 5.46 shows the area of farming in spring time from 1987 to 2013. According to this figure, the area increased between 1987 and 2007 and then it decreased. The minimum area was 10 km<sup>2</sup> in 2011-spring and the maximum area was 108 km<sup>2</sup> in 2007-spring.



**Figure 5.46:** Farming area in spring time – Supervised classification.

By comparing farming results in spring and summer times of same years, it could be understood that the area of farming body in spring time was less than summer time. Figure 5.47 shows that the maximum change was about 182 km<sup>2</sup> between spring and summer times of 2011.



**Figure 5.47:** Comparing the results of farming class in spring and summer times – Supervised classification.

The areas of different classes obtained from supervised classification in spring and winter times show decreases for water class and increases for salt and salt soil classes. Table (5.3) shows the results of all classes in spring and winter times.

**Table 5.3:** Supervised classification results (km<sup>2</sup>) in spring and winter times.

Year	Water	Salt	Salty soil	Soil	Farming	Total area
1987	5344	0	646	581	61	6632
2007	4626	30	1341	527	108	6632
2011 <sup>1</sup>	2713	687	2155	553	10	6118
2013	3000	323	2530	752	27	6632
2014 <sup>2</sup>	2169	742	2414	770	-	6095

<sup>1</sup>Classified results of DMC satellite. The classified area was 6118 km<sup>2</sup> in 2011 year.

<sup>2</sup>Classified results of 2014-February. The total classified area was 6095.

According to the results of supervised classification in table 5.3, the total classified area was 6632 km<sup>2</sup> in all years but there were two exceptions in 2011-spring and 2014-February. In 2011 year DMC satellite was used and the study area covered by this image was smaller compared to the area covered by Landsat data. Also, the study area covered in 2014-February was smaller than other dates because a frame was enough to analyze water changes in Urmia Lake. There was also no farming class in 2014-February because of the especial condition in winter time that it made difficult to analysis farming bodies. In other words, there was no agricultural activity during winter and farming areas seemed soil during this season.

Table 5.4 shows the total area of all classes at summer time. The results of supervised classification in summer time show increases in the area of water and

decreases in the area of salt and salty soil from 1984 to 1995. It also shows decreasing trend in the area of water and increasing trend in the area of salt and salty soil from 1995 to 2013.

**Table 5.4:** Supervised Classification results (km<sup>2</sup>) in Summer Time.

Year	Water	Salt	Salty soil	Soil	Farming	Total area
1984	4970	315	643	584	120	6632
1987	5082	275	571	590	114	6632
1990	5092	65	733	616	126	6632
1995	5982	0	63	536	51	6632
1998	5513	94	379	580	66	6632
2000	4679	23	1271	589	70	6632
2006	4058	406	1357	653	158	6632
2007	4095	88	1638	634	177	6632
2009	3222	269	2478	545	118	6632
2010	3013	391	2553	506	169	6632
2011	2674	542	2428	796	192	6632
2012 <sup>1</sup>	2709	445	2750	572	65	6541
2013	1852	1209	2877	518	176	6632

<sup>1</sup>Classified results of DMC satellite. The classified area was 6541 km<sup>2</sup> in 2012 year.

According to the results of supervised classification in table (5.4) the total classified area was 6632 km<sup>2</sup> in all years but there was an exception in 2012. In 2012 year, DMC satellite was used and the study area was smaller compared to area covered by Landsat data. Water surface area of Urmia Lake increased from 1984 to 1995 and then it decreased from 1995 to 2013 and the area of salt and salty soil areas increased during this time.

### 5.2.3 Comparing The Results Of Unsupervised And Supervised Classification

By comparing the results of unsupervised and supervised methods it could be concluded that there were differences between the results of supervised classification and unsupervised classification. According to Figure 5.48 to 5.57, the results of different classification methods weren't same and sometimes there were noticeable differences between the results of unsupervised classification and supervised classification.

To have an accurate classification, the importance of having knowledge about the study area and gathering control points to examine the accuracy of classification were important tasks that needs to be conducted. Gathered control points using GPS

in 2014-February and a collection of control points which gathered using Google Earth in August month of 2010, 2011, and 2013 were used in this study to conduct the accuracy assessment of classifications in mentioned years. ERDAS IMAGINE was used to check the accuracy of classification to select best results.

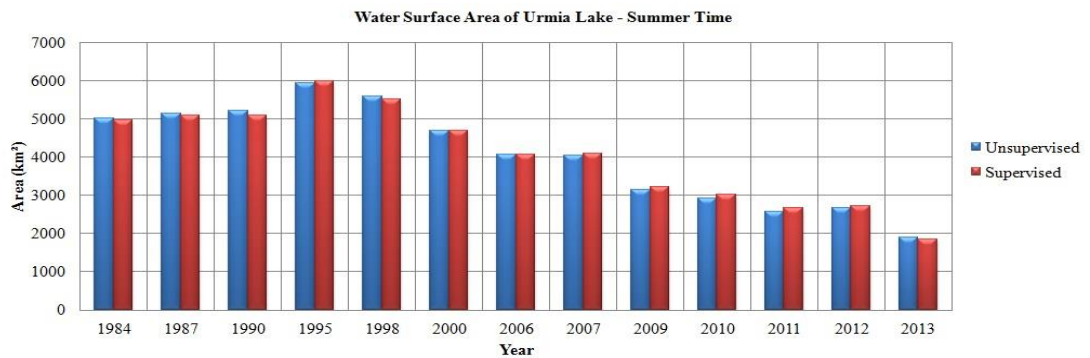


**Figure 5.48:** Comparing the results of water area in summer time.

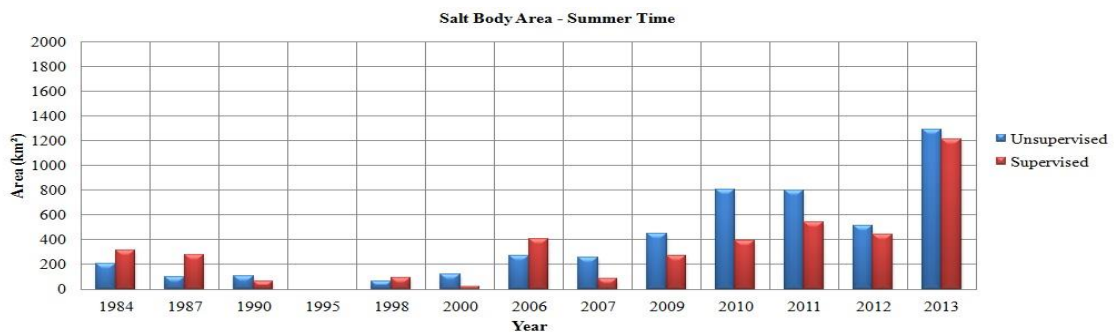


**Figure 5.49:** Comparing the results of salt area in summer time.

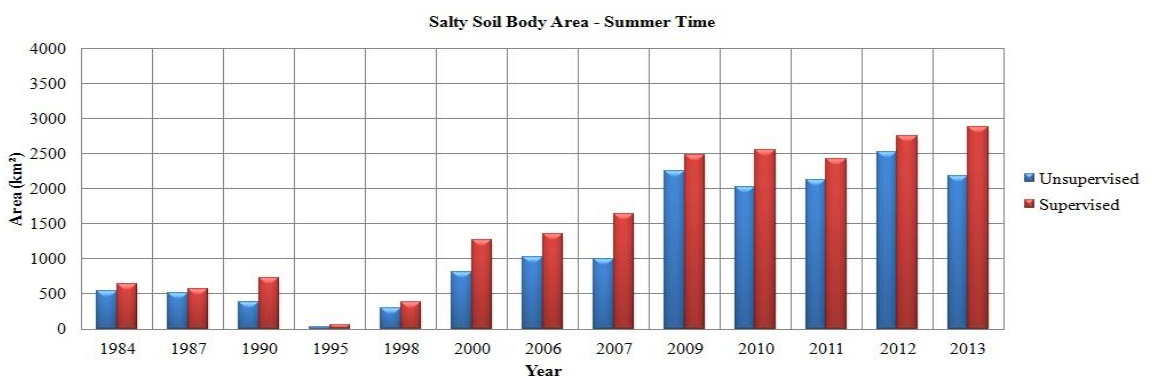


**Figure 5.50:** Comparing the results of salty soil area in summer time.

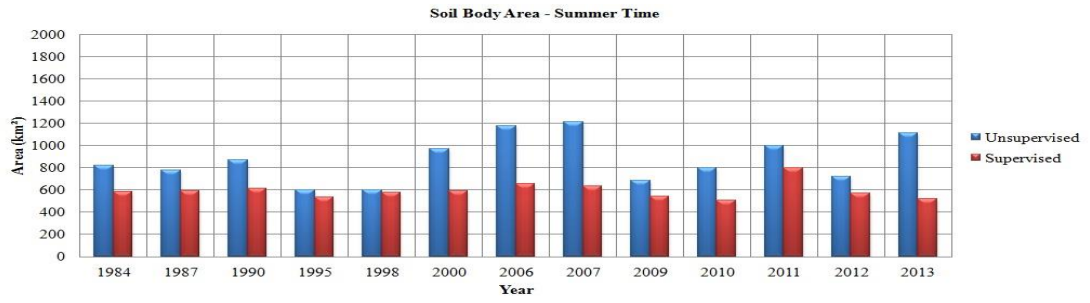


**Figure 5.51:** Comparing the results of soil class in summer time.

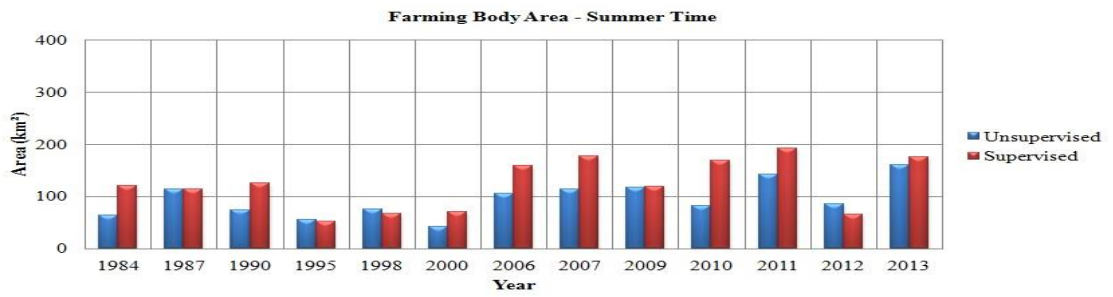


**Figure 5.52:** Comparing the results of farming class in summer time.

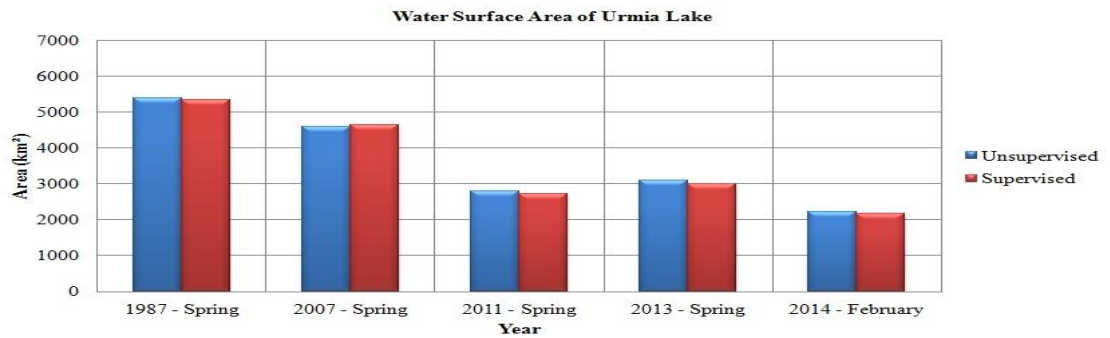


**Figure 5.53:** Comparing the results of water class in spring and winter times.

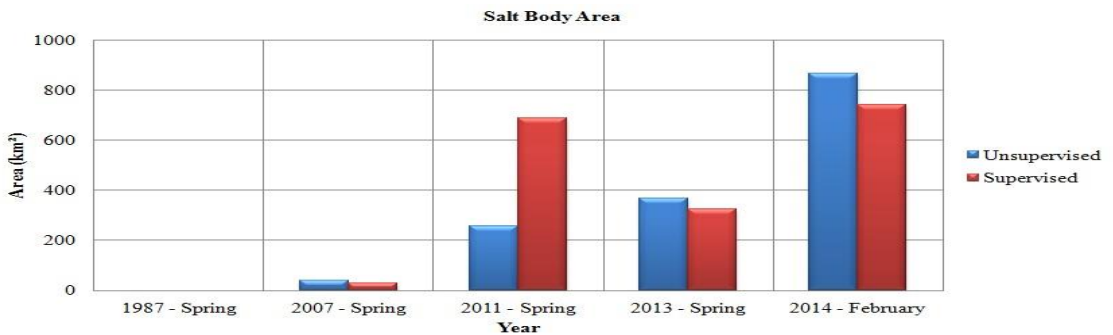


**Figure 5.54:** Comparing the results of salt class in spring and winter times.

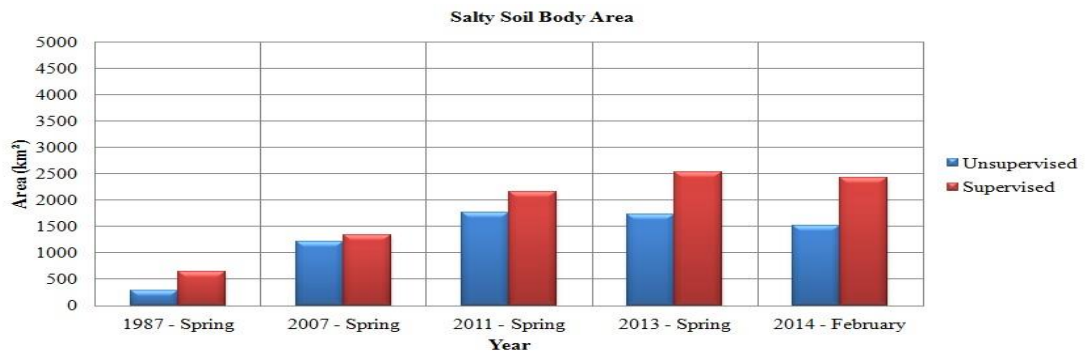


**Figure 5.55:** Comparing the results of salty soil class in spring and winter times.

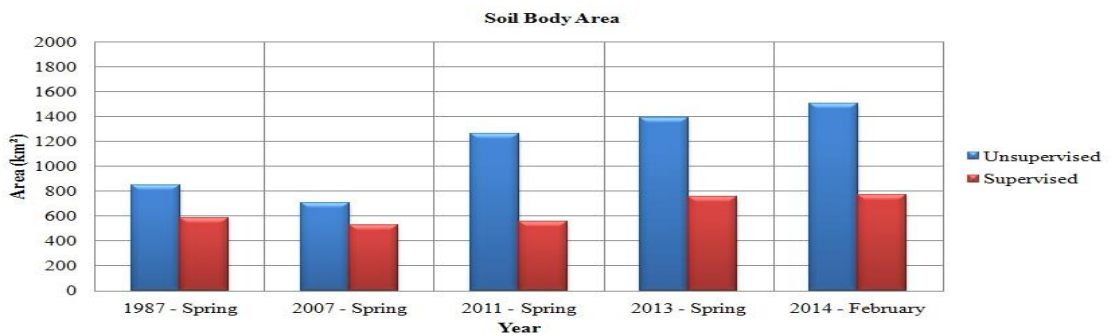


**Figure 5.56:** Comparing the results of soil class in spring and winter times.

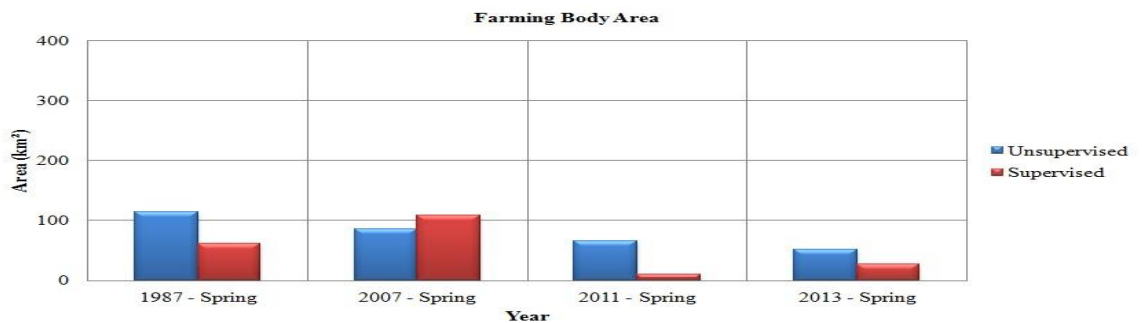


**Figure 5.57:** Comparing the results of farming class in spring time.

The purpose of quantitative accuracy assessment is the identification and measurement of map errors. It involves comparison of a site on a map (classified data) against field or photo information (reference data) for the same site. All accuracy assessments include four fundamental steps: 1) design the sample, 2) collect data, 3) build and test the error matrix, and 4) analyze the results. Therefore, Accuracy assessment is a general term to compare the classification results to geographical data that are assumed to be true, in order to determine the accuracy of the classification process. Usually, the assumed-true data are derived from ground



truth data. There are two methods which are using control points for accuracy assessment. These methods are random reference pixels and defined control points. The first method is based on selection control points automatically and the second method is based on using control points gathered from truth references like maps, GPS, Google Earth, and etc[51].

*When reference pixels are selected by the analyst, it is often tempting to select the same pixels for testing the classification that was used in the training samples. This biases the test, since the training samples are the basis of the classification. By allowing the reference pixels to be selected at random, the possibility of bias is lessened or eliminated[51].*

The number of reference pixels is an important factor in determining the accuracy of the classification. It has been shown that more than 250 reference pixels are needed to estimate the mean accuracy of a class to within plus or minus five percent. ERDAS IMAGINE uses a square window to select the reference pixels. The size of window can be defined by the analyst. Three different types of distribution are offered for selecting random pixels[51]:

- Random: No rules are used
- Stratified random: The number of points is stratified to the distribution of thematic layer classes.
- Equalized random: Each class has an equal number of random points.

Defined control points method is used when truth control points are available to check the accuracy of classification. Control points which were used in this study were collected using GPS and Google Earth and then they were edited and imported to ERDAS IMAGINE to check the accuracy of unsupervised and supervised classification.

A minimum of 50 samples for each land cover category is a good ‘rule of thumb’ as a starting point. If the area is excessively large (greater than 1 million acres) or the classification has a large number of categories (greater than 12) then the sample size may need to increase (e.g., 75 to 100 per category). Sample sizes can also be adjusted depending on the relative importance of each category or the inherent variability within each category[51].

The results concluded from the accuracy assessment include two kinds of reports which are named error matrix and accuracy report. The error matrix simply compares the reference points to the classified points in a C\*C matrix, where c is the number of classes including class 0. The accuracy report calculates statistics of the percentages of accuracy, based upon the results of the error matrix. The Kappa coefficient expresses the proportionate reduction in error generated by a classification process compared with the error of a completely random classification. In other words, Kappa coefficient measures the relationship between beyond chance agreement and expected disagreement. For example, a value of 0.82 implies that the classification process is avoiding 82 percent of the errors that a completely random classification generates[51].

Table 5.5 to 5.8 shows the error matrix, accuracy report and Kappa statistics of unsupervised and supervised classification in 2010-Summer. Producer's accuracy is calculated by dividing the total number of correct sample units in favorite class category by the total number of that class sample units in the reference data (Column Total). User's accuracy which make an information decision is calculated by dividing the total number of correct pixels in the favorite class by the total number of pixels classified as that class (Row Total). In other words, although producer's accuracy percent of favorite class have been identified as that class areas, only user's accuracy percent of the area called for that class on the map are actually that favorite class on the ground. For example, 94.87% of the soil areas have been identified as the soil in the table 5.6 but only 64.91% of the areas called soil on the map are actually soil on the ground. Overall accuracy is the sum of correctly classified samples divided by the total number of samples in the error matrix. Other useful analyses of the error matrix are possible for the advanced user, including Kappa analysis (for statistically determining if one error matrix is significantly different than another), Weighted Kappa analysis (for instances when not all errors have equal importance). According to the results of accuracy assessment in 2010-summer, the overall accuracy of supervised classification was more than unsupervised classification and the overall Kappa statistics of supervised classification was also better than unsupervised. Producer's accuracy and user's accuracy results and kappa statistics of water body in both methods were same and the results of other classes are available in below tables.

**Table 5.5:** Error Matrix of ISODATA - 2010 – Summer.

Classified Data		Reference Data				
Class Name	Water	Salt	Salty Soil	Soil	Farming	Total
Water	40	0	0	0	0	40
Salt	0	35	0	0	0	35
Salty Soil	0	3	23	2	0	28
Soil	0	2	17	37	1	57
Farming	0	0	0	0	40	40
Total	40	40	40	39	41	200

**Table 5.6:** Accuracy totals and Kappa statistics of ISODATA - 2010 – Summer.

Class Name	Reference Totals	Classified Totals	Number Correct	Producer Accuracy	User Accuracy	Kappa
Water	40	40	40	100.00%	100.00%	1.0000
Salt	40	35	35	87.50%	100.00%	1.0000
Salty Soil	40	28	23	57.50%	82.14%	0.7768
Soil	39	57	37	94.87%	64.91%	0.5641
Farming	41	40	40	97.56%	100.00%	1.0000
Totals	200	200	175			

Overall Classification Accuracy = 87.50%, Overall Kappa Statistics = 0.8438

**Table 5.7:** Error Matrix of Maximum Likelihood - 2010 – Summer.

Classified Data		Reference Data				
Class Name	Water	Salt	Salty Soil	Soil	Farming	Total
Water	40	0	0	0	0	40
Salt	0	32	0	0	0	32
Salty Soil	0	7	33	4	0	44
Soil	0	1	7	33	0	41
Farming	0	0	0	2	41	43
Total	40	40	40	39	41	200

**Table 5.8:** Accuracy Totals and Kappa Statistics Maximum Likelihood - 2010 – Summer.

Class Name	Reference Totals	Classified Totals	Number Correct	Producer Accuracy	User Accuracy	Kappa
Water	40	40	40	100.00%	100.00%	1.0000
Salt	40	32	32	80.00%	100.00%	1.0000
Salty Soil	40	44	33	82.50%	75.00%	0.6875
Soil	39	41	33	84.62%	80.49%	0.7576
Farming	41	43	41	100.00%	95.35%	0.9415
Totals	200	200	179			

Overall Classification Accuracy = 89.50%, Overall Kappa Statistics = 0.8687

Table 5.9 to 5.12 shows the error matrix, accuracy report and Kappa statistics of unsupervised and supervised classification in 2011-Summer. The results of accuracy assessment in 2011-summer was an exception between studying dates and the overall accuracy of unsupervised was better than supervised method in this year, but it should be considered that the overall accuracy and overall kappa statistics results were very close to each in two classification methods. Water class results in unsupervised method were better than supervised. The results of other classes are available in below tables.

**Table 5.9:** Error Matrix of ISODATA - 2011 – Summer.

Classified Data		Reference Data				
Class Name	Water	Salt	Salty Soil	Soil	Farming	Total
Water	40	0	0	0	0	40
Salt	0	36	0	0	0	36
Salty Soil	0	4	29	5	0	38
Soil	0	0	11	33	6	50
Farming	0	0	0	2	34	36
Total	40	40	40	40	40	200

**Table 5.10:** Accuracy Totals and Kappa Statistics of ISODATA - 2011 – Summer.

Class Name	Reference Totals	Classified Totals	Number Correct	Producer Accuracy	User Accuracy	Kappa
Water	40	40	40	100.00%	100.00%	1.0000
Salt	40	36	36	90.00%	100.00%	1.0000
Salty Soil	40	38	29	72.50%	76.32%	0.7039
Soil	40	50	33	82.50%	66.00%	0.5750
Farming	40	36	34	85.00%	94.44%	0.9306
Totals	200	200	172			

Overall Classification Accuracy = 86.00%, Overall Kappa Statistics = 0.8250

**Table 5.11:** Error Matrix of Maximum Likelihood - 2011 – Summer.

Classified Data		Reference Data				
Class Name	Water	Salt	Salty Soil	Soil	Farming	Total
Water	40	0	0	1	0	41
Salt	0	24	0	0	0	24
Salty Soil	0	15	38	5	1	59
Soil	0	1	2	32	3	38
Farming	0	0	0	2	36	38
Total	40	40	40	40	40	200

**Table 5.12:** Accuracy Totals and Kappa Statistics Maximum Likelihood - 2011 - Summer.

Class Name	Reference Totals	Classified Totals	Number Correct	Producer Accuracy	User Accuracy	Kappa
Water	40	41	40	100.00%	97.00%	0.9695
Salt	40	24	24	60.00%	100.00%	1.0000
Salty Soil	40	59	38	95.00%	64.41%	0.5551
Soil	40	38	32	80.00%	84.21%	0.8026
Farming	40	38	36	90.00%	94.74%	0.9342
Totals	200	200	170			

Overall Classification Accuracy =85.00%, Overall Kappa Statistics = 0.8125

Table 5.13 to 5.16 shows the error matrix, accuracy report and Kappa statistics of unsupervised and supervised classification in 2013-Summer. According to the results of accuracy assessment in 2013-summer, the overall accuracy of supervised classification was better than unsupervised classification and the overall Kappa statistics of supervised classification was also better than unsupervised. Producer's accuracy and user's accuracy and kappa statistics results of water class in supervised classification were higher than unsupervised classification. Results of other classes are available in below tables.

**Table 5.13:** Error Matrix of ISODATA - 2013 – Summer.

Classified Data Class Name	Reference Data					
	Water	Salt	Salty Soil	Soil	Farming	Total
Water	43	0	0	1	0	44
Salt	7	40	0	0	0	47
Salty Soil	0	4	23	1	0	28
Soil	0	7	27	36	4	74
Farming	0	0	0	2	38	40
Total	50	51	50	40	42	233

**Table 5.14:** Accuracy Totals and Kappa Statistics of ISODATA - 2013 – Summer.

Class Name	Reference Totals	Classified Totals	Number Correct	Producer Accuracy	User Accuracy	Kappa
Water	50	44	43	86.00%	97.73%	0.9711
Salt	51	37	40	78.43%	85.11%	0.8093
Salty Soil	50	28	23	46.50%	82.14%	0.7726
Soil	40	74	36	90.50%	48.65%	0.3801
Farming	42	40	38	90.48%	95.00%	0.9390
Totals	233	233	180			

Overall Classification Accuracy = 77.25%, Overall Kappa Statistics = 0.7171

**Table 5.15:** Error Matrix of Maximum Likelihood - 2013 – Summer.

Classified Data		Reference Data				
Class Name	Water	Salt	Salty Soil	Soil	Farming	Total
Water	44	0	0	1	0	45
Salt	6	31	0	0	0	37
Salty Soil	0	20	47	7	2	76
Soil	0	1	3	29	4	36
Farming	0	0	0	3	36	39
Total	50	51	50	40	42	233

**Table 5.16:** Accuracy Totals and Kappa Statistics Maximum Likelihood - 2013 – Summer.

Class Name	Reference Totals	Classified Totals	Number Correct	Producer Accuracy	User Accuracy	Kappa
Water	50	45	44	88.00%	97.78%	0.9717
Salt	51	37	31	60.78%	83.78%	0.7924
Salty Soil	50	76	47	94.00%	61.84%	0.5142
Soil	40	36	29	72.50%	80.56%	0.7653
Farming	42	39	36	85.71%	92.31%	0.9062
Totals	233	233	187			

Overall Classification Accuracy = 80.26%, Overall Kappa Statistics = 0.7523

Table 5.17 to 5.20 show the error matrix and accuracy report an Kappa statistics of unsupervised and supervised classification in 2014-February. According to the results of accuracy assessment in 2014-February, the overall accuracy of supervised classification was better than unsupervised classification and the overall Kappa statistics of supervised classification was also better than unsupervised. Producer's accuracy and user's accuracy and kappa statistics results of water class in supervised classification were higher than unsupervised classification. The results of the other classes could be compared according to the values mentioned in below tables.'

**Table 5.17:** Error Matrix of ISODATA - 2014 – February.

Classified Data		Reference Data			
Class Name	Water	Salt	Salty Soil	Soil	Total
Water	39	2	0	0	41
Salt	1	29	2	0	32
Salty Soil	0	9	13	0	22
Soil	0	0	25	40	65
Total	40	40	40	40	160

**Table 5.18:** Accuracy Totals and Kappa Statistics of ISODATA - 2014 – February.

Class Name	Reference Totals	Classified Totals	Number Correct	Producer Accuracy	User Accuracy	Kappa
Water	40	41	39	97.50%	95.12%	0.9350
Salt	40	32	29	72.50%	90.63%	0.8750
Salty Soil	40	22	13	32.50%	59.09%	0.4545
Soil	40	65	40	100.00%	61.54%	0.4872
Totals	160	160	121			

Overall Classification Accuracy = 75.63%, Overall Kappa Statistics = 0.6750

**Table 5.19:** Error Matrix of Maximum Likelihood - 2014 – February.

Classified Data Class Name	Reference Data				
	Water	Salt	Salty Soil	Soil	Total
Water	39	1	0	0	40
Salt	0	32	1	0	33
Salty Soil	1	7	39	2	49
Soil	0	0	0	38	38
Column Total	40	40	40	40	160

**Table 5.20:** Accuracy Totals and Kappa Statistics of Maximum Likelihood - 2014 – February.

Class Name	Reference Totals	Classified Totals	Number Correct	Producer Accuracy	User Accuracy	Kappa
Water	40	40	39	97.50%	97.50%	0.9667
Salt	40	33	32	80.00%	96.97%	0.9596
Salty Soil	40	49	39	97.50%	79.59%	0.7279
Soil	40	38	38	95.00%	100.00%	1.000
Totals	160	160	148			

Overall Classification Accuracy = 92.50% , Overall Kappa Statistics = 0.9000

According to the results of accuracy assessment, producer's accuracy and user's accuracy of the water body class in supervised classification were better than unsupervised classification in the study dates except 2011. Kappa statistics value of the water class in both unsupervised and supervised methods was the same in 2010. It had a higher value in unsupervised rather than supervised in 2011. Also, it had a higher value in supervised method rather than unsupervised in 2013 and 2014.

Producer's accuracy of the salt class of the unsupervised classification method was better than supervised in the study dates except 2014-February. User's accuracy of the salt class in both unsupervised and supervised was the same in 2010 and 2011. Also, user's accuracy of unsupervised in 2013 was better than supervised and in contrast; user's

accuracy of unsupervised in 2014 was less than supervised. Kappa statistics of both methods were same in 2010 and 2011. Also, kappa statistics of unsupervised were higher than supervise in 2013 and less than supervised method in 2014.

Producer's accuracy of salty soil class in supervised classification method was better than unsupervised in all studied dates. User's accuracy of salty soil class in unsupervised was better than supervised in all dates except 2014. Kappa statistics of unsupervised methods were better than supervised in all dates except 2014.

Producer's accuracy of soil class in unsupervised classification method was better than supervised in all studied dates. User's accuracy of soil class in unsupervised was less than supervised in all dates. Kappa statistics of unsupervised methods were less than supervised in all studied dates.

Producer's accuracy of farming class of the supervised classification method was better than supervised in all studied dates except 2013. User's accuracy of farming class in unsupervised was higher than supervised in all dates except 2011. Kappa statistics of unsupervised methods were higher than supervised in all studied dates except 2011.

In conclusion, the overall classification accuracy and overall Kappa Statistics of supervised classification in all studied dates were better than unsupervised classification except 2011-summer. In 2011, there was a minor difference between the results of unsupervised and supervised classification. Therefore, it could be concluded that determination water surface area of Urmia Lake using supervised classification is better than unsupervised classification and the accuracy of this method is better than unsupervised classification.

Figure 5.58 shows a correlation between calculated water surface area of Urmia Lake in summer time using supervised classification method and water surface elevation changes in summer time using HYDROWEB data. The correlation coefficient value is 0.952997382. This value shows high positive correlation between the water surface area and water surface elevation changes in Urmia Lake from 1995 to 2013.



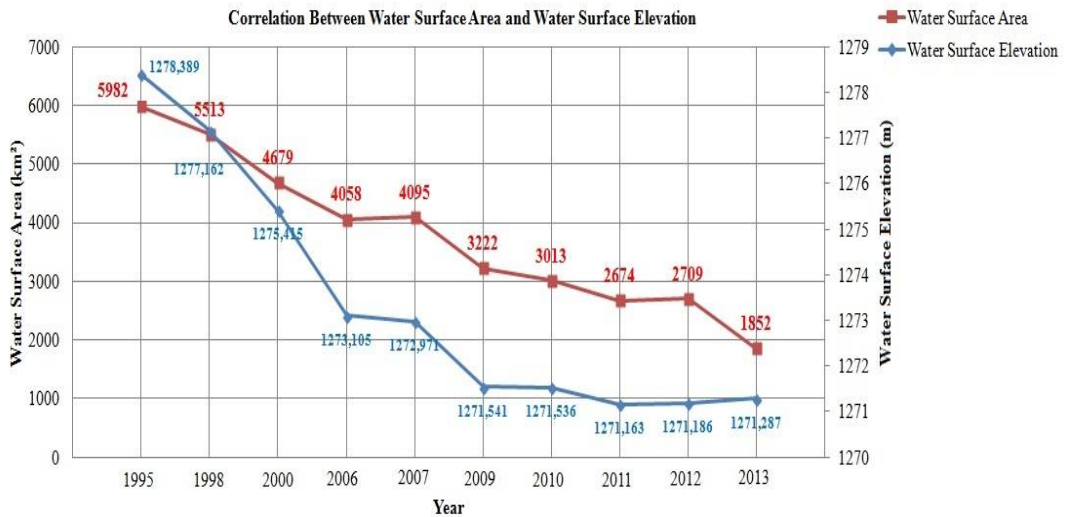


**Figure 5.58:** Correlation between water surface area and water surface elevation changes in summer time.

Figure 5.59 shows a correlation between calculated water surface area of Urmia Lake in summer time using supervised classification method and water surface elevation data of Iran's Energy Ministry which were captured on the fifteenth day of November. The correlation coefficient value is 0.980961507. This value shows high positive correlation between the water surface area and water surface elevation changes on Urmia Lake from 1995 to 2013. Water surface elevation values of HYDROWEB and Energy Ministry of Iran are a little different from each other. Available water surface elevation values from Energy Ministry of Iran are belong to fifteenth day of November during 1966 to 2013 and water surface elevation values of HYDROWEB are belong to different days and months during 1992 to 2013. The water surface elevation values of HYDROWEB were decimal. To have a better analysis, these dates were converted to day, month, and year format. Then, the average value of water surface elevation was calculated during summer time using June, July, and August months of each year.

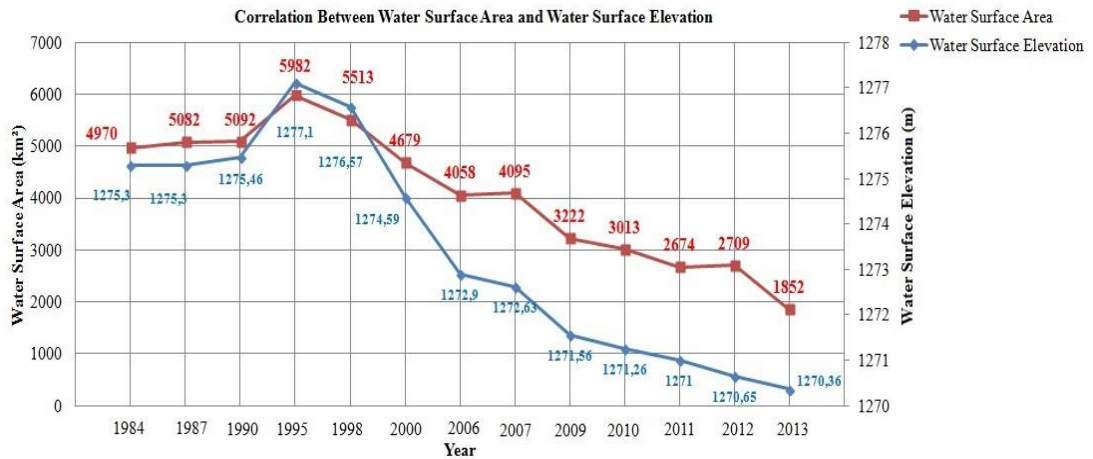


**Figure 5.59:** Correlation between water surface area (summer) and water surface elevation (November) changes

### 5.3 Analyzing the results of NDVI, NDWI, NDDI, NDSI , AND SI

#### 5.3.1 Normalized Difference Vegetation Index (NDVI)

Normalized Difference Vegetation Index (NDVI) is calculated using red and infrared bands of remotely sensed images and it gives information about the spatial distribution and condition of vegetated areas. Eq.(5.10) shows the related formula to calculate the NDVI value.

$$NDVI = \frac{\rho_{NIR} - \rho_{Red}}{\rho_{NIR} + \rho_{Red}} \quad (5.10)$$

Where  $\rho_{NIR}$  is reflectance value of infrared band and  $\rho_{Red}$  is the reflectance value of band red of the remote sensing system. NDVI values are between -1 and 1 and they can be used to analyze vegetated and non vegetated areas. Water, snow, and ice usually have NDVI value less than 0, bare soils values are between 0 and 0.1, sparse vegetation such as shrubs and grasslands or sensing crop values are between 0.2 and 0.5, and peak growth stage values are between 0.6 and 1. Leaf structure, maturation, water content and mesophyll arrangement impact the amount of spectral reflectance from different wavelengths for a selected vegetation type[28,47]. NDVI maps of Landsat-5 TM images were produced in ERDAS IMAGINE and NDVI maps of Landsat-8 images were produced in ENVI using band math. Band 3 in Landsat-5 TM

and band 4 in Landsat-8 refer red bands which are needed to calculate NDVI according to mentioned formula. Band 4 of Landsat-5 TM and band 5 of Landsat-8 refer also as NIR band.

To produce NDVI maps and analyze them, the extracted results from ERDAS IMAGINE and ENVI were analyzed in ArcGIS. To analyze vegetation changes in the study area, it was better to separate water bodies and non-water bodies from each other. MNDWI index was used to separate water bodies from non-water bodies according to Eq.(5.11).

$$MNDWI = \frac{(\rho_{Green} - \rho_{SWIR})}{(\rho_{Green} + \rho_{SWIR})} \quad (5.11)$$

MNDWI indice was applied in ENVI using band math and water bodies were separated from nonwater bodies using thresholding value 0 by consideration that the cover type is water if  $MNDWI > 0$  and it is nonwater if  $MNDWI \leq 0$ [8]. Then the results were converted to shape file. Figures 5.60 and 5.61 show example of MNDWI results including different kinds of water bodies and the location of some dams in Urmia Lake's catchment area. According to the results of this study, MNDWI by thresholding 0 was a good indice to separate water bodies from non-water bodies, but it is important to know that thresholding 0 can also consider some salt bodies and wet salt bodies or wet salty soil areas as water body. Water surface area of Urmia Lake was extracted using MNDWI by considering thresholding 0 and the results were very different from other methods which were used in this study. Water indice does not only count for water class, but also considers any wet areas in the study like different soil types or vegetation. The results of water surface area of Urmia Lake using MNDWI were calculated too.



**Figure 5.60:** Some kinds of water bodies in the study area – Photos taken by Yusuf Alizade Govarchin Ghale in land study.

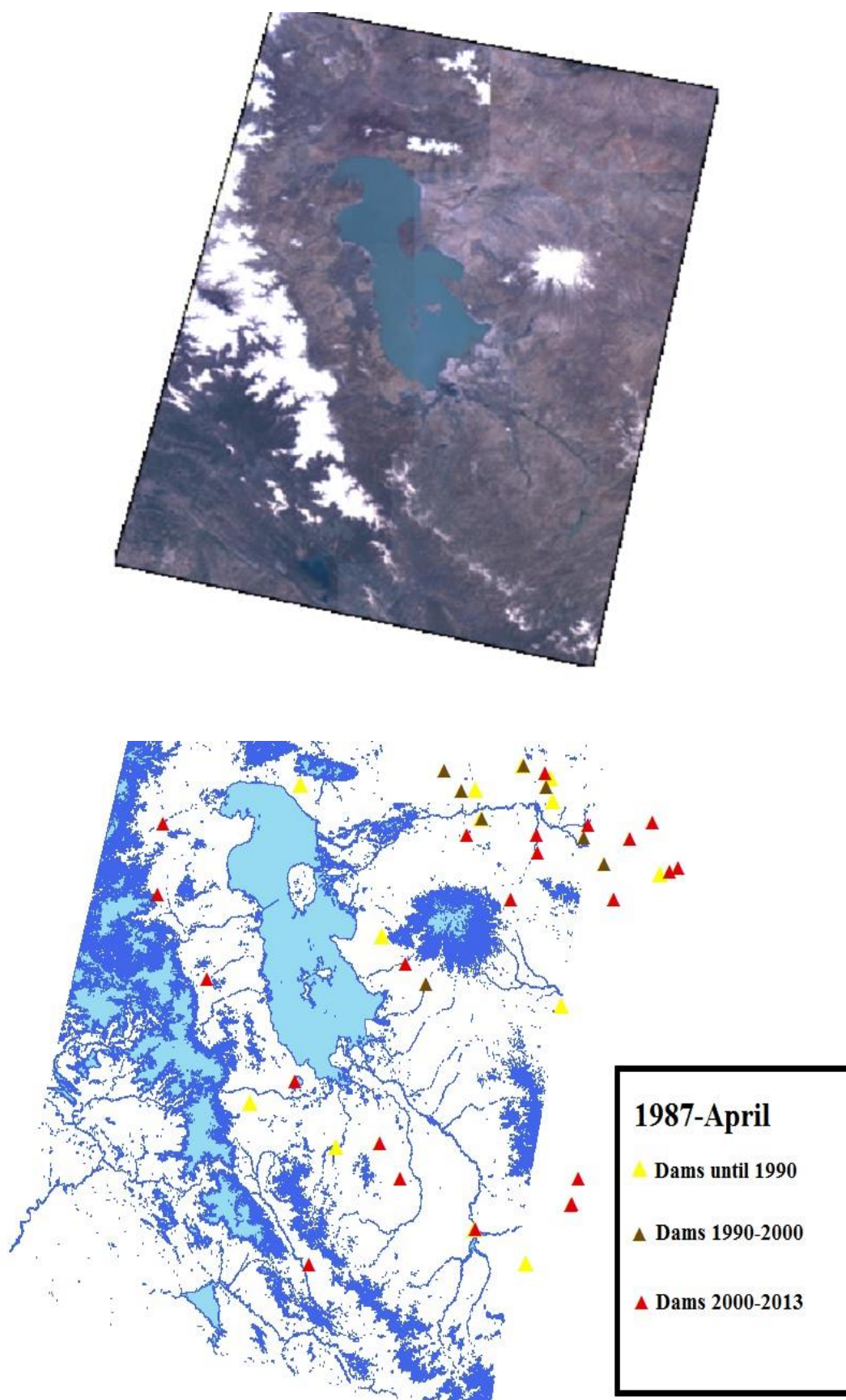


**Figure 5.61:** Extracted areas using MNDWI- Landsat-5 TM -1987 – spring.

Thresholding 0 was used to calculate MNDWI in this study because there were many water body types, including water, snow, clouds, rivers, streams, dams, dirty water and clean water.

In the final step of production NDVI maps, water bodies were masked in ArcGIS and NDVI values of non-water bodies between 0 and 1 reclassified in ArcGIS to compare the results in different years. Figures 5.62 and 5.63 show NDVI maps at summer time of 1984, 1987, 1990, 2000, 2006, 2010, 2011, and 2013.

To have a good comparison and analysis, the maps were beside each other by considering different dates. The area of NDVI classes also were calculated to give a true view about changes which happened in the study area.

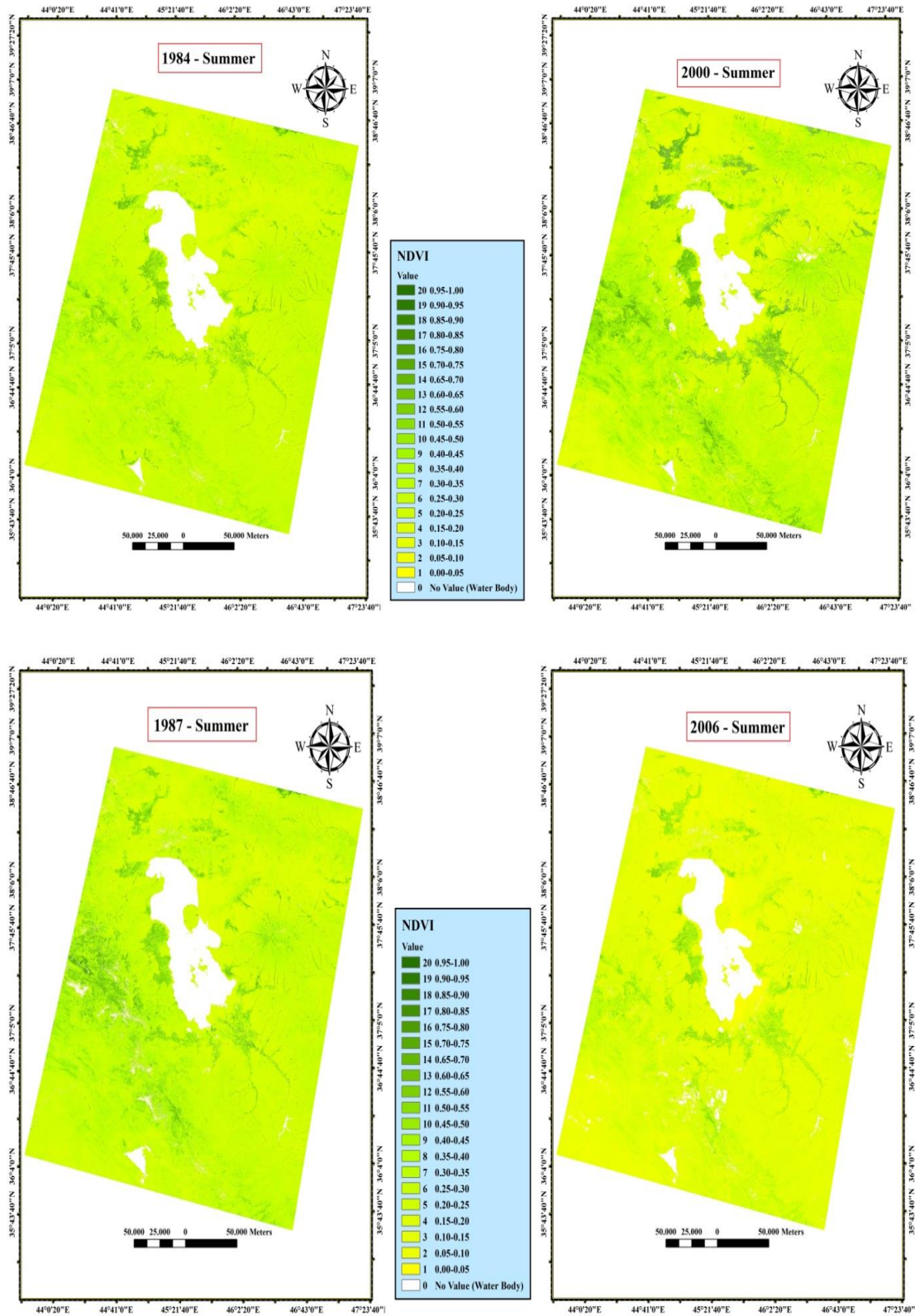


**Figure 5.62:** NDVI maps in summer time of 1984, 1987, 2000, and 2006.

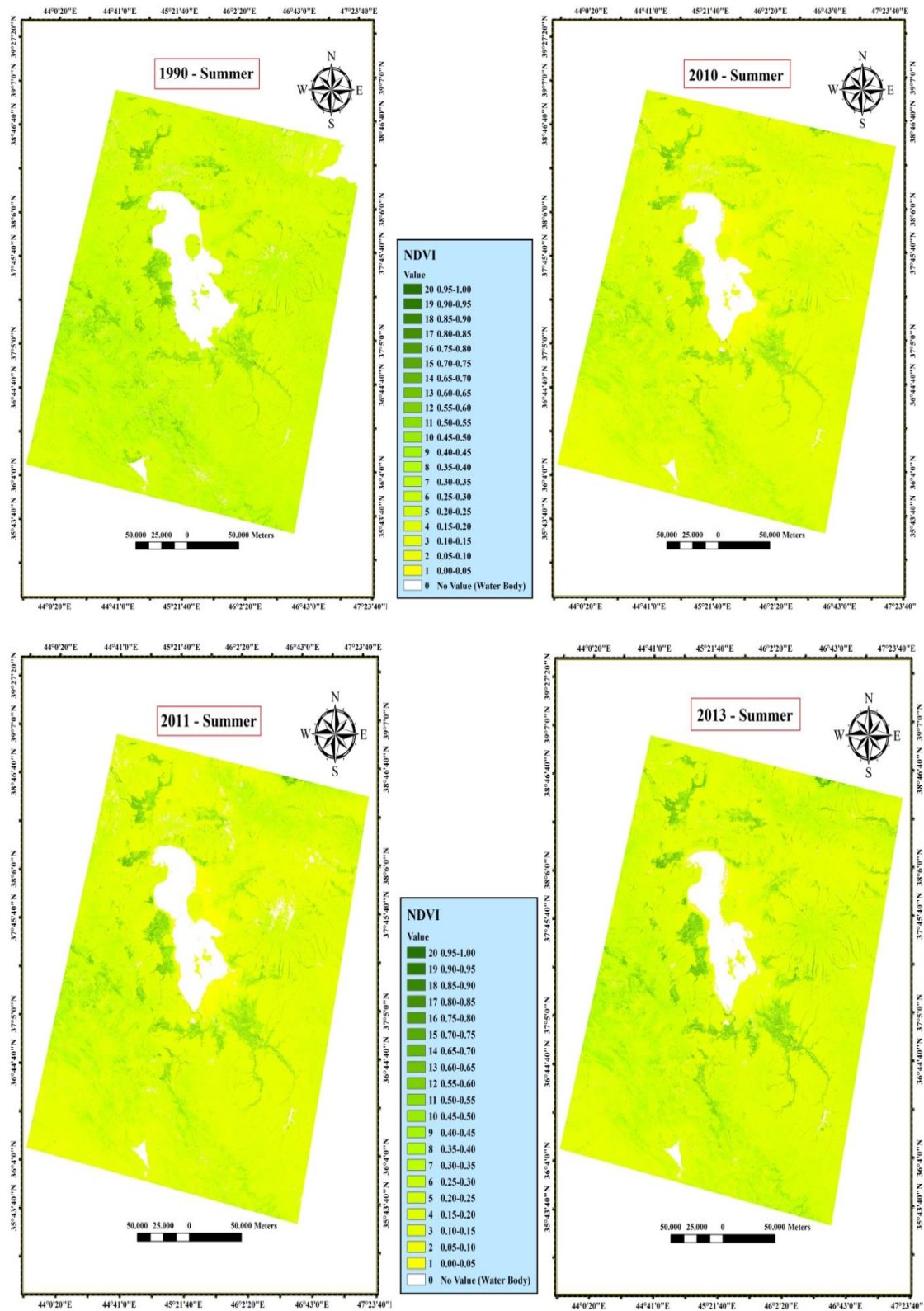


**Figure 5.63:** NDVI maps in summer time of 1990, 2010, 2011, and 2013.

According to NDVI maps, yellow color shows low NDVI value and sparse or vegetation. Green color shows high NDVI value and dense vegetation. The



vegetation changes occurred in the study area between 2000 and 2006. The intensity of vegetation increased in the west and south part of Urmia Lake, since the yellow color intensity has been increased in the vicinity of Urmia Lake especially in the East and south parts of Lake.

To analyze NDVI results, NDVI values were classified into 3 groups, including values between 0 and 0.1, values between 0.1 and 0.5 and finally, values between 0.5 and 1. Figure 5.64 shows values between 0 and 0.1 including bare soil, barren rock, sparse desert vegetation and sand. The minimum area of this class was about 3 km<sup>2</sup> in 1987 and the maximum area of it, was about 24025 km<sup>2</sup> in 2006-August. The study area changes between 2000 and 2006 were considerable and NDVI value changes were significant during this time.

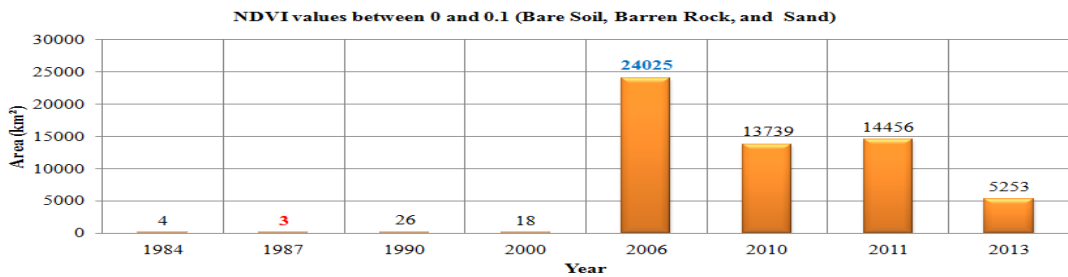


**Figure 5.64:** NDVI values between 0 and 0.1.

NDVI values between 0.1 and 0.5 show sparse vegetation such as shrubs and grasslands or senescing crops (Figure 5.65). The minimum area of this class was about 55847 km<sup>2</sup> in 2006 year and the maximum area was about 79565 km<sup>2</sup> in 2000 year. The total area of this class decreased between 2000 and 2006 years and it increased from 2006 to 2013.

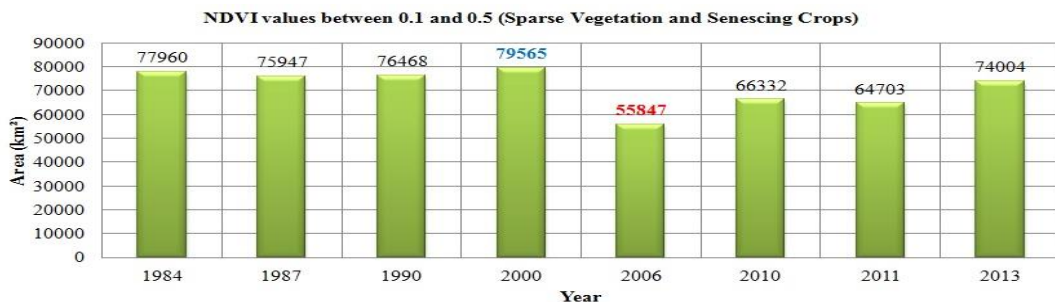


**Figure 5.65:** NDVI values between 0.1 and 0.5.

High NDVI values (approximately 0.6 to 0.9) show dense vegetation such as that found in temperate and tropical forests or crops at their peak growth stage[69] (Figure 5.66). The minimum area of this class was about 1228 km<sup>2</sup> in 2006 and the maximum area of it was 4345 km<sup>2</sup> in 1987. Although, the total are of this class decreased between 1987 and 2006, and it increased from 2006 to 2013. The results show a high amount of changes occurred between 2000 and 2006 and the percentage of the high NDVI values decreased from 2000 to 2006. This was mainly caused as a result of land cover changes such as many vegetation types in study area were converted to bare soil, barren rock, sparse desert vegetation and sand from 2000 to 2006. After this time, vegetation types of study area changed to reach their last state between 1984 to 2000.

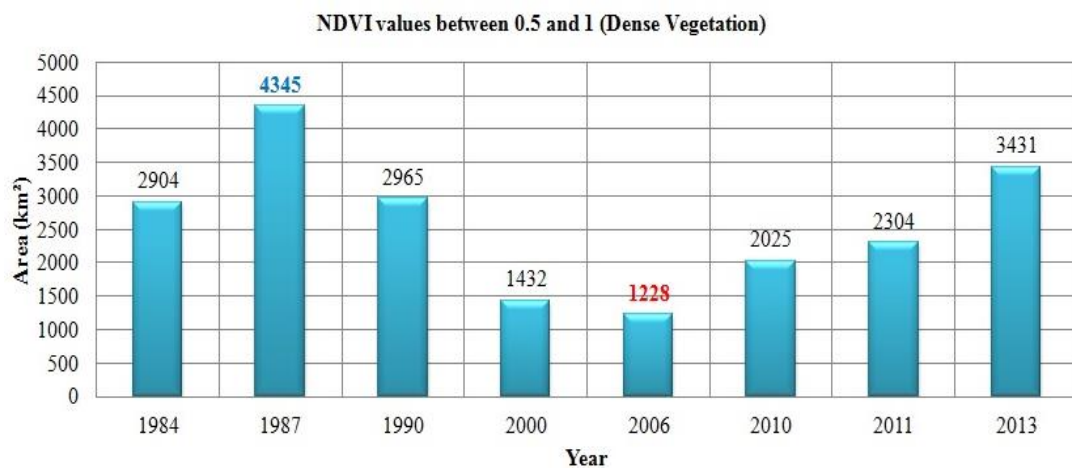


**Figure 5.66:** NDVI values between 0.5 and 1.

The area of different NDVI classes is shown in Table 5.21. Values mentioned in Area (0-0.1) column illustrates the area of NDVI class including NDVI values between 0 and 0.1 and Values mentioned in Area (0.1-0.5) column illustrates the area of NDVI class including NDVI values between 0.1 and 0.5 and Values mentioned in Area (0.5-1) column shows the area of NDVI class including NDVI values between 0.5 and 1. The total classified area of each year was different from other years because their water bodies were different from each other. Water bodies were masked to analyze NDVI changes in non-water bodies. By analyzing the results of NDVI figures and table 5.21 it could be concluded that there were three period in vegetation changes in study area. The first period was from 1984 to 2000 when there were little changes in NDVI values of the study area. The second period was from

2000 to 2006 showing an increase of the area of low NDVI values. The third period was from 2006 to 2013 showing and increasing of the area of high NDVI values.

**Table 5.21:** NDVI results (km<sup>2</sup>) in summer time.

Year	Area (0-0.1)	Area (0.1-0.5)	Area (0.5-1)	Total Area (km <sup>2</sup> )
1984	4	77960	2904	80868
1987	3	75947	4345	80295
1990	26	76468	2965	79459
2000	18	79565	1432	81015
2006	24025	55847	1228	81100
2010	13739	66332	2025	82096
2011	14456	64703	2304	81463
2013	5253	74004	3431	82688

### 5.3.2 Calculation of Water Surface Area Using NDVI and Unsupervised

#### Classification

To calculate water surface area of Urmia Lake, a different method was used in this study that integrates NDVI and unsupervised classification. Based on the literature search, this approach has not been applied to a lake study previously. This method helps to save time and avoid from operator mistakes. It is based on the unsupervised classification of NDVI values. To use this method, first of all NDVI images was created in ERDAS IMAGINE, then unsupervised classification (ISODATA) was applied to classify the study area just into two classes including water body and non-water body. Table 5.22 shows the results of 4 methods which were used in this study to calculate the water surface area of Urmia Lake in summer time. According to table 5.22 the results of supervised classification and NDVI based unsupervised classification are very close to each other. MNDWI (thresholding 0) values are very high and exaggerated rather than other methods because of thresholding 0. Thresholding zero cause some salt bodies be considered as water body and it is clear even by visual interpretation of satellite images and google earth.

**Table 5.22:** Water surface area (km<sup>2</sup>) of Urmia Lake using 4 methods – Summer.

Year	Unsupervised Classification	Supervised Classification	NDVI Based Unsupervised	MNDWI (Thresholding 0)
1984	5005	4970	4935	5141
1987	5128	5082	5076	5227
1990	5200	5092	5035	5308
1995	5946	5982	5948	5983
1998	5597	5513	5530	5715
2000	4697	4679	4600	4927
2006	4057	4058	4100	4392
2007	4049	4095	4116	4490
2009	3130	3222	3218	4042
2010	2922	3013	3027	3922
2011	2562	2674	2762	4030
2013	1897	1852	1998	3373

To check the accuracy of NDVI based unsupervised, the accuracy assessment process was done in summer time of 2010, 2011, and 2013 using control points. Table 5.23 to 5.28 show the results of accuracy assessment in mentioned dates. Overall classification accuracy and overall kappa statistics of this method are higher than unsupervised classification and supervised classification methods which were explained in previous sections but it is important to consider that in NDVI based unsupervised classification, the NDVI was classified just into two classes. This method could be used when the aim of the study is obtaining water surface area, and other land cover classes are out of important. Moreover, this is an automated method which can decrease and remove operator mistakes during classification.

**Table 5.23:** Error Matrix of NDVI-Unsupervised - 2010- Summer.

Classified data	Reference Data		
	Water body	Nonwater Body	Row Total
Water	40	0	40
Nonwater	0	160	160
Column Total	40	160	200

**Table 5.24:** Accuracy Totals and Kappa Statistics of NDVI-Unsupervised - 2010 – Summer.

Class Name	Refrence Totals	Classified Totals	Number Correct	Producer Accuracy	User Accuracy	Kappa
Water	40	40	40	100.00%	100.00%	1.0000
Nonwater	160	160	160	100.00%	100.00%	1.0000
Totals	200	200	148			
Overall Classification Accuracy = 100.00% , Overall Kappa Statistics =1.0000						

**Table 5.25:** Error Matrix of NDVI-Unsupervised - 2011- Summer.

Classified Data		Reference Data	
Class Name	Water body	Nonwater Body	Row Total
Water	40	4	44
Nonwater	0	156	156
Column Total	40	160	200

**Table 5.26:** Accuracy Totals and Kappa Statistics of NDVI-Unsupervised - 2011 – Summer.

Class Name	Reference Totals	Classified Totals	Number Correct	Producer Accuracy	User Accuracy	Kappa
Water	40	44	40	100.00%	90.91%	0.8864
Nonwater	160	156	156	97.50%	100.00%	1.0000
Totals	200	200	196			

Overall Classification Accuracy = 98.00% , Overall Kappa Statistics =0.9398

**Table 5.27:** Error Matrix of NDVI-Unsupervised - 2013- Summer.

Classified Data		Reference Data	
Class Name	Water body	Nonwater Body	Row Total
Water	45	2	47
Nonwater	5	181	186
Column Total	50	183	213

**Table 5.28:** Accuracy Totals and Kappa Statistics of NDVI-Unsupervised - 2013 – Summer.

Class Name	Reference Totals	Classified Totals	Number Correct	Producer Accuracy	User Accuracy	Kappa
Water	50	47	45	90.00%	95.74%	0.9723
Nonwater	183	186	181	98.91%	97.31%	0.8747
Totals	233	233	226			

Overall Classification Accuracy = 97.00%, Overall Kappa Statistics =0.9091

### 5.3.3 Normalized Difference Water Index (NDWI)

Normalized Difference Water Index (NDWI) is another indice that can be used for the determination of vegetation water content (VWC) based on physical principles. Eq.(5.12) shows the related formula to calculate NDWI in Landsat images.

$$NDWI = \frac{\rho_{NIR} - \rho_{SWIR}}{\rho_{NIR} + \rho_{SWIR}} \quad (5.12)$$

Where  $\rho_{SWIR}$  is the reflectance or radiance in a short wave infrared wavelength band and  $\rho_{NIR}$  is the reflectance or radiance in a near infrared wavelength band. For Landsat-5 TM NIR and SWIR correspond to bands 4 and 5 respectively, and for Landsat-8 NIR and SWIR correspond to bands 5 and 6 respectively.

NDWI values are between -1 and 1, minus values indicate dry vegetation types or less vegetation water content areas and positive values indicate green vegetation types or high vegetation water content areas. NDWI can be used to analyze vegetation changes in the study area like NDVI but it should be considered that NDWI does not remove completely the background soil reflectance effects, similar to NDVI. In other words, low NDWI values mean low percentage of water in vegetation and higher NDWI values mean higher percentage of water in vegetation types [27,28,29]. NDWI values were calculated in ENVI using band math and then their water bodies were masked like NDVI maps using MNDWI shape files in ArcGIS. In final step, they were reclassified and converted to maps in ArcGIS. Figures 5.67 and 5.68 show NDWI maps at summer time of 1984, 1987, 1990, 2000, 2006, 2010, 2011, and 2013.

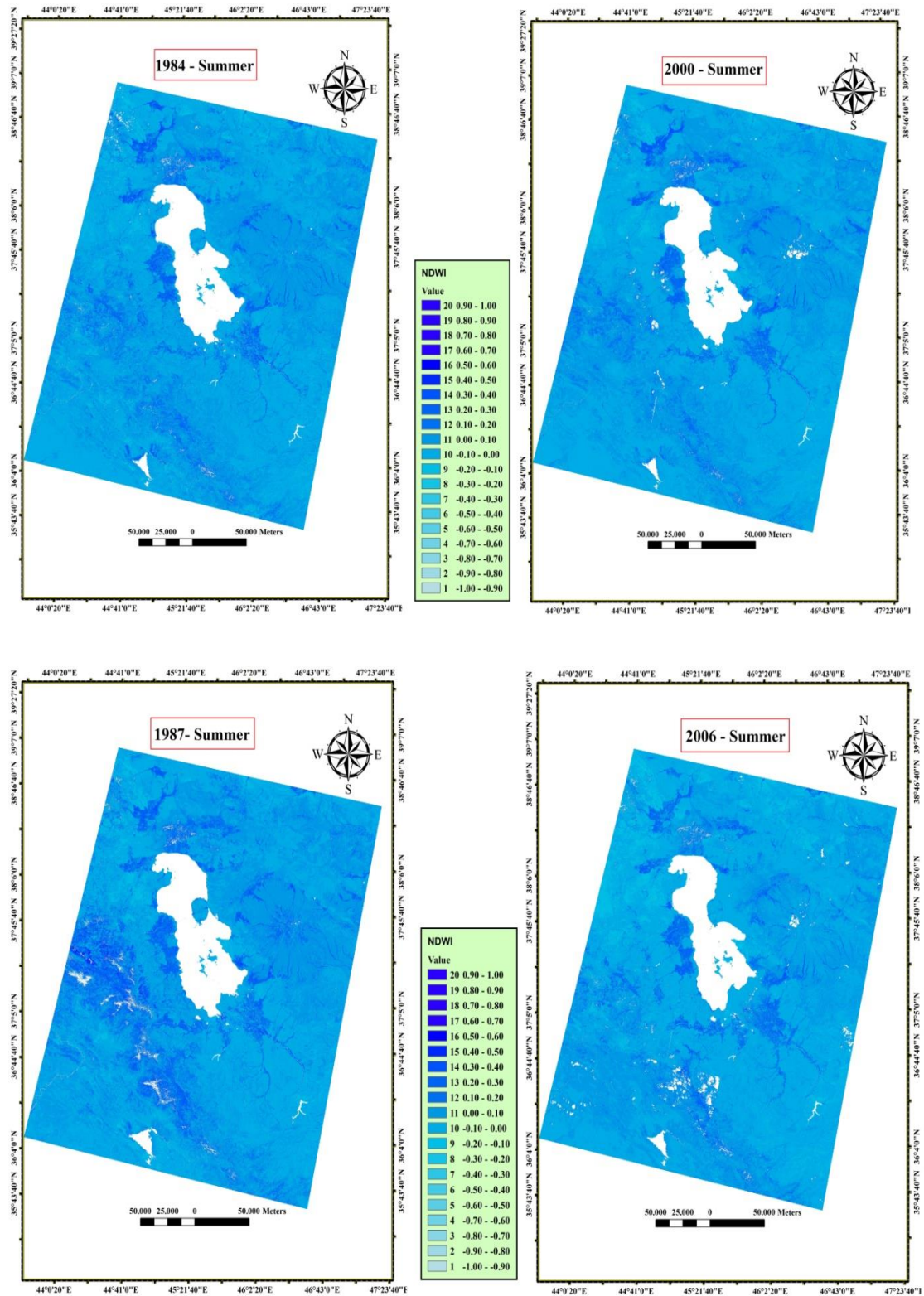
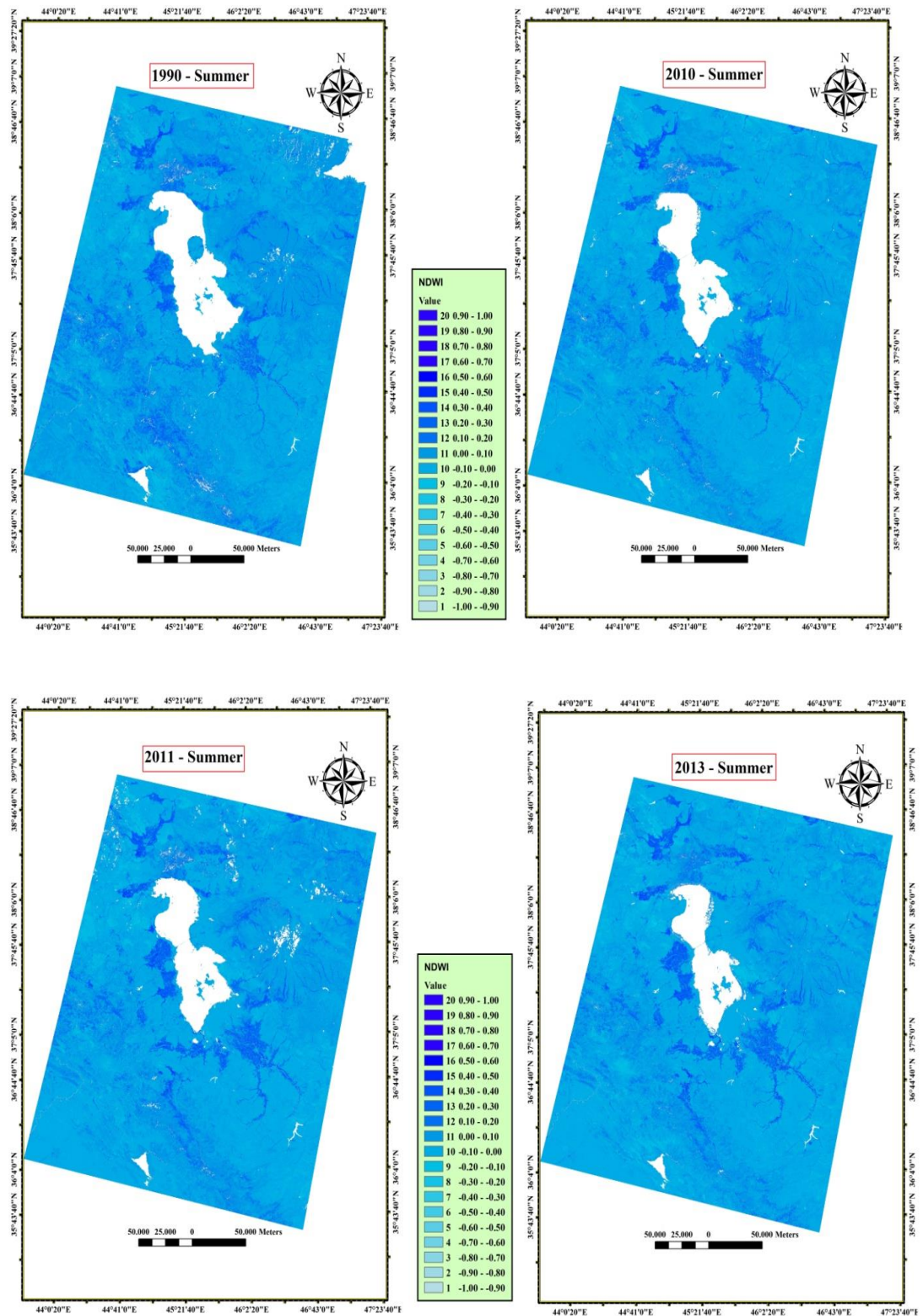


Figure 5.67: NDWI maps in summer time of 1984, 1987, 2000, and 2006.



**Figure 5.68:** NDWI maps in summer time of 1990, 2010, 2011, and 2013.

According to NDWI maps, light blue color shows low NDWI values and dry vegetation types and blue color shows high NDWI values and green vegetation types. By considering all study area, it could be understood that green vegetation types



were more separated in the northwest, west and south parts of Urmia Lake. To analysis NDWI results , NDWI values were classified into 3 groups, including values between -1 and 0, values between 0 and 0.5 and finally values between 0.5 and 1. Figure 5.69 shows the area of values between -1 and 0. The minimum area of this class was about 34518 km<sup>2</sup> in 1987 and the maximum area of it, was about 53462 km<sup>2</sup> in 2013. The total area of this class decreased between 1984 and 1987 and it increased from 1987 to 2013.

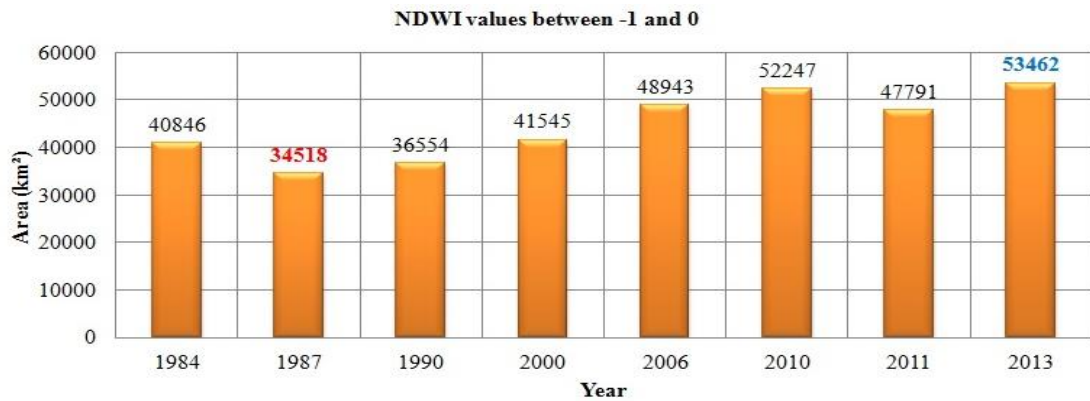


**Figure 5.69:** NDWI values between -1 and 0.

Figure 5.70 shows the area of values between 0 and 0.5. The minimum area of this class was about 29176 km<sup>2</sup> in 2013 and the maximum area of it, was about 45757 km<sup>2</sup> in 1987. The total area of this class increased between 1984 and 1987 and it decreased from 1987 to 2013.

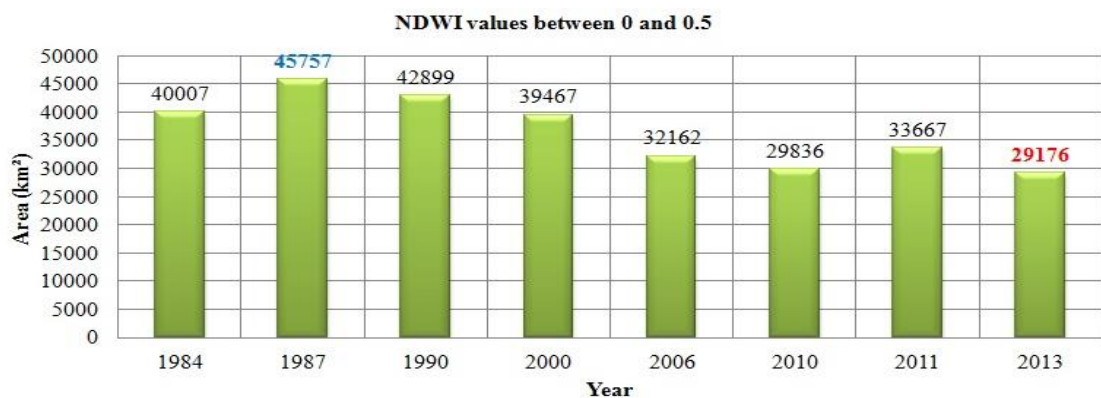


**Figure 5.70 :** NDWI values between 0 and 0.5.

Figure 5.71 shows the area of values between 0.5 and 1. The minimum area of this class was about 2 km<sup>2</sup> in 2006 and the maximum area of it, was about 56 km<sup>2</sup> in

2013. The total area of this class increased between 1984 and 1987 and it decreased from 1987 to 2006, and finally it increased from 2006 to 2013.

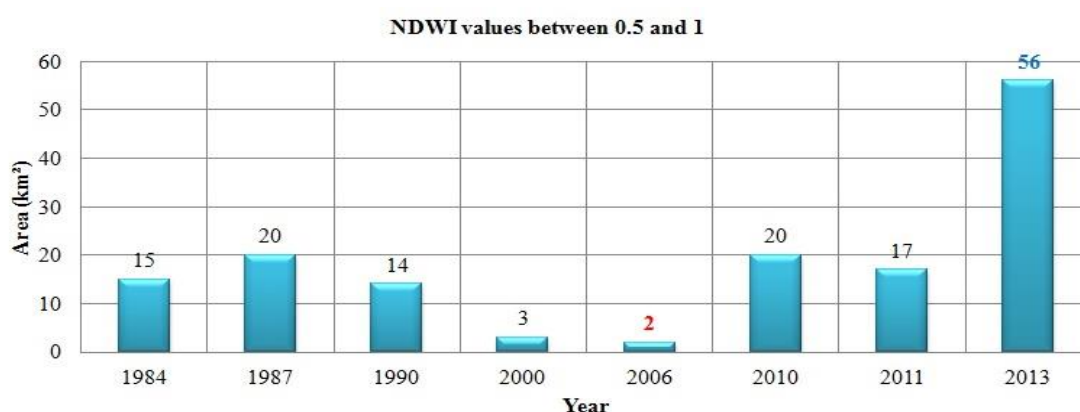


**Figure 5.71:** NDWI values between 0.5 and 1.

Table 5.29 shows the area of different NDWI classes. Values mentioned in Area (-1-0) column illustrates the area of NDWI class, including NDWI values between -1 and 0 and Values mentioned in Area (0-0.5) column shows the area of NDWI class, including NDWI values between 0 and 0.5 and Values mentioned in Area (0.5-1) column illustrates the area of NDWI class, including NDWI values between 0.5 and 1. The total classified area of each year was different from other years because their water bodies were different from each other and water bodies were masked to analyze NDWI changes in non-water bodies. By analyzing the results of NDWI maps and table 5.29 it could be concluded that NDWI values changed in the study area from 1984 to 2013 especially between 2000 and 2013.

**Table 5.29:** NDWI results (km<sup>2</sup>) in summer time.

Year	Area (-1-0)	Area (0-0.5)	Area (0.5-1)	Total Area
1984	40846	40007	15	80868
1987	34518	45757	20	80295
1990	36554	42899	14	79467
2000	41545	39467	3	81015
2006	48943	32162	2	81107
2010	52247	29836	20	82103
2011	47791	33667	17	81475
2013	53462	29176	56	82694

#### 5.3.4 Normalized Difference Drought Index (NDDI)

Normalized Difference Drought Index NDDI was generated from NDVI and NDWI using Eq.(5.13) to analyze drought condition in study area. NDDI combines information from visible, NIR, and SWIR bands. NDDI values are between 0 and 100. High values, especially values which are between 10 and 100 show high intensity of drought in the study area.

$$NDDI = \frac{NDVI - NDWI}{NDVI + NDWI} \quad (5.13)$$

NDDI values were calculated in ENVI, then their water bodies masked in ArcGIS and finally, they were reclassified and converted to maps in ArcGIS. Figures 5.72 and 5.73 show NDDI maps in summer time of 1984, 1987, 1990, 2000, 2006, 2010, 2011, and 2013. To understand changes in the study area NDDI values between 10 and 100 were assigned to red color. According to NDDI maps, NDDI values between 10 and 100 increased from 2000 to 2006. The increases of these values in the study area was realitiden to the increasing intensity of drought condition in the study area. By considering NDDI maps, it could be concluded that NDDI values between 10 and 100 were increased especially in north, south-east and east parts of Urmia Lake in summer time of 2006, 2010, 2011, and 2013. Moreover to have a good comparison and analysis NDDI changes in the study area, total area of NDDI classes was calculated in 3 groups. The first class includes values between 0 and 2, the second class includes values between 2 and 10, and finally the third class includes values between 10 and 100.

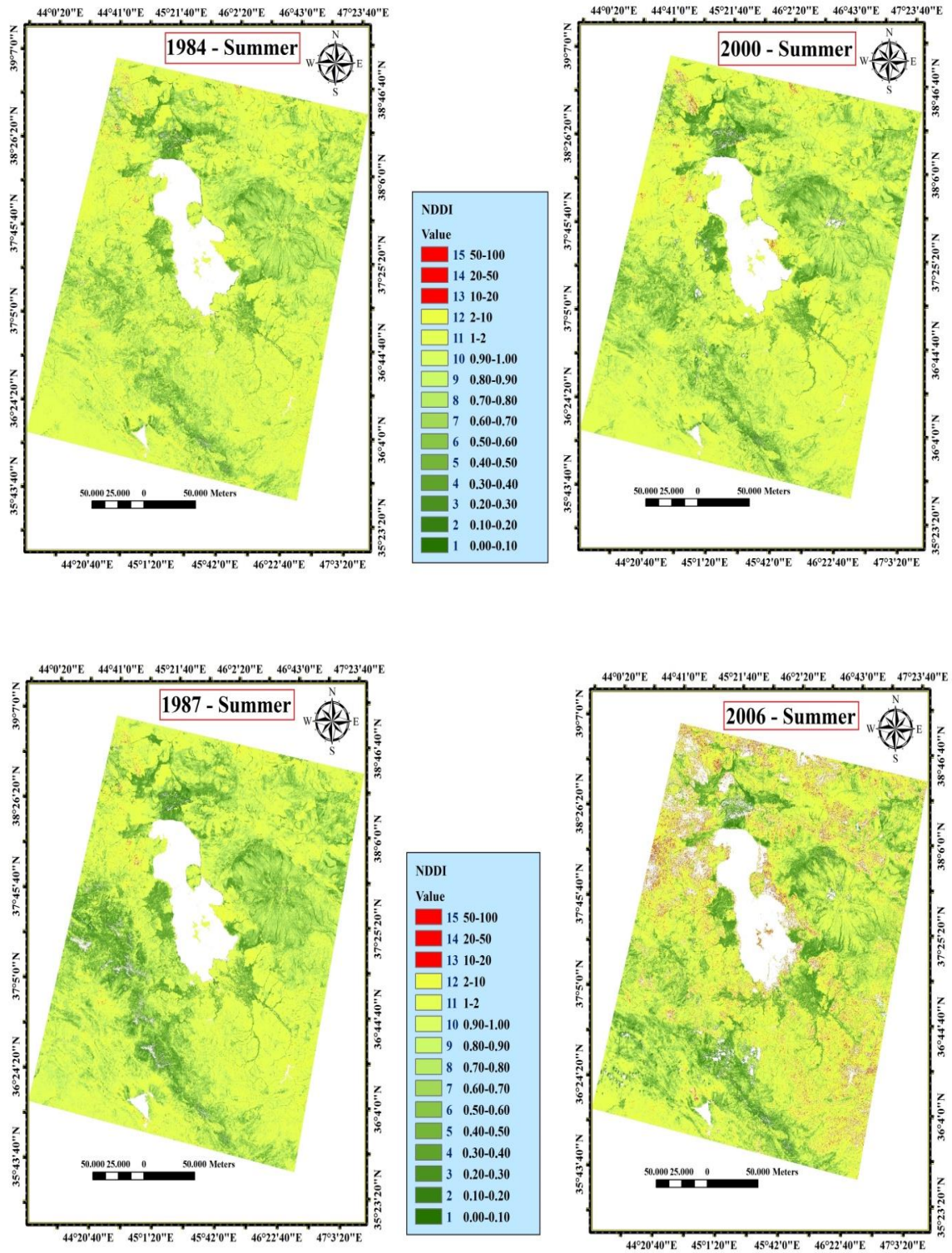
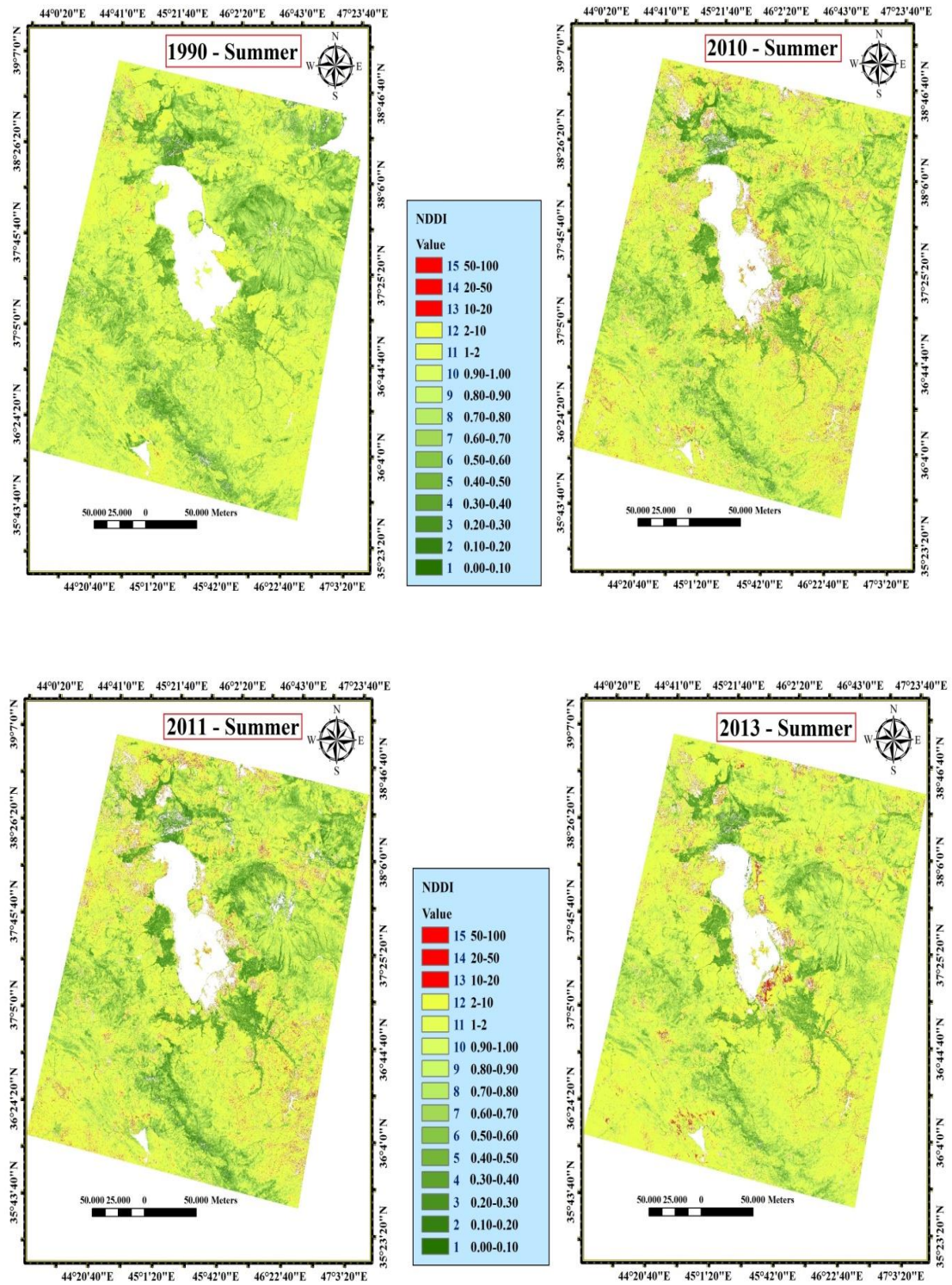


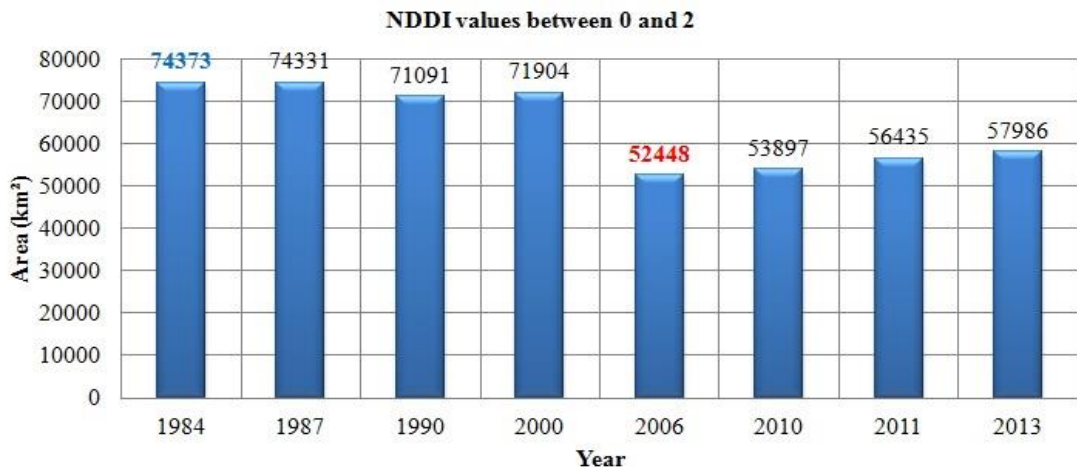
Figure 5.72: NDDI maps in summer time of 1984, 1987, 2000, and 2006.



**Figure 5.73:** NDDI maps in summer time of 1990, 2010, 2011, and 2013.

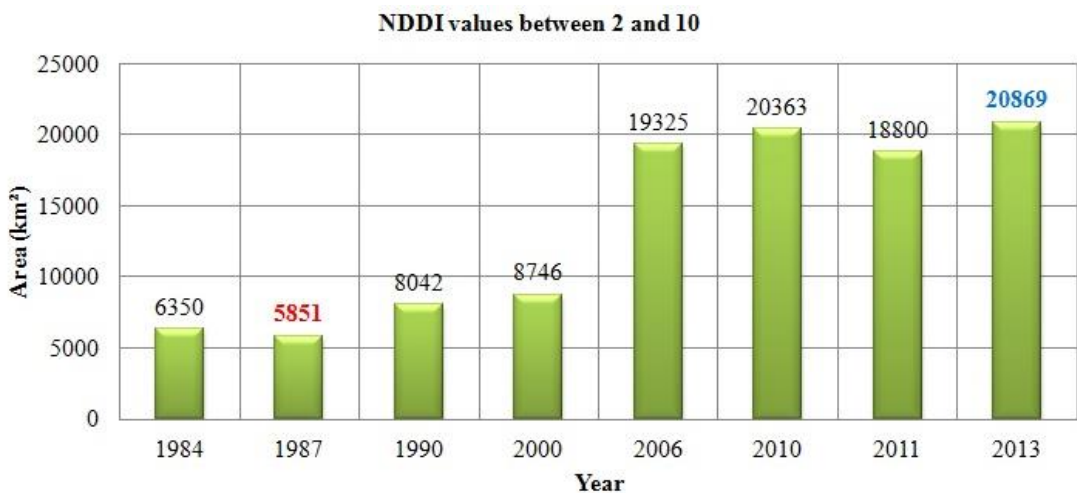
Figure 5.74 shows the area of values between 0 and 2. These values illustrate the normal condition in the study area. The minimum area of this class was about 52448 km<sup>2</sup> in 2006 and the maximum area of it, was about 74373 km<sup>2</sup> in 1984. The study area changes between 2000 and 2006 were considerable. NDDI value changes were

significant during this time. The total area of this class decreased between 2000 and 2006 years and it increased from 2006 to 2013 years.



**Graph 5.74:** NDDI values between 0 and 2.

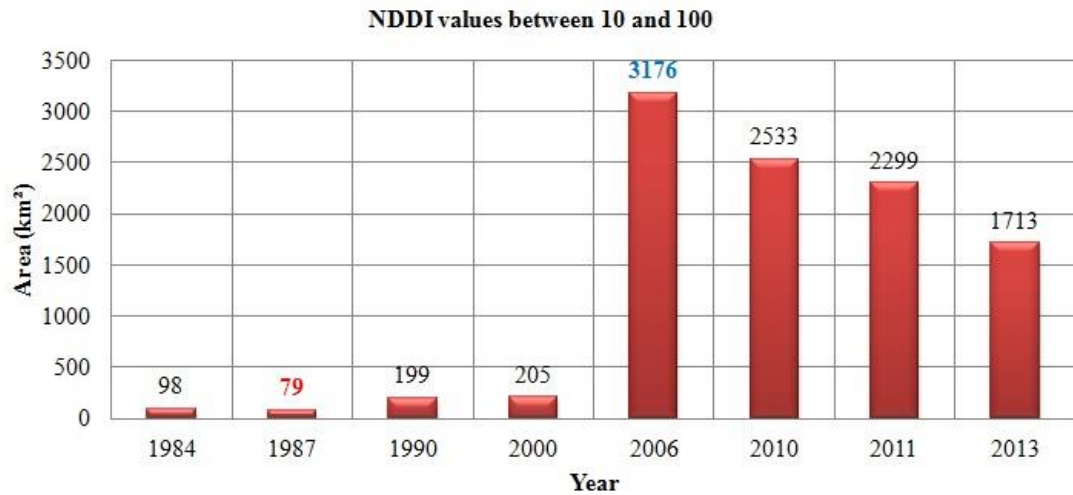
Figure 5.75 shows the area of values between 2 and 10. These values show normal condition in study area. The minimum area of this class was about 5851 km<sup>2</sup> in 1987 and the maximum area of it, was about 20869 km<sup>2</sup> in 2013. The study area changes between 2000 and 2006 were considerable. NDDI value changes were significant during this time. The total area of this class increased extremely between 2000 and 2006 years.



**Graph 5.75:** NDDI values between 2 and 10.

Figure 5.76 shows the area of NDDI values between 10 and 100. These values illustrate a drought condition in the study area. The minimum area of this class was

about 79 km<sup>2</sup> in 1987 and the maximum area of it, was about 3176 km<sup>2</sup> in 2006. The study area changes between 2000 and 2006 were considerable and NDDI value changes were significant during this time. The total area of this class increased extremely between 2000 and 2006 years and it decreased from 2006 to 2013 years.



**Graph 5.76:** NDDI values between 10 and 100.

According to the NDDI maps, NDDI values show considerable changes between 2000 and 2006. Totally, drought conditions increased between 2000 and 2013 but the intensity of this change was very significant from 2000 to 2006 and it decreased from 2006 to 2013. Moreover, close areas of Urmia Lake affected more than other regions because of existence salt areas in these regions. Also, west and southwest parts of study area affected less than other parts.

### 5.3.5 Normalized Differential Salinity Index (NDSI) and Salinity Index (SI)

Normalized Differential Salinity Index (NDSI) was used for identification of soil salinity changes in the study area. Salt-affected soils can be determined using Normalized Difference Vegetation Index (NDVI), and Normalized Differential Salinity Index (NDSI) as well. NDSI helps to generate a color composite image to isolate and interpret salt-affected lands. NDSI values are between -1 and 1, smaller values show less salt-affected areas and higher values show high salt-affected areas.. Eq.(5.14) show related formula to calculate NDSI value in Landsat images.

$$NDSI = \frac{\rho_{Red} - \rho_{NIR}}{\rho_{Red} + \rho_{NIR}} \quad (5.14)$$

Where  $\rho_{Red}$  is the reflectance or radiance in a red wavelength band and  $\rho_{NIR}$  is the reflectance or radiance in a near infrared wavelength band[23,24,25,26]. NDSI values were calculated in ENVI and then their water bodies were masked in ArcGIS. In final step, they were classified and converted to maps in ArcGIS. Figures 5.77 and 5.78 show NDSI maps at summer time of 1984, 1987, 1990, 2000, 2006, 2010, 2011, and 2013. Green color shows low NDSI values and less salt affected areas and yellow color shows high NDSI values and high salt affected areas.

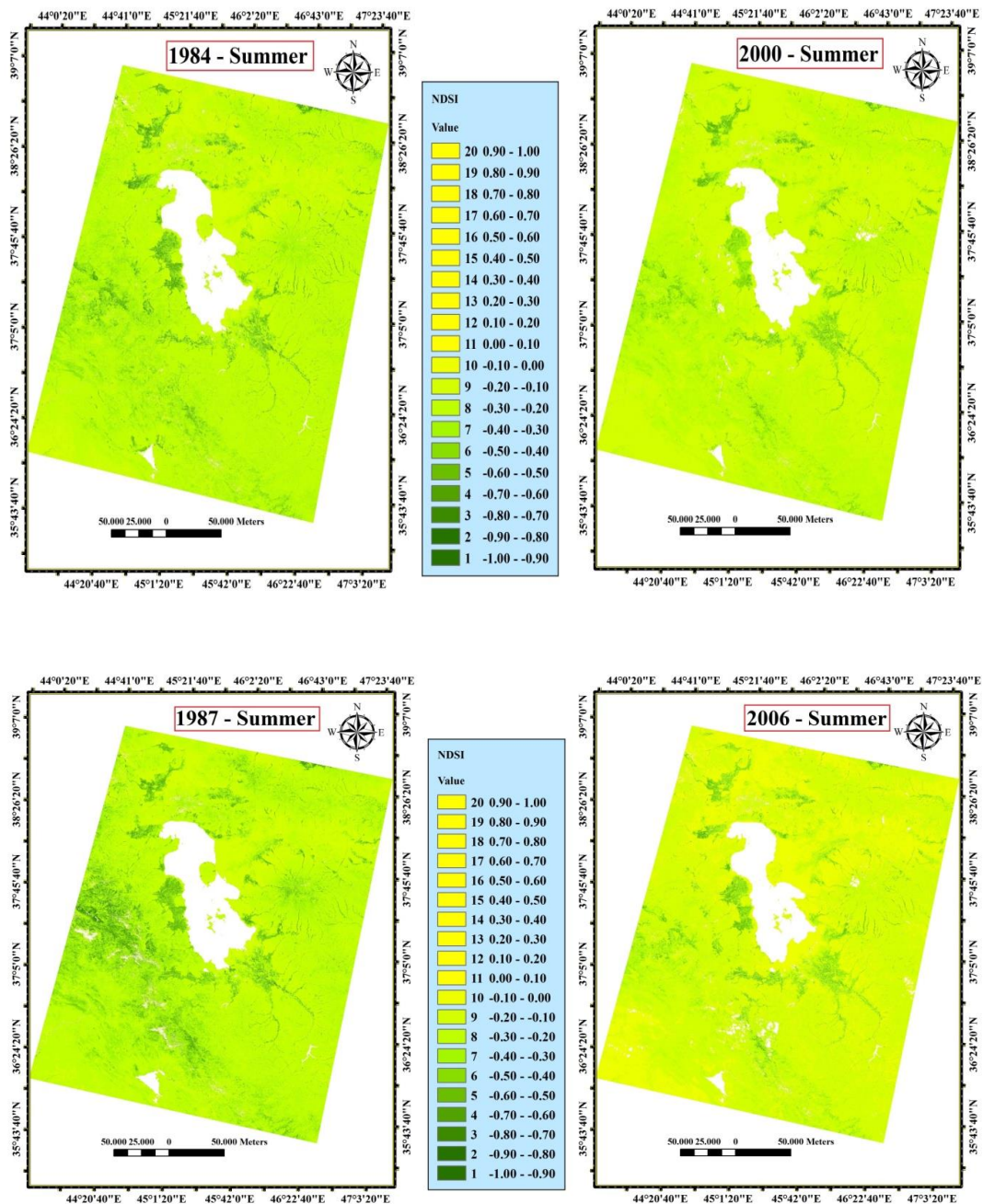
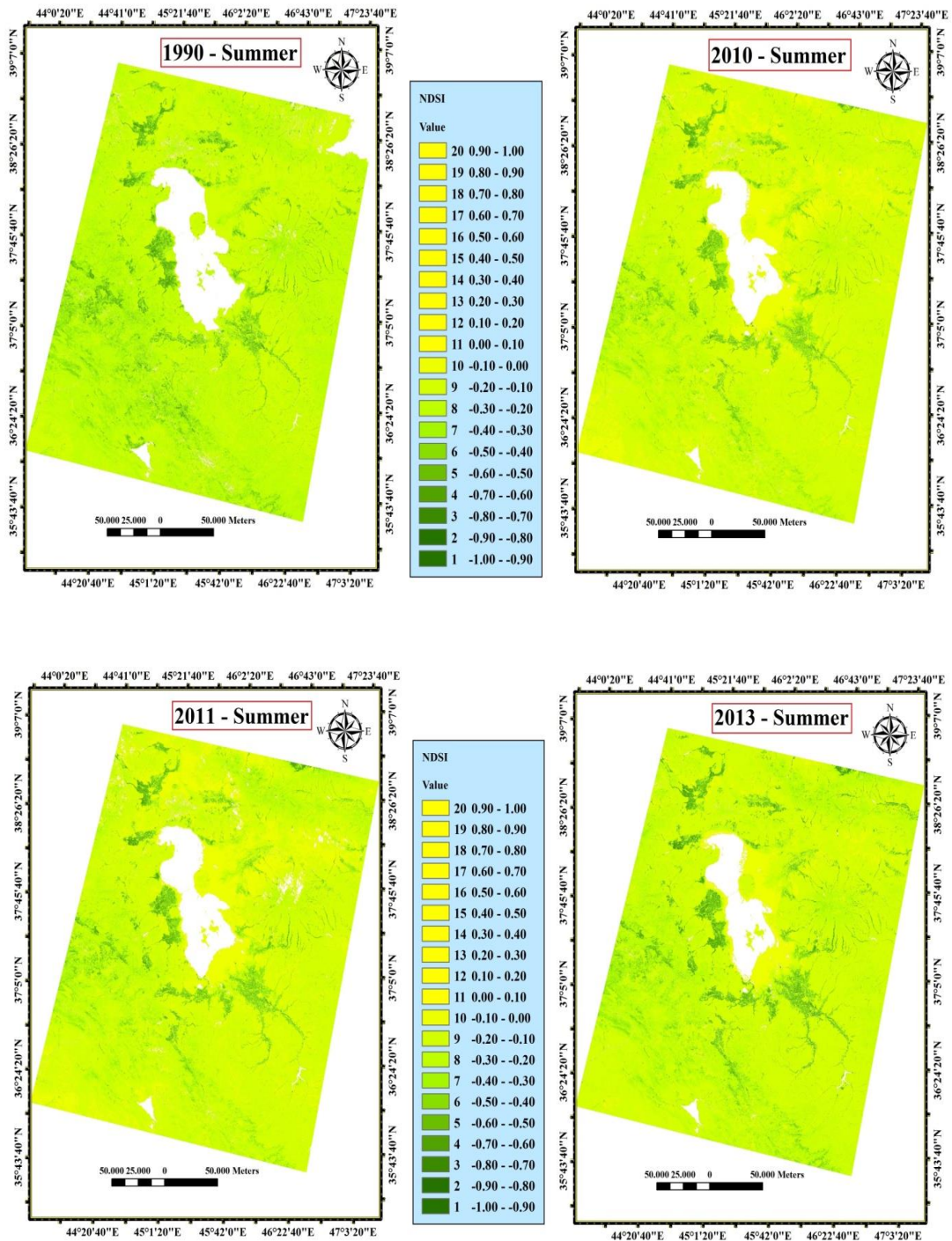


Figure 5.77: NDSI maps in summer time of 1984, 1987, 2000, and 2006.





**Figure 5.78:** NDSI maps in summer time of 1990, 2010, 2011, and 2013.

According to NDSI maps, soil salinity changes occurred in the study area, especially from 2000 to 2006 and the salinity increased in the study area especially in the east and south parts of Urmia Lake. Salt affected areas between 1984 and 2000 covered smaller parts and less changes rather than years between 2000 and 2013 in which high percentage of study area changed to salt-affected areas.

Salinity Index (SI) which was another indice to analyze soil salinity was used in this study to monitor and analyze changes in study area. SI values are between 0 and 1, smaller values show less salt-affected areas and higher values show high salt-affected areas. Eq.(5.15) shows the related formula to calculate salinity Index.

$$SI = \frac{\rho_{Green} + \rho_{Red}}{2} \quad (5.15)$$

Where  $\rho_{Green}$  is the reflectance or radiance in a green wavelength band and  $\rho_{Red}$  is the reflectance or radiance in a red wavelength band. SI values were calculated in ENVI and then their water bodies were masked in ArcGIS using shapefiles extracted by MNDWI. In the final step, they were classified and converted to maps in ArcGIS. Figures 5.79 to 81 show SI maps at summer time of 1984, 1987, 1990, 2000, 2006, 2010, 2011, and 2013. Green color shows low SI values and less salt affected areas and yellow color shows high SI values and high salt affected areas.

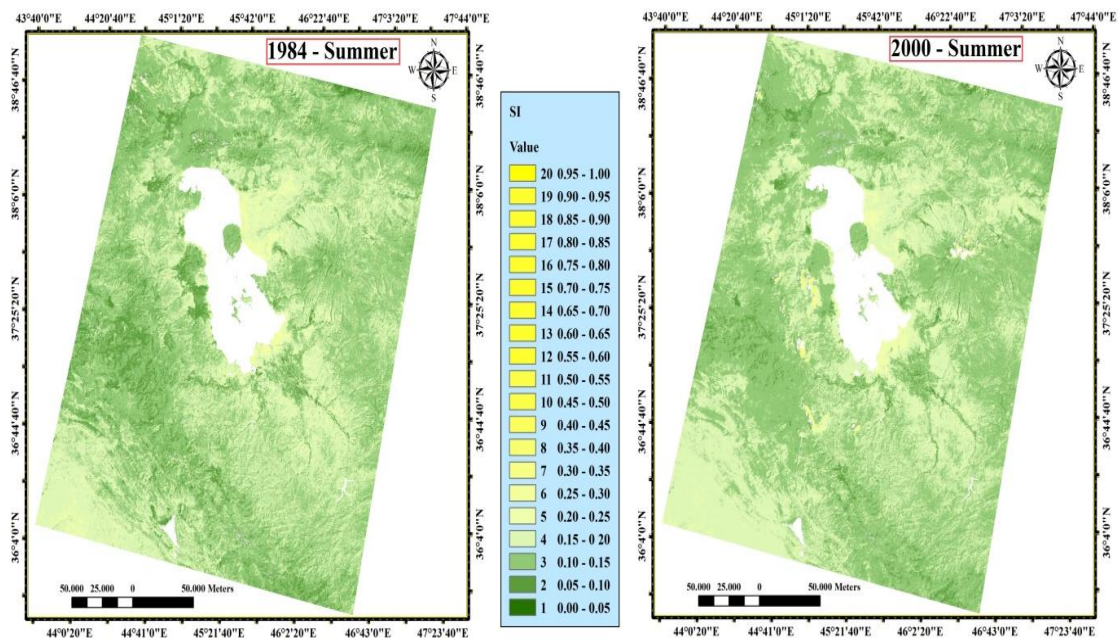


Figure 5.79: SI maps in summer time of 1984 and 2000.

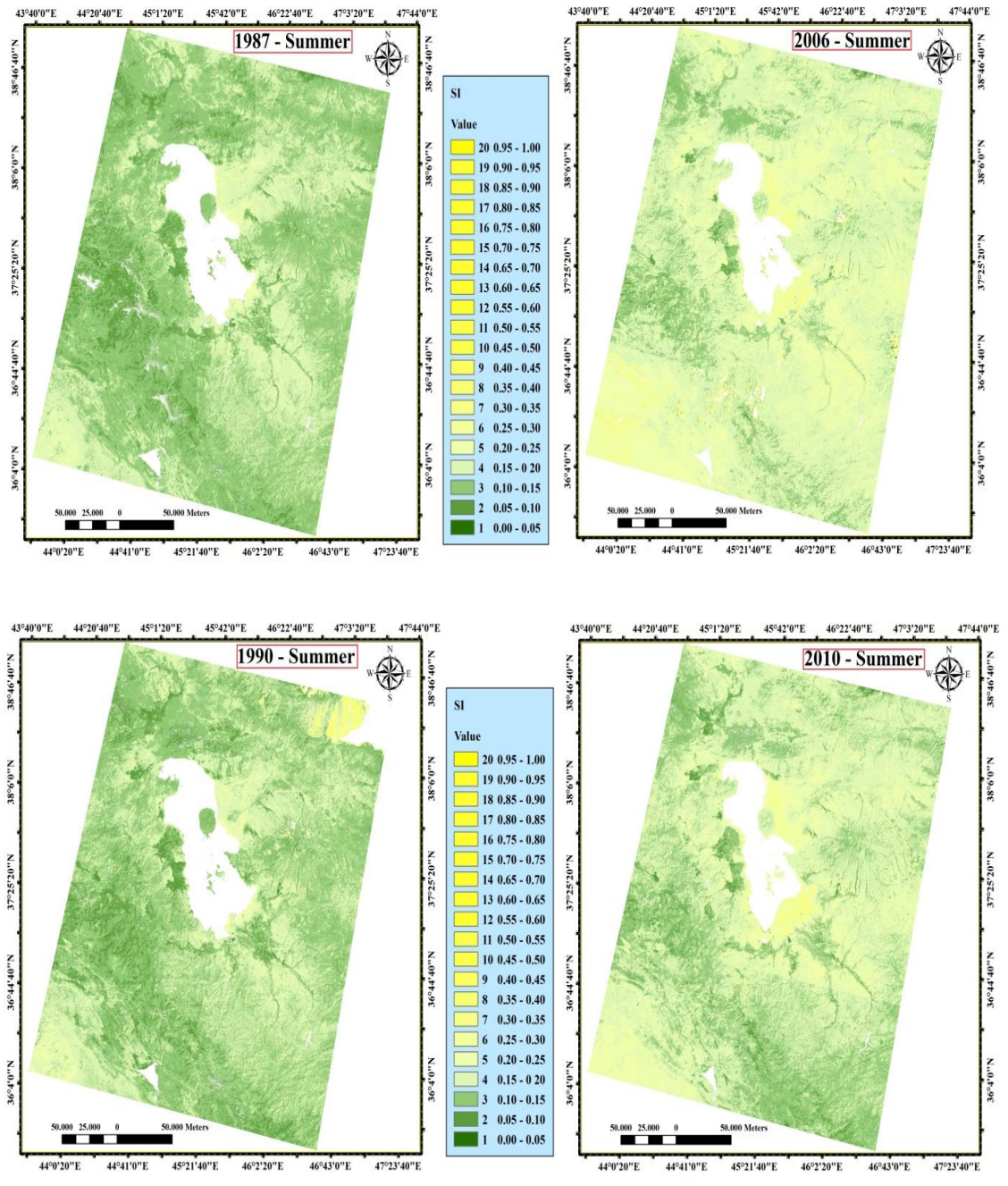
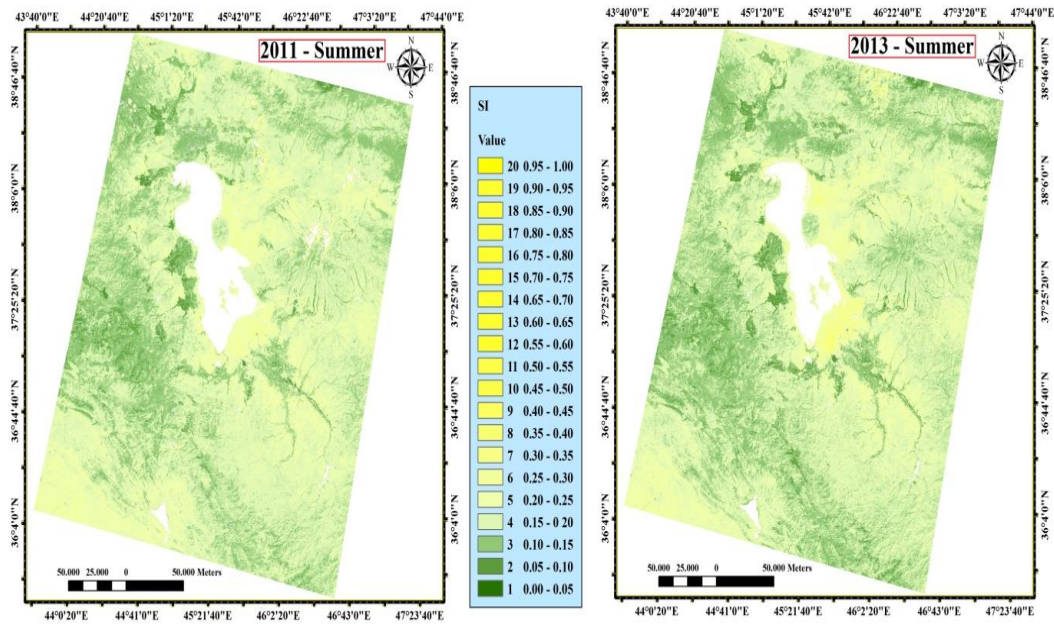


Figure 5.80: SI maps in summer time of 1987, 1990, 2006, and 2010.



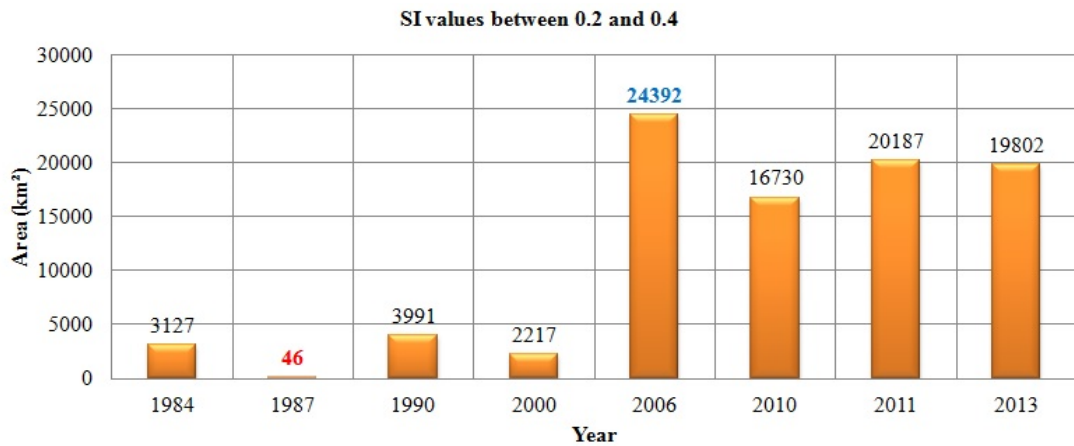
**Figure 5.81:** SI maps in summer time of 2011 and 2013.

According to SI maps, soil salinity changes occurred in the study area, especially between 2000 and 2006. The salinity increased in the study area especially in the east and south parts of Urmia Lake. The study area changes between 2000 and 2013 were considerable and SI value changes were significant during this time. Moreover, to have a good comparison and analysis SI changes, SI values reclassified and the area of each class in different years were compared. The area of SI classes was calculated in 3 groups. The first class includes values between 0 and 0.2, the second class includes values between 0.2 and 0.4, and finally, the third class includes values between 0.4 and 1. Figure 5.82 shows the area of values between 0 and 0.2. The minimum area of this class was about 56566 km<sup>2</sup> in 2006 and the maximum area of it, was about 80250 km<sup>2</sup> in 1987. The total area of this class decreased significantly between 2000 and 2006 years.



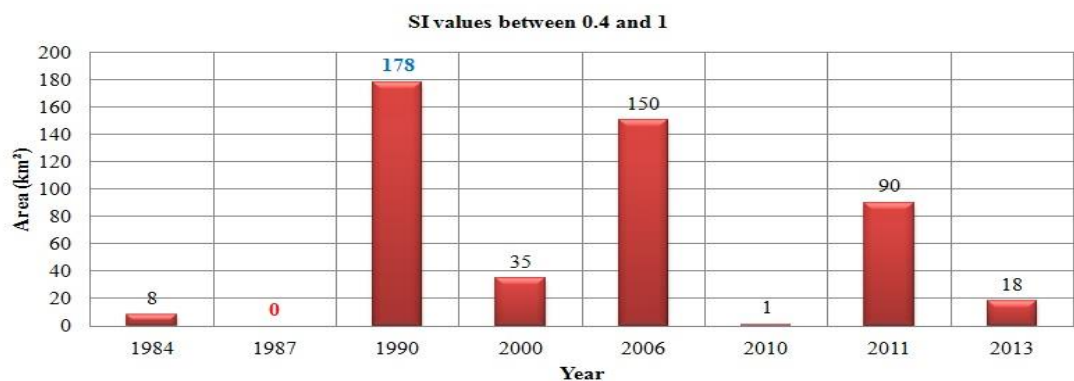
**Figure 5.82:** SI values between 0 and 0.2.

Figure 5.83 shows the area of values between 0.2 and 0.4. The minimum area of this class was about 46 km<sup>2</sup> in 1987 and the maximum area of it, was about 24392 km<sup>2</sup> in 2006. The study area changes between 2000 and 2006 were considerable and SI value changes were significant during this time. The total area of this class increased between 2000 and 2006 years and it decreased from 2006 to 2013 years.



**Figure 5.83:** SI values between 0.2 and 0.4.

Figure 5.84 shows the area of values between 0.4 and 1. The minimum area of this class was about zero km<sup>2</sup> in 1987 and the maximum area of it, was about 178 km<sup>2</sup> in 1990. The values of this class show high salt affected areas in the study area. By considering SI classes it could be understood that areas between 0 and 0.4 were better to analyze salinity changes in the study area because the covered area using this class was very large rather than other classes. The area of values between 0.4 and 1 was very small rather than other classes.



**Figure 5.84:** NDSI values between 0.4 and 1.

The area of each SI class is shown in Table 5.30. Values mentioned in Area (0- 0.2) column illustrates the area of SI class, including SI values between 0 and 0.2 and values mentioned in Area (0.2-0.4) column shows the area of SI class, including SI values between 0.2 and 0.4 and values mentioned in Area (0.4-1) column illustrates the area of SI class including SI values between 0.4 and 1. The total classified area of each year was different from each other because their water bodies were different from each other and water bodies were masked to analysis SI changes of non-water bodies. By analyzing the results of SI maps and table 5.30 it could be concluded that the study area changes between 2000 and 2013 were considerable and 2006 year could also be considered as the most salt affected year between studied years from 1984 to 2013.

**Table 5.30:** SI results (km<sup>2</sup>) in summer time.

Year	Area (0-0.2)	Area (0.2-0.4)	Area (0.4-1)	Total Area
1984	77733	3127	8	80868
1987	80250	46	0	80296
1990	75298	3991	178	79467
2000	78763	2217	35	81015
2006	56566	24392	150	81108
2010	65373	16730	1	82104
2011	61197	20187	90	81474
2013	62874	19802	18	82694

To analyze salinity changes in water surface of Urmia Lake, Salinity Index (SI) was used. Salinity Index values were calculated in ENVI using band math and masked in ArcGIS using shapefiles of water bodies extracted from MNDWI results to keep the salinity values of water surface of Urmia Lake. In other words, salinity index results and shapefiles of water surface area of Urmia Lake extracted by MNDWI were used to analyze salinity changes in water and some salinity areas which were stucked to Urmia lake. Figures 5.86 and 5.87 show the SI maps of water surface of Urmia Lake in summer time of 1984, 1987, 1990, 2000, 2006, 2010, 2011, and 2013. To check the accuracy of these results unsupervised classification maps in conjunction with SI maps were used beside each other to analyze and compare changes in water surface area of Urmia Lake and its saline vicinity. When the study area classified into 150 clusters using ISODATA, water class of Urmia Lake showed 2 specifics classes from 2000 to 2013. Figure 5.85 shows unsupervised classification results before recoding and editing. According to field study and visual interpretation, pale blue color in

figure 5.85 in 2013 year can be known as saturated water body having a low amount of water and high percentage of salinity in comparison to other parts of Urmia Lake. It can also be known as shallow water body, but it seems that saturated water body would be more appropriate naming for this class because shallow water body should be in all study dates and the depth of Urmia Lake is changeable in different parts of Urmia Lake during all studied years but there is no specific cluster between 1984 and 2000 like those which are between 2000 and 2013. Moreover, by analyzing water surface area changes from 2000 to 2013, it could be understood that drying of Urmia Lake was started from saturated water parts, especially south and east parts of Urmia Lake that belong to this class in the last years.

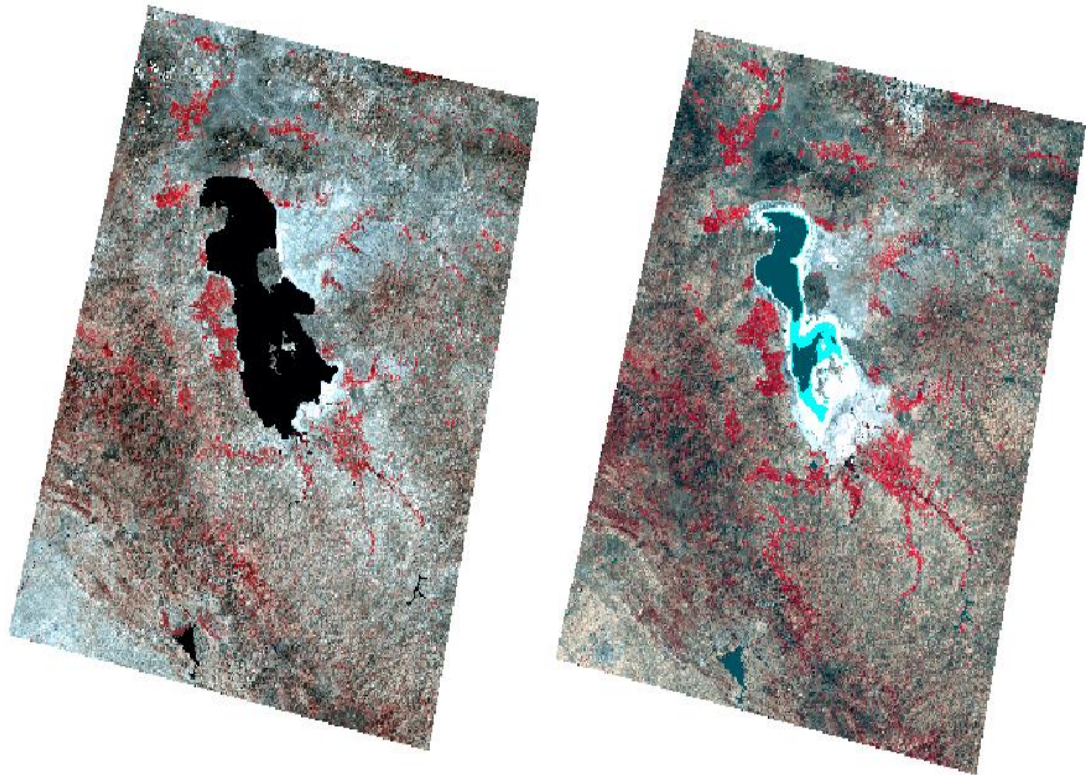


**Figure 5.85:** Unsupervised classification results in 1984-summer (Left) and 2013-summer (Right).

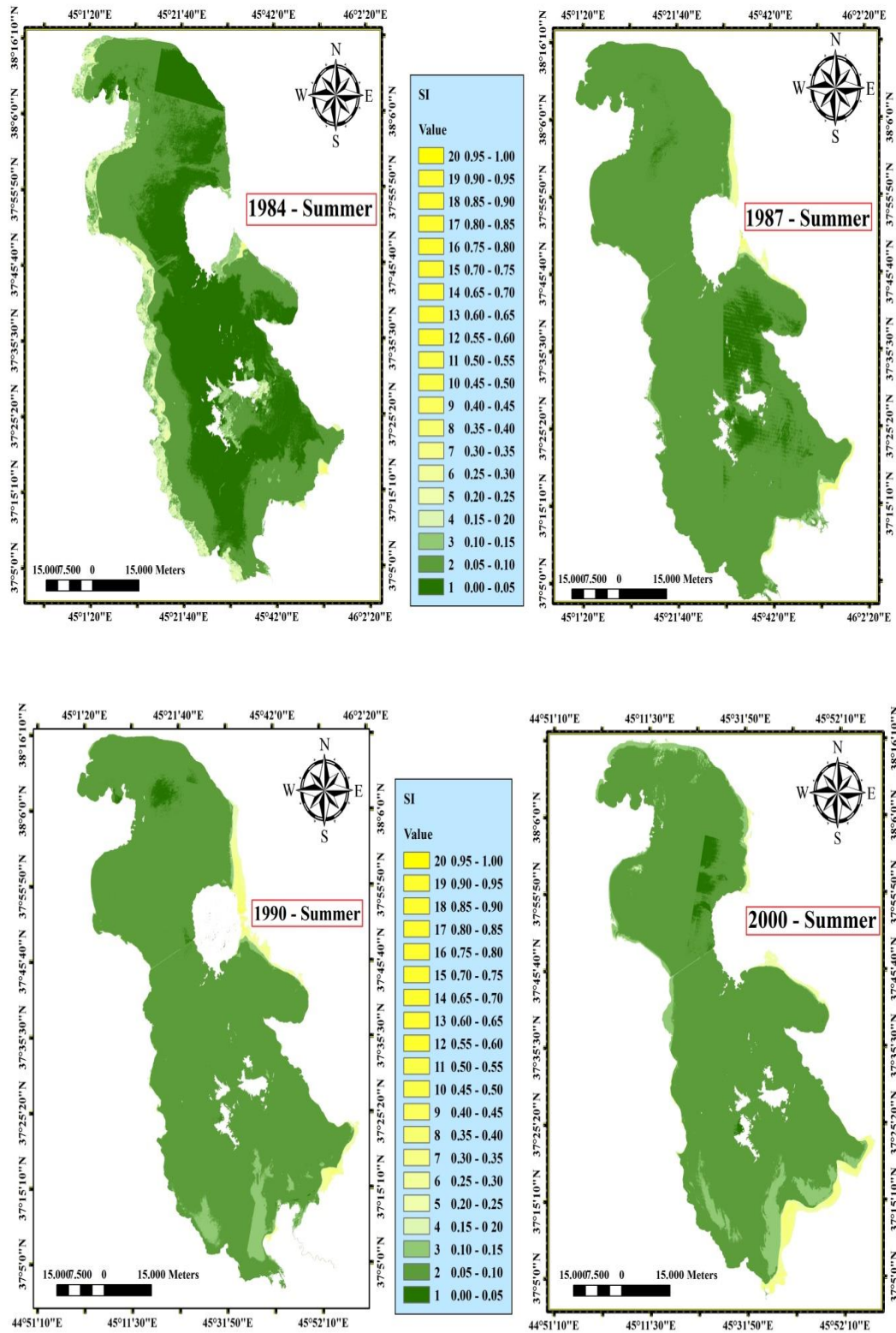


**Figure 5.86:** SI maps of Urmia Lake in summer time of 1984, 1987, 2000 and 2006.



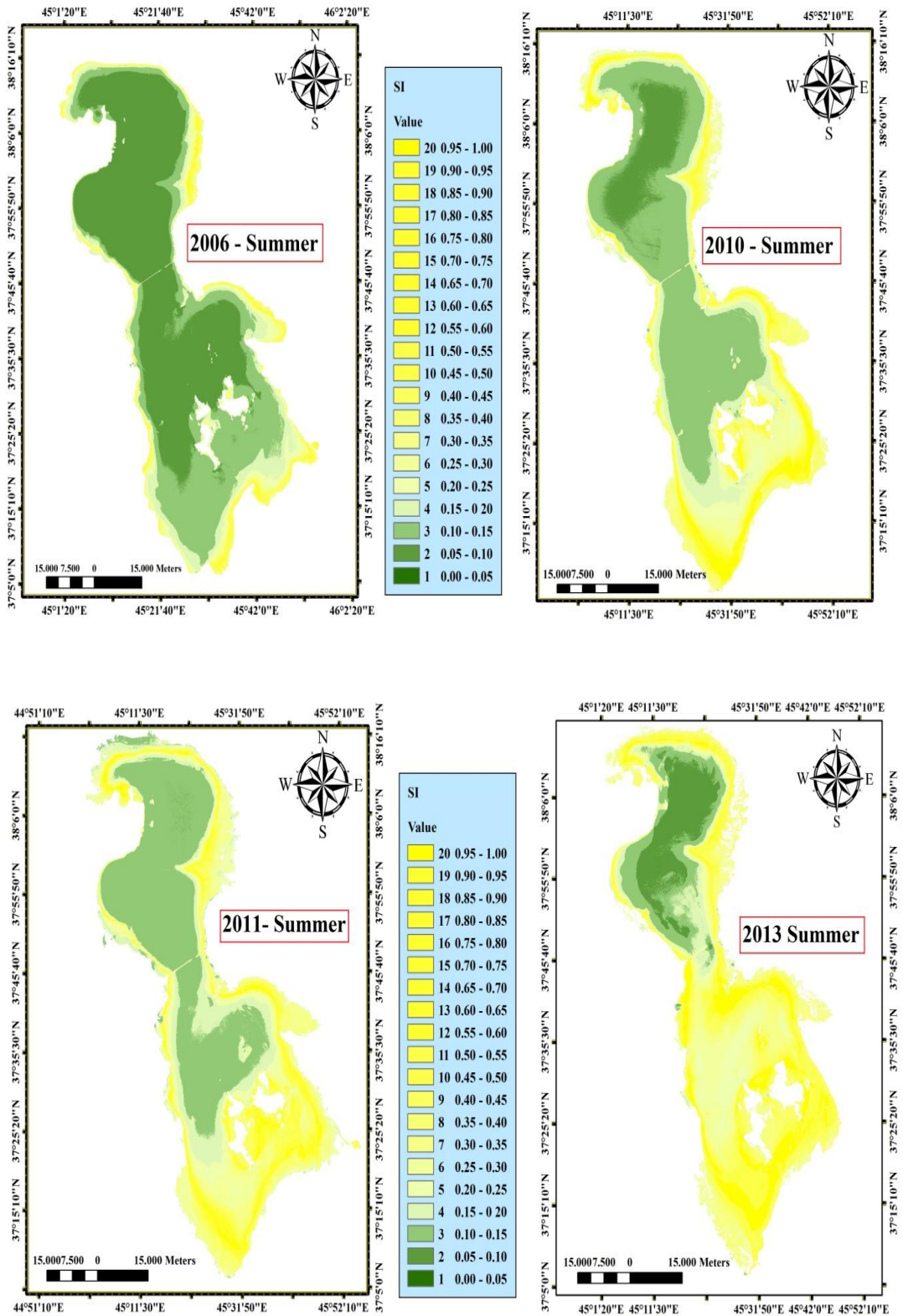


**Figure 5.87:** SI maps of Urmia Lake in summer time of 1990, 2010, 2011 and 2013.

Figure 5.88 shows the results of SI maps and unsupervised classification maps at summer time of 2006, 2010, and 2011 beside each other. By considering two

different classes for water and totally three classes which are named water, shallow water (saturated water), and salt, adaptation between the results of SI maps and unsupervised classification maps is clear. In all figures, number one is SI maps and number two is SI maps having values between 0.3 and 1 assigned to red color and number three is unsupervised map including 3 classes. According to these figures, salt class in unsupervised map matches to high SI values and saturated or shallow water class matches to SI values less than those ones matched to salt body. Finally, other SI classes having smaller values conform to water class of unsupervised classification maps and they show salinity changes in other parts of the water area.

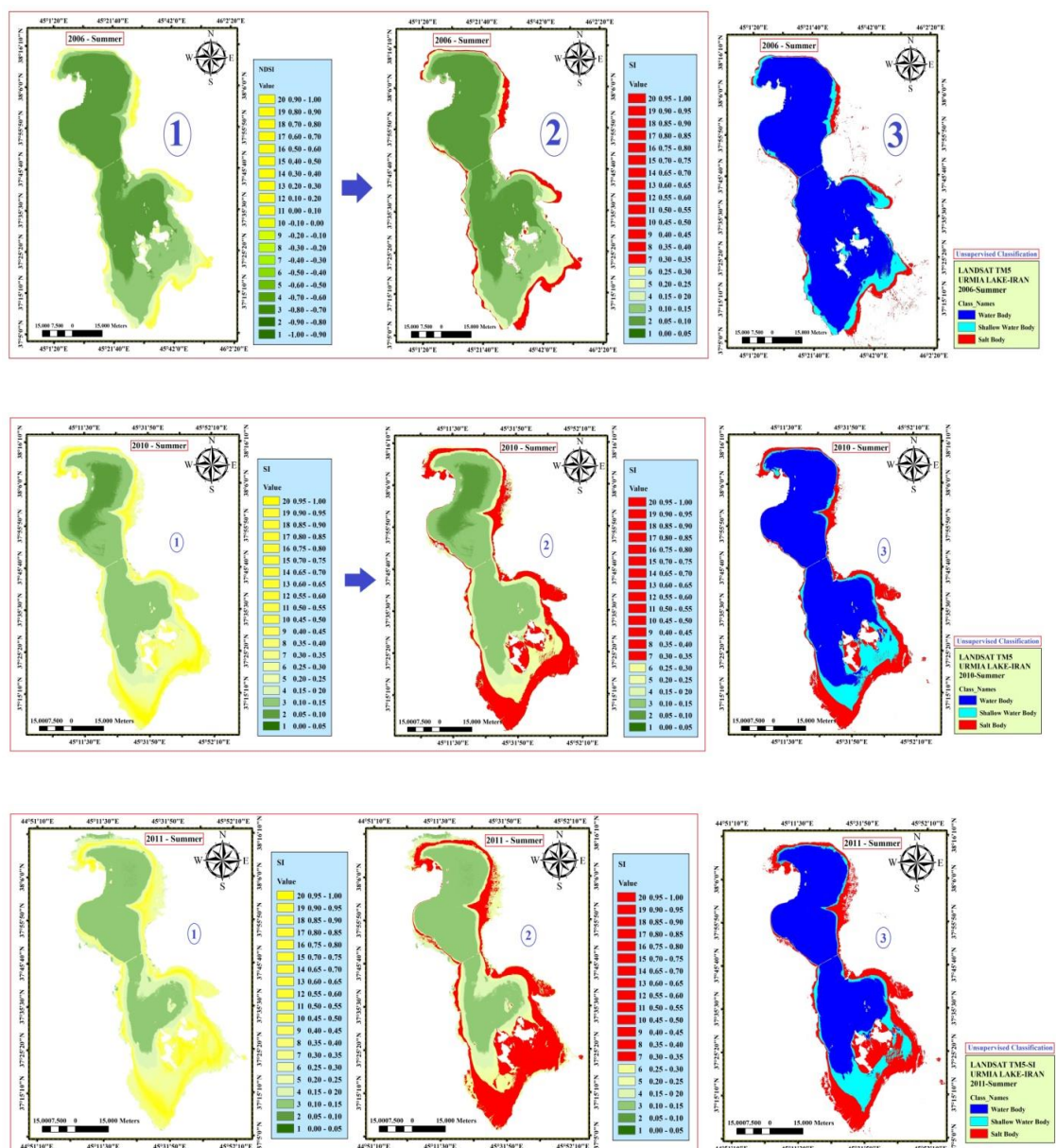


Figure 5.88: Comparing SI and unsupervised classification maps of Urmia lake.

In SI maps of water body, yellow color presents high SI values and high salt affected areas. Green color shows low SI values and less salt affected areas in the study area. Water salinity changes occurred in the study area from 1984 to 2013 but the intensity of changes was very high and considerable from 2000 to 2013 and the salinity percentage of water body increased extremely especially between 2006 and 2013.

#### 5.4 Analyzing Meteorological Data

20 synoptic stations were selected around Urmia Lake to analyze meteorological changes in the study area. Ordinary Kriging approach was applied to meteorological data obtained from all 20 synoptic stations to prepare prediction and standard error prediction maps of annual precipitation and mean air temperature in August month by considering that many Landsat frames which were used in this study during summer time were collected in August month. Moreover, Standardized Precipitation Index (SPI) was applied to 7 synoptic stations using long time period precipitation data to monitor drought and climate change between 1984 and 2011. The meteorological condition of 5 stations which were close to Urmia Lake were analyzed using air temperature, precipitation, and humidity data. Figure 5.89 shows climate zones in Iran. According to this figure, Urmia lake is located in cold zone and the weather condition around Urmia Lake is cold or very cold.

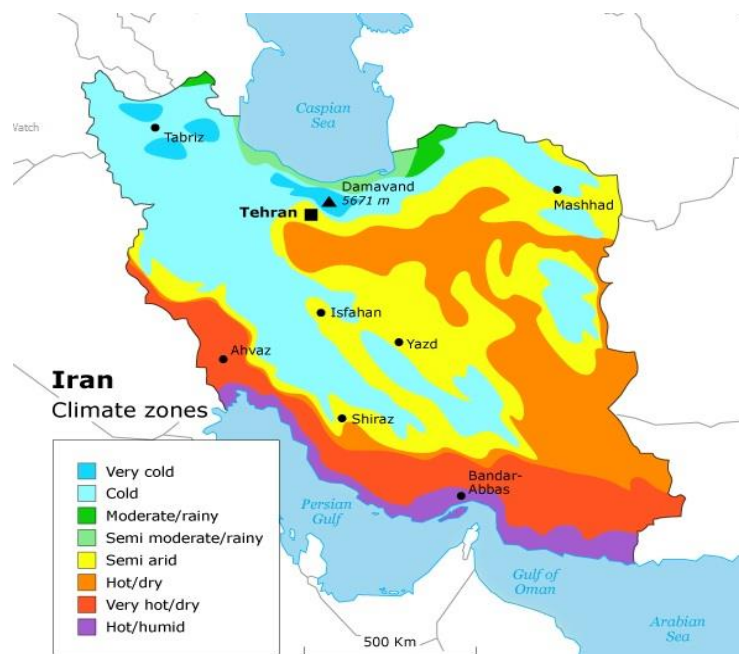


Figure 5.89: Climate zones of Iran[67].

### **5.4.1 Geostatistical Analysis**

Geostatistics is a specific type of statistics dealing with spatial databases on regionalized variables. It is a relatively new discipline developed in the 1960s primarily by mining engineers who were facing the problem of evaluating recoverable reserves in mining deposits. The applications of geostatistics have spread from the original metal mining topics in such diverse fields as soil science, oceanography, hydrogeology, agriculture, environmental science, and more recently health science. Recently GIS has emerged as an innovative and important component of many projects in geoscience and meteorology and it can be used to map and analyze the geographical distribution of different kinds of data: GIS has proven to be useful for geomatics research purposes, decision-making, planning, management and dissemination of information.

#### **5.4.1.1 Kriging To Temperature Data**

Ordinary kriging provides a prediction map and a standard error map that shows the uncertainty related to the predicted values. In this study, mean temperature values of 20 synoptic stations in August month from 2000 to 2011 were analyzed using ordinary kriging to understand temperature changes in study area. Table 5.31 shows the value of mean temperature of August month between 2000 and 2011 in synoptic stations. There were some missing data in 2000 year because some meteorological stations were established in 2006 year. Thirteen meteorological stations are located in West Azerbaijan and seven meteorological stations are located in East Azerbaijan. Figures 5.90 and 5.91 show prediction maps of mean air temperature in August month of 2000, 2006, 2007, 2009, 2010, and 2011. Because of missing data in 2000 year, the maps of this year doesn't seem appropriate to analyze changes in the study area, however its results were shown in this study to understand the difference between maps with enough data and missing data.

**Table 5.31:** Mean temperature values (°C) in August month.

Sta.Code	2000	2006	2007	2009	2010	2011
Gharaziyaaddin	-	29	26	23.6	27.1	26.3
Khoy	25.6	27.1	25.1	23.2	25.5	24.4
Salmas	-	25.5	23.6	22.2	23.7	23.8
Kahriz	-	26.3	24.4	22.8	24.6	24.3
Urmia	24.4	24.7	23.4	21.5	23.3	22.8
Ushnaviye	-	24	22.3	21.4	22.5	21.8
Sulduz	-	24.6	23,2	22.2	23.7	23.3
Piranshahr	25.9	27	25.4	24.2	26.1	25.2
Sardasht	27.4	28.8	26.8	25.9	27.9	26.7
Mahabad	26	26.4	24.9	24.4	25.6	25.6
Bukan	-	26.6	25	24.2	25.3	25.1
Shahindej	-	-	25.8	24.2	25.8	25.6
Miyandoab	-	25.8	24	22.8	24.4	24.2
Maragheh	26.3	28.2	26.6	25.2	27.1	26.5
Bonab	26.3	27.3	26	24.7	26.6	26.5
Bostanabad	-	22.5	20.9	19.7	20.8	20.7
Sahand	25.3	27.1	24.8	22.7	25.2	24.2
Tabriz	27	28.8	26.6	25	26.8	26.1
Marand	25.7	27.8	24.5	22.7	25.8	24.8
Ahar	22.7	24.1	21.5	19.9	21.9	21

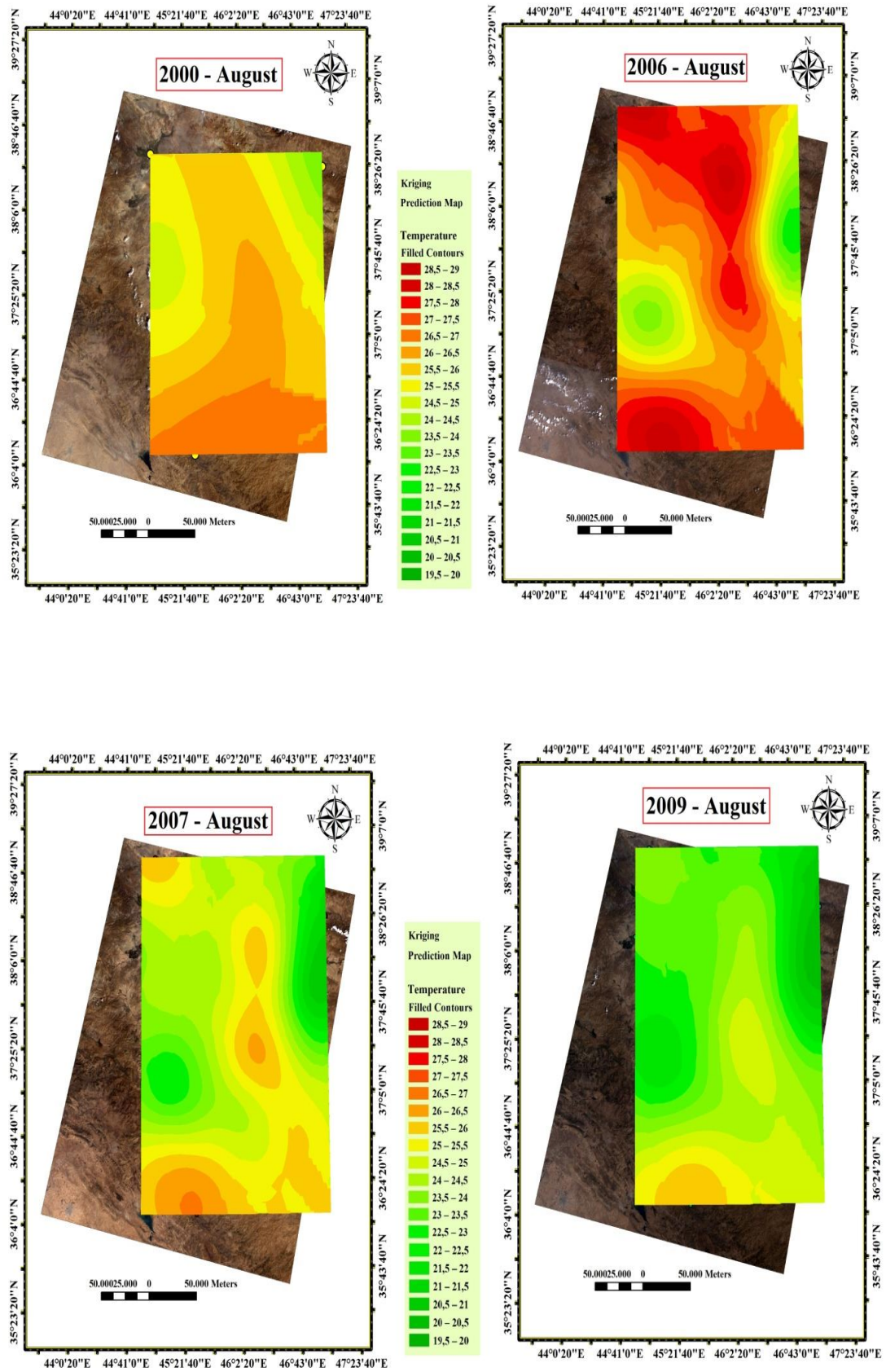
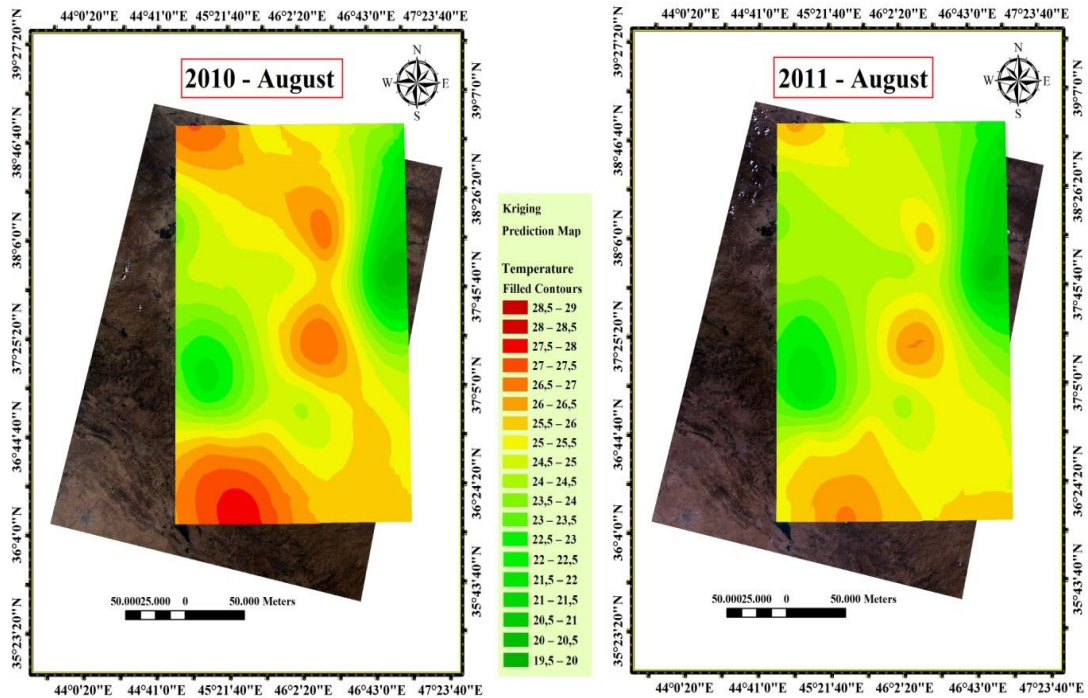
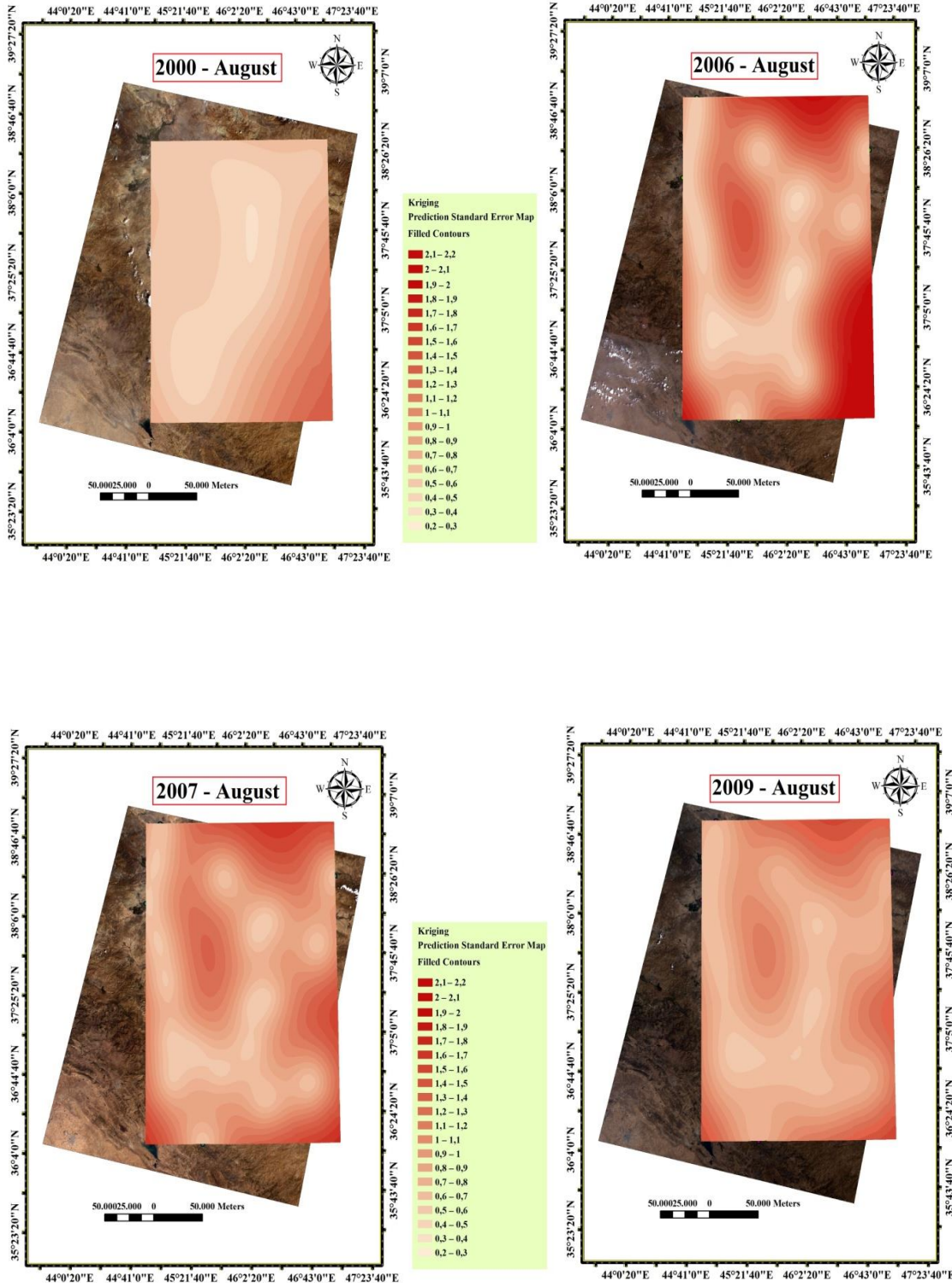


Figure 5.90: Prediction maps of air temperature in August month from 2000 to 2009.



**Figure 5.91:** Prediction maps of air temperature in 2010 and 2011.

According to prediction maps of mean air temperature in August month, 2006 and 2010 years seemed the warmest years and 2009 seemed the coldest year between studied years. Analyzing climate condition in 2000 year didn't seem very easy and possible because of missing data in this year. South, east, and northeast parts of Urmia Lake had warmer climate rather than other parts and west part of Urmia Lake had colder weather rather than other parts. Temperature increased from 2000-August to 2006-August and then it decreased from 2006-August to 2009-August. Then it increased from 2009-August to 2010-August and it decreased again from 2010-August to 2011-August. Figures 5.92 and 5.93 show prediction standard error maps in August month from 2000 to 2011. The kriging outcome in these figures indicated the standard error values were smaller in the neighborhoods of synoptic stations where data were available. The standard error values tend to increase toward the borders of the prediction area and on the Urmia Lake's surface which no observations were available. Moreover, standard error maps showed smaller values in 2007 and 2009 years in comparing to 2006, 2010, and 2011 years. In other words, standard error maps indicated the largest values in 2011 and the smallest values in 2009.



**Figure 5.92:** Prediction standard error map of air temperature in August month from 2000 to 2009.



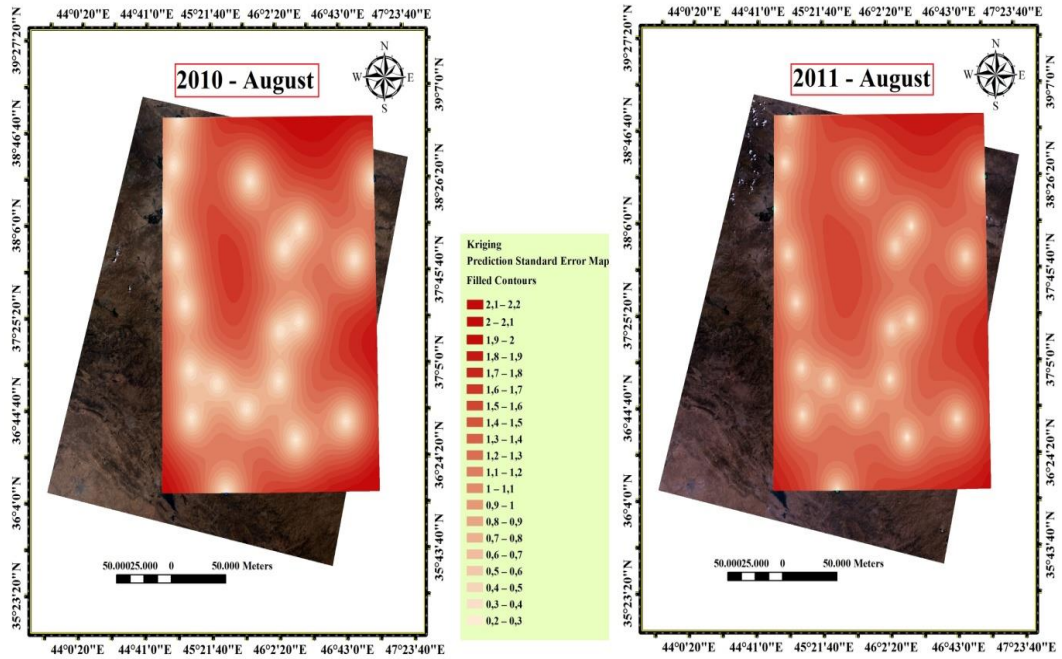


**Figure 5.93:** Prediction standard error map of air temperature in August month of 2010 and 2011.

#### 5.4.1.2 Kriging To Precipitation Data

Table 5.32 shows the value of annual precipitation from 2000 to 2011 in synoptic stations. There were some missing data in 2000 such as temperature in the previous section. Thirteen meteorological stations are located in West Azerbaijan and seven meteorological stations are located in East Azerbaijan. Figures 5.94 and 5.95 show prediction maps of annual precipitation in 2000, 2006, 2007, 2009, 2010, and 2011.

**Table 5.32:** Annually precipitation values (mm).

Sta.Code	2000	2006	2007	2009	2010	2011
Gharaziyaaddin	-	295.2	420.1	410.4	394.5	442.8
Khoy	207.1	269.8	287.6	275.4	245.3	320.4
Salmas	-	256.1	232.2	283.6	333	227.4
Kahriz	-	308.6	297.8	297.9	275	396.8
Urmia	230.6	427.7	264.8	292	329.3	409
Ushnaviye	-	640.3	397.2	334.8	328.6	532.3
Sulduz	-	537.9	314.6	518.8	230.1	375.8
Piranshahr	577.2	744.9	583.6	572.2	564.1	769.5
Sardasht	689.1	1018.8	621.2	800.9	676.2	865.3
Mahabad	313.3	578.1	331.2	334.4	255.1	436.2
Bukan	-	581.5	292.3	699.4	272.3	392.8
Shahindej	-	-	284.1	338.3	314.2	435.4
Miyandoab	-	422.7	197.2	278.4	222.8	360.5
Maragheh	175.5	395.8	245	258.5	201.3	295.8
Bonab	150.5	456.1	-	256.6	224.9	301.3
Bostanabad	-	363.2	310.8	261.2	253.3	481.1
Sahand	178.3	363.2	310.9	261.4	253.6	481.3
Tabriz	205	305.1	229.9	241.9	183.9	282.2
Marand	233.4	390.9	415.5	430.5	424.9	406.4
Ahar	243.5	283.5	335.3	182.9	276.4	337.8

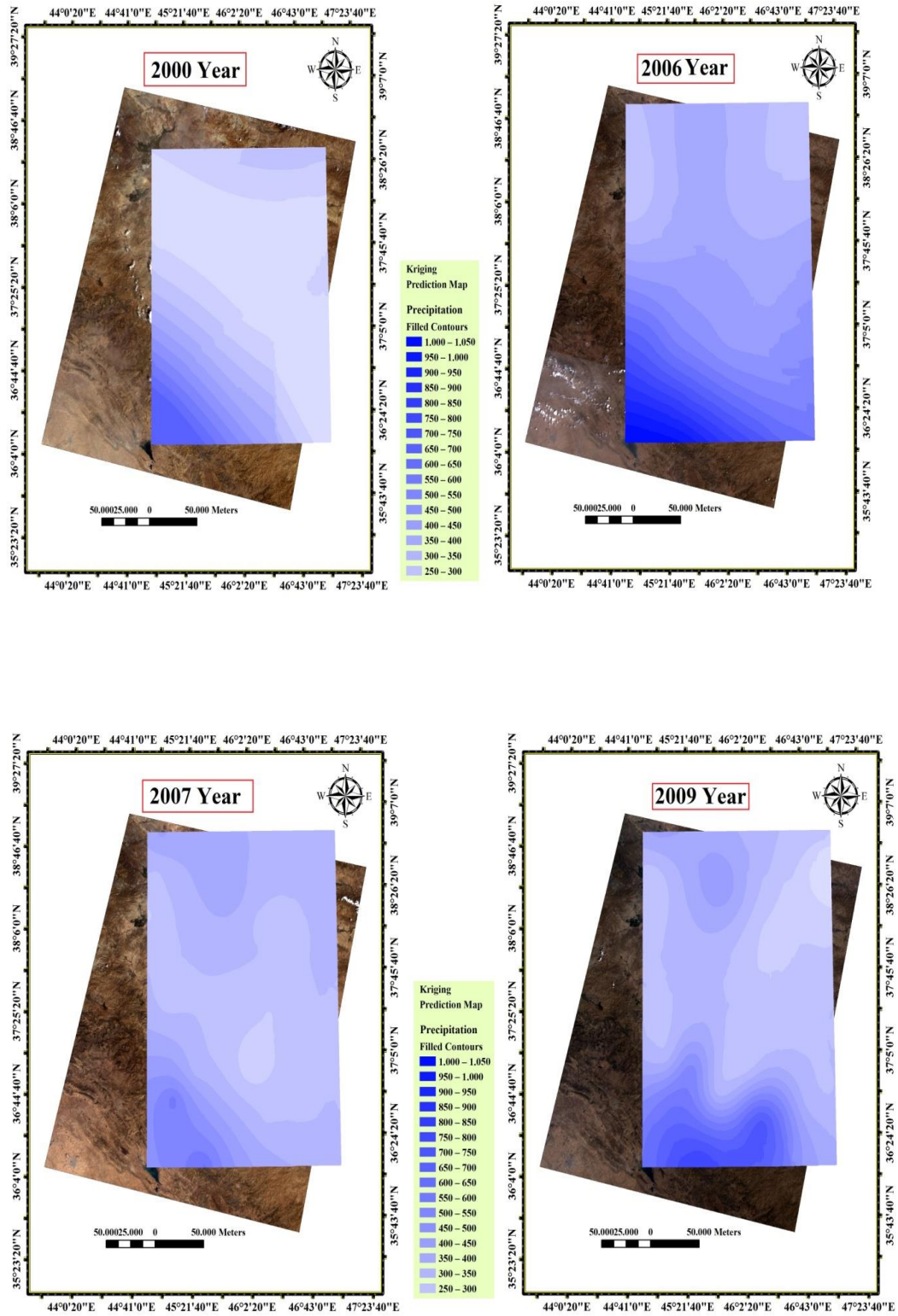


**Figure 5.94:** Prediction maps of annual precipitation from 2000 to 2009.

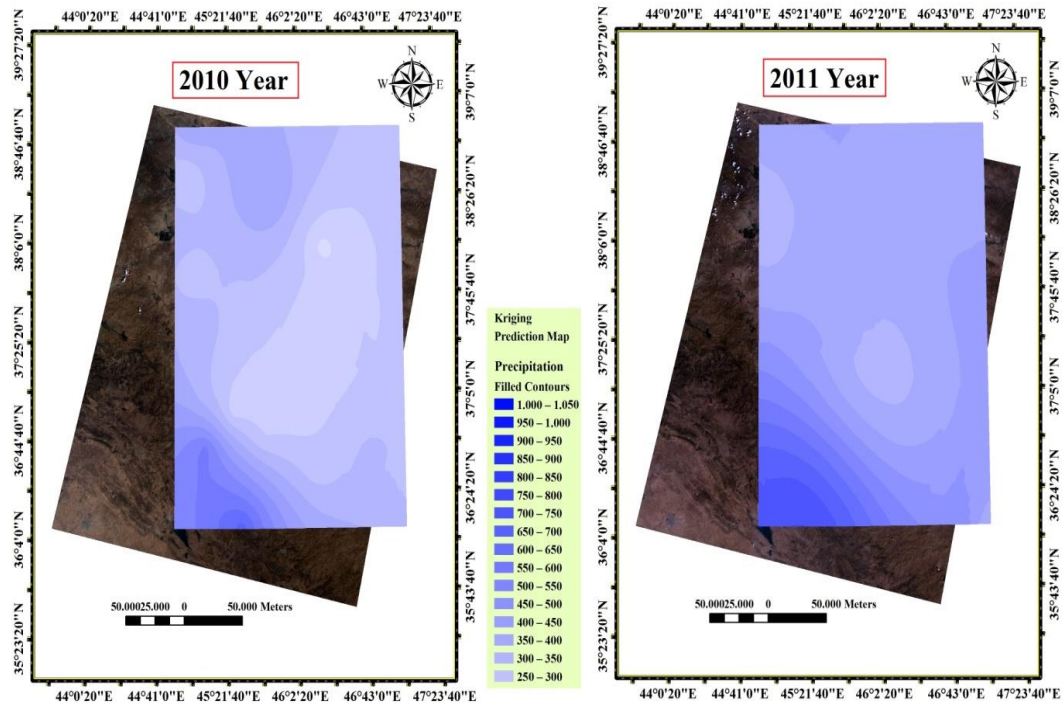


**Figure 5.95:** Prediction maps of annual precipitation in 2010 and 2011.

According to prediction maps of annual precipitation, more precipitation amount was received in 2006 and 2009, especially in the south-west part of Urmia Lake. Also in 2010, less rainfall was received compared to other years. Analyzing climate condition in 2000 year didn't seem very easy and possible because of missing data in this year. South, southwest and northwest parts of Urmia Lake had more rainfall rather than other parts. East and northeast parts of Urmia Lake had less rainfall rather than other parts. Rainfall increased from 2000 to 2006 and then it decreased between 2006 and 2007 and then it increased from 2007 to 2009. Then it decreased between 2009 and 2010 and finally, it increased from 2010 to 2011. Figures 5.96 and 5.97 show prediction standard error maps of annual precipitation from 2000 to 2011. The kriging outcomes in these figures indicated the standard error values were smaller in the neighborhoods of synoptic stations where data were available. The standard error values tend to increase toward the borders of the prediction area and on the Urmia Lake's surface which no observations were available. Moreover, standard error maps had smaller values in 2006 and 2011 years in comparing to 2007, 2009, and 2010 years. In other words, standard error maps indicated the largest values in 2009 and the smallest values in 2006.

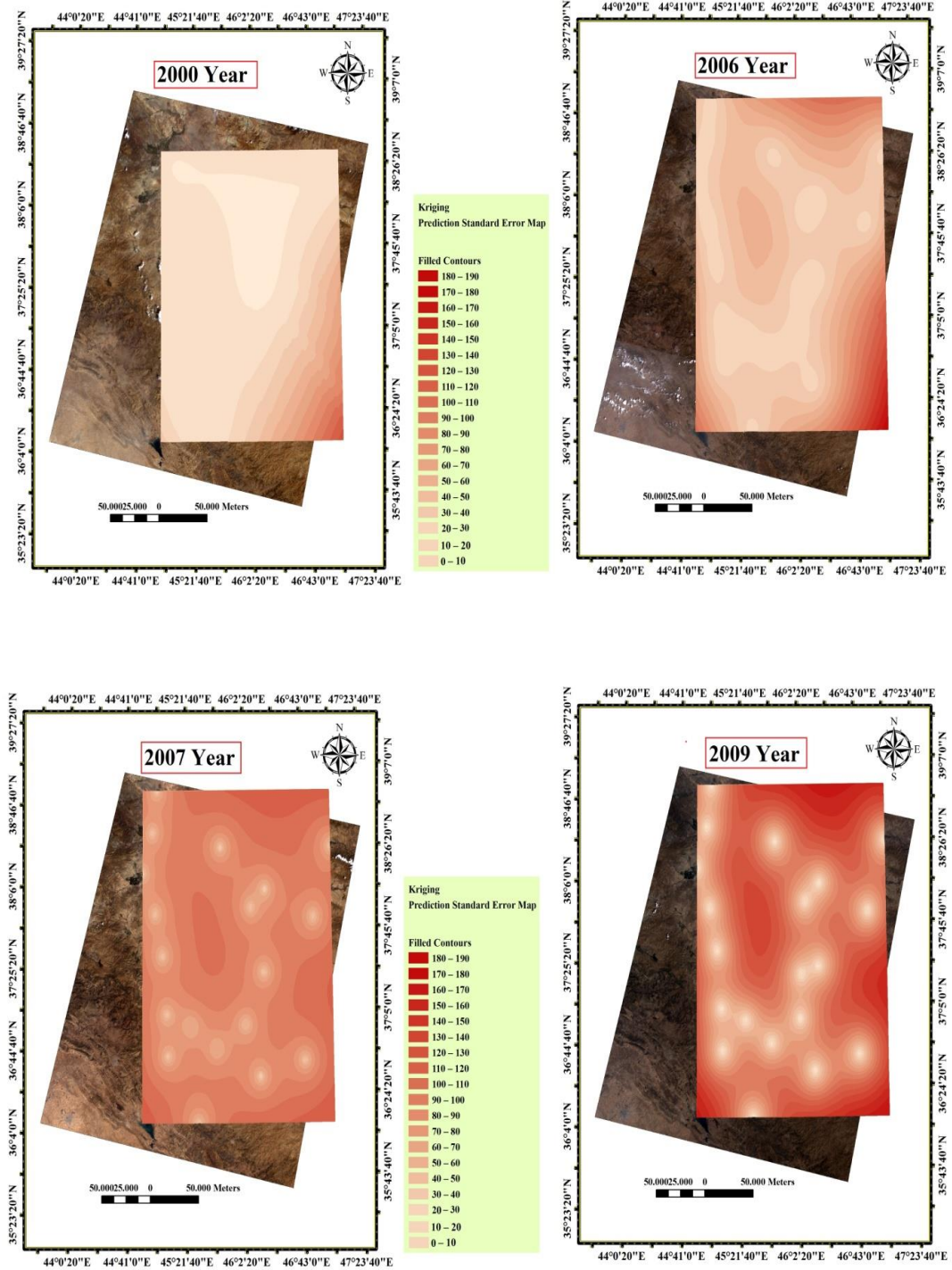


**Figure 5.96:** Prediction standard error maps of annual precipitation from 2000 to 2009.

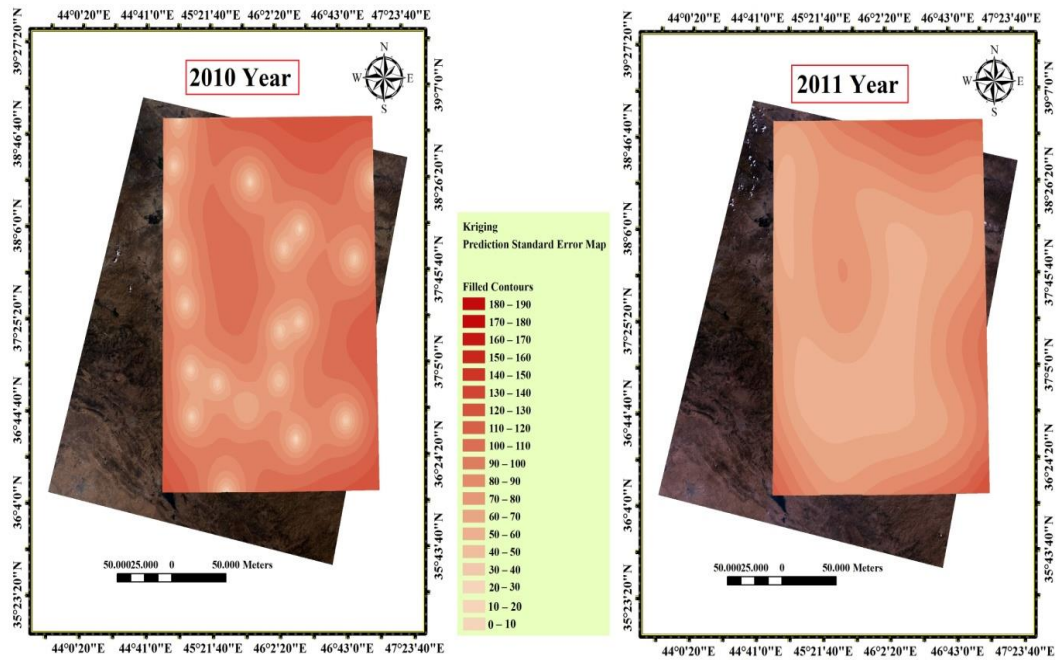


**Figure 5.97:** Prediction standard error maps of annual precipitation in 2010 and 2011.

According to the results of geostatistical analysis, 2006 seemed as the warmest year with more rainfall compared to other studied dates. The kriging maps in these figures indicated the standard error values were smaller in the neighborhoods of synoptic stations where data were available. The standard error values tend to increase toward the borders of the prediction area and on the Urmia Lake’s surface where no observations were available. Unfortunately, creating rainfall maps in 2000 year was not appropriate because of missing data in this year.

#### 5.4.2 Standardized Precipitation Index (SPI)

SPI\_SL\_6.exe is used in this study to calculate monthly SPI values in 7 synoptic stations. Precipitation values were edited and prepared monthly using long time period and then they were analyzed in SPI\_SL\_6.exe and the results of all months in all years were obtained. Finally the results of SPI were determined as 1-month SPI, 3-Month SPI, 6-Month SPI, 9-month SPI, 12-mont SPI, and finally 24-month SPI and the SPI values of June, July, and August in studied years when Urmia Lakes changes were analyzed using satellite images were compared in this study to understand drought changes in the study area from 1984 to 2011. Moreover, the SPI values of Urmia station which was the closest and the most important station

between others, were compared in all months between 1984 and 2011 when Urmia Lake's changes when analyzed using satellite images. SPI values of this station were compared in all years between 1998 and 2011 by considering that water surface area of Urmia Lake decreased extremely from 1998 to 2013. Ideally, at least 20-30 years of monthly values, with 50-60 years (or more) being optimal and preferred are used to calculate SPI values in SPI\_SL\_6.exe. Figure 5.98 shows the synoptic stations which were used in this study to calculate the SPI values.

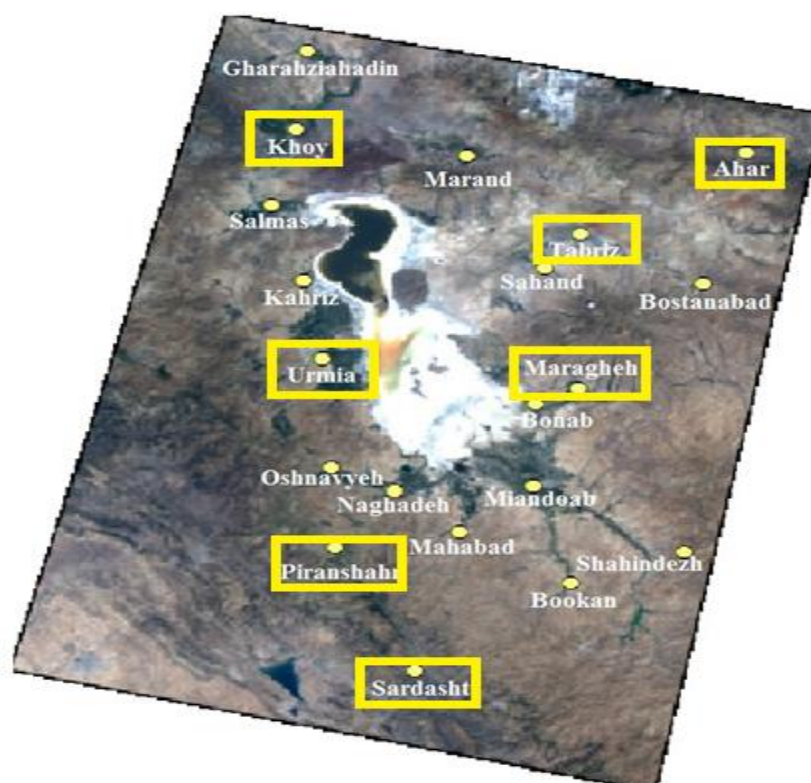


**Figure 5.98:** Location of synoptic stations which were used to calculate SPI.

Table 5.33 shows the time period of data of each station which were used in this study.

**Table 5.33:** Meteorological stations, which were used to calculate SPI.

Sta.code	Time period
Urmia	1951-2011
Tabriz	1951-2011
Khoy	1960-2011
Maragheh	1984-2011
Ahar	1986-2011
Piranshahr	1986-2011
Sardasht	1988-2011

Table 5.34 shows Mackee and others (1993) SPI Values and related drought intensity. The values of this table was used in this study to interpret changes in study area[44,65].

**Table 5.34: SPI Values and drought intensity.**

SPI Value	Drought Intensity
2 and more	Extremely wet
1.5 to 1.99	Very wet
1 to 1.49	Moderately wet
-0.99 to 0.99	Near normal
-1 to -1.49	Moderately dry
-1.5 to -1.99	Severely dry
-2 and less	Extremely dry

#### 5.4.2.1 SPATIO-temporal Analysis Of Different SPIs

There is no single definition of drought and it can be generally grouped into meteorological, agricultural, hydrological and socioeconomic droughts. Drought is a very complex hazard to define and detect. It spans multiple sectors and timescales. Just as there is no single definition of drought, there is no single drought index that meets the requirements of all applications. That said, a real strength of the SPI is its ability to be calculated for many timescales, which makes it possible to deal with many of the drought types described above. The ability to compute the SPI on multiple timescales allows for temporal flexibility in the evaluation of precipitation conditions in relation to water supply.

The SPI was designed to quantify the precipitation deficit for multiple timescales, or moving averaging windows. These timescales reflect the impacts of drought on different water resources needed by various decision-makers. Meteorological and soil moisture conditions (agriculture) respond to precipitation anomalies on relatively short timescales, for example 1-6 months, whereas streamflow, reservoirs, and groundwater respond to longer-term precipitation anomalies of the order of 6 months up to 24 months or longer. So, for example, one may want to look at a 1- or 2-month SPI for meteorological drought, anywhere from 1-month to 6-month SPI for agricultural drought, and something like 6-month up to 24-month SPI or more for hydrological drought analyses and applications. The SPI can be calculated from 1



month up to 72 months. Statistically, 1–24 months is the best practical range of application. This 24-month cutoff is based on Standardized Precipitation Index User Guide<sup>7</sup> Guttman’s recommendation of having around 50–60 years of data available. Unless one has 80–100 years of data, the sample size is too small and the statistical confidence of the probability estimates on the tails (both wet and dry extremes) becomes weak beyond 24 months. In addition, having only the minimum 30 years of data (or less) shortens the sample size and weakens the confidence. Technically, one could run the SPI on less than 30 years of data bearing in mind, however, the statistical limitations and weaker confidence pointed out above[44].

### 1-month SPI

A 1-month SPI map is very similar to a map displaying the percentage of normal precipitation for a 30-day period. In fact, the derived SPI is a more accurate representation of monthly precipitation because the distribution has been normalized. For example, a 1-month SPI at the end of August compares the 1-month precipitation total for August in that particular year with the August precipitation totals of all the years on record. Because the 1-month SPI reflects short-term conditions, its application can be related closely to meteorological types of drought along with short-term soil moisture and crop stress, especially during the growing season. The 1-month SPI may approximate conditions represented by the Crop Moisture Index, which is part of the Palmer Drought Severity Index suite of indices. Interpretation of the 1-month SPI may be misleading unless climatology is understood. In regions where rainfall is normally low during a month, large negative or positive SPIs may result even though the departure from the mean is relatively small. The 1-month SPI can also be misleading with precipitation values less than the normal in regions with a small normal precipitation total for a month. As with a percent of normal precipitation map, useful information is contained in the 1-month SPI maps, but caution must be observed when analysing them. It should be considered that in theory, the SPI can be calculated on a sub-monthly basis, but in practice this is not recommended. It is highly recommended that the user look at a minimum averaging window of 4 weeks.

### 3-month SPI

The 3-month SPI provides a comparison of the precipitation over a specific 3-month period with the precipitation totals from the same 3-month period for all the years included in the historical record. In other words, a 3-month SPI at the end of August compares the June–July–August precipitation total in that particular year with the June - July - August precipitation totals of all the years on record for that location. Each year data is added, another year is added to the period of record, thus the values from all years are used again. The values can and will change as the current year is compared historically and statistically to all prior years in the record of observation. A 3-month SPI reflects short- and medium-term moisture conditions and provides a seasonal estimation of precipitation. In primary agricultural regions, a 3-month SPI might be more effective in highlighting available moisture conditions than the slow-responding Palmer Index or other currently available hydrological indices. It is important to compare the 3-month SPI with longer timescales. A relatively normal or even a wet 3-month period could occur in the middle of a longer-term drought that would only be visible over a long period. Looking at longer timescales can prevent misinterpretation believing that a drought might be over when in fact it is just a temporary wet period. Continuous and persistent drought monitoring is essential to determine when droughts begin and end. This helps avoid “false alarms” when going into and coming out of drought. Having a set of “triggers” in place, which are tied to actions within a drought plan, can help ensure this. As with the 1-month SPI, the 3-month SPI may be misleading in regions where it is normally dry during any given 3-month period. Large negative or positive SPIs may be associated with precipitation totals not very different from the mean. This caution can be explained with the Mediterranean climate of California and around northern Africa and southern Europe, where very little rain falls or is expected over distinct periods of the year. Because these periods are characterized by little rain, the corresponding historical totals will be small, and relatively small deviations on either side of the mean could result in large negative or positive SPIs. Conversely, this time period can be a good indicator for some monsoon regions around the world.

### 6-month SPI

The 6-month SPI compares the precipitation for that period with the same 6-month period over the historical record. For example, a 6-month SPI at the end of

September compares the precipitation total for the April–September period with all the past totals for that same period. The 6-month SPI indicates seasonal to medium-term trends in precipitation and is still considered to be more sensitive to conditions at this scale than the Palmer Index. A 6-month SPI can be very effective in showing the precipitation over distinct seasons. For example, a 6-month SPI at the end of March would give a very good indication of the amount of precipitation that has fallen during the very important wet season period from October through March for certain Mediterranean locales. Information from a 6-month SPI may also begin to be associated with anomalous streamflows and reservoir levels, depending on the region and time of year.

#### 9-month SPI

The 9-month SPI provides an indication of inter-seasonal precipitation patterns over a medium timescale duration. Droughts usually take a season or more to develop. SPI values below -1.5 for these timescales are usually a good indication that dryness is having a significant impact on agriculture and may be affecting other sectors as well. Some regions may find that the pattern displayed by the map of the Palmer Index is closely related the 9-month SPI maps. For other areas, the Palmer Index is more closely related to the 12-month SPI. This time period begins to bridge a short-term seasonal drought to those longer-term droughts that may become hydrological, or multi-year, in nature.

#### 12-month up to 24-month SPI

The SPI at these timescales reflects long-term precipitation patterns. A 12-month SPI is a comparison of the precipitation for 12 consecutive months with that recorded in the same 12 consecutive months in all previous years of available data. Because these timescales are the cumulative result of shorter periods that may be above or below normal, the longer SPIs tend to gravitate toward zero unless a distinctive wet or dry trend is taking place. SPIs of these timescales are usually tied to streamflows, reservoir levels, and even groundwater levels at longer timescales. In some locations, the 12-month SPI is most closely related with the Palmer Index, and the two indices can reflect similar conditions.

Table A.1 to A.3 in APPENDIX A show the SPI results in Ahar station during summer time. SPI-1 means 1-month SPI, SPI-2 means 2-month SPI, SPI-3 means 3-

month SPI, SPI-6 means 6-month SPI, SPI-9 means 9-month SPI, SPI-12 means 12-month SPI and finally SPI-24 means 24-month SPI. Figure 5.99 shows also the drought condition in study area. SPI values in result tables in APPENDIX A with different colors presented by below legend. Colorless values which are -0.99 and 0.99 present normal condition[44].

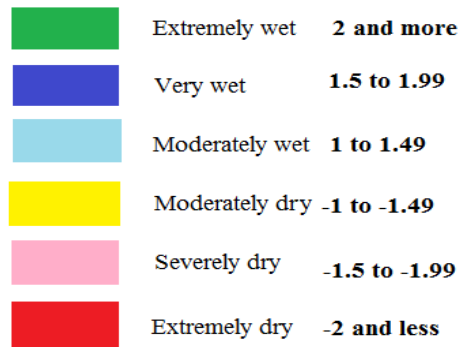


**Figure 5.99:** SPI values and ranges.

According to table A.1 to A.3 1995-summer could be considered as a wet time in Ahar station and 2000-summer, and 2009-summer could be considered as dry times when Urmia Lake land cover changes were analyzed using satellite images. According to tables A.4 to A.6 most SPI values show normal condition or moderately dry condition in Khoy station and 1987-summer and 2000-summer could be considered as dry times between 1984 and 2011. According to tables A.7 to A.9 1995-summer could be considered as a wet time in Maragheh station and 2000-summer, and 2009-summer could be considered as dry times between studied dates. According to tables A.10 to A.12 2000-summer can be considered as a dry time in Piranshahr station. SPI values show normal condition in most times. According to tables A.13 to A.15 1995-summer can be considered as a wet time in Sardasht station and 2000-summer, and 2009-summer could be considered as dry times between studied dates. According to tables A.16 to A.18 1990-summer, 2000-summer and 2009-summer can be considered as dry times in Tabriz station and other dates include normal condition. Moderately dry is also considerable between studied dates according to results of 6-SPI month. According to tables A.19 to A.21 1995-summer could be considered as a wet time in Urmia station and 2000-summer, and 2006-summer could be considered as dry times between studied dates.

Table A.22 to A.39 show SPI values of Urmia station in all months of years when Urmia Lake's land cover changes were analyzed using satellite images. Moreover SPI values are available between 1998 to 2011 when the surface area of Urmia Lake started to decrease.

According to SPI values of Urmia Station, 1995 year could be considered as a wet year and 1987, 1999, 2000, 2001, 2005, 2006, and 2008 could be considered as dry years which were studied between 1984 and 2011. These results show a considerable change in SPI values of 1999, 2000, and 2001, then the condition seemed normal until 2005. In 2005 and 2006 a drought condition was considerable again and the condition changed to normal after this time in 2007. Then, it's changed to drought condition in 2008. Finally, SPI values show moderately dry condition in 2009 and normal condition in 2010 and 2011.

In conclusion, SPI values totally show that there was normal condition in studying synoptic stations from 1984 to 1999. Drought condition started in the study area from 1999 about 10 years from 1999 to 2009 but it should be considered that drought condition didn't cover all years from 1999 to 2009. In other words, 2003,2004, and 2007 years could be considered as years with normal condition.

### 5.4.3 Analyzing Meteorological Data Of 5 Close Stations To Urmia Lake

Temperature, precipitation, and humidity changes were analyzed monthly and annually in 5 near stations around Urmia Lake accordingg to figures in APPENDIX A to comprehend the meteorological changes in study area. Figure 5.100 shows the location of 5 analyzed stations which are close to Urmia Lake.

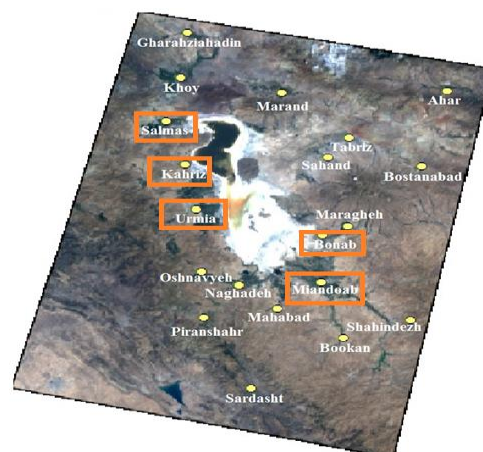


**Figure 100** : Synoptic stations location which are close to Urmia Lake.

#### **5.4.3.1 Temperature Data**

Temperature data of Salmas station is available during 2002 to 2011. According to temperature figures in APPENDIX B the mean temperature has the minimum value in January and the maximum value in August or July. According to annual figures temperature increased considerably in 2010 year and this year is the warmest year during last years. The air temperature decreased after 2010.

Temperature data of Kahriz station is available during 2006 to 2011. According to APPENDIX B the mean temperature has the minimum value in January and the maximum value in August or July. According to annual figures temperature increased considerably in 2006 and 2010 year and these years are the warmest years during last years. The air temperature decreased after 2010.

Temperature data of Urmia station are available from 1984 to 2011. According to APPENDIX B the mean temperature has the minimum value in January or December and the maximum value in August or July. According to annual figures, mean daily temperature decreased during years of 1987 and 1995 and then it increased after that time. According to annual figures temperature increased considerably in 2010 year and this year is the warmest year during last 30 years. The air temperature decreased after 2010.

Temperature data of Miandoab station is available during 2006 to 2011. According to APPENDIX B the mean daily temperature has the minimum value in January or December and the maximum value in August or July. According to annual figures temperature increased considerably in 2010 year and this year is the warmest year during last years. The air temperature decreased after 2010.

Temperature data of Bonab station are available during 2000 to 2011. According to APPENDIX B the mean daily temperature has the minimum value in January or December and the maximum value in August or July. According to annual figures temperature increased considerably in 2010 year and this year is the warmest year during last 11 years. The air temperature decreased after 2010.

Finally, air temperature changes show considerable changes in 2006, and 2010 years and these years can be considered as the warmest years. Air temperature in studying stations decreased after 2010. Urmia station data which is available in long term period show normal condition until 2000 years and after this time air temperature

started increasing from 2000 to 2010 but this increasing doesn't cover all studied years between 2000 and 2010. In other words some years show normal condition during 2000 to 2010 and some years show increasing in temperature. Air temperature reaches its maximum value in 2010 and then it decreased.

#### **5.4.3.2 Precipitation Data**

Precipitation data of Salmas station is available during 2002 to 2011. According to APPENDIX B the precipitation has the minimum value in summer and the maximum value in spring or winter. The minimum amount of precipitation is in 2005 and the maximum amount of precipitation is in 2010. Precipitation figures haven't regular form like temperature figures and the amount of precipitation is different in different months, seasons and years.

Precipitation data of Kahriz station is available during 2006 to 2011. According to APPENDIX B the precipitation has the minimum value in summer and the maximum value in spring or winter. The minimum amount of precipitation is in 2008 and the maximum amount of precipitation is in 2011. Precipitation graphs haven't regular form like temperature graphs and the amount of precipitation in 2011 is very large rather than other years.

Precipitation data of Urmia station is available during 1984 to 2011. According to APPENDIX B the precipitation has the minimum value in summer and the maximum value in spring or winter. The minimum amount of precipitation is in 2005 and the maximum amount of precipitation is in 1994. Precipitation decreased during years of 1994 and 2002 and it is increased during years of 2006 and 2011.

Precipitation data of Miandoab station is available during 2006 to 2011. According to APPENDIX B the precipitation has the minimum value in summer and the maximum value in spring or winter. The minimum amount of precipitation is in 2007 and the maximum amount of precipitation is in 2006. Precipitation figures haven't regular form like temperature figures and the amount of precipitation in 2011 is very large rather than 2010.

Precipitation data of Bonab station is available during 2000 to 2011. According to APPENDIX B the precipitation has the minimum value in summer and the maximum value in spring or winter. The minimum amount of precipitation is in 2000 and the

maximum amount of precipitation is in 2006. Precipitation figures haven't regular form like temperature figures and the amount of precipitation in 2006 is very large rather than other years.

Finally, precipitation changes show the most value of precipitation in 2006, 2010, and 2011. Precipitation figures doesn't have regular changes and forms such as temperature figures. It seems considerable that the maximum amount of precipitation in studied stations is belong to warmest years. In the other words, 2006 and 2010 have at the same time most amount of precipitation and air temperature. It is possible that high temperature cause most evaporation and most evaporation cause most rainfall in study area.

#### **5.4.3.3 Humidity Data**

According to APPENDIX B humidity data of Salmas station show the minimum value in summer and the maximum value in winter. The minimum amount of humidity is in 2008 and the maximum amount of humidity is in 2007. Humidity figures show regular changes in winter, spring, summer and autumn. Also increasing humidity in 2011 is very noticeable in recent years.

Humidity data of Kahriz station show the minimum value in summer and the maximum value in winter. The minimum amount of humidity is in 2008 and the maximum amount of humidity is in 2007. Humidity figures show regular changes in winter, spring, summer and autumn. Also the amount of increasing humidity in 2011 is very noticeable in recent years.

Humidity data of Urmia station show the minimum value in summer and the maximum value in winter. The minimum amount of humidity is in 2000 and 2001 and the maximum amount of humidity is in 1993 and 1994. Humidity figures show regular changes in winter, spring, summer and autumn. Also the amount of increasing humidity in 2011 is very noticeable rather than 2010.

Humidity data of Miandoab station show the minimum value in summer and the maximum value in winter. The minimum amount of humidity is in 2010 and the maximum amount of humidity is in 2006. Humidity graphs show regular changes in winter, spring, summer and autumn. Also the amount of increasing humidity in 2011 is very noticeable recent years.



Humidity data of Bonab station show the minimum value in summer and the maximum value in winter. The minimum amount of humidity is in 2010 and the maximum amount of humidity is in 2003. Humidity figures show regular changes in winter, spring, summer and autumn. Also the amount of increasing humidity in 2011 is very noticeable recent years.

Finally, humidity changes show the minimum value in 2000, 2006, 2008, and 2010 especially in 2008. Humidity decreased during recent years but its changes aren't regular. The increasing humidity in 2011 rather to previous years is considerable.

In conclusion, analyzing meteorological data using geostatistics analysis, Standardized Precipitation Index (SPI), and figures prove changes in air condition during 2000 to 2010 and there is a dry condition during these years, but this condition isn't regular and the air condition of some years like 2003, 2004, 2007 seems normal. The air condition started to be better after 2010. Moreover, air condition seems better rather to other years during 1987 to 1998 especially 1995 year has the best air condition in comparing to other years. 2006 and 2010 years have high temperature values and 2010 at the same time can be also considered as a year with high amount of precipitation in recent years.



## 6. CONCLUSION AND RECOMMENDATIONS

The main purpose of this study was multi-temporal change detection on Urmia Lake and its catchment area using remote sensing and geographical information systems (GIS) for the last 30 years from 1984 to 2014. In total 95 satellite images and meteorological data from 20 synoptic stations around Urmia Lake were analyzed in this study in order to better understand the changes which have occurred in the study area during the last 30 years. Additionally a comprehensive database was prepared which included historical information from affected dams (from years 1970-2013), underground water resources (from years 1972-2012), population statistics of West Azerbaijan and East Azerbaijan (from years 1985 to 2010), water surface elevation of Urmia Lake (from years 1966 to 2013). A land study of Urmia Lake was also completed during different seasons over the last few years in order to assess recent changes. For the land study control points were collected using GPS in order to ensure the results were accurate in their classification. Google Earth was another source of control for accuracy and comparison.

Unsupervised classification (ISODATA) and supervised classification (Maximum Likelihood) methods were used in this study to classify Urmia Lake from 1984 to 2014. Table (6.1) and (6.2) show the results of unsupervised and supervised classification from 1984 to 2014. According to these tables, the results of both methods were different from each other. To choose the best result an accuracy assessment process using control points from 2010 to 2014 was used. According to the results of the accuracy assessment process, the overall classification accuracy and overall Kappa statistics using the supervised classification method were shown to be better than the unsupervised classification for every time period except the summer of 2011. Therefore, to analyze the water surface area of Urmia Lake using supervised classification was determined to be better than unsupervised classification. In this process another method, which was named NDVI, based unsupervised classification was used to calculate water surface area of Urmia Lake. The results of this method

were very close to the supervised classification results. After an accuracy assessment was completed to check the accuracy of this method, the results were acceptable. This method proved to be an easy and time saving method which can be used to calculate the area of a water body, like of Urmia Lake, when the aim is surface area determination only.

**Table 6.1:** Unsupervised Classification Results.

Year	Water	Salt	Salty Soil	Soil	Farming	Total
1984-Summer	5005	205	542	816	64	6632
1987-Spring	5379	0	289	850	114	6632
1987-Summer	5128	98	518	774	114	6632
1990-Summer	5200	104	386	868	74	6632
1995-Summer	5946	0	35	596	55	6632
1998-Summer	5597	63	295	602	75	6632
2000-Summer	4697	118	806	969	42	6632
2006-Summer	4057	273	1022	1175	105	6632
2007-Spring	4592	41	1206	707	86	6632
2007-Summer	4049	257	1001	1211	114	6632
2009-Summer	3130	449	2255	681	117	6632
2010-Summer	2922	806	2026	796	82	6632
2011-Spring*	2800	255	1765	1262	65	6147
2011-Summer	2562	798	2130	1000	142	6632
2012-Summer*	2668	513	2525	723	85	6514
2013-Spring	3090	367	1735	1389	51	6632
2013-Summer	1897	1290	2176	1108	161	6632
2014-February*	2215	865	1515	1500	-	6095

\* Classified results of DMC satellite (2011-spring and 2012-summer) and Landsat-8 (2014-February). The classified areas are different and smaller than classified areas using Landsat-5 images.

According to the results of supervised classification the total classified area is 6632 km<sup>2</sup> in all years the three exceptions being the 2011-Spring, 2012-Summer and 2014-February. In 2011 and 2012 years images from the DMC satellite were used and the classified area was shown to be smaller than other dates when compared to the Landsat data. Also, the study area in 2014-February is smaller than the other time periods because a single frame was enough to analyze water body changes in Urmia Lake. There was also no farming classifications made in 2014-February as winter time made it difficult to assess the farming activity.

**Table 6.2:** Supervised Classification Results.

Year	Water	Salt	Salty Soil	Soil	Farming	Total
1984-Summer	4970	315	643	584	120	6632
1987-Spring	5344	0	646	581	61	6632
1987-Summer	5082	275	571	590	114	6632
1990-Summer	5092	65	733	616	126	6632
1995-Summer	5982	0	63	536	51	6632
1998-Summer	5513	94	379	580	66	6632
2000-Summer	4679	23	1271	589	70	6632
2006-Summer	4058	406	1357	653	158	6632
2007-Spring	4626	30	1341	527	108	6632
2007-Summer	4095	88	1638	634	177	6632
2009-Summer	3222	269	2478	545	118	6632
2010-Summer	3013	391	2553	506	169	6632
2011-Spring*	2713	687	2155	553	10	6118
2011-Summer	2674	542	2428	796	192	6632
2012-Summer*	2709	445	2750	572	65	6541
2013-Spring	3000	323	2530	752	27	6632
2013-Summer	1852	1209	2877	518	176	6632
2014-February*	2169	742	2414	770	-	6095

\* Classified results of DMC satellite (2011-spring and 2012-summer) and Landsat-8 (2014-February). The classified areas are different and smaller than classified areas using Landsat-5 images.

According to supervised classification results, water surface area of Urmia Lake increased from 1984 to 1995 and then decreased from 1995 to 2013. The severity of the decreasing water surface area from 1998-2000 is also noticeable. From 1998 until 2000 the water surface area difference is about 834 km<sup>2</sup>. The maximum surface area of Urmia Lake was 5982 km<sup>2</sup> in 1995 and the minimum area was 1852 km<sup>2</sup> in 2013. Water surface area decreased about 873 km<sup>2</sup> from 2007 to 2009 and it could be compared to the decreasing surface area in the years 1998 and 2000. From 1998 until 2013 Urmia Lake saw a yearly decrease in surface area in all but two years. During the summers of 2006 and 2007 the lake remained relatively stable with a 37 km<sup>2</sup> increase over 2006. A second similar exception was during 2011 and 2012 when the water surface area of Urmia Lake increased a similar 35 km<sup>2</sup>. It must also be noted that immediately afterward in 2013 the lake decreased rapidly by nearly 857 km<sup>2</sup>.

The minimum area of the salt class was near zero km<sup>2</sup> in 1995 while the maximum area of this class was 1209 km<sup>2</sup> in 2013. The salt area decreased from 1984 to 1995 and then it increased from 1995 to 2013. The minimum area of salty soil class was about 63 km<sup>2</sup> in 1995 and the maximum area was 2877 km<sup>2</sup> in 2013. Notable, is the

considerable increase of salty soil area of about 840 km<sup>2</sup> from 2007 to 2009. More than 4000 km<sup>2</sup> of Urmia Lake's area was converted to salt and salty soil bodies from 1995 to 2013. Water surface area changes from 1984 to 2013 are presented in table (6.3) by considering the maximum area in 1995 according to the results of supervised classification. According to the results of this table about 70% of water surface area of Urmia Lake was lost from 1995-Summer to 2013-Summer.

**Table 6.3:** Water surface area changes of Urmia Lake from 1984 to 2013 in Summer time.

Year	Area (km <sup>2</sup> )	Remaining Area (%)	Drought Area (%)
1984	4970	83.08	16.92
1987	5082	84.95	15.05
1990	5092	85.12	14.88
1998	5513	92.15	7.85
2000	4679	78.21	21.79
2006	4058	67.83	32.17
2007	4095	68.45	31.55
2009	3222	53.86	46.14
2010	3013	50.36	49.64
2011	2674	44.70	55.30
2012	2709	45.28	54.72
2013	1852	30.95	69.05

Two reasons were presented by researchers to explain the drying and decreasing water surface area of Urmia Lake from 1998 to 2013. These reasons are firstly human activities resulting in wrong management of water bodies and agricultural activities in Urmia Lake's catchment area and secondly, global warming. There is great debate over which of these reasons should be considered as primary. However to understand the role of these two reasons, human activities were analyzed using dams, underground water resources, and population statistics. There are, in total, 103 dams in the West Azerbaijan and East Azerbaijan provinces. Of these dams 56 are located in Urmia Lake's catchment area. 14 dams were established from 1970 to 1990, and 10 dams were made from 1990-2000, and 32 dams were built from 2000 to 2014. Moreover, there are additional dams which are under construction or in the study stage. These dams play a critical role in developing agriculture areas in Urmia Lake's catchment area, but it also means an increase in irrigation and water usage. The total cultivation area using dams supplied water was about 102966 Hectare in 1999 and it increased to 192648 Hectare in 2013. Annual adjustable water volume of all dams in Urmia lake's catchment area was about 2060.30 million m<sup>3</sup> in 2013 while

the annual agricultural water consumption was about 1320.28 million m<sup>3</sup>. According to these statistics, cultivation areas using water supplied from dams doubled from the periods of 1970-1999 until 1999-2013. Annual drinking water consumption was 389.04 million m<sup>3</sup> in 2013 year. In looking forward, it should be considered that the population of both West Azerbaijan and East Azerbaijan increased during recent years. Moreover, water consumption of each Iranian is 2 times the global average for water consumption. According to population statistics, the population of both West Azerbaijan and East Azerbaijan increased about 1.800.000 during 1985 to 2010. By increasing population and farming areas, underground water, which supply some part of Urmia Lake's water reserve has been decreased like surface water bodies because of establishment of different dams. Human impacts on Urmia lake and its environment are excessive. Therefore, it seems that the main reason of drying Urmia Lake might be human activities most probably. Mechanisms between land surface and atmosphere interactions need to be investigated carefully to understand the impact of human activities on regional climate of Urmia lake. Human activities might be influencing regional climate as well. To this end, for further studies a regional climate model with multi temporal land cover data could be run to understand the impact of the changing landscape on regional climate of the region.

Table (6.3) shows the information about dams in Urmia Lake's catchment area which were established from 1970 to 2000. Table (6.4) also shows the information for some dams in Urmia Lake's catchment area which are established from 2000 to 2014. Most of these dams were established in the study area for the purpose of furthering agricultural activities. Figure 6.1 shows the location of some dams in Urmia Lake's catchment area.

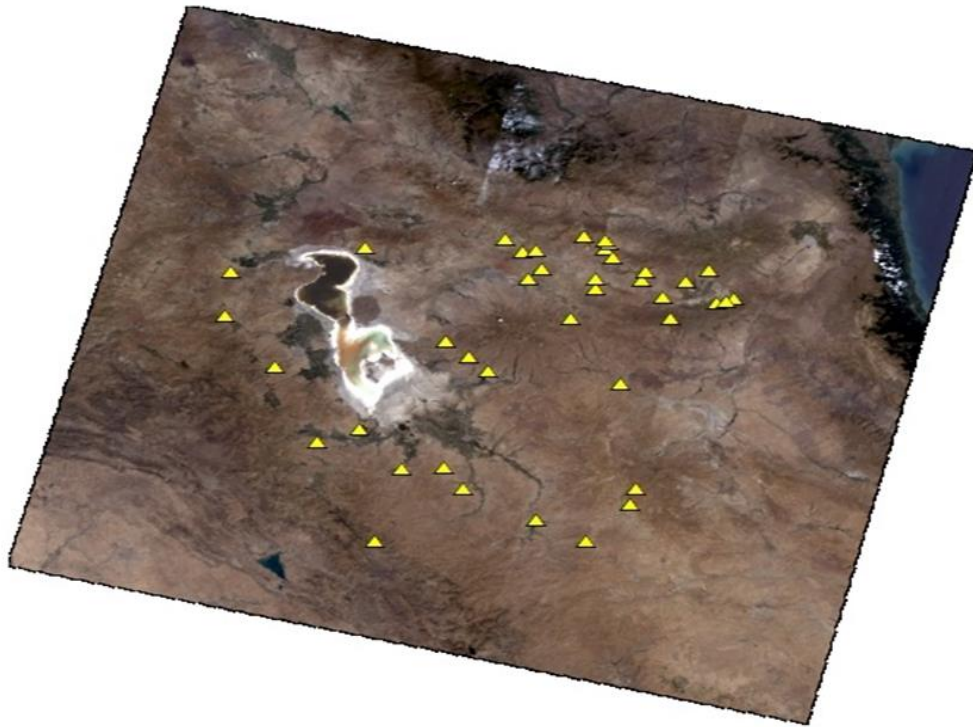


**Figure (6.1):** Location of some dams in Urmia Lake’s catchment area – Landsat-8 - Mosaic of 9 frames.

**Table 6.4:** Established dams between 1970 and 2000.

Dam’s Name	Annual Adjustable Water (million m <sup>3</sup> )	Cultivation area (Hectare)	Operation Year
Mahabad	197.8	18200	1970
Shahid Kazemi	605	66165	1971
Khormalu	0.32	65	1979
Barugh Heris	0.15	45	1982
Amand-1	0.25	25	1983
Haft Cheshmeh	0.3	25	1984
Molla Yaghub	4	800	1984
Ghazi Kandi	1.5	240	1984
Yengejel Heris	1	60	1984
Til	0.7	70	1985
Maghsudlu	1.8	360	1985
Amand-2	0.25	25	1985
Hacha Su	3.1	220	1986
Dehgorji	0.45	300	1988
Amand Tabriz	4	400	1993
Yengeje Azer	3	500	1993
Alaviyan	123.4	14535	1995
Nahand	32	-	1996
Param	4	400	1997
Dash Esparan	0.45	80	1997
Ardalan	4.5	269	1998
Gavdush Abad	2.5	182	1999



**Table 6.5:** Some of dams established between 2000 and 2014.

Dam's Name	Annual Adjustable Water (million m <sup>3</sup> )	Cultivation area (Hectare)	Operation Year
Hasanlu	94	14500	2000
Malak Kiyani	10	600	2000
Tajyare Sarab	4.5	600	2003
Kurd Kandi	6.03	500	2003
Ghushkhana	0.14	-	2003
Ghurichay	0.8	115	2004
Ertefa Kazemi	425	328	2005
Shaharchay	199	12690	2005
Gheysaragh	2.8	325	2006
Kanespi	1.79	500	2009
Sarugh	51.8	4900	2009
Zola	132.5	30300	2010
Sanjagh	1	350	2010
Chughan	3.2	362	2011
Vergil	2.3	700	2012
Ahmad Abad	5.9	450	2012
Khorasane	2.5	400	2013
Heris Shabestar	0.15	25	-
Vangh Oliya	2	-	-
Gavdush Abad	2.5	182	-
Chinag Bulagh	0.3	150	-
Mingh Khaki	0.45	80	-
Gultapa	0.6	200	-
Mingh Sangi	0.3	50	-

Underground water sources which include deep wells, semi deep wells, aqueducts, and water fountains are another source that provides needed water for irrigation and agricultural developing. Discharge water from underground water sources was 1534 million m<sup>3</sup> from 1984 to 1985 with an increase to 2156 during 2011 to 2012. Moreover, discharge water from underground water sources increased by 400 million m<sup>3</sup> alone from 1998 to 1999. According to the available statistics from underground water sources during 1972 to 2012, there are totally 74336 semi deep wells and 8047 deep wells in Urmia Lake's catchment area in 2012.

Meteorological data using Geostatistic Analysis, Standardized Precipitation Index (SPI), precipitation data, temperature and humidity data were applied to better understand the climate changes in the study area during recent years. Climate condition seemed better from 1987 to 1998 (1995 year was notable for its wet air condition). The results showed the normal condition in studied synoptic stations from 1984 to 1999. Drought conditions began in the study area in 1999 and basically continued for 10 years during until 2009. The changes in SPI values from normal

condition to dry condition during 1999 to 2001 are considerable. The only normal years from 1999-2009 appear to be 2003, 2004, and 2007. Finally, SPI values show moderately dry condition in 2009 and normal condition during 2010 and 2011. According to the geostatistics analysis results, 2006 was the hottest year with more rainfall compared to the other studied periods. The air temperatures in 2006 and 2010 were the warmest while following years cooled down. In 2006 and 2010 the high temperatures were also years of increased precipitation compared to other years. Therefore, in general, the meteorological analysis showed changes toward a dry climatic condition from 1999 until 2010 but these changes were not regular.

Analyzing water surface area changes of Urmia Lake and climate condition changes is very important in determining whether climate change or human activity is the primary reason for the decrease in the water surface area. For example, 2011 saw increased precipitation levels compared to the dry years of 2009 and 2010, yet instead of increasing or maintaining, the water surface area of the lake decreased disproportionately during 2011. This draws into question, the true impact of climate change alone on the water surface area.

The report of Drought Risk Management Plan For Lake Urmia Basin which was An integrated plan to save the lake that was drawn by stakeholders, which was facilitated by the United Nation Development Program (UNDP) Conservation of Iranian Wetlands Project (CIWP) is also considerable. This plan was developed With the cooperation of the Urmia Lake provinces, the Integrated Management Plan for Lake Urmia Basin (IMPLUB). This study investigated possible causes of Urmia Lake decline by estimating trends in the time series for hydro-climatic variables of the basin. 4 non-parametric statistical tests (Mann- Kendall, Theil-Sen, Spearman Rho, Sen's T) were applied to estimate trends in the annual and seasonal time series for temperature, precipitation, and streamflow at 81 stations throughout the basin. The results showed significant increasing trends in temperature throughout the basin and area-specific precipitation trends (Figure 6.2).

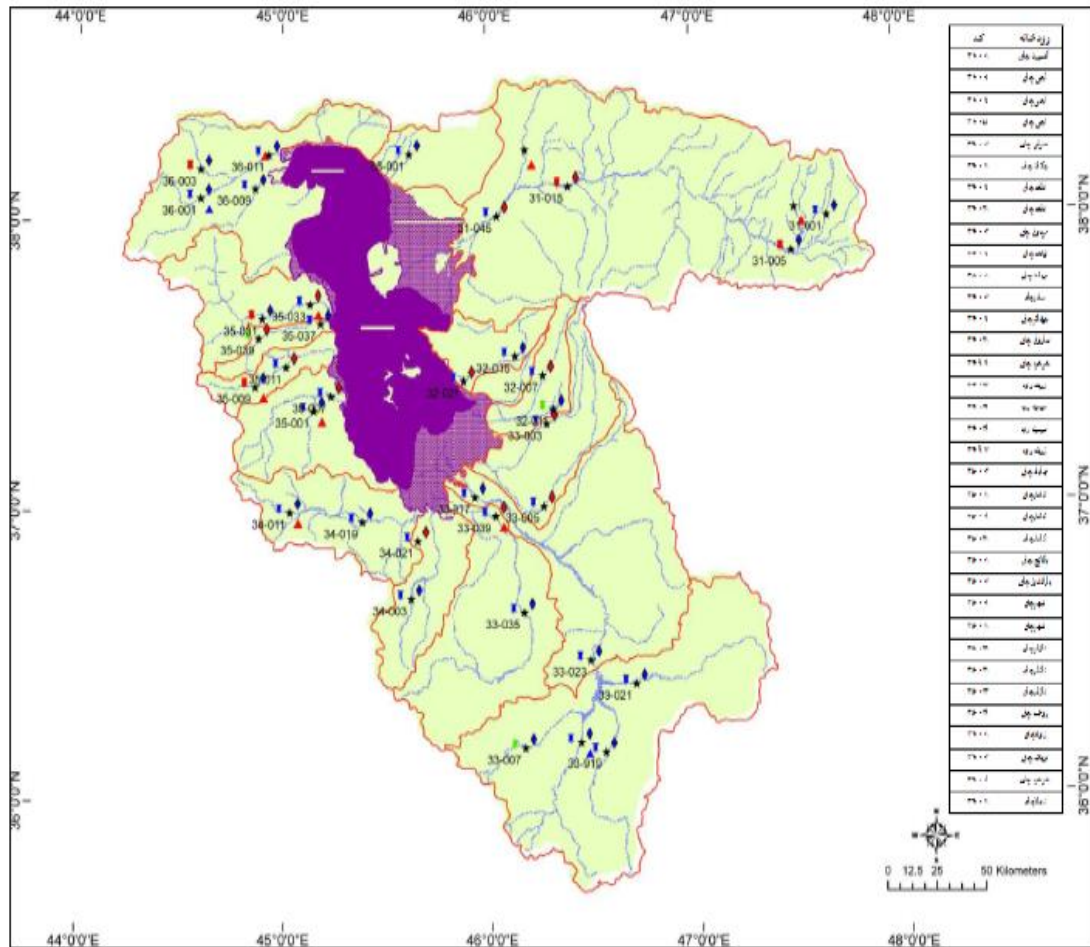


**Figure 6.2 :** Trends in hydro-climatic stations of Urmia Lake basin ( ▲ = significant increase in temperature; ◆ = significant decrease in discharge; ■ = significant decrease in rainfall).

The tests also confirmed a general decreasing trend in basin streamflow that was more pronounced in the downstream stations. This can be attributed to over-exploitation of the upper sub-catchments.

The rivers Jighati (Zarrinerood), Tatau (Siminerood), Soyugh Bulagh chay (Mahabad), Gadar chay, Baranduz chay, Shahar chay, Roze chay, Nazlu chay, Zola chay, Tasuj chay, Aji chay, and Sufi Chay rivers provide 75% of the inflow water to Urmia Lake while underground water sources, precipitation, and flood water provide 25% of the water inflow. When comparing this climate and nature controlled inflow sources to population and agricultural activities during recent years, it seems more probable that the primary reason of the drying of Urmia Lake must be human activities such as improper water and agricultural management in the catchment area.

Table (6.6) shows the results of minimum and maximum area of different classes of Normalized Difference Vegetation Index (NDVI), Normalized Difference Water Index (NDWI), Salinity Index (SI), and Normalized Difference Drought Index (NDDI) in the summers of 1984, 1987, 1990, 2000, 2006, 2010, 2011 and 2013. The Salinity Index (SI) was also used to monitor the salinity changes of water surface area of Urmia Lake in this study and the results were compared to the unsupervised classification results. It seems this index can be used to accurately monitor salinity changes of water surface area of Urmia Lake.

**Table 6.6:** Minimum and maximum area (km<sup>2</sup>) of Indexes.

Index Ranges	Minimum area (km <sup>2</sup> ) -Year	Maximum area-Year
NDVI (0-0.1)	3-1987	24025-2006
NDVI (0.1-0.5)	55847-2006	79565-2000
NDVI (0.5-1)	1228-2006	4345-1987
NDWI (-1 - 0)	34518-1987	53462-2013
NDWI (0-0.5)	29176-2013	45756-1987
NDWI (0.5-1)	2-2006	56-2013
NDDI (0-2)	52448-2006	74373-1984
NDDI (2-10)	5851-1987	20869-2013
NDDI (10-100)	79-1987	3176-2006
SI (0-0.2)	56566-2006	80250-1987
SI (0.2-0.4)	46-1987	24392-2006
SI (0.4-1)	0-1987	178-1990

According to the results of these mentioned indexes, 2006 can be considered as a year with the highest soil salinity value, least NDVI, least NDWI, and most severe drought conditions. 1987 can be considered as the year with the lowest soil salinity value, highest NDVI, highest NDWI, and least drought like conditions. Changes in every index, which was used in this study is considerable from 2000 to 2006. It can be concluded that the study area faced an important change in vegetation, vegetation water content, and salinity levels. The water surface area of Urmia Lake decreased nearly 2000 km<sup>2</sup> from 5982 km<sup>2</sup> in 1995 to 4058 km<sup>2</sup> in 2006. In other words, 32% of Urmia Lake dried up during the period of 1995 until 2006. It then decreased another 2000 km<sup>2</sup> from 4058 km<sup>2</sup> in 2006 to 1852 km<sup>2</sup> in 2013. It appears obvious that more conservative water and agricultural monitoring and management program should be designed for Urmia Lake's catchment area if Urmia Lake is to be rescued and recovered. Remote sensor data in conjunction with field survey would be a valuable asset for such monitoring program. In addition, GIS technology could be effectively used to conduct spatial and temporal analysis within Urmia Lake and its

catchment area in order to support the decision making process. The touristic and industrial potential of Urmia Lake and its catchment area along with its geopolitical position of both west Azerbaijan and East Azerbaijan could also create opportunities. Trade with neighbor countries such as Turkey, Azerbaijan, Iraq and Armenia could be a good way to reduce agricultural activities around Urmia Lake and concentrate on other economic activities. Moreover, a good study of different types of crops in Urmia Lake's catchment area and analyzing their benefits in compared to the amount of water used to grow up them is necessary to reduce crops which have high water consumption amount.



## REFERENCES

- [1] **Ekercin, S.** (2007). Multitemporal change detection on the Salt Lake and its vicinity by integration remote sensing and geographical information systems. PhD thesis. ITU.
- [2] **Ridley, B.K.** (1984). Remote Sensing: Basic Principles-Cambridge University Press-Second edition.
- [3] **Clarke, K, C** (2011). Getting started with Geographical Information Systems-Fifth Edition.
- [4] **Eimanifar, A. Mohebbi, F.** (2007). Urmia Lake (Northwest Iran): a brief review. Saline Systems, doi:10.1186/1746-1448-3-5-BioMed Central.
- [5] **Ehsani, A. Malekzadeh-Viayeh, R. Moradi, M. Seyyed-Ghoreishi, A.** (2012). Documentation and analysis of the ecological changes in Urmia Lake in a 40-year period. Urmia University.
- [6] **Zarghami, M.** (2011). Effective watershed management; Case study of Urmia Lake, Iran. Lake and Reservoir Management, An International Journal of the North American Lake Management Society. 27:87–94.
- [7] **Sima, S. Tajrishy, M.** (2013). Using satellite data to extract volume-area-elevation relationships for Urmia Lake, Iran. Journal of Great Lakes Research, 39, 90-99.
- [8] **Ji, L. Wylie, B. Zhang L.** (2009). Analysis of dynamic thresholds of the Normalized Difference Water Index-Photogrammetric Engineering & Remote Sensing Vol. 75, No. 11, November 2009, pp. 1307–1317.
- [9] **Abrishamchi, A. Ahmadalipour, A. Shafiee Jood, M. Sima, S. Tajrishy, M.** (2012). Monitoring Urmia Lake area variation using MODIS satellite data. World Environmental and Water Resources Congress 2012: Crossing Boundaries © ASCE 2012.
- [10] **Alsheikh, A, A. Ghorbandi, A. Nouri, N.** (2007). Coastline change detection using remote sensing. International Journal of Environment Sciences. Tech., 4 (1): 61-66. ISSN: 1735-1472.
- [11] **Ghobadi, Y. Kabiri, K. Pirasteh, S. Pradhan, B.** (2012). Manifestation of Remotely Sensed Data Coupled With Field Measured Meteorological Data for an Assessment of Degradation of Urmia Lake. Asia Pacific Conference on Environmental Science and Technology, 395-401.
- [12] **Chipman, J, W. Kiefer, R, W. Lillesand, T, M.** (2008). Remote Sensing and Image Interpretation-Sixth edition.
- [13] **Canada Center for Remote Sensing (CCRS), Remote Sensing Tutorial.**

Fundamentals of Remote Sensing.

- [14] **Engineering and Design Remote Sensing, Engineer Manual (2003).** Department of the army, US army corps of engineers, Washington, DC.
- [15] **GIS by ESRI .**(2004). What is ArcGIS.
- [16] **Shamsi, U.M.** (2005). GIS applications for Water, Waste water, and Storm Water Systems.
- [17] **Chang, K.T.** (2008). Programming ArcObjects with VBA, A task-oriented approach-Second Edition.
- [18] **Amrollahi. Mohabbad, H. Sima. Rezvantalab.** (2011). Investigation of recent changes in Urmia Salt Lake. International Journal of Chemical and Environmental Engineering. 2(3): pp. 168-171.
- [19] **Aahmadi, R. Eimanifar, A. Esmaeili Dahsht, L. Negarestan, H. Mohebbi, F.** (2010).The fluctuations of physicochemical factors and phytoplankton populations of Urmia Lake, Iran. Iraninan Journal of Fisheries Sciences, 9(3) 368-381.
- [20] **Mather, P, M.** (2004). Computer Processing of Remotely-Sensed Images-Third Edition.
- [21] **Crowley, G.** (2008). DMC Product Manual for the DMC Europe 2007 coverage. DMC International Imaging Ltd.
- [22] **United Nation Development Program.** (2012). Drought risk management plan for Lake Urmia basin, Working group on sustainable management of water resources and agriculture, Regional council of Lake Urmia basin management.
- [23] **Liang, Shunlin.** (2004). Quantitative Remote Sensing of Land Surface.
- [24] **Levin, N.** (1999). Fundamentals of Remote Sensing.
- [25] **Canty, M, J. Cohen, W, B. Schroeder, T, A. Song, C. Yang, Zhiqiang.** (2006). Radiometric correction of multi-temporal Landsat data for characterization of early successional forest patterns in western Oregon. Remote Sensing of Environmental, 103, 16-26.
- [26] **Aguado, I. Chuvieco, E. Riano, D. Salas, J.** (2003). Assessment of Different Topographic Corrections in Landsat-TM Data for Mapping Vegetation Types. IEEE Transactions on geosciences and Remote Sensing, 41, 1056-1061,ISSN: 0196-2892.
- [27] **Toutin, T.** (2003). Review Paper: Geometric Processing of Remote Sensing Images: Models, Algorithms and methods. International Journal of Remote Sensing.Vol. 25, No 10, 1893-1924.
- [28] **Rawashdeh, S, B, A.** (2012). Assessment of Change Detection Method Based on Normalized Vegetation Index in Environmental Studies. Internatinal Journal of Applied Science and Engineering. 10, 2: 89-97.



- [29] **Ritter, T.** (2006). Drought and its effect on vegetation, comparison of Landsat NDVI for Drought and non-drought years related to Land use Land cover classifications. EES 5053.
- [30] **Brown, J, F. Gu, Y. Verdin, J, P. Wardlow, B.** (2007). A five-year analysis of MODIS NDVI and NDWI for grassland drought assessment over the central Great Plains of the United States. *Geophysical Research Letters*, Vol. 34, L06407, doi:10. 1029/2006GL029127.
- [31] **Anderson, M. Chen, D. Cosh, M. Doriaswamy, P. Jackson, T, J. Hunt, E, R. Walthall, C.** (2003). Vegetation water content mapping using Landsat data derived normalized difference water index for corn and soybeans. *Remote Sensing of Environment* 92, 475-482.
- [32] **Al-Khaier, F.** (2003). Soil salinity detection using satellite remote sensing. International institute for geo-information science and earth observation enschede, the Netherlands.
- [33] **Ahmed, M. Al-Khafaji, A.** (2013). Assessment Environmental Changes in Al-Habbaniya Lake and Surrounding Areas in the Central Part of Iraq. *Journal of Natural Sciences Research*, ISSN 2225-0921, 8-16.
- [34] **Goossens, R. Alavi Panah, S, K.** (2001). Relationship Between the Landsat TM, MSS DATA and Soil Salinity. *J. Agri. Sci. Technol.* Vol. 3, 21-31.
- [35] **Abdul-Qadir, A, M. Benni, T, J.** (2010). Monitoring and evaluation of soil salinity in term of spectral response using Landsat images and GIS in mesopotamianplain/IRAQ. *Journal of Iraqi Desert Studies.* Vol 2, No. 2, 19-32.
- [36] **Arquero, A. Martinez, E. Renza, D. Sanchez, J.** (2010). Drought Estimation Maps by Means of Multidate Landsat Fused Images. *Remote Sensing for Science, Education, and Natural and Cultural Heritage.* 775-782.
- [37] **Bohling, G.** (2005). Introduction to Geostatistics and Variogram Analysis, C&PE 940, Assistant Scientist, Kansas Geological Survey.
- [38] **Oliver, M.A. Webster, R.** (2007). *Geostatistics for Environmental Scientists.* Second edition.
- [39] **Bohling, G.** (2005). Kriging, C&PE 940, 19 October 2005. Assistant Scientist, Kansas Geological Survey
- [40] **Matheron, G.** (1963). Principles of Geostatistics. *Economic Geology*, December 1963, v. 58, p. 1246-1266.
- [41] **Heidari, A. Mahmodi, Sh. Taghizadeh Mehrijardi, R. Zareian Jahromi, M.** (2008). Spatial Distribution of Groundwater Quality with Geostatistics (Case Study: Yazd-Ardakan Plain). *World Applied Sciences Journal* 4 (1): 09-17, 2008 ISSN 1818-4952.
- [42] **Murthy, C.S. Naresh Kumar, M. Roy, P.S. Secha Sai, M.V.R.** (2009). On the use of Standardized Precipitation Index (SPI) for drought intensity assessment. *Meteorol. Appl.* 16: 381-389.
- [43] **Avci, D, Z, U. Karaman, M. Ozelkan, E. Papila, I.** (2011), Drought

determination by using land surface temperature and Normalized Difference Vegetation Index.

- [44] **World Meteorological Organization.** (2012). Standardized Precipitation Index, User Guide.
- [45] **Anderson, G, L. Haas, R, H. Hanson, J, D.** (1993). Evaluating Landsat Thematic Mapper Derived Vegetation Indices for Estimating Above-Ground Biomass on Semiarid Rangelands. *Remote Sens. Environ.* 45, 165-175.
- [46] **Evans, J, P. Geerken, R. Zaitchik, B.** (2005). Classifying rangeland vegetation type and coverage from NDVI time series using Fourier Cycle Similarity. *International Journal of Remote Sensing*, 24, 5535-5554.
- [47] **Osaki, K.** (2000). Seasonal changes of NDVI calculated by JERS data with higher spatial resolution. *International Archives of Photogrammetry and Remote Sensing*, 170-173.
- [48] **Akar, I.** (2011). Determination of water surface changes and landuse changes of Acigol (Turkey) – Urmia (Iran) Lakes’ vicinity using multi-temporal satellite imageries. Master thesis. Marmara University.
- [49] **Arbiol, R. Magarinos, A. Martinez, L. Perez, F.**(2013). Development fo NDVI WMS geoservice from reflectance DMC Imagery at ICC. <http://www.icc.cat/eng/>.
- [50] **Ogunbadewa, E, Y.** (2013). A comparative assessment of UK-DMC and Landsat-7 ETM+satellite data. Research article. Volume 33, Number 2, 166-173.
- [51] **Leica Geosystems.** (2008). ERDAS Field Guide. Volum Two.
- [52]<<http://www.gisagmaps.com>>, date retrieved 10.09.2013.
- [53]< <https://landsat.usgs.gov>>, date retrieved 20.10.2012.
- [54]< <http://earthexplorer.usgs.gov>>, date retrieved 20.10.2012.
- [55]< <https://earth.esa.int>>, date retrieved 10.5.2013.
- [56]< <https://directory.eoportal.org>>, date retrieved 10.8.2013.
- [57]< <http://www.nrcan.gc.ca/earth-sciences/geomatics>>, date retrieved 10.11.2012.
- [58]< <http://daminfo.wrm.ir/fa/dam/stats>>, date retrieved 10.11.2013.
- [59]< <http://www.nrcan.gc.ca/earth-sciences/geomatics>>, data retrieved 10.10. 2013
- [60]< <http://www.legos.obs-mip.fr/>>, data retrieved 05.07. 2013
- [61]< <http://www.wrs.wrm.ir>>, data retrieved 05.10. 2013
- [62]< <http://www.amar.org.ir>>, data retrieved 10.10. 2013
- [63]< <http://resources.arcgis.com/en> >, data retrieved 10.01. 2014
- [64]< <http://gmao.gsfc.nasa.gov/>>, data retrieved 20.01. 2014
- [65]< <http://drought.unl.edu> />, data retrieved 20.01. 2014
- [66]< <http://www.ajol.info/index.php> />, data retrieved 20.01. 2013

[67]< <http://fanack.com/en/countries/iran/>>, data retrieved 20.01. 2014

[68]< <http://www.eoearth.org/view/article/155839/>>, data retrieved 20.01. 2014

[69]< <http://phenology.cr.usgs.gov/> />, data retrieved 20.01. 2013



## **APPENDICES**

**APPENDIX A:** Tables

**APPENDIX B:** Figures

## APPENDIX A

**Table A.1:** SPI values of Aahar Station – June Month.

Year	Rainfall	SPI-1	SPI-3	SPI-6	SPI-9	SPI-12	SPI-24
1987	25,3	0,44	-0,74	-1,26	-1,19	-1,05	-99
1990	4,3	-0,81	-0,5	-0,21	0,56	1,09	-0,02
1995	54,7	1,25	0,47	0,56	1,3	1,06	2,08
1998	11	-0,22	-0,62	-0,42	-1,02	-0,74	-0,42
2000	1,8	-1,25	-2,43	-1,49	-0,89	-0,37	-0,21
2006	6	-0,62	-0,17	0,16	-0,27	-0,48	-0,86
2007	25,7	0,46	0,82	0,58	0,45	0,5	-0,08
2009	16,3	0,07	-1,46	-2,14	-1,78	-1,76	-2,52
2010	18,6	0,18	1,17	1,34	1	1,31	-0,24
2011	13,7	-0,06	0,58	0,7	-0,49	-0,96	0,27

**Table A.2:** SPI values of Aahar Station – July Month.

Year	Rainfall	SPI-1	SPI-3	SPI-6	SPI-9	SPI-12	SPI-24
1987	0,5	-0,89	-0,48	-0,98	-0,95	-1,05	-99
1990	0	-1,02	-1,45	-0,71	-0,61	1,04	-0,19
1995	2,6	-0,37	0,11	0,27	1,02	1,05	1,86
1998	16,9	1,37	-0,13	-0,4	-0,32	-0,5	-0,33
2000	0,6	-0,87	-2,16	-1,72	-1,82	-0,35	-0,43
2006	11	0,83	-0,65	-0,08	0,21	-0,31	-1
2007	21	1,69	0,54	0,97	0,57	0,66	0,17
2009	0,8	-0,81	-1,7	-2,28	-2,48	-1,9	-2,75
2010	0	-1,02	1,02	1,2	1,1	1,23	-0,39
2011	3,3	-0,22	0	0,67	-0,12	-0,83	0,29

**Table A.3:** SPI values of Aahar Station – August Month.

Year	Rainfall	SPI-1	SPI-3	SPI-6	SPI-9	SPI-12	SPI-24
1987	24,8	1,63	0,71	-0,49	-0,73	-0,63	-99
1990	0	-0,5	-1,66	-0,65	-0,6	0,91	-0,65
1995	0	-0,5	0,88	0,31	0,39	1,01	1,6
1998	0	-0,5	-0,03	-0,65	-0,24	-0,48	-0,33
2000	0	-0,5	-2,04	-2,14	-1,92	-0,85	-0,41
2006	0	-0,5	-0,54	-0,42	0,07	-0,32	-0,97
2007	6	0,43	0,76	0,9	0,68	0,73	0,24
2009	3	0,1	-0,38	-1,87	-2,2	-1,76	-2,73
2010	5,8	0,41	-0,18	1,1	1,06	1,22	-0,3
2011	5,5	0,38	-0,26	0,47	0,3	-0,79	0,34

**Table A.4:** SPI values of Khoy Station – June Month.

Year	Rain	SPI-1	SPI-3	SPI-6	SPI-9	SPI-12	SPI-24
1984	0	-1,77	-1,5	-0,23	-0,71	-0,86	0,56
1987	0,1	-1,75	-2,75	-2,48	-1,38	-1,76	-0,59
1990	0	-1,77	-1,07	-0,67	-0,4	-0,38	-1,02
1995	18,6	0,04	-1,6	-1,9	-1,1	-1,12	-0,54
1998	11,5	-0,36	0,24	-0,49	-1,1	-0,91	-1,12
2000	7	-0,71	-0,35	-0,82	-1,19	-1,41	-1,69
2006	1,1	-1,51	-0,44	-0,37	-0,87	-0,99	-0,31
2007	22	0,2	0,28	-0,11	-0,26	-0,01	-0,66
2009	65,1	1,5	-0,43	-0,84	-1,11	-0,61	-1,12
2010	11	-0,4	0,59	0,5	0,24	0,94	0,2
2011	27,7	0,43	0,95	0,46	-0,44	-0,65	0,18

**Table A.5:** SPI values of Khoy Station – July Month.

Year	Rain	SPI-1	SPI-3	SPI-6	SPI-9	SPI-12	SPI-24
1984	1,6	-0,61	-0,85	-0,62	-0,66	-0,92	0,28
1987	0,6	-0,89	-3,34	-2,47	-1,64	-1,73	-0,59
1990	0	-1,2	-1,48	-0,92	-1,21	-0,37	-1,47
1995	28,2	1,41	-0,47	-1,4	-0,81	-0,64	-0,28
1998	1,3	-0,68	0,36	-0,5	-0,91	-1,3	-1,18
2000	0	-1,2	-1,31	-1,13	-1,54	-1,39	-1,69
2006	27,2	1,37	-0,55	-0,42	-0,32	-0,63	-0,23
2007	24,4	1,24	0,21	0,36	-0,18	-0,04	-0,48
2009	8,8	0,3	-0,08	-0,85	-1,48	-0,84	-1,27
2010	2,5	-0,43	0,32	0,66	0,36	0,84	0,01
2011	15,6	0,78	0,34	0,6	-0,09	-0,44	0,24

**Table A.6:** SPI values of Khoy Station – August Month.

Year	Rain	SPI-1	SPI-3	SPI-6	SPI-9	SPI-12	SPI-24
1984	0	-0,74	-2,48	-0,74	-0,74	-0,99	0,28
1987	4,8	0,3	-1,66	-3,15	-2,45	-1,6	-0,54
1990	4	0,18	-1,89	-1,06	-1,12	-0,31	-1,65
1995	0	-0,74	0,47	-1,28	-1,21	-0,73	-0,31
1998	1	-0,43	-0,9	-0,29	-0,68	-1,24	-1,19
2000	8	0,71	-0,82	-0,82	-1,2	-1,3	-1,62
2006	4,8	0,3	0,03	-0,73	-0,35	-0,53	-0,19
2007	17,2	1,54	0,91	0,64	0,21	0,13	-0,33
2009	2,9	-0,01	1,21	-0,54	-1,1	-0,81	-1,42
2010	3,7	0,13	-0,68	0,61	0,16	0,83	0,02
2011	1,1	-0,4	0,4	0,68	0,23	-0,45	0,22

**Table A.7: SPI values of Maragheh Station – June Month.**

Year	Rain	SPI-1	SPI-3	SPI-6	SPI-9	SPI-12	SPI-24
1984	1,5	-0,25	1,07	0,82	-99	-99	-99
1987	2,4	-0,09	-0,83	-0,23	0,19	0,11	0,57
1990	0	-0,79	-0,26	-0,33	0,22	0,15	-0,44
1995	47,2	2,24	1,14	1,09	1,15	1,34	1,55
1998	0,1	-0,69	-0,18	0,27	-0,04	-0,02	-0,29
2000	5	0,24	-0,63	-1,12	-1,38	-1,48	-1,68
2006	0	-0,79	0,07	0,76	0,09	0,01	0,03
2007	0	-0,79	0,49	0,05	0,44	0,37	0,21
2009	18,8	1,18	-1,32	-1,9	-1,35	-1,11	-2,24
2010	5,1	0,25	0,47	-0,09	0,3	0,58	-0,27
2011	0	-0,79	0,79	0,55	-0,37	-0,45	0,08

**Table A.8: SPI values of Maragheh Station – July Month.**

Year	Rain	SPI-1	SPI-3	SPI-6	SPI-9	SPI-12	SPI-24
1984	0,6	0,33	0,93	1,06	-99	-99	-99
1987	0	0,09	-0,41	0	-0,05	0,11	0,56
1990	0,2	0,21	-0,94	-0,45	-0,05	0,15	-0,44
1995	11,2	1,63	0,97	1,3	1,32	1,42	1,59
1998	10,4	1,56	0,49	0,3	0,19	-0,03	-0,22
2000	0	0,09	-0,44	-1,16	-1,37	-1,49	-1,77
2006	0	0,09	0,11	0,86	0,27	0,01	-0,01
2007	0,9	0,41	-0,21	0,25	-0,24	0,38	0,21
2009	0	0,09	-0,37	-1,86	-2,12	-1,12	-2,25
2010	0	0,09	0,56	0,08	0,22	0,58	-0,27
2011	0	0,09	-0,17	0,56	-0,21	-0,45	0,08

**Table A.9: SPI values of Maragheh Station – August Month.**

Year	Rain	SPI-1	SPI-3	SPI-6	SPI-9	SPI-12	SPI-24
1984	0	0,18	-0,61	1,21	-99	-99	-99
1987	4	1,11	0,01	-0,22	-0,34	0,15	0,57
1990	0	0,18	-1,39	-0,5	-0,19	0,15	-0,58
1995	0	0,18	2,23	1,23	1,06	1,4	1,56
1998	0	0,18	0,36	0,46	0,32	-0,02	-0,22
2000	1,4	0,63	0,01	-0,82	-1,23	-1,44	-1,74
2006	0	0,18	-1,8	-0,19	0,45	0,01	-0,01
2007	2	0,76	-0,45	0,2	-0,2	0,39	0,22
2009	0	0,18	0,87	-1,51	-2,13	-1,09	-2,25
2010	1,1	0,56	-0,01	0,16	-0,1	0,58	-0,26
2011	1	0,54	-0,92	0,7	0,2	-0,44	0,09



**Table A.10:** SPI values of Piranshahr Station – June Month.

Year	Rain	SPI-1	SPI-3	SPI-6	SPI-9	SPI-12	SPI-24
1987	3	0,01	-0,64	-0,29	0,28	0,25	-99
1990	0	-0,4	0,58	-0,05	-0,14	-0,18	-1,03
1995	19,9	1,49	0,84	-0,51	0,55	0,61	0,88
1998	6,2	0,39	-0,23	0,13	-0,33	-0,36	-0,35
2000	0	-0,4	-0,33	-0,49	-0,92	-0,93	-1,85
2006	0	-0,4	0,56	1,2	0,23	0,23	0,09
2007	0	-0,4	0,66	0,31	-0,09	-0,13	0,04
2009	29	2,01	-0,28	-0,77	-0,38	-0,27	-1,09
2010	5,6	0,33	0,47	0,34	0,27	0,3	0
2011	2,1	-0,11	1,4	1,29	0,29	0,27	0,33

**Table A.11:** SPI values of Piranshahr Station – July Month.

Year	Rain	SPI-1	SPI-3	SPI-6	SPI-9	SPI-12	SPI-24
1987	0	0,4	-0,67	0,12	0,49	0,25	-99
1990	0	0,4	-2,51	0,05	-0,19	-0,18	-1,04
1995	0	0,4	0,45	-0,05	0,42	0,61	0,88
1998	0	0,4	0,16	-0,21	-0,2	-0,37	-0,35
2000	1	0,69	-1,07	-0,94	-0,95	-0,97	-1,85
2006	0	0,4	0,31	1,52	0,36	0,23	0,09
2007	1	0,69	0,06	0,42	0,12	-0,13	0,04
2009	0	0,4	-0,03	-0,22	-1,27	-0,28	-1,1
2010	0	0,4	0,4	0,55	0,3	0,3	-0,01
2011	1,5	0,86	0,67	1,21	0,4	0,28	0,34

**Table A.12:** SPI values of Piranshahr Station – August Month.

Year	Rain	SPI-1	SPI-3	SPI-6	SPI-9	SPI-12	SPI-24
1987	0	0,29	-0,4	-0,12	-0,28	0,25	-99
1990	0	0,29	-1,02	0,15	-0,38	-0,18	-1,11
1995	0	0,29	1,17	0,33	-0,3	0,6	0,86
1998	0	0,29	0,05	0,28	-0,24	-0,36	-0,35
2000	0	0,29	-0,78	-0,55	-0,75	-0,95	-1,82
2006	0	0,29	-1,02	0,22	0,68	0,21	0,09
2007	22	2,21	1,35	0,79	0,27	0,01	0,11
2009	0	0,29	1,67	0,2	-1,09	-0,28	-1,17
2010	0	0,29	-0,03	0,84	0,2	0,3	-0,01
2011	0,7	0,55	-0,2	1,55	0,78	0,28	0,34

**Table A.13: SPI values of Sardasht Station – June Month.**

Year	Rain	SPI-1	SPI-3	SPI-6	SPI-9	SPI-12	SPI-24
1990	2,6	0,04	-0,3	-0,92	-0,4	-0,42	-1,13
1995	33,6	2,57	1,91	1,61	1,92	1,92	1,57
1998	2	-0,06	0,05	1,33	1,23	1,23	0,54
2000	2	-0,06	-0,87	-0,56	-1,08	-1,11	-1,71
2006	0	-0,43	0,81	1,51	0,72	0,73	0,54
2007	2,4	0,01	0,23	-0,2	-0,66	-0,69	0
2009	4,1	0,27	-0,25	-0,65	-0,77	-0,74	-1,59
2010	1,8	-0,09	0,55	0,36	0,57	0,57	-0,14
2011	8,1	0,76	1,24	0,94	-0,08	-0,1	0,22

**Table A.14: SPI values of Sardasht Station – July Month.**

Year	Rain	SPI-1	SPI-3	SPI-6	SPI-9	SPI-12	SPI-24
1990	0	0,21	-0,87	-1,08	-0,48	-0,42	-1,13
1995	0	0,21	1,04	1,78	1,89	1,91	1,56
1998	4	1,13	0,5	1,29	1,2	1,23	0,52
2000	0,7	0,4	-0,6	-1,19	-0,99	-1,1	-1,72
2006	0	0,21	0,8	1,49	0,82	0,72	0,54
2007	2,2	0,77	-1,29	0,13	-0,53	-0,68	0,01
2009	0	0,21	-0,97	-0,15	-1,17	-0,74	-1,59
2010	0	0,21	1	0,6	0,39	0,57	-0,14
2011	0,3	0,29	0,93	0,82	0,02	-0,1	0,22

**Table A.15: SPI values of Sardasht Station – August Month.**

Year	Rain	SPI-1	SPI-3	SPI-6	SPI-9	SPI-12	SPI-24
1990	0	0,55	-0,55	-0,53	-1,06	-0,42	-1,15
1995	0	0,55	2,35	1,94	1,48	1,91	1,56
1998	0	0,55	0,01	1,46	1,18	1,23	0,52
2000	0	0,55	-0,53	-1,18	-0,9	-1,1	-1,71
2006	0	0,55	-0,97	0,13	1,15	0,7	0,54
2007	7	1,63	0,7	-0,11	-0,66	-0,65	0,01
2009	0	0,55	-0,28	0,11	-1,02	-0,76	-1,61
2010	2	0,59	-0,34	0,72	0,31	0,57	-0,14
2011	0	0,55	0,33	1,08	0,48	-0,1	0,22

**Table A.16:** SPI values of Tabriz Station Station – June Month.

Year	Rain	SPI-1	SPI-3	Spi-6	SPI-9	SPI-12	SPI-24
1984	0,2	-1,46	-1,21	-0,97	-1,19	-1	-0,61
1987	1,8	-0,91	-1,1	-0,7	-0,51	-0,62	-0,42
1990	0	-1,65	-1,5	-1,51	-0,63	-0,59	-1,59
1995	20,3	0,58	-0,34	-0,78	0,09	-0,06	0,45
1998	1,2	-1,06	-0,14	-0,27	-0,83	-0,58	-0,89
2000	23	0,69	-1,01	-1,21	-0,75	-0,71	-1,48
2006	0	-1,65	-1,02	0,23	-0,32	-0,43	-0,51
2007	8,9	-0,07	0,27	-0,11	0,32	0,11	-0,26
2009	34	1,1	-1,04	-0,99	-0,91	-0,55	-2,06
2010	6,9	-0,24	-0,17	-0,43	-0,23	-0,08	-0,47
2011	0,7	-1,22	0,65	0,24	-0,69	-0,75	-0,59

**Table A.17:** SPI values of Tabriz Station Station – July Month.

Year	Rain	SPI-1	SPI-3	Spi-6	SPI-9	SPI-12	SPI-24
1984	7,1	0,59	-0,15	-1,12	-0,93	-0,94	-0,58
1987	1	-0,2	-1,41	-0,43	-0,84	-0,68	-0,41
1990	1,4	-0,12	-2,7	-1,72	-1,63	-0,61	-1,7
1995	0	-0,49	-0,4	-0,92	-0,01	-0,08	0,4
1998	16,3	1,26	0,39	-0,1	-0,44	-0,6	-0,83
2000	0	-0,49	-1,01	-1,45	-1,62	-0,87	-1,67
2006	0,3	-0,37	-1,73	-0,43	-0,16	-0,47	-0,74
2007	1,5	-0,1	0,01	-0,02	-0,41	0,12	-0,26
2009	0	-0,49	-0,7	-1,04	-1,64	-0,82	-2,09
2010	0,4	-0,34	-0,39	-0,4	-0,23	-0,09	-0,61
2011	11,4	0,94	0,16	0,56	-0,42	-0,62	-0,49

**Table A.18:** SPI values of Tabriz Station Station – August Month.

Year	Rain	SPI-1	SPI-3	Spi-6	SPI-9	SPI-12	SPI-24
1984	0	0,02	-0,76	-1,09	-0,89	-1	-0,58
1987	0	0,02	-1,38	-1,04	-0,99	-0,71	-0,41
1990	0	0,02	-1,76	-1,42	-1,9	-0,74	-1,95
1995	0	0,02	0,1	-0,75	-0,6	-0,08	0,33
1998	9	1,13	0,37	0,14	-0,12	-0,45	-0,74
2000	0,5	0,12	0,24	-1,32	-1,69	-0,86	-1,77
2006	0	0,02	-2,46	-1,26	0	-0,52	-0,74
2007	9	1,13	0,06	0,49	-0,33	0,23	-0,21
2009	0	0,02	0,65	-0,73	-1,44	-0,81	-2,2
2010	10	1,22	-0,05	-0,51	-0,4	0,05	-0,52
2011	4,5	0,68	-0,09	0,69	0	-0,69	-0,45

**Table A.19:** SPI values of Urmia Station Station – June Month.

Year	Rain	SPI-1	SPI-3	SPI-6	SPI-9	SPI-12	SPI-24
1984	2	-0,8	0,26	-0,45	-0,85	-0,86	-0,16
1987	3,2	-0,58	-1,61	-1,58	-0,67	-0,65	-0,08
1990	0,5	-1,26	-0,88	-1,06	-0,09	-0,21	-0,88
1995	16,2	0,5	0,77	0,28	1,01	1,2	1,81
1998	0,1	-1,51	-0,52	-0,53	-1,16	-0,68	-0,98
2000	5	-0,34	-1,42	-1,42	-1,85	-1,94	-2,5
2006	0,4	-1,31	-0,31	-0,08	-0,73	-0,86	-1,46
2007	24,3	0,88	0,09	-0,46	0,79	0,71	-0,05
2009	32,7	1,2	-1,08	-1,11	-0,25	-0,28	-1,24
2010	3,3	-0,57	0,98	0,64	0,68	0,86	0,36
2011	9,5	0,07	0,96	0,83	0	0,15	0,61

**Table A.20:** SPI values of Urmia Station Station – July Month.

Year	Rain	SPI-1	SPI-3	SPI-6	SPI-9	SPI-12	SPI-24
1984	0,5	-0,15	1,12	-0,25	-0,63	-0,81	-0,16
1987	0	-0,45	-1,9	-1,14	-0,98	-0,77	-0,07
1990	4,1	0,43	-1,29	-1,26	-0,92	-0,15	-0,86
1995	24,3	1,62	0,23	0,55	1,2	1,34	1,82
1998	4,2	0,44	-0,68	-0,7	-1,01	-1,23	-0,93
2000	0	-0,45	-1,96	-1,48	-1,98	-1,85	-2,46
2006	0,1	-0,32	-0,83	-0,2	-0,54	-0,81	-1,54
2007	28,8	1,8	0,59	0,16	0,1	0,93	0,14
2009	0	-0,45	-0,45	-0,88	-1,6	-0,28	-1,43
2010	0	-0,45	0,6	0,72	0,77	0,82	0,35
2011	0,2	-0,27	0,04	0,72	0,08	0,15	0,59

**Table A.21:** SPI values of Urmia Station Station – August Month.

Year	Rain	SPI-1	SPI-3	SPI-6	SPI-9	SPI-12	SPI-24
1984	0	0,06	-1,27	-0,23	-0,59	-0,9	-0,16
1987	1	0,27	-0,97	-1,63	-1,46	-0,75	-0,07
1990	0	0,06	-0,91	-1,14	-1,23	-0,16	-1,04
1995	0	0,06	0,99	0,45	0,3	1,32	1,79
1998	0	0,06	-0,95	-0,42	-0,81	-1,21	-0,92
2000	0	0,06	-0,86	-1,32	-1,74	-1,88	-2,45
2006	2	0,45	-1,27	-0,72	-0,34	-0,81	-1,52
2007	1,3	0,33	1,38	0,33	-0,28	0,91	0,12
2009	0	0,06	0,74	-0,52	-1,36	-0,28	-1,43
2010	27,2	2,78	0,67	1,09	0,76	1,05	0,5
2011	9	1,36	0,17	0,98	0,59	-0,03	0,64

**Table A.22:** SPI values of Urmia Station – 1984 Year.

Month	SPI-1	SPI-3	SPI-6	SPI-9	SPI-12	SPI-24
Jan	-0,97	-0,91	-1,09	-0,49	-1,52	-0,14
Feb	0,03	-0,85	-1,17	-1,05	-1,23	-0,08
Mar	-0,66	-1,16	-1,54	-1,61	-1,15	-0,31
Apr	-1,83	-1,52	-1,76	-1,89	-1,28	-0,46
May	1,54	0,03	-0,4	-0,76	-0,71	-0,14
Jun	-0,8	0,26	-0,45	-0,85	-0,86	-0,16
Jul	-0,15	1,12	-0,25	-0,63	-0,81	-0,16
Aug	0,06	-1,27	-0,23	-0,59	-0,9	-0,16
Sep	-0,49	-1,14	0,05	-0,59	-0,96	-0,18
Oct	-0,51	-0,89	0,59	-0,61	-0,97	-0,79
Nov	1,5	0,84	0,43	0,18	-0,15	-1,06
Dec	-0,23	0,69	0,46	0,4	-0,17	-1,01

**Table A.23:** SPI values of Urmia Station – 1987 Year.

Month	SPI-1	SPI-3	SPI-6	SPI-9	SPI-12	SPI-24
Jan	-2,14	-0,05	0,25	0,74	1,19	0,18
Feb	1,02	-0,27	0,55	1,13	1,22	0,29
Mar	-0,41	-0,67	0,24	0,3	0,6	0,1
Apr	-0,65	-0,37	-0,4	-0,18	0,29	0,06
May	-1,58	-1,49	-1,37	-0,62	-0,13	-0,11
Jun	-0,58	-1,61	-1,58	-0,67	-0,65	-0,08
Jul	-0,45	-1,9	-1,14	-0,98	-0,77	-0,07
Aug	0,27	-0,97	-1,63	-1,46	-0,75	-0,07
Sep	-0,07	-0,77	-1,82	-1,66	-0,77	-0,06
Oct	1,79	1,59	0,28	-0,18	-0,24	0,43
Nov	-0,46	0,98	0,62	-0,65	-0,7	0,35
Dec	2,55	2,17	2,08	0,72	0,28	0,97

**Table A.24:** SPI values of Urmia Station – 1990 Year.

Month	SPI-1	SPI-3	SPI-6	SPI-9	SPI-12	SPI-24
Jan	0,66	0,23	1,26	0,52	-0,36	-0,43
Feb	-0,52	-0,54	1	0,7	-0,22	-0,63
Mar	-0,65	-0,58	0,62	0,49	-0,56	-0,87
Apr	0,06	-0,68	-0,46	0,39	-0,05	-0,63
May	-0,96	-0,97	-1,13	0,01	-0,21	-0,74
Jun	-1,26	-0,88	-1,06	-0,09	-0,21	-0,88
Jul	0,43	-1,29	-1,26	-0,92	-0,15	-0,86
Aug	0,06	-0,91	-1,14	-1,23	-0,16	-1,04
Sep	-0,49	-0,41	-1,03	-1,12	-0,17	-1,03
Oct	-0,05	-0,36	-1,44	-1,52	-1,16	-1,21
Nov	-1,51	-1,39	-1,83	-1,79	-1,73	-1,28
Dec	0,98	-0,43	-0,67	-1,25	-1,27	-1,26

**Table A.25: SPI values of Urmia Station – 1995 Year.**

Month	SPI-1	SPI-3	SPI-6	SPI-9	SPI-12	SPI-24
Jan	0,09	1,79	1,77	1,84	1,87	2,44
Feb	0,59	-0,05	1,77	2,02	1,8	2,48
Mar	-0,92	-0,52	0,93	1,23	1,65	2,24
Apr	1,49	0,7	1,49	1,6	1,72	2,33
May	-0,41	0,23	0,09	1,29	1,49	1,83
Jun	0,5	0,77	0,28	1,01	1,2	1,81
Jul	1,62	0,23	0,55	1,2	1,34	1,82
Aug	0,06	0,99	0,45	0,3	1,32	1,79
Sep	1,07	1,42	1,03	0,53	1,17	1,84
Oct	-0,45	-0,16	-0,06	0,37	1,1	1,83
Nov	0,23	-0,05	0,3	0,25	0,15	1,62
Dec	-1,03	-0,77	-0,19	0,41	0,07	1,48

**Table A.26: SPI values of Urmia Station – 1998 Year.**

Month	SPI-1	SPI-3	SPI-6	SPI-9	SPI-12	SPI-24
Jan	0,67	-0,89	-1,18	-0,5	-0,56	-0,74
Feb	-1,27	-1	-1,47	-0,52	-0,79	-0,95
Mar	0,23	-0,13	-1,15	-0,45	-1,12	-0,95
Apr	0,11	-0,3	-0,79	-1,03	-0,61	-0,96
May	-0,27	-0,2	-0,66	-1,12	-0,57	-1,01
Jun	-1,51	-0,52	-0,53	-1,16	-0,68	-0,98
Jul	0,44	-0,68	-0,7	-1,01	-1,23	-0,93
Aug	0,06	-0,95	-0,42	-0,81	-1,21	-0,92
Sep	0,64	0,18	-0,55	-0,53	-1,14	-0,91
Oct	-1,29	-0,9	-1,23	-1,09	-1,37	-0,97
Nov	-1,77	-2,2	-2,56	-1,25	-1,47	-1,11
Dec	0,03	-1,88	-1,87	-1,64	-1,32	-1,26

**Table A.27: SPI values of Urmia Station – 1999 Year.**

Month	SPI-1	SPI-3	SPI-6	SPI-9	SPI-12	SPI-24
Jan	-0,33	-1,57	-1,91	-2,06	-1,51	-1,3
Feb	-0,44	-0,68	-1,82	-2,22	-1,4	-1,42
Mar	-0,49	-1,01	-2,09	-2,27	-1,81	-1,78
Apr	-0,95	-1,22	-1,89	-2,18	-2,27	-1,72
May	-0,06	-1,05	-1,25	-2,02	-2,29	-1,66
Jun	-0,34	-0,95	-1,36	-2,05	-2,12	-1,66
Jul	0	-0,41	-1,28	-1,77	-2,05	-2,05
Aug	0,75	-0,36	-1,1	-1,26	-1,95	-2,01
Sep	0,43	0,08	-0,98	-1,32	-2	-1,97
Oct	0,34	0,32	-0,31	-1,22	-1,75	-1,85
Nov	-0,81	-0,48	-0,76	-1,34	-1,43	-1,88
Dec	-1,79	-1,22	-1,31	-1,72	-1,84	-1,98

**Table A.28:** SPI values of Urmia Station – 2000 Year.

Month	SPI-1	SPI-3	SPI-6	SPI-9	SPI-12	SPI-24
Jan	0,03	-1,66	-1,15	-1,31	-1,65	-2,01
Feb	-0,71	-1,4	-1,38	-1,61	-1,75	-2,03
Mar	-0,1	-0,62	-1,4	-1,58	-1,67	-2,12
Apr	-0,4	-0,73	-1,51	-1,36	-1,44	-2,3
May	-1,97	-1,17	-1,69	-1,85	-2,02	-2,61
Jun	-0,34	-1,42	-1,42	-1,85	-1,94	-2,5
Jul	-0,45	-1,96	-1,48	-1,98	-1,85	-2,46
Aug	0,06	-0,86	-1,32	-1,74	-1,88	-2,45
Sep	-0,03	-0,96	-1,65	-1,52	-1,93	-2,49
Oct	0,15	-0,1	-1,58	-1,62	-2,15	-2,31
Nov	0,64	0,31	-0,08	-1	-1,38	-1,82
Dec	-0,06	0,2	-0,07	-1,15	-1,22	-1,91

**Table A.29:** SPI values of Urmia Station – 2001 Year.

Month	SPI-1	SPI-3	SPI-6	SPI-9	SPI-12	SPI-24
Jan	0,01	0,21	-0,04	-0,99	-1,15	-1,78
Feb	-0,73	-0,69	-0,26	-0,58	-1,18	-1,88
Mar	-0,49	-0,96	-0,55	-0,83	-1,4	-1,87
Apr	-1,19	-1,45	-0,98	-1,07	-1,64	-1,94
May	-0,41	-1,38	-1,51	-1,2	-1,43	-2,09
Jun	-0,8	-1,45	-1,66	-1,23	-1,43	-2,07
Jul	-0,12	-0,88	-1,72	-1,24	-1,33	-2,01
Aug	0,06	-1,25	-1,56	-1,62	-1,31	-2,03
Sep	-0,37	-1,07	-1,69	-1,77	-1,33	-2,06
Oct	-0,45	-0,81	-1,37	-2,12	-1,6	-2,22
Nov	0,07	-0,49	-1	-1,74	-1,75	-2,02
Dec	0,3	-0,33	-0,66	-1,64	-1,75	-1,86

**Table A.30:** SPI values of Urmia Station – 2002 Year.

Month	SPI-1	SPI-3	SPI-6	SPI-9	SPI-12	SPI-24
Jan	0,84	0,35	-0,18	-0,77	-1,4	-1,62
Feb	-0,58	0,19	-0,36	-0,73	-1,4	-1,67
Mar	0,36	0,27	-0,16	-0,4	-1,1	-1,53
Apr	1,03	0,57	0,55	0,23	-0,19	-1,11
May	0,51	0,81	0,7	0,33	0,13	-0,75
Jun	-1,26	0,64	0,56	0,23	0,1	-0,76
Jul	-0,32	0,01	0,33	0,36	0,1	-0,73
Aug	0,06	-1,97	0,48	0,42	0,1	-0,73
Sep	-0,49	-1,32	0,42	0,39	0,1	-0,73
Oct	-0,8	-1,23	-0,62	-0,04	0,05	-0,85
Nov	-0,05	-0,74	-1,33	0,01	0,02	-1,02
Dec	0,49	-0,4	-0,75	0	0,08	-0,96

**Table A.31:** SPI values of Urmia Station – 2003 Year.

Month	SPI-1	SPI-3	SPI-6	SPI-9	SPI-12	SPI-24
Jan	-1,5	-0,62	-1,16	-0,99	-0,3	-1,05
Feb	-0,32	-0,71	-1,15	-1,62	-0,27	-1,06
Mar	0,92	0,05	-0,37	-0,65	-0,01	-0,67
Apr	0,5	0,63	0,14	-0,23	-0,28	-0,33
May	-1,19	0,2	-0,19	-0,6	-0,87	-0,46
Jun	0,07	-0,38	-0,33	-0,55	-0,73	-0,38
Jul	-0,45	-1,2	-0,07	-0,37	-0,68	-0,37
Aug	0,06	-0,4	0,03	-0,31	-0,67	-0,37
Sep	-0,49	-1,39	-0,62	-0,48	-0,68	-0,37
Oct	0,47	0,2	-0,91	-0,13	-0,43	-0,23
Nov	0,22	0,16	-0,14	-0,02	-0,29	-0,2
Dec	0,23	0,2	-0,1	-0,48	-0,39	-0,22

**Table A.32:** SPI values of Urmia Station – 2004 Year.

Month	SPI-1	SPI-3	SPI-6	SPI-9	SPI-12	SPI-24
Jan	0,03	-0,02	-0,06	-0,79	-0,14	-0,31
Feb	-0,13	-0,18	-0,11	-0,34	-0,12	-0,29
Mar	-1,27	-1,15	-0,66	-0,98	-0,92	-0,58
Apr	0	-0,85	-0,73	-0,71	-1,15	-0,9
May	1,3	0,24	0,05	0,01	-0,12	-0,62
Jun	-0,6	0,67	-0,08	-0,05	-0,2	-0,58
Jul	1,24	1,13	0,12	0,03	-0,01	-0,45
Aug	0,06	0,18	0,18	0,02	-0,01	-0,45
Sep	-0,49	0,55	0,68	-0,03	-0,01	-0,45
Oct	-0,78	-1,21	0,55	-0,26	-0,3	-0,45
Nov	0,57	-0,12	-0,19	-0,02	-0,13	-0,3
Dec	-0,53	-0,38	-0,32	0,25	-0,29	-0,46

**Table A.33:** SPI values of Urmia Station – 2005 Year.

Month	SPI-1	SPI-3	SPI-6	SPI-9	SPI-12	SPI-24
Jan	-0,26	-0,18	-0,75	0,26	-0,31	-0,32
Feb	0,08	-0,68	-0,65	-0,69	-0,28	-0,3
Mar	-2,13	-1,53	-1,4	-1,42	-0,41	-0,83
Apr	-0,94	-1,65	-1,37	-1,73	-0,71	-1,18
May	0,18	-1,42	-1,54	-1,51	-1,54	-0,97
Jun	-1,21	-0,85	-1,57	-1,53	-1,52	-1,01
Jul	-0,27	-0,33	-1,53	-1,33	-1,66	-0,98
Aug	0,7	-0,94	-1,56	-1,62	-1,57	-0,95
Sep	-0,22	-0,4	-1	-1,61	-1,58	-0,94
Oct	-0,86	-0,86	-0,87	-1,94	-1,7	-1,14
Nov	-0,41	-1,1	-1,55	-2,07	-2	-1,27
Dec	-0,74	-1,42	-1,69	-1,86	-2,19	-1,45



**Table A.34:** SPI values of Urmia Station – 2006 Year.

Month	SPI-1	SPI-3	SPI-6	SPI-9	SPI-12	SPI-24
Jan	0,44	-0,75	-1,18	-1,26	-1,86	-1,31
Feb	1,54	0,66	-0,33	-0,67	-1,38	-1,06
Mar	-0,69	0,38	-0,69	-0,92	-1,17	-0,97
Apr	0,38	0,35	-0,16	-0,48	-0,64	-0,88
May	-0,28	-0,48	-0,13	-0,66	-0,89	-1,48
Jun	-1,31	-0,31	-0,08	-0,73	-0,86	-1,46
Jul	-0,32	-0,83	-0,2	-0,54	-0,81	-1,54
Aug	0,45	-1,27	-0,72	-0,34	-0,81	-1,52
Sep	-0,22	-0,66	-0,5	-0,2	-0,82	-1,51
Oct	2,19	2	0,99	0,86	0,43	-0,64
Nov	1,04	2,01	1,69	0,79	0,86	-0,49
Dec	-0,44	1,9	1,79	1,05	0,95	-0,5

**Table A.35:** SPI values of Urmia Station – 2007 Year.

Month	SPI-1	SPI-3	SPI-6	SPI-9	SPI-12	SPI-24
Jan	-1,25	0,08	1,54	0,8	0,71	-0,55
Feb	-0,61	-1,57	1,26	0,98	0,28	-0,66
Mar	0,13	-0,87	1,16	1,09	0,52	-0,35
Apr	0,26	-0,12	-0,14	0,93	0,47	-0,12
May	-0,21	-0,14	-0,81	0,68	0,5	-0,22
Jun	0,88	0,09	-0,46	0,79	0,71	-0,05
Jul	1,8	0,59	0,16	0,1	0,93	0,14
Aug	0,33	1,38	0,33	-0,28	0,91	0,12
Sep	-0,49	1,21	0,36	-0,2	0,91	0,12
Oct	-0,86	-1,13	0	-0,22	-0,22	0,12
Nov	-0,46	-1,17	-0,11	-0,27	-0,76	0,11
Dec	-0,22	-1,18	-0,64	-0,44	-0,77	0,16

**Table A.36:** SPI values of Urmia Station – 2008 Year.

Month	SPI-1	SPI-3	SPI-6	SPI-9	SPI-12	SPI-24
Jan	0,16	-0,73	-1,24	-0,54	-0,49	0,14
Feb	0,79	0,18	-0,75	-0,09	-0,21	0
Mar	-1,76	-0,69	-1,43	-1,14	-0,7	-0,11
Apr	-1,64	-1,49	-1,63	-1,97	-1,32	-0,47
May	-1,05	-2,66	-1,77	-2,25	-1,67	-0,61
Jun	0,05	-1,88	-1,74	-2,09	-1,84	-0,52
Jul	0,11	-1,04	-1,84	-1,84	-2,17	-0,49
Aug	0,19	-0,25	-2,44	-1,7	-2,14	-0,5
Sep	0,84	0,21	-1,77	-1,64	-2,02	-0,45
Oct	2,23	2,12	1,05	-0,14	-0,48	-0,43
Nov	-0,79	1,44	1,2	-0,61	-0,5	-0,83
Dec	-0,97	1,06	1,02	-0,39	-0,66	-0,92

**Table A.37:** SPI values of Urmia Station – 2009 Year.

Month	SPI-1	SPI-3	SPI-6	SPI-9	SPI-12	SPI-24
Jan	-1,04	-2,12	0,74	-0,01	-0,82	-0,85
Feb	-1,88	-2,53	0,29	0,11	-1,35	-0,99
Mar	0,76	-0,46	0,52	0,51	-0,56	-0,79
Apr	-1,19	-0,67	-1,64	-0,01	-0,46	-1,11
May	-1,64	-0,83	-1,79	-0,46	-0,58	-1,35
Jun	1,2	-1,08	-1,11	-0,25	-0,28	-1,24
Jul	-0,45	-0,45	-0,88	-1,6	-0,28	-1,43
Aug	0,06	0,74	-0,52	-1,36	-0,28	-1,43
Sep	1,99	1,2	-0,62	-0,77	-0,06	-1,19
Oct	-0,24	0,56	-0,15	-0,72	-1,46	-1,14
Nov	1	0,96	1,04	0,06	-0,64	-0,76
Dec	0,3	0,49	0,78	-0,24	-0,44	-0,71

**Table A.38:** SPI values of Urmia Station – 2010 Year.

Month	SPI-1	SPI-3	SPI-6	SPI-9	SPI-12	SPI-24
Jan	-0,49	0,57	0,63	0,13	-0,32	-0,75
Feb	-0,23	-0,45	0,49	0,65	-0,14	-0,94
Mar	0,46	-0,14	0,19	0,46	-0,29	-0,55
Apr	0,96	0,65	0,74	0,79	0,45	-0,03
May	1,02	1,11	0,75	1,07	1,19	0,4
Jun	-0,57	0,98	0,64	0,68	0,86	0,36
Jul	-0,45	0,6	0,72	0,77	0,82	0,35
Aug	2,78	0,67	1,09	0,76	1,05	0,5
Sep	-0,37	1,1	1,12	0,76	0,79	0,45
Oct	-0,2	0,51	0,6	0,77	0,84	-0,24
Nov	-1,84	-1,85	-1,05	0,38	0,14	-0,33
Dec	-0,58	-1,91	-1,23	0,11	-0,02	-0,31

**Table A.39:** SPI values of Urmia Station – 2011 Year.

Month	SPI-1	SPI-3	SPI-6	SPI-9	SPI-12	SPI-24
Jan	0,44	-1,45	-0,84	-0,28	0,17	-0,13
Feb	-0,76	-0,69	-1,72	-1,4	0,09	-0,08
Mar	0,67	0,28	-0,98	-0,76	0,19	-0,1
Apr	1,45	1,02	0,2	0,27	0,44	0,5
May	0,32	1,13	0,68	-0,01	0,09	0,75
Jun	0,07	0,96	0,83	0	0,15	0,61
Jul	-0,27	0,04	0,72	0,08	0,15	0,59
Aug	1,36	0,17	0,98	0,59	-0,03	0,64
Sep	1,41	1,06	1,09	0,92	0,13	0,56
Oct	0,53	0,93	0,46	0,96	0,33	0,68
Nov	0,63	0,81	0,68	1,16	0,8	0,58
Dec	-1,35	0,09	0,34	0,89	0,78	0,45

## APPENDIX B

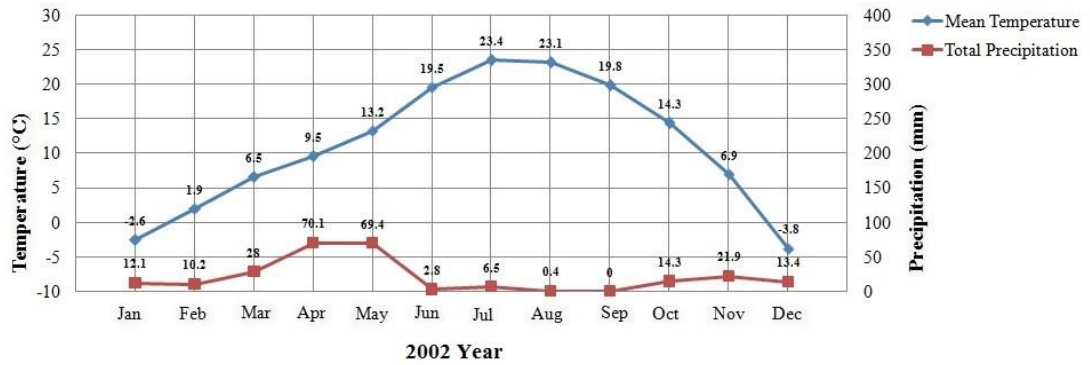


Figure B.1 : Mean temperature and total precipitation of Salmas station in 2002.

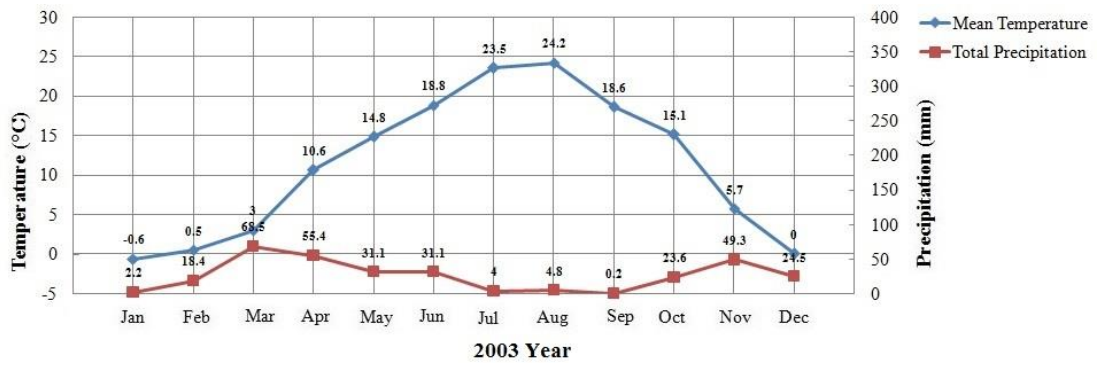


Figure B.2 : Mean temperature and total precipitation of Salmas station in 2003.

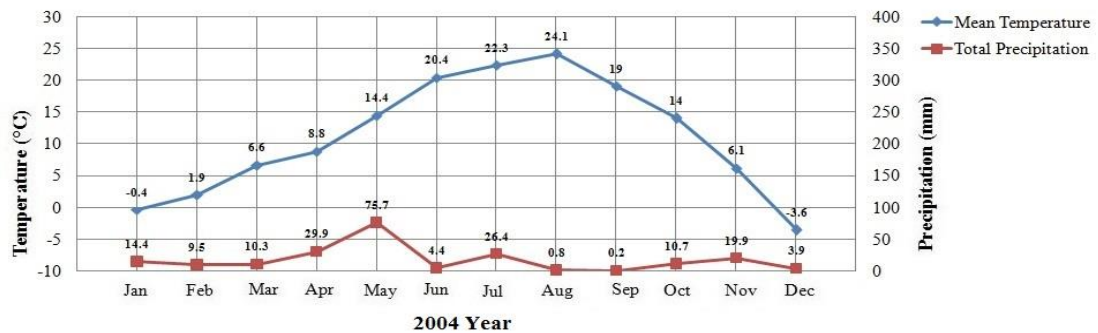


Figure B.3 : Mean temperature and total precipitation of Salmas station in 2004.

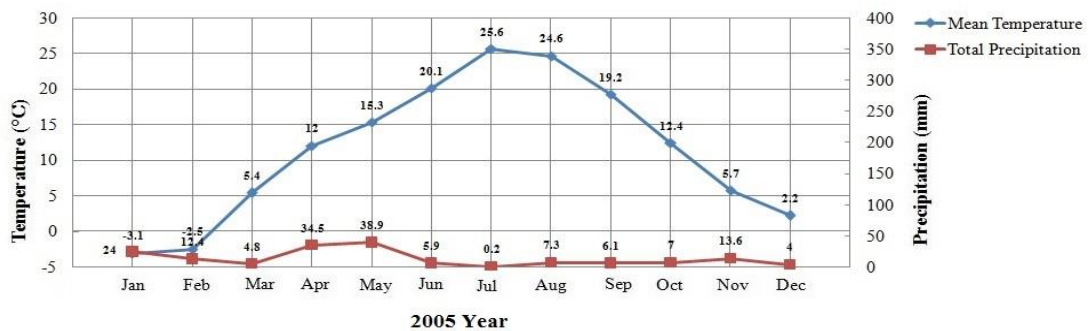


Figure B.4 : Mean temperature and total precipitation of Salmas station in 2005.

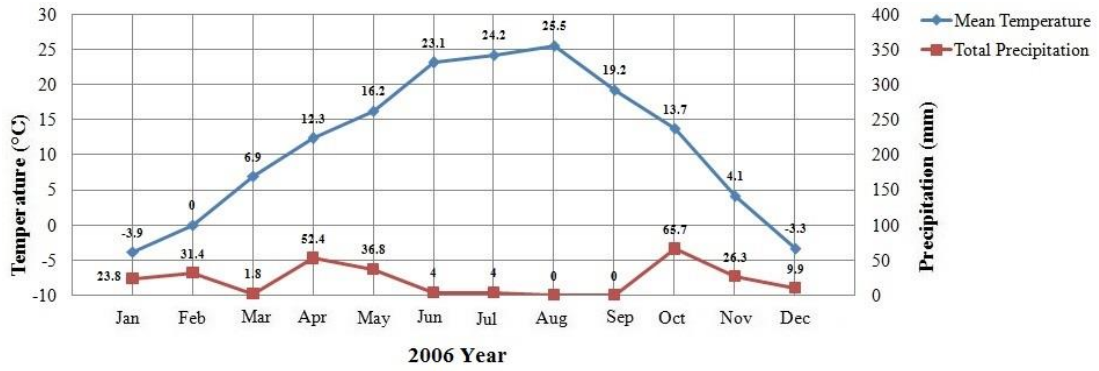


Figure B.5 : Mean temperature and total precipitation of Salmas station in 2006.

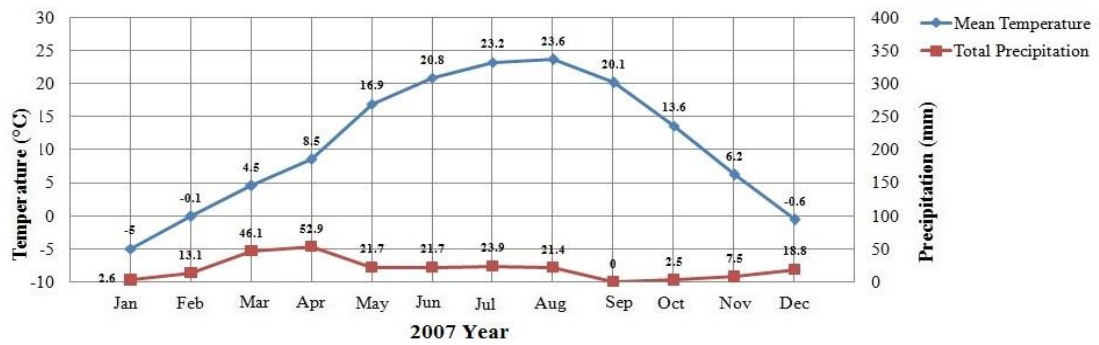


Figure B.6 : Mean temperature and total precipitation of Salmas station in 2007.

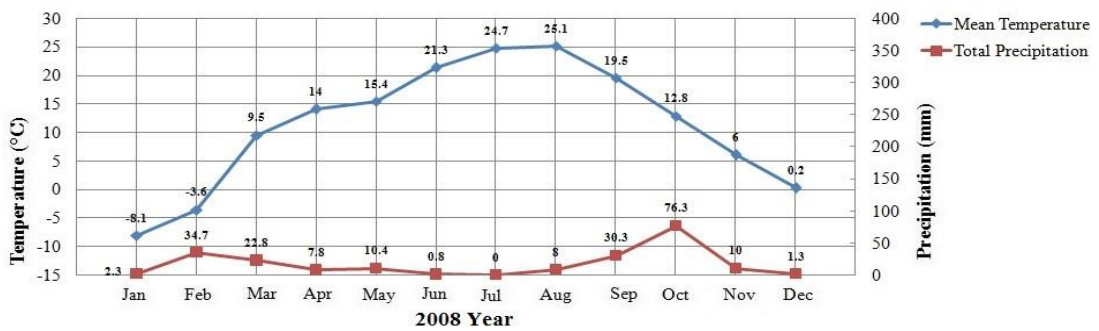


Figure B.7 : Mean temperature and total precipitation of Salmas station in 2008.

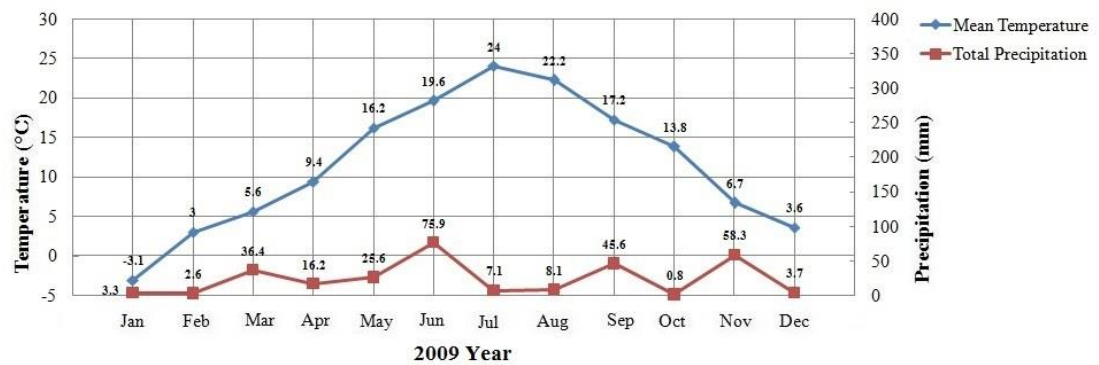


Figure B.8 : Mean temperature and total precipitation of Salmas station in 2009.

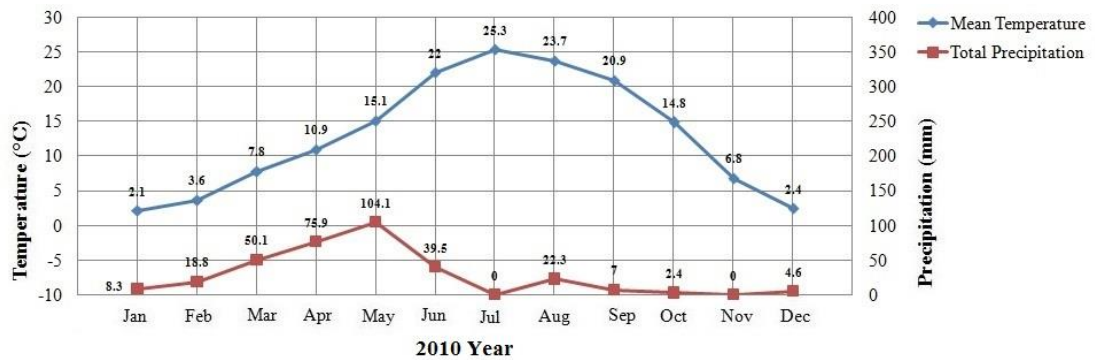


Figure B.9 : Mean temperature and total precipitation of Salmas station in 2010.

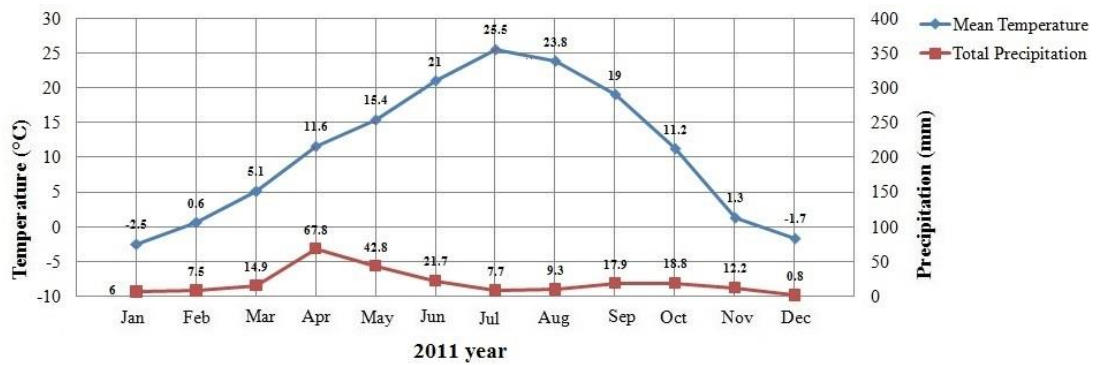


Figure B.10 : Mean temperature and total precipitation of Salmas station in 2011.

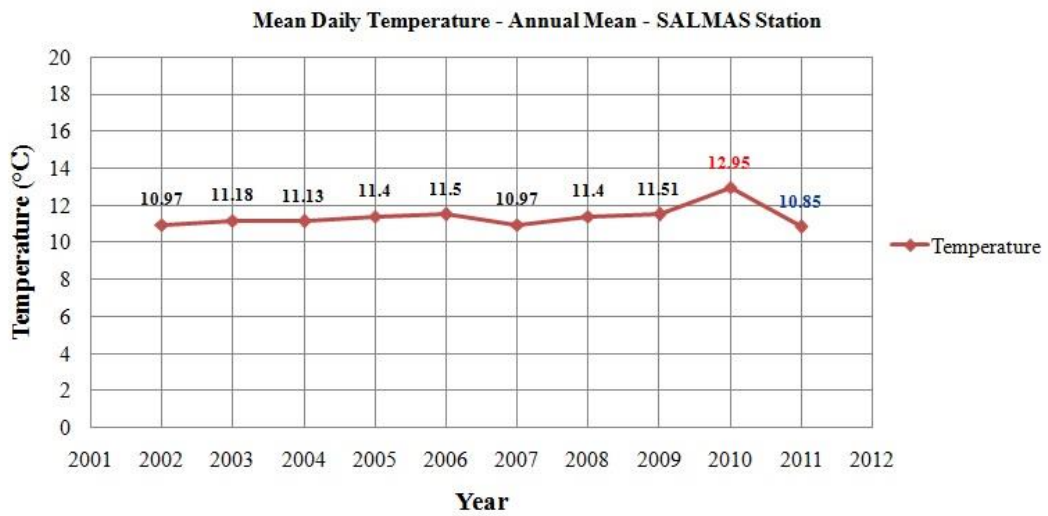


Figure B.11 : Mean temperature and total precipitation of Salmas station in 2012.

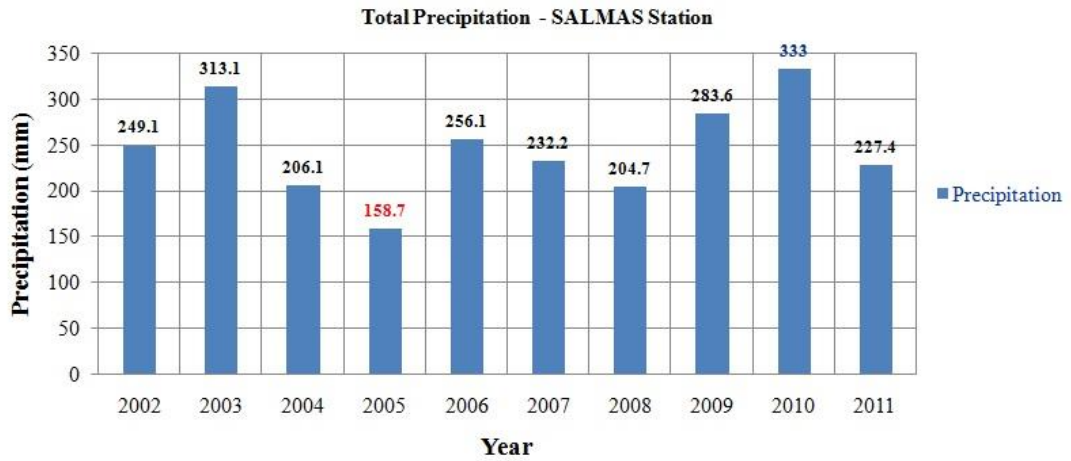


Figure B.12 : Annual precipitation of Salmas station.

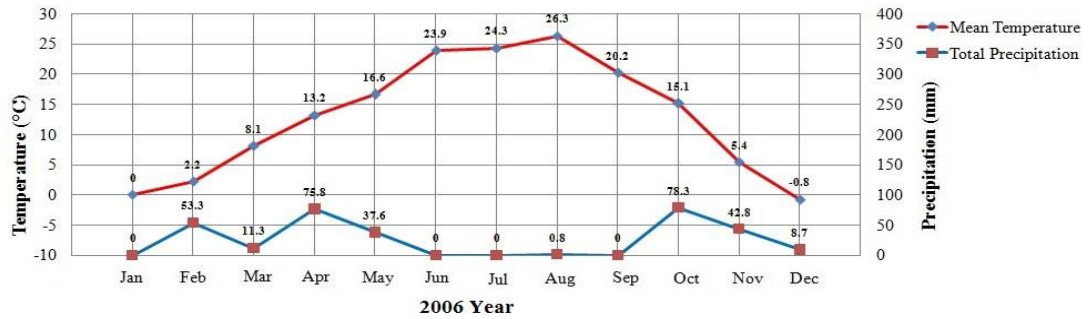


Figure B.13 : Mean temperature and total precipitation of Kahriz station in 2006.

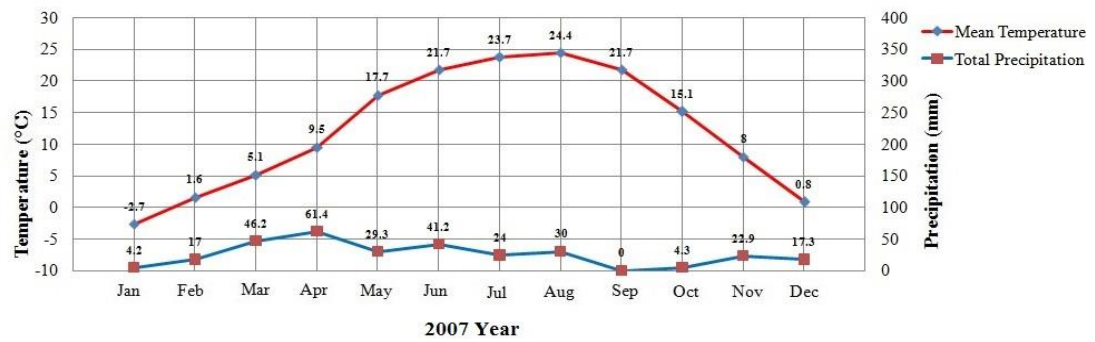


Figure B.14 : Mean temperature and total precipitation of Kahriz station in 2007.

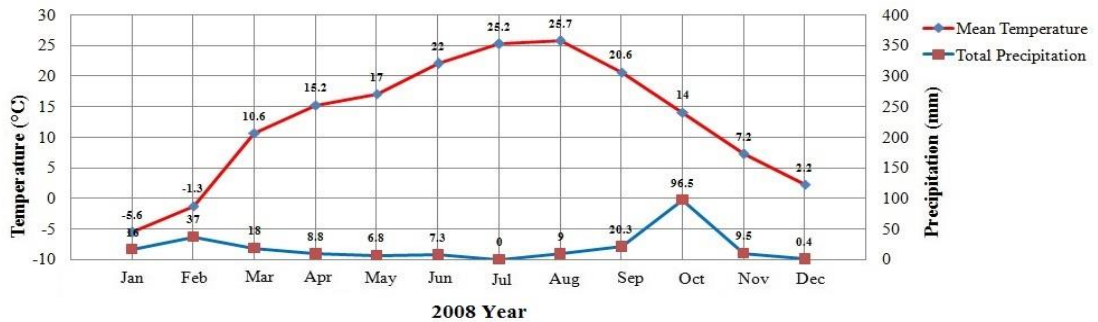


Figure B.15 : Mean temperature and total precipitation of Kahriz station in 2008.

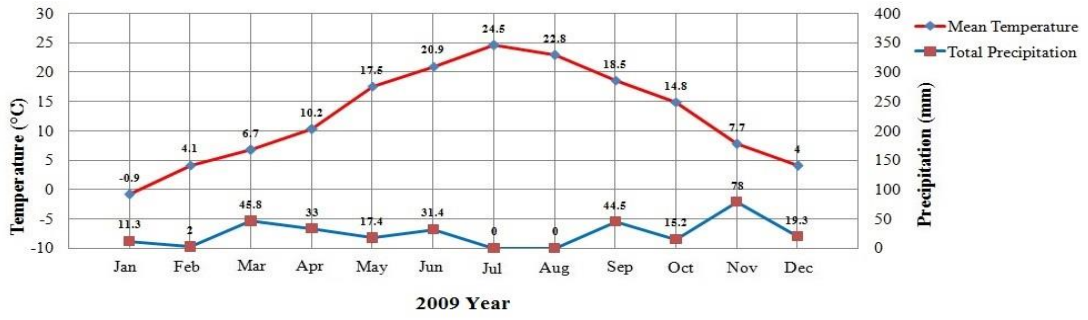


Figure B.16 : Mean temperature and total precipitation of Kahriz station in 2009.

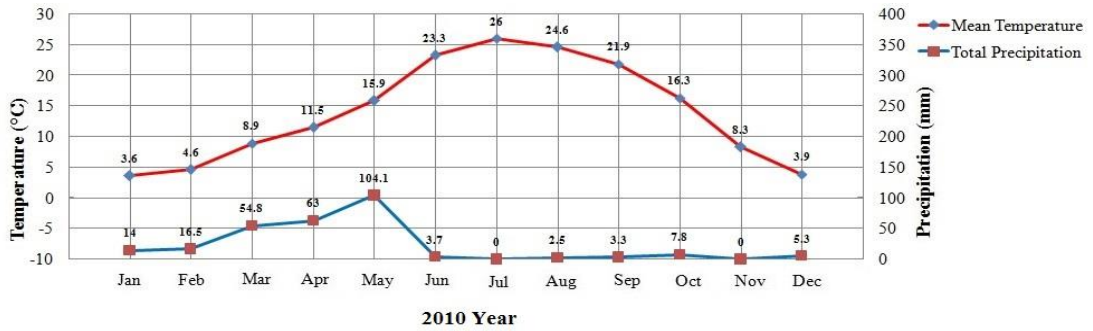


Figure B.17: Mean temperature and total precipitation of Kahriz station in 2010.

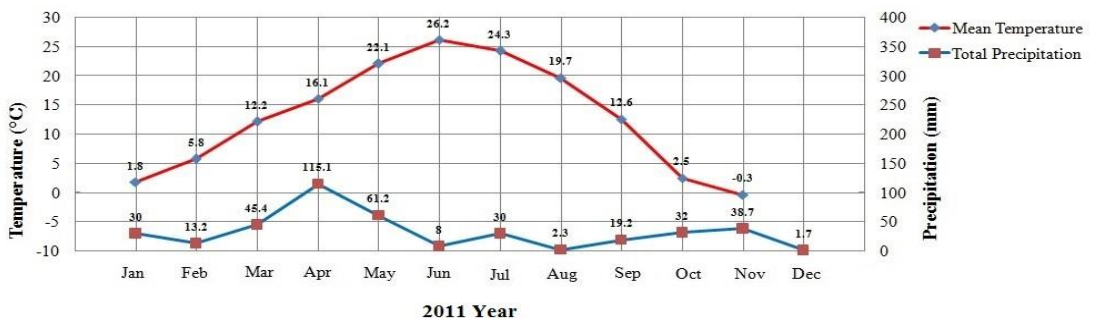


Figure B.18 : Mean temperature and total precipitation of Kahriz station in 2011.

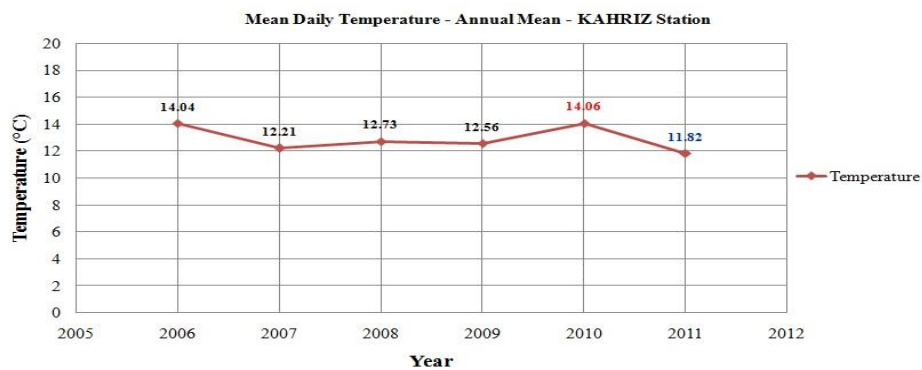
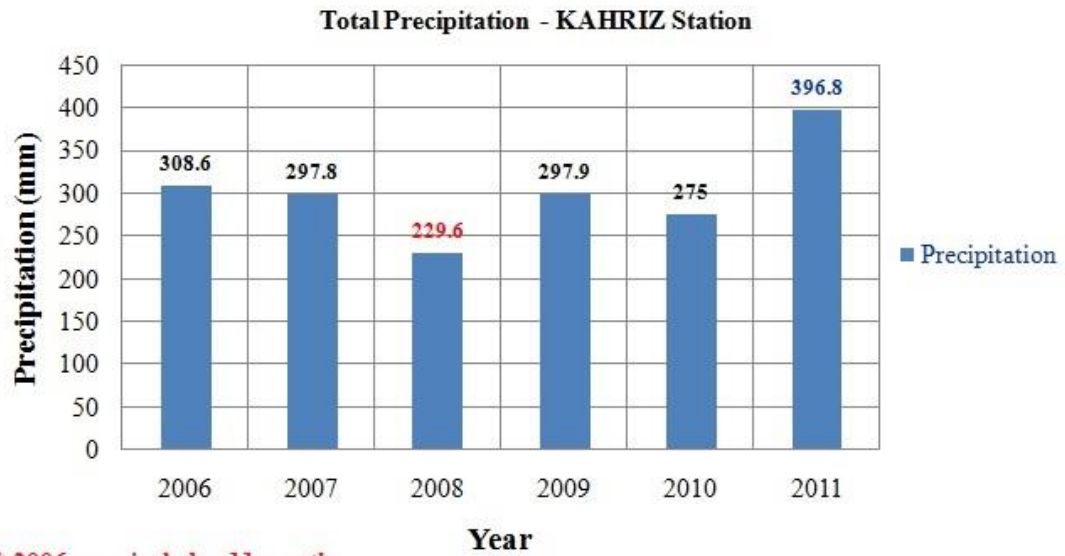
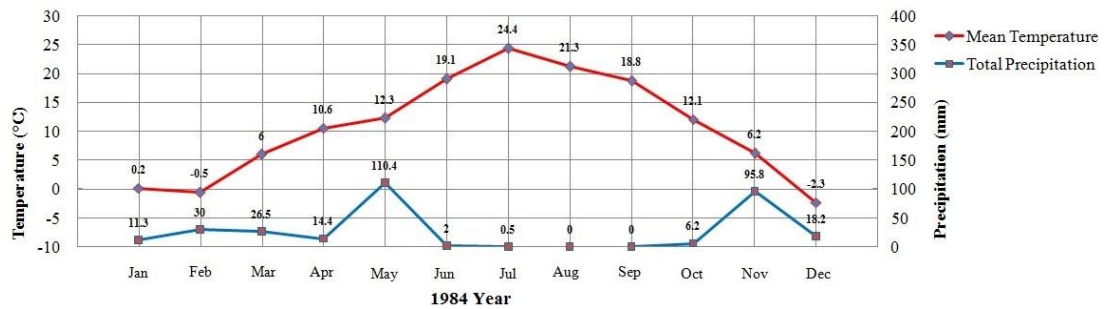


Figure B.19 : Annual mean temperature of Kahriz station.



**Figure B.20 :** Annual precipitation of Kahriz station.



**Figure B.21 :** Mean temperature and total precipitation of Urmia station in 1984.

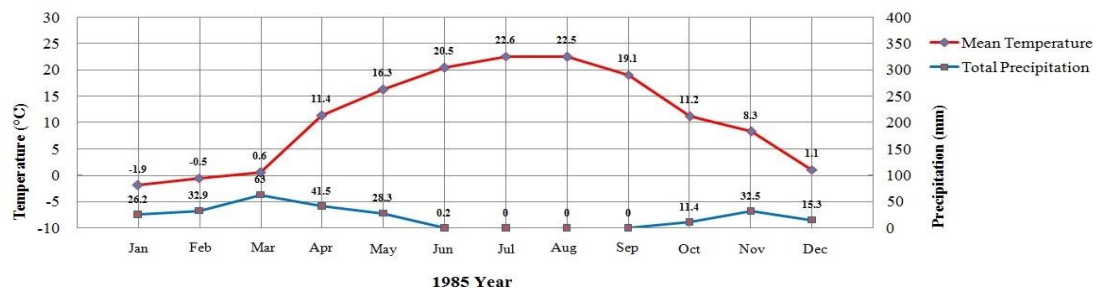


**Figure B.22 :** Mean temperature and total precipitation of Urmia station in 1985.

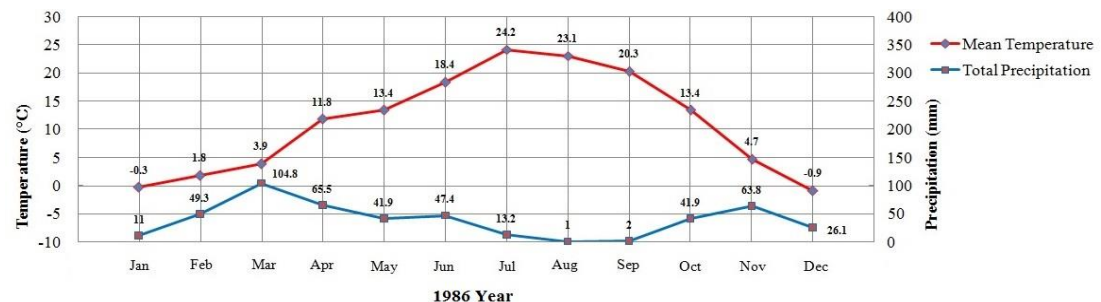


**Figure B.23 :** Mean temperature and total precipitation of Urmia station in 1986.



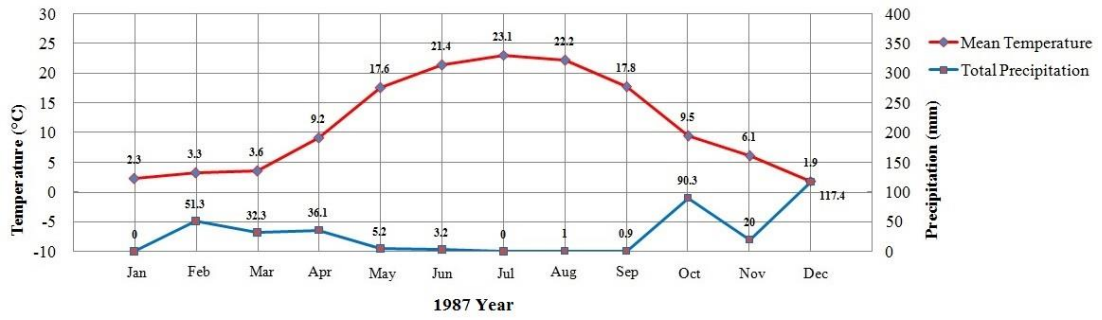


Figure B.24 : Mean temperature and total precipitation of Urmia station in 1987.

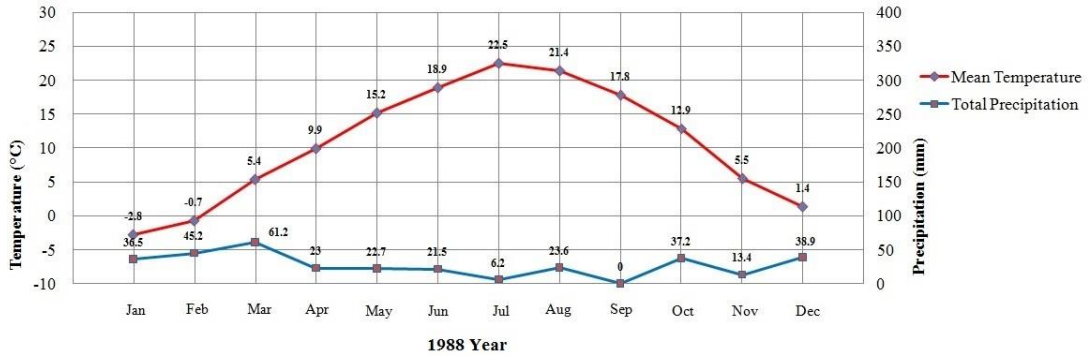


Figure B.25 : Mean temperature and total precipitation of Urmia station in 1988.

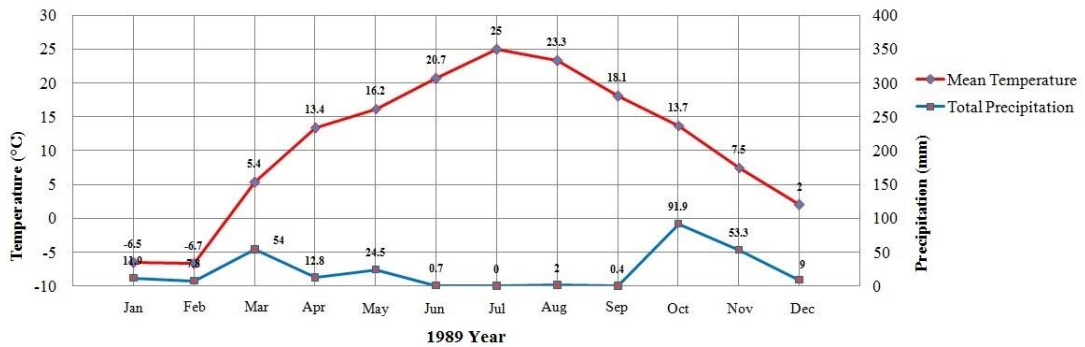


Figure B.26 : Mean temperature and total precipitation of Urmia station in 1989.

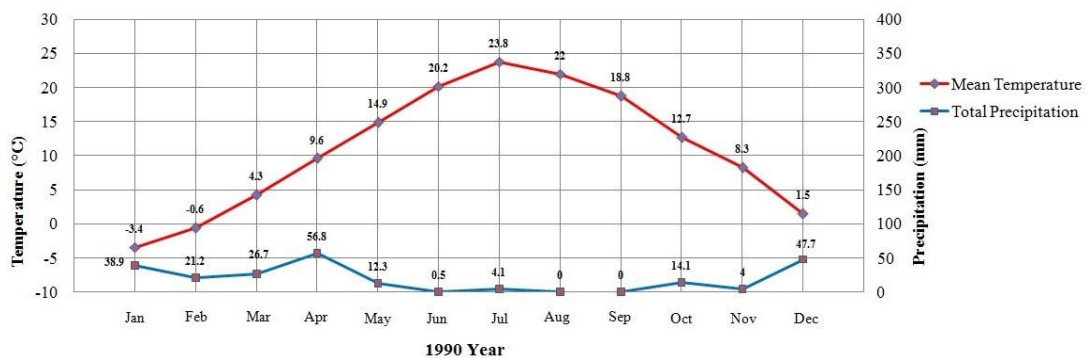


Figure B.27 : Mean temperature and total precipitation of Urmia station in 1990.

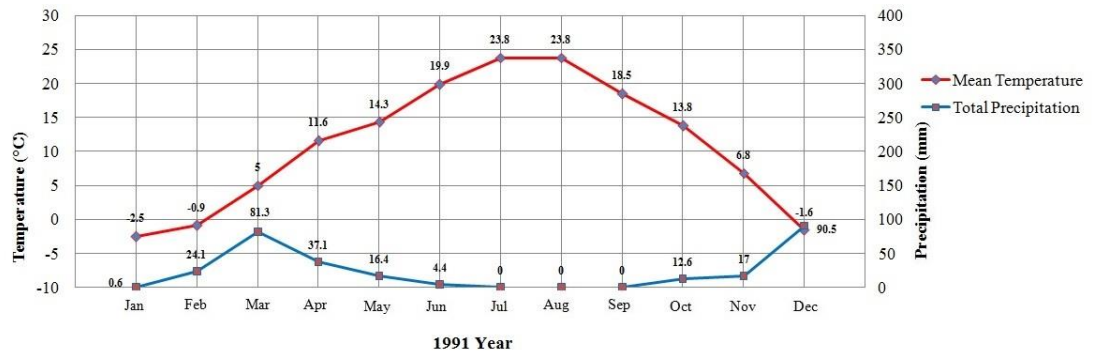


Figure B.28 : Mean temperature and total precipitation of Urmia station in 1991.

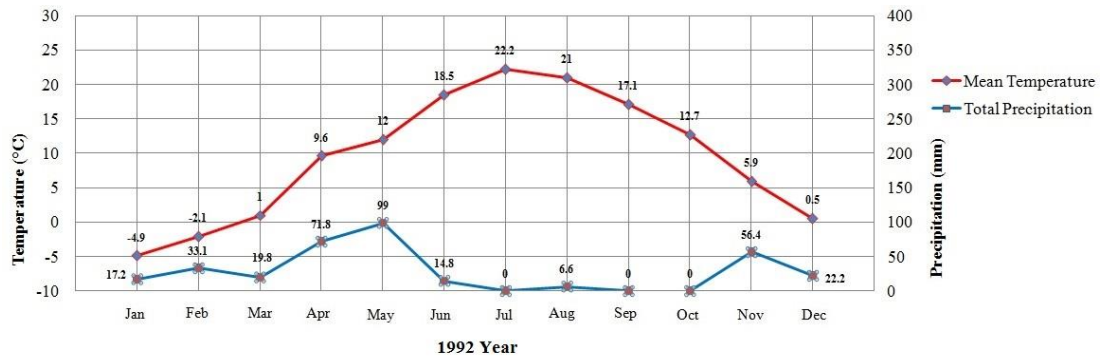


Figure B.29 : Mean temperature and total precipitation of Urmia station in 1992.

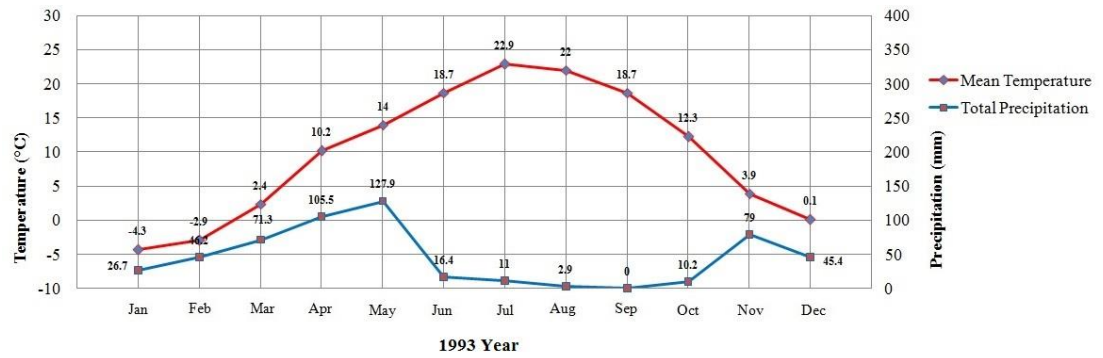


Figure B.30 : Mean temperature and total precipitation of Urmia station in 1993.

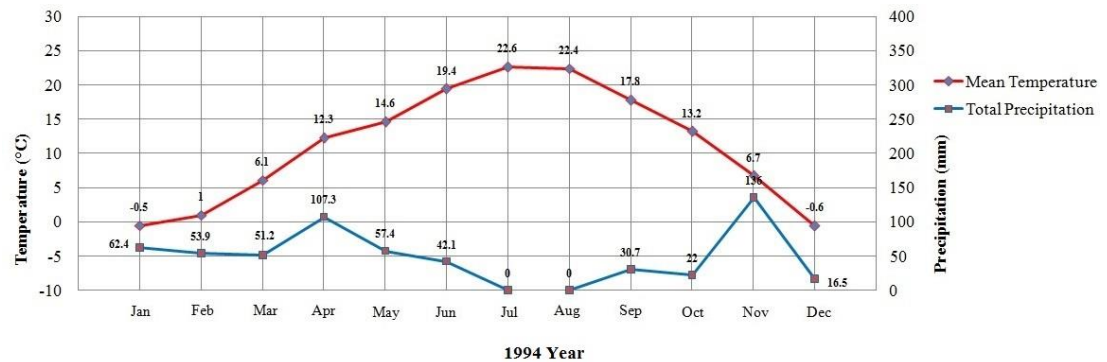


Figure B.31 : Mean temperature and total precipitation of Urmia station in 1994.



Figure B.32 : Mean temperature and total precipitation of Urmia station in 1995.

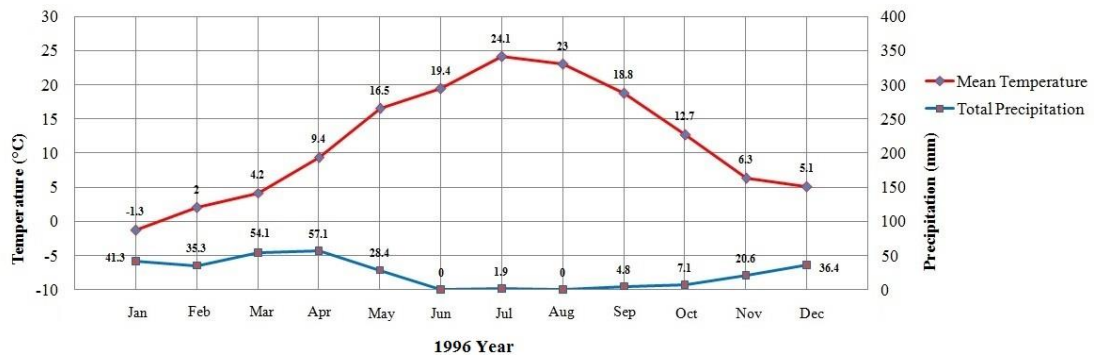


Figure B.33 : Mean temperature and total precipitation of Urmia station in 1996.

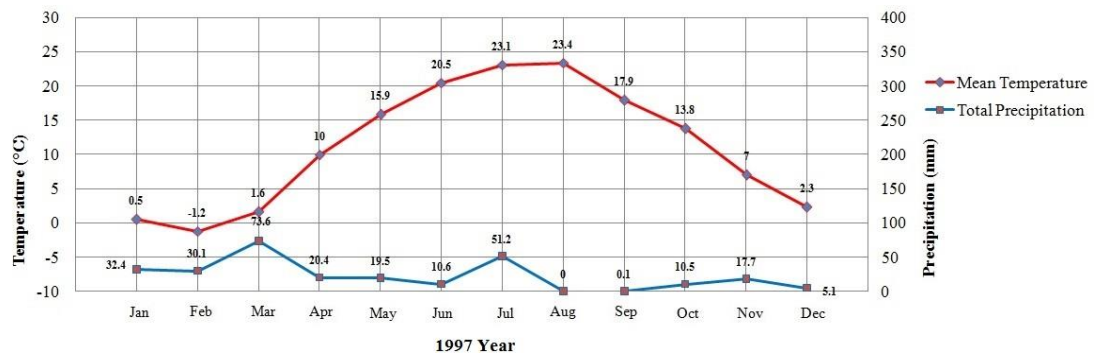


Figure B.34 : Mean temperature and total precipitation of Urmia station in 1997.

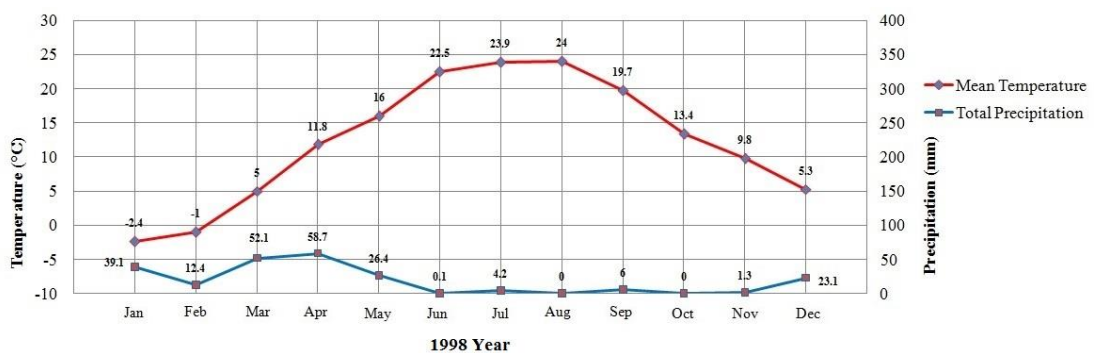


Figure B.35 : Mean temperature and total precipitation of Urmia station in 1998.

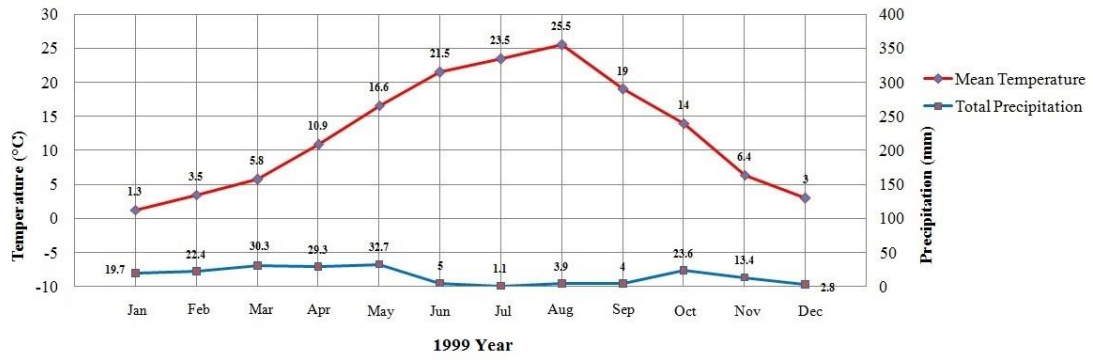


Figure B.36 : Mean temperature and total precipitation of Urmia station in 1999.

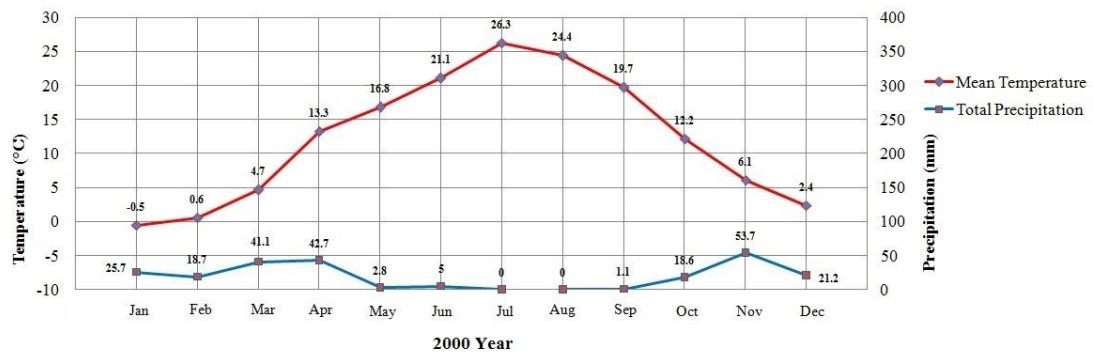


Figure B.37 : Mean temperature and total precipitation of Urmia station in 2000.

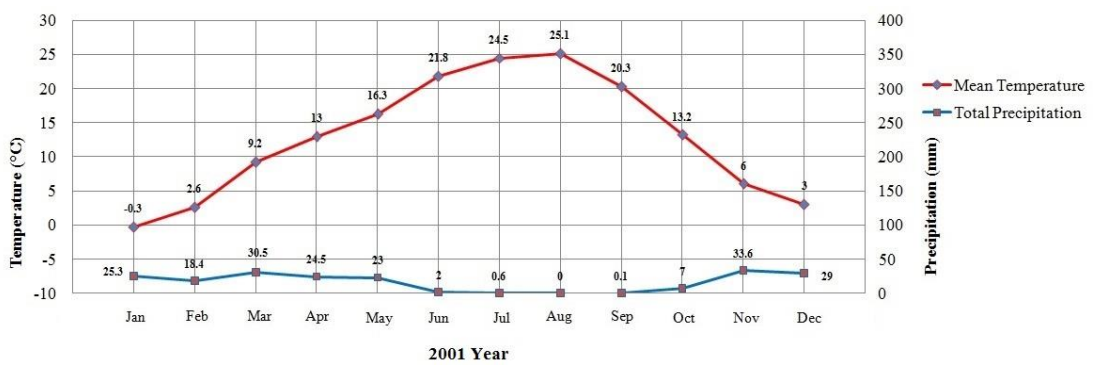


Figure B.38 : Mean temperature and total precipitation of Urmia station in 2001.

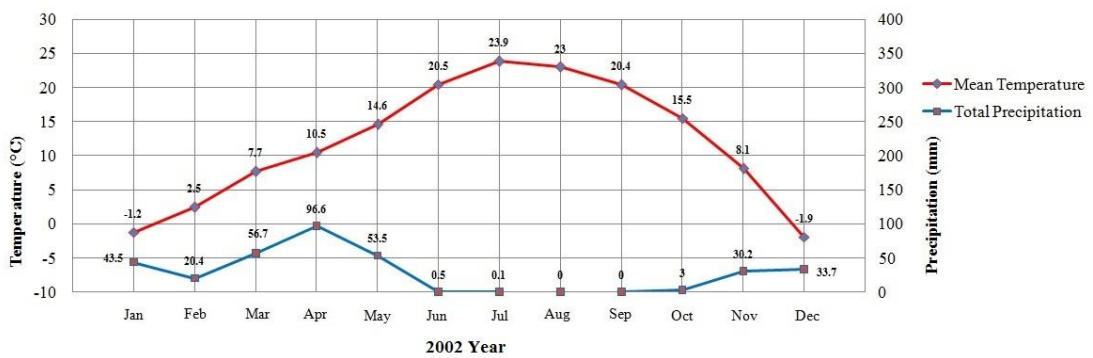


Figure B.39 : Mean temperature and total precipitation of Urmia station in 2002.

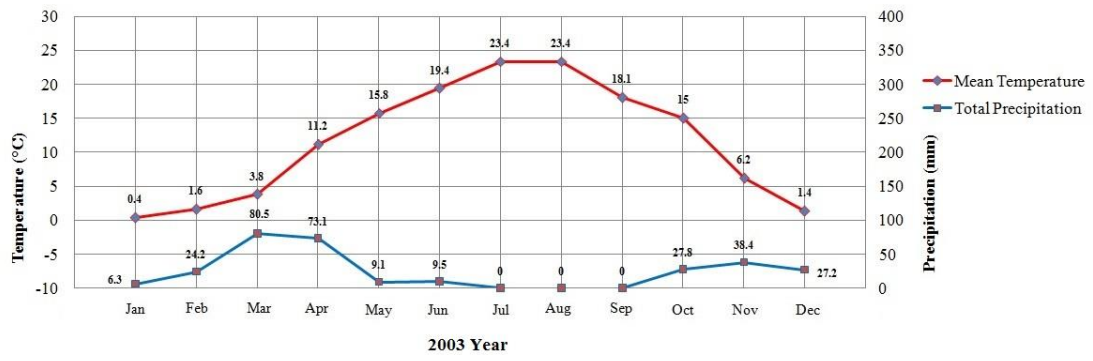


Figure B.40 : Mean temperature and total precipitation of Urmia station in 2003.

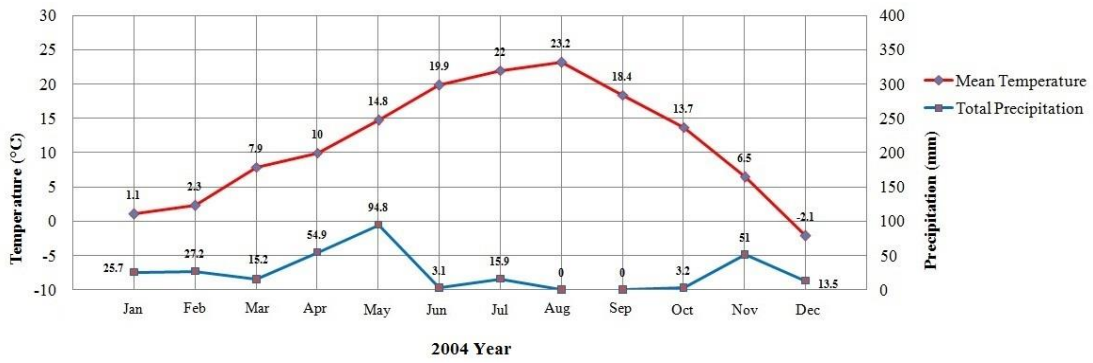


Figure B.41 : Mean temperature and total precipitation of Urmia station in 2004.

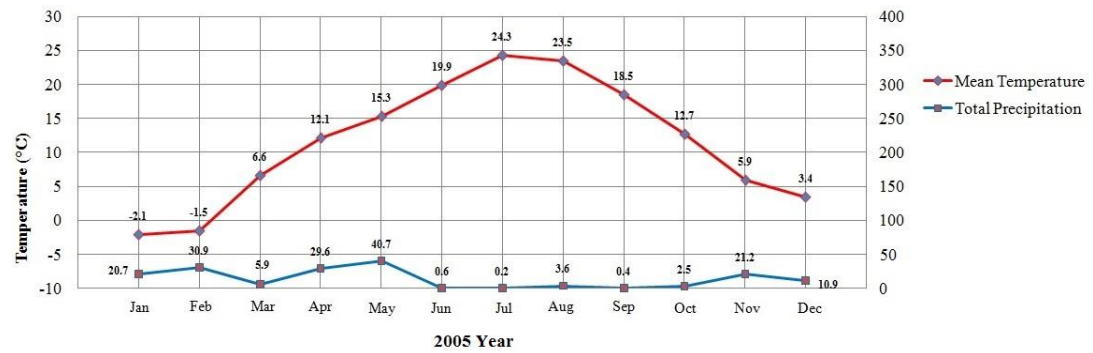


Figure B.42 : Mean temperature and total precipitation of Urmia station in 2005.

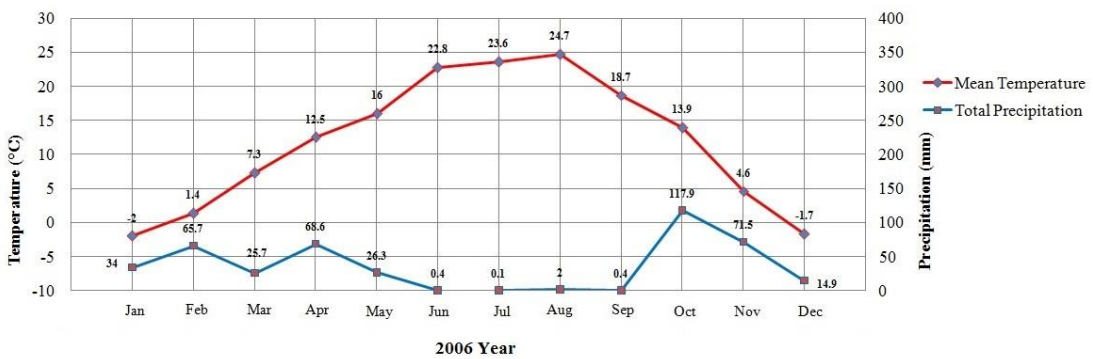


Figure B.43 : Mean temperature and total precipitation of Urmia station in 2006.

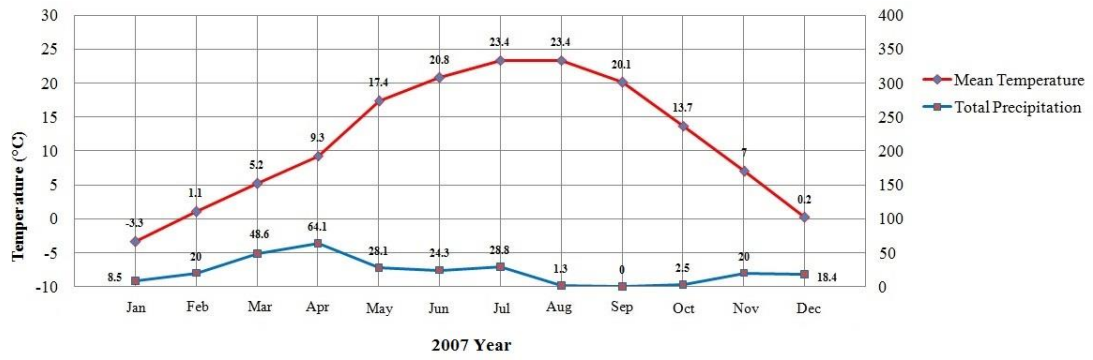


Figure B.44 : Mean temperature and total precipitation of Urmia station in 2007.

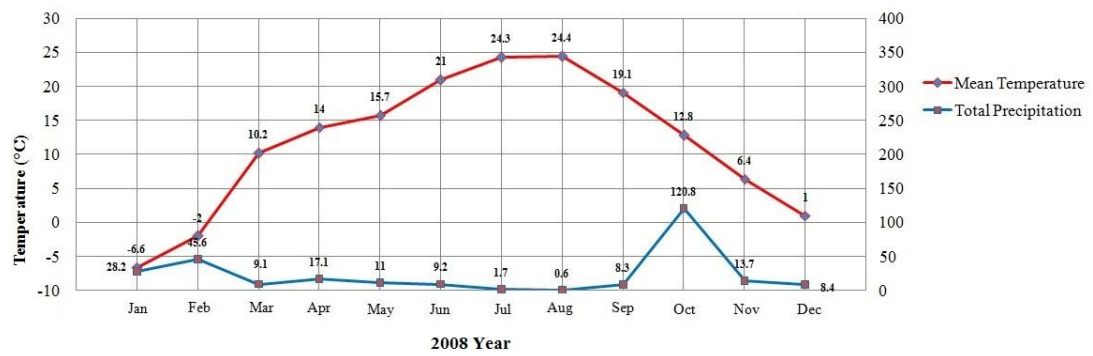


Figure B.45 : Mean temperature and total precipitation of Urmia station in 2008.

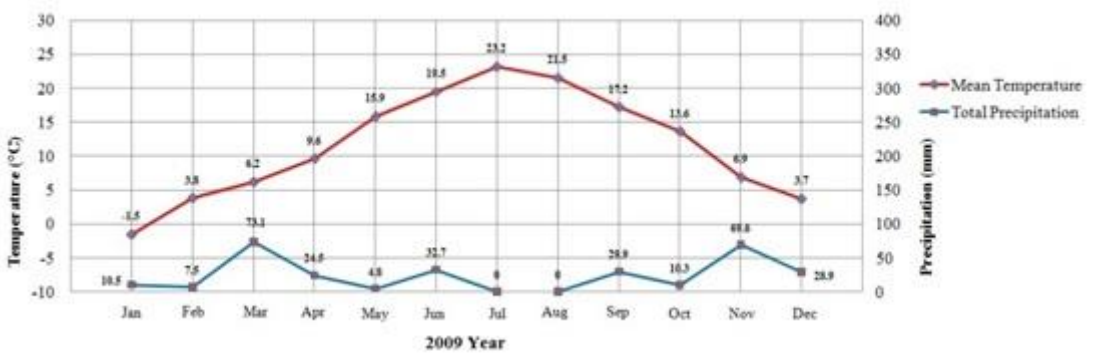


Figure B.46 : Mean temperature and total precipitation of Urmia station in 2009.

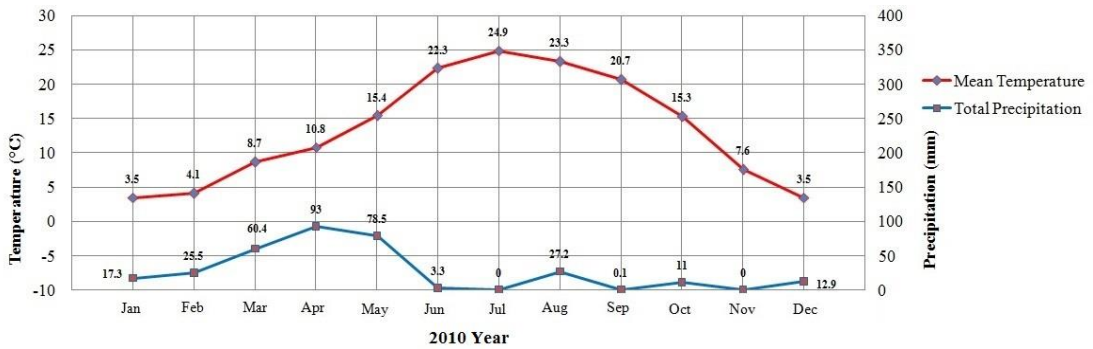


Figure B.47 : Mean temperature and total precipitation of Urmia station in 2010.

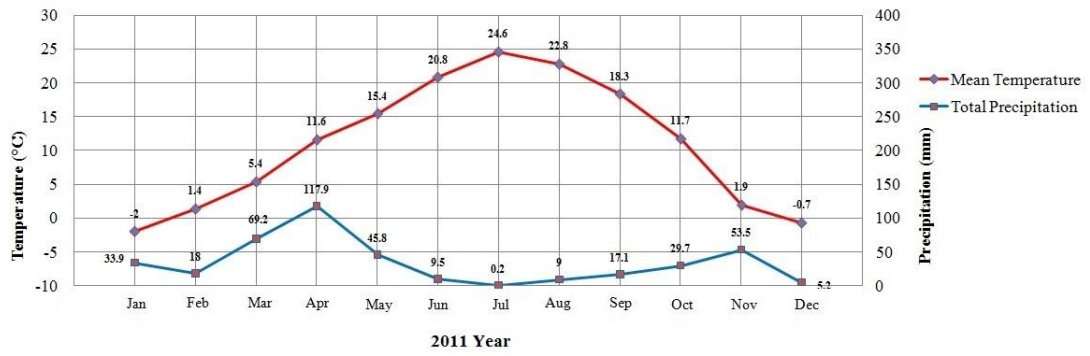


Figure B.48 : Mean temperature and total precipitation of Urmia station in 2011.

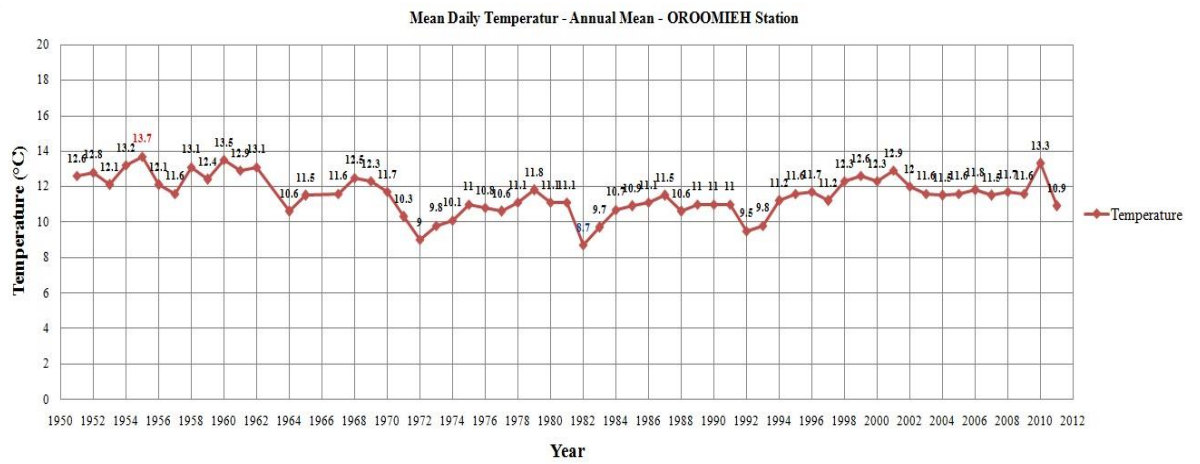


Figure B.49 : Annual mean temperature of Urmia station.

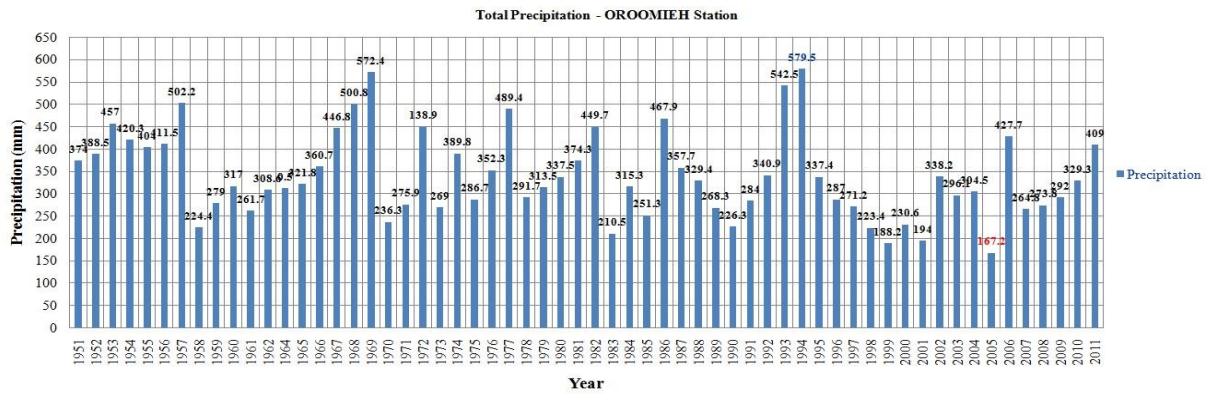


Figure B.50 : Annual precipitation of Urmia station in 2002.

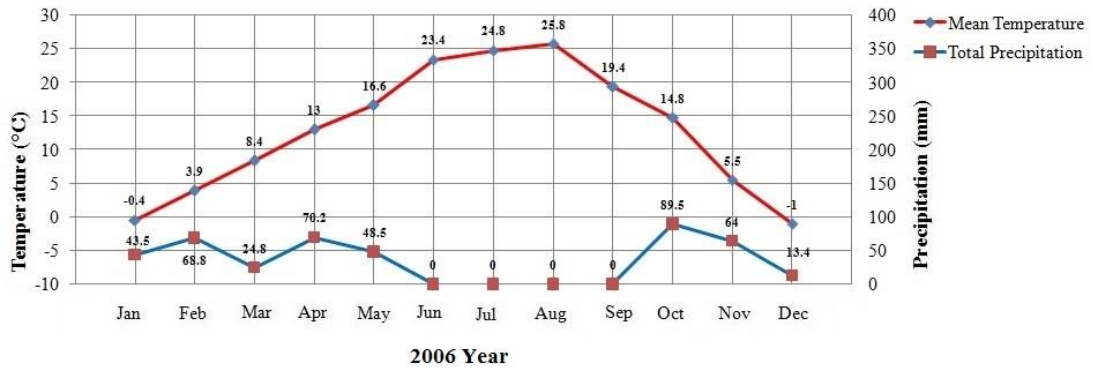


Figure B.51 : Mean temperature and total precipitation of Miandoab station in 2006.

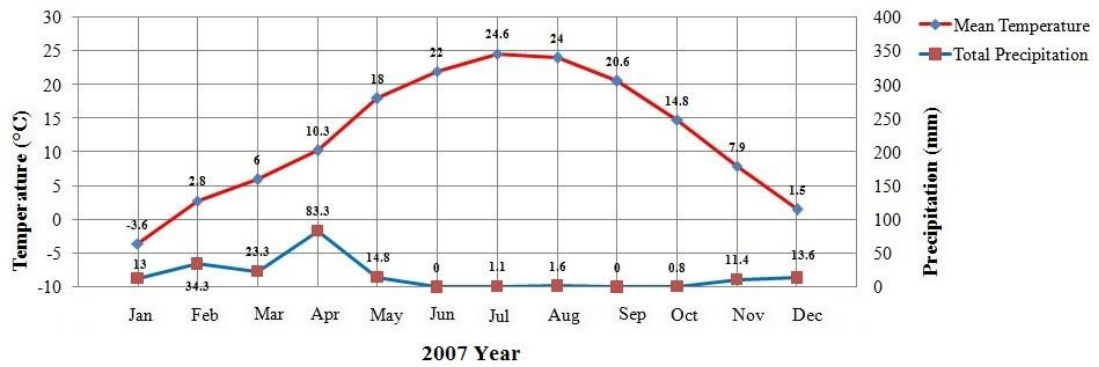


Figure B.52 : Mean temperature and total precipitation of Miandoab station in 2007.

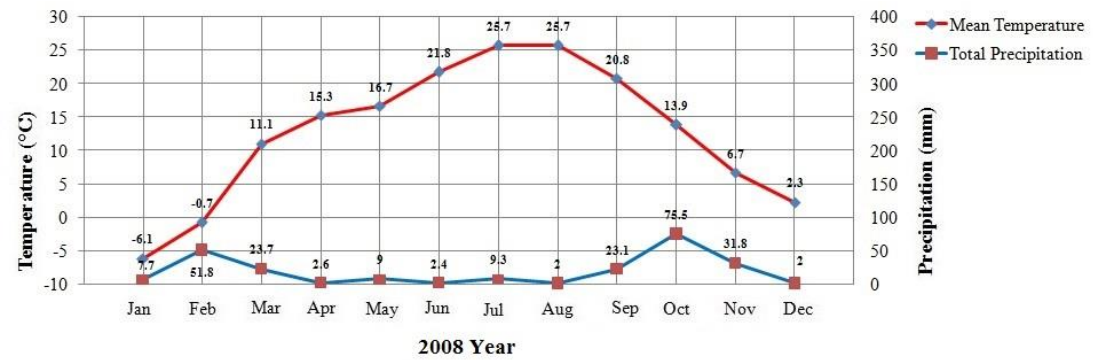


Figure B.53 : Mean temperature and total precipitation of Miandoab station in 2008.

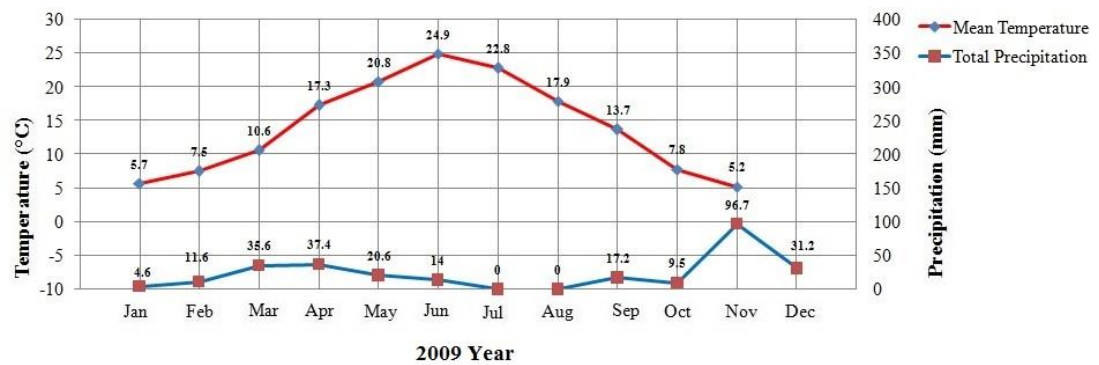


Figure B.54 : Mean temperature and total precipitation of Miandoab station in 2009.



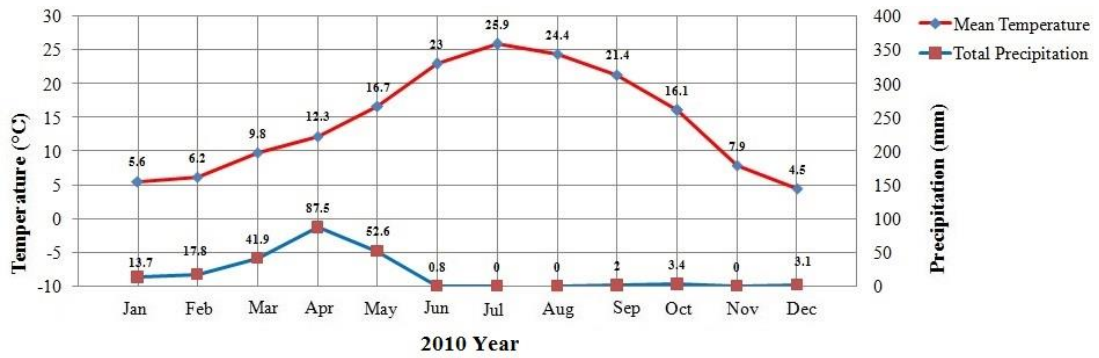


Figure B.55 : Mean temperature and total precipitation of Miandoab station in 2010.

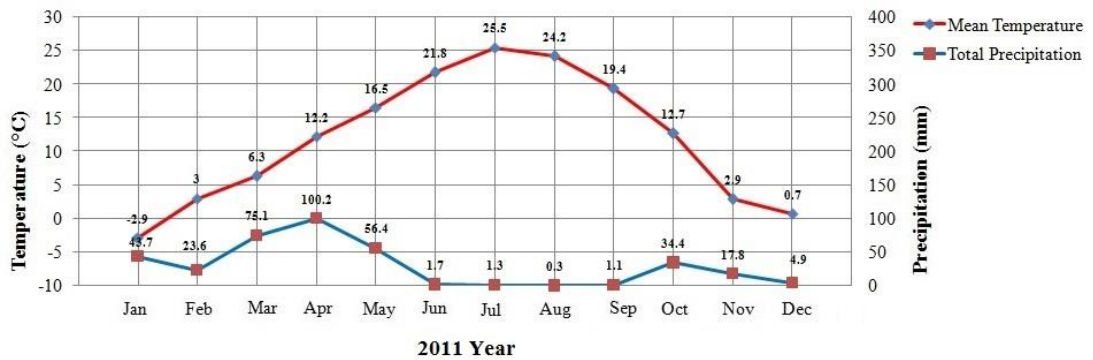


Figure B.56 : Mean temperature and total precipitation of Miandoab station in 2011.

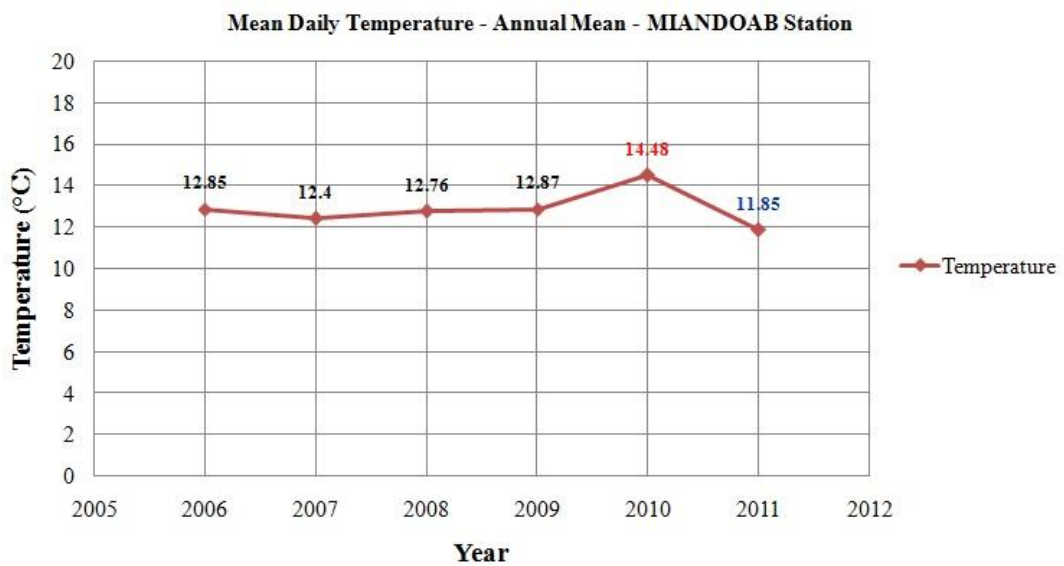
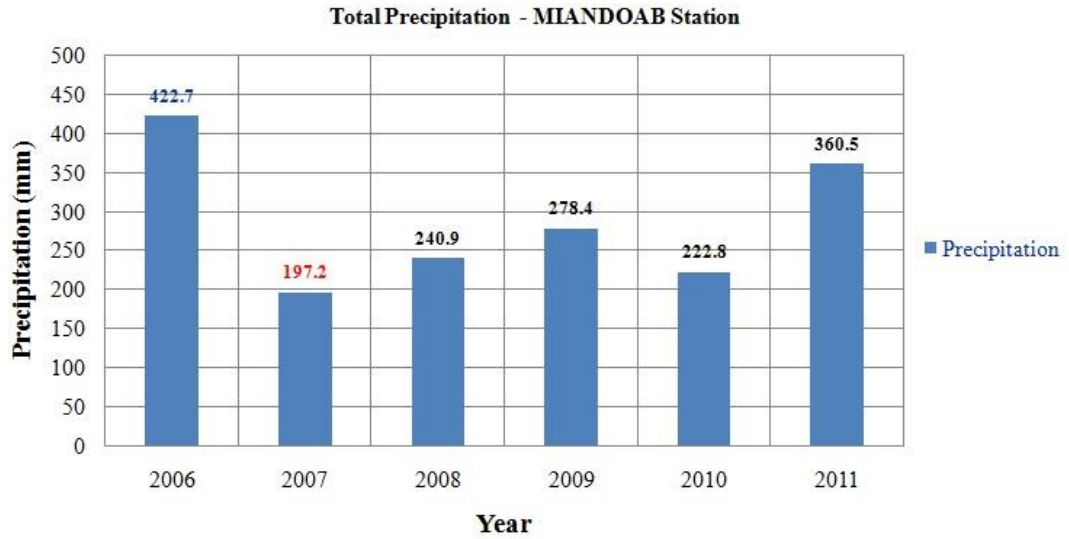
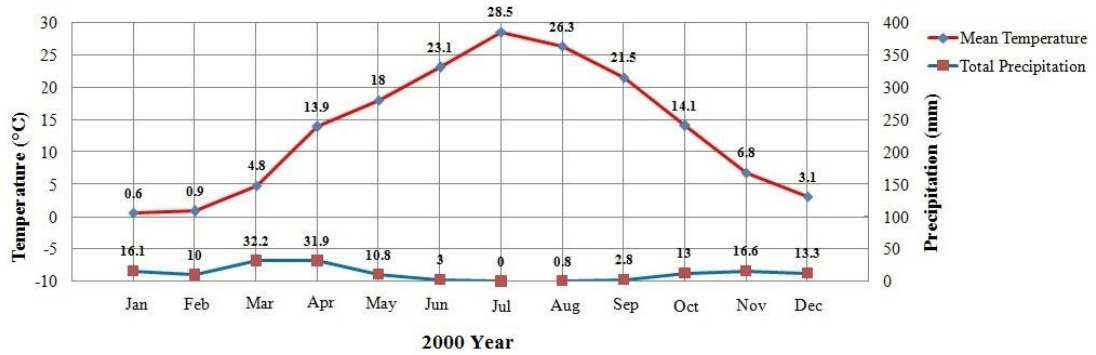


Figure B.57 : Annual mean temperature of Miandoab station.



**Figure B.58 :** Annual precipitation of Miandoab station.



**Figure B.59 :** Mean temperature and total precipitation of Bonab station in 2000.

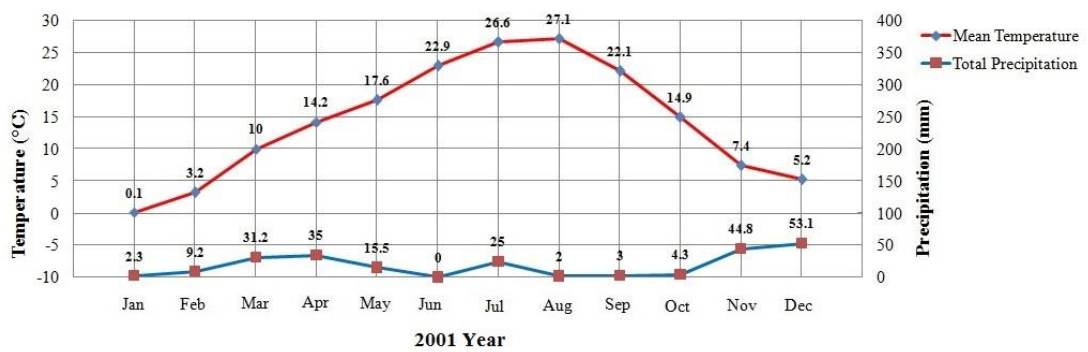


**Figure B.60 :** Mean temperature and total precipitation of Bonab station in 2001.

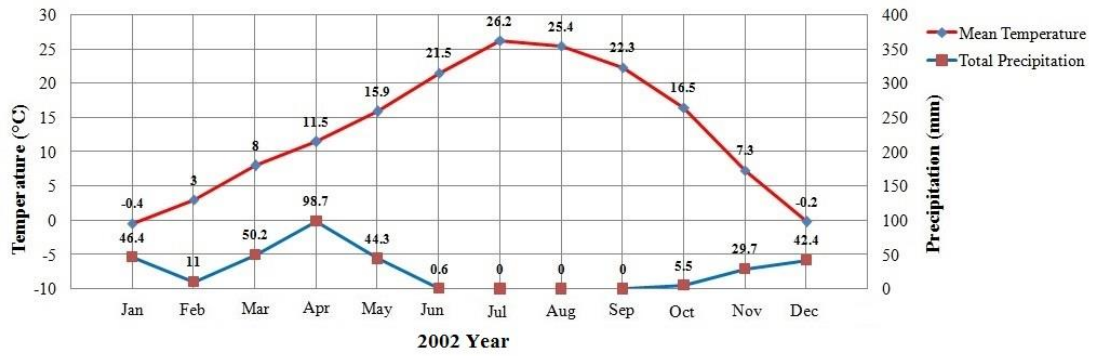


Figure B.61 : Mean temperature and total precipitation of Bonab station in 2002.

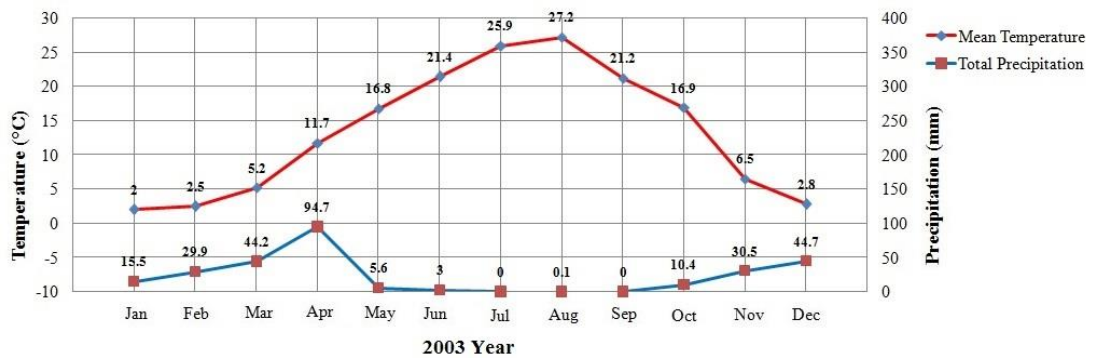


Figure B.62 : Mean temperature and total precipitation of Bonab station in 2003.

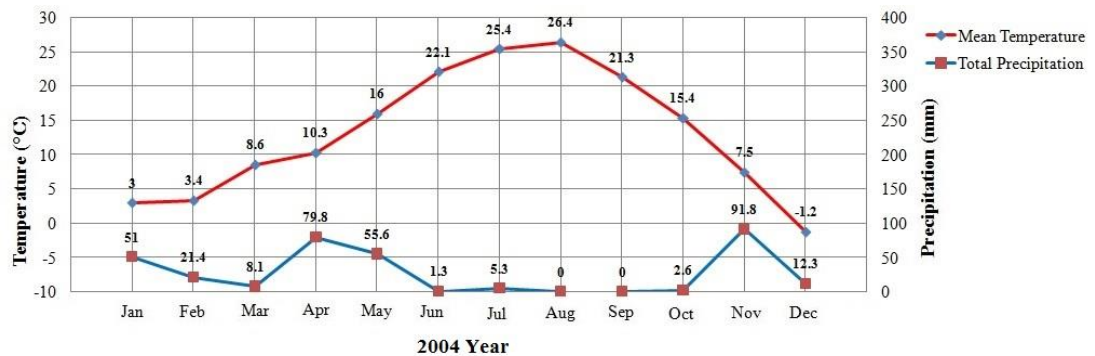


Figure B.63 : Mean temperature and total precipitation of Bonab station in 2004.

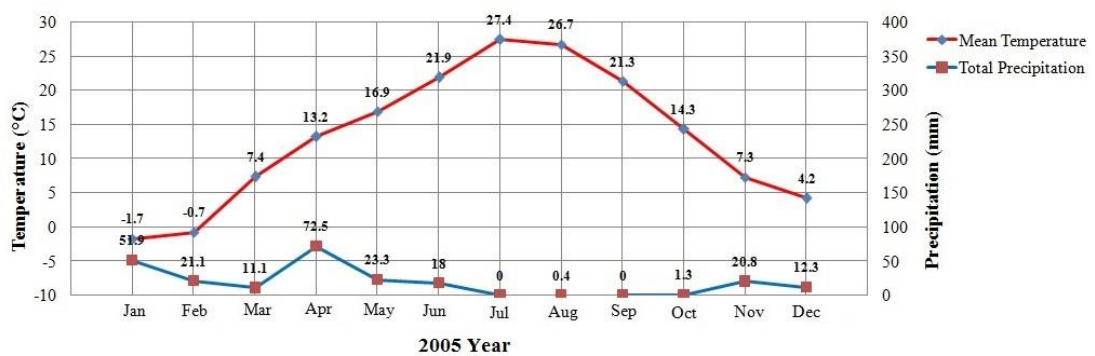


Figure B.64 : Mean temperature and total precipitation of Bonab station in 2005.

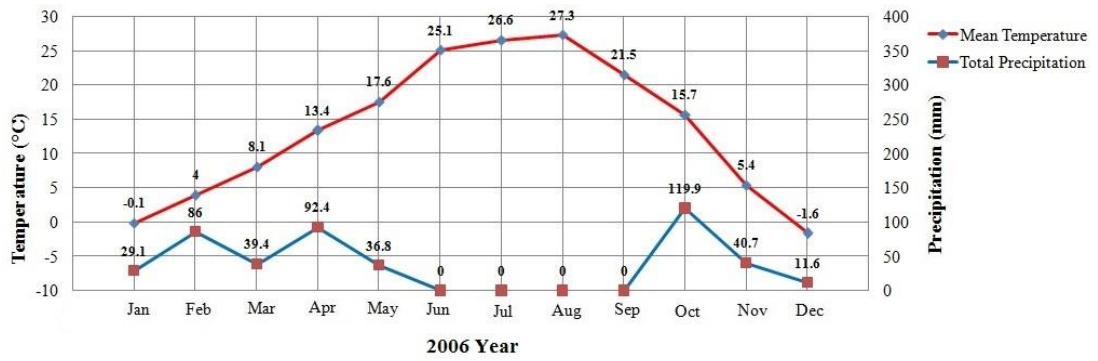


Figure B.65 : Mean temperature and total precipitation of Bonab station in 2006.

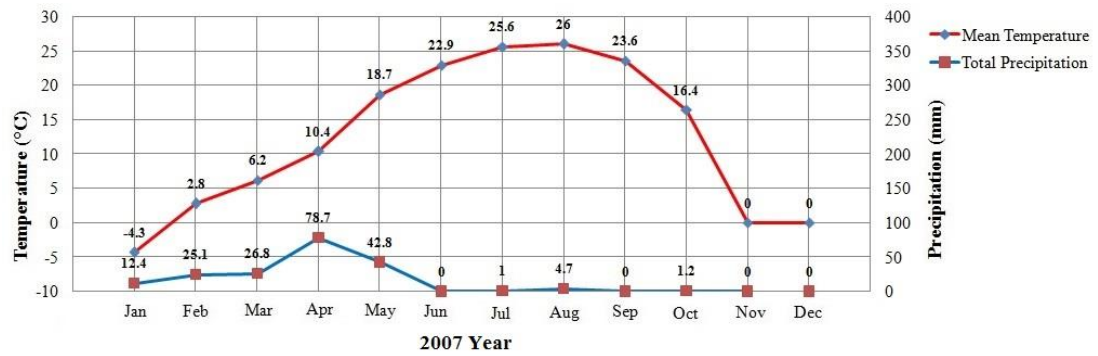


Figure B.66 : Mean temperature and total precipitation of Bonab station in 2007.

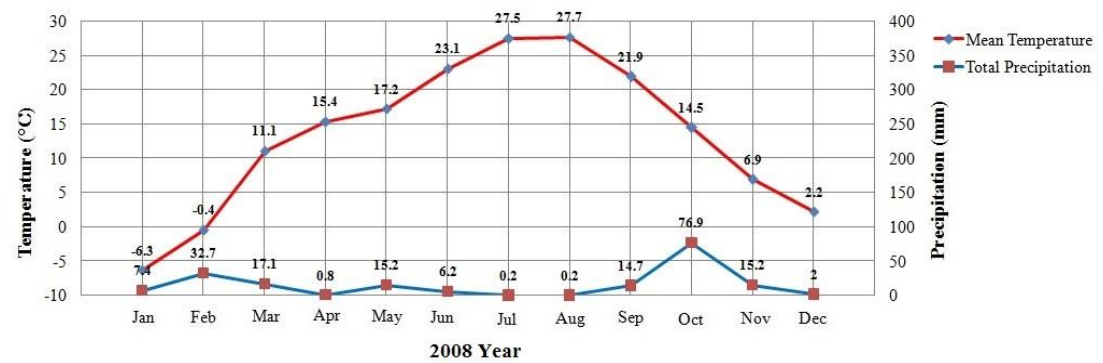


Figure B.67 : Mean temperature and total precipitation of Bonab station in 2008.

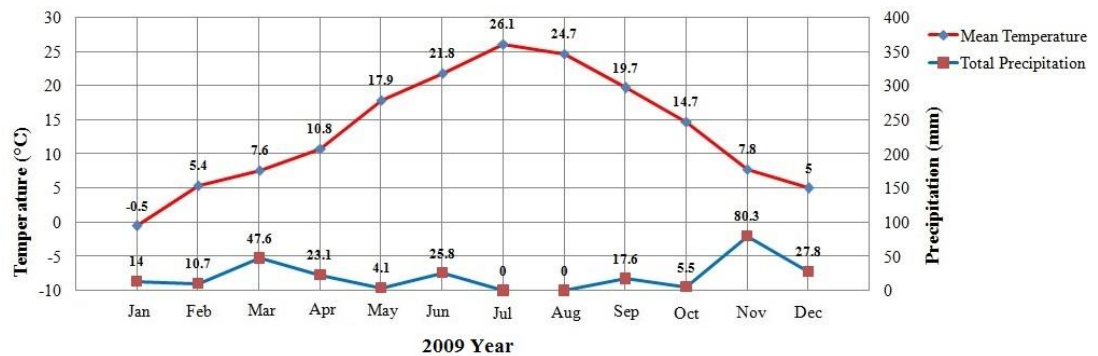


Figure B.68 : Mean temperature and total precipitation of Bonab station in 2009.

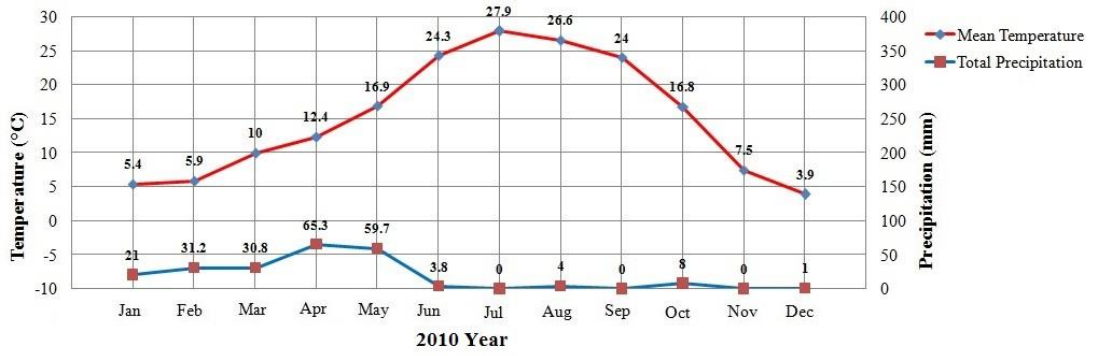


Figure B.69 : Mean temperature and total precipitation of Bonab station in 2010.

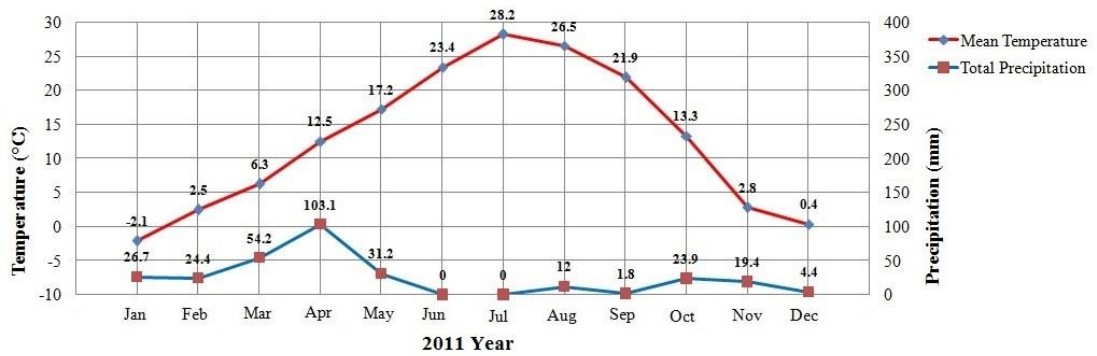


Figure B.70 : Mean temperature and total precipitation of Bonab station in 2011.

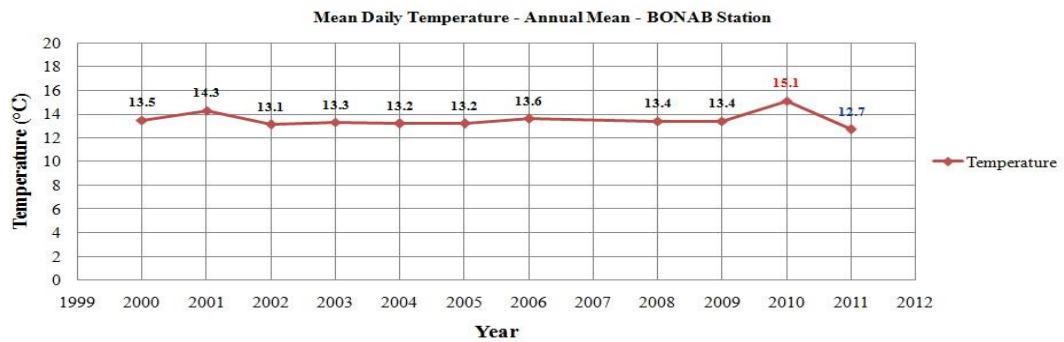


Figure B.71 : Annual Mean temperature and total precipitation of Bonab.

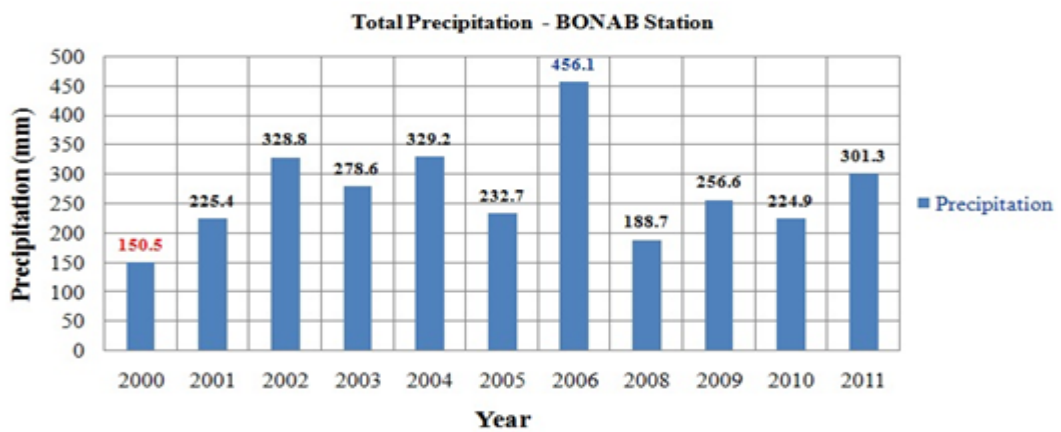
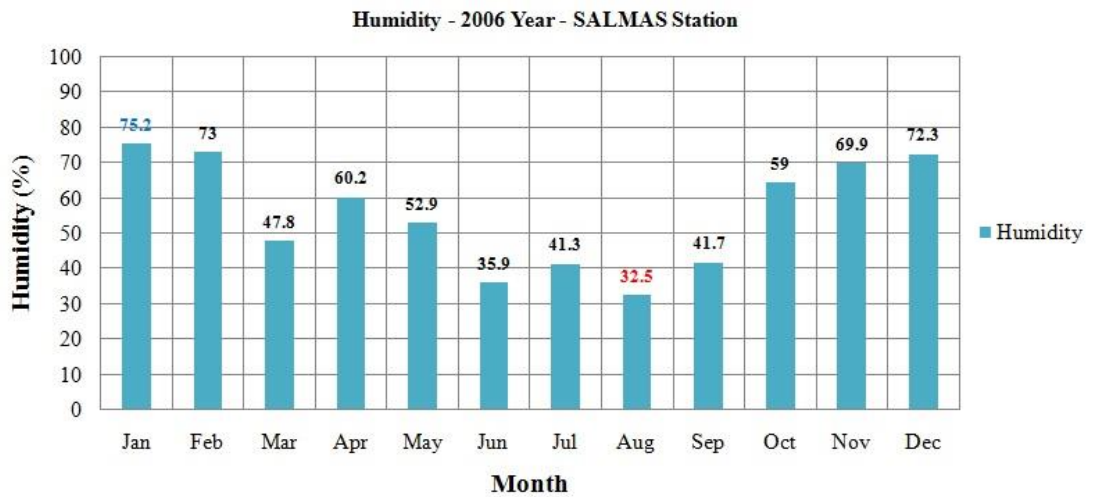
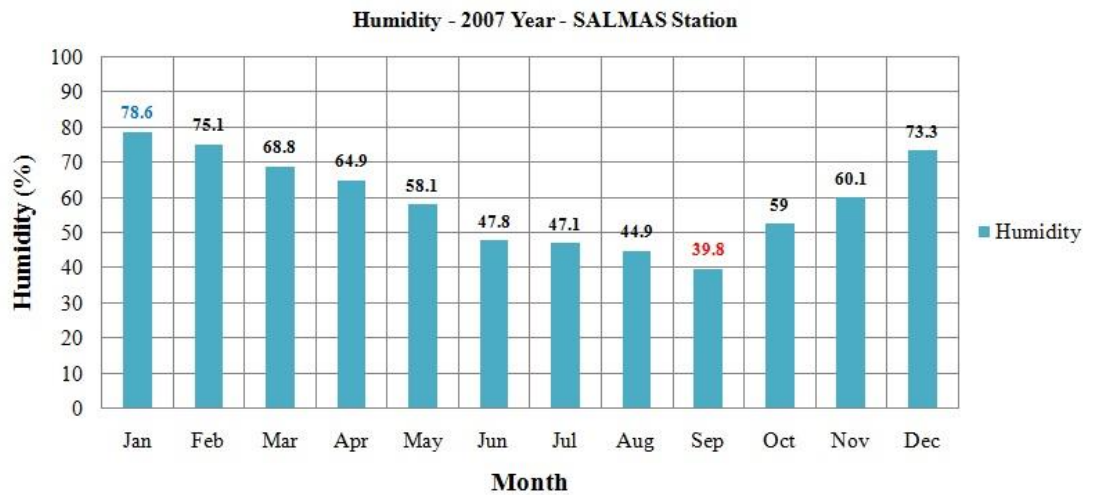


Figure B.72 : Annual precipitation of Bonab station.



**Figure B.73 : Humidity of Salmas station in 2006.**



**Figure B.74 : Humidity of Salmas station in 2007.**

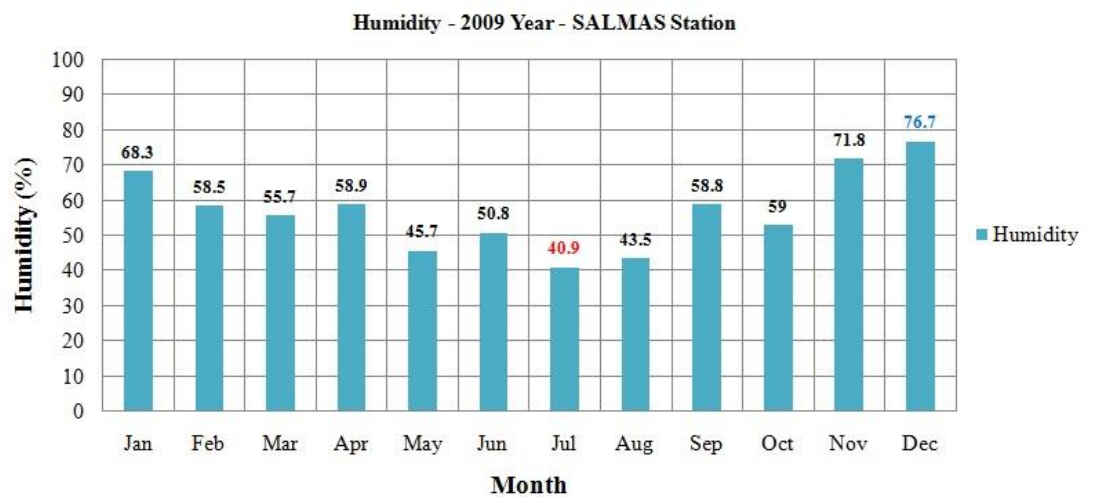


**Figure B.75 : Humidity of Salmas station in 2009.**

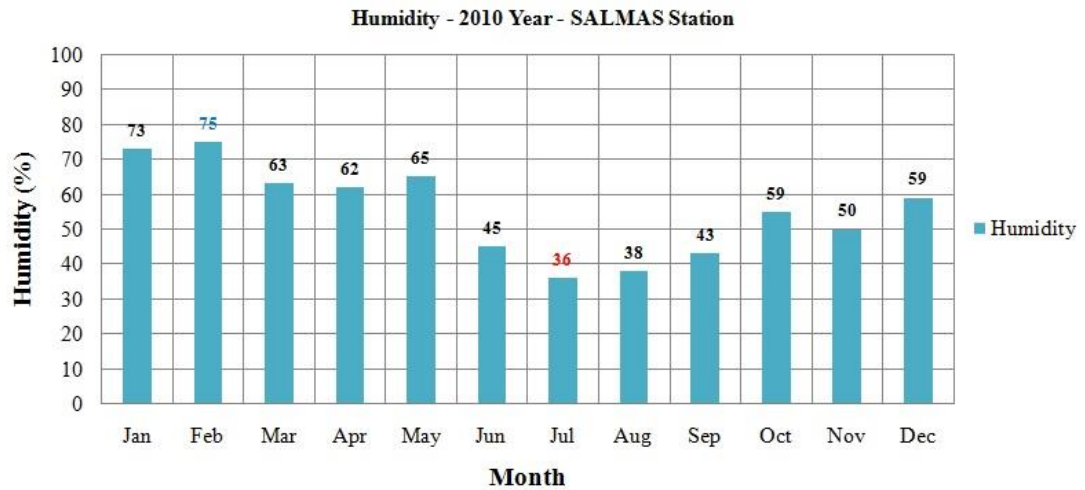


**Figure B.76 :** Humidity of Salmas station in 2010.

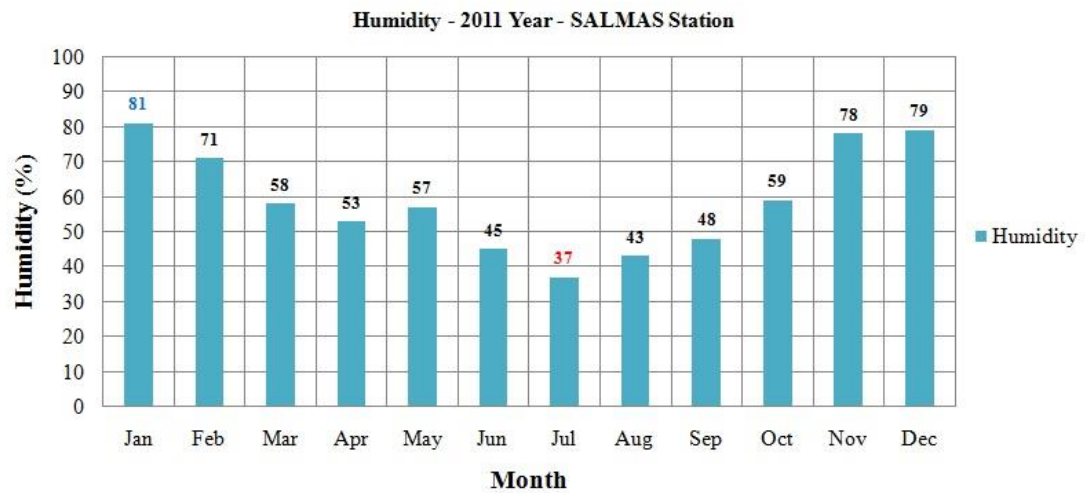


**Figure B.77 :** Humidity of Salmas station in 2011.

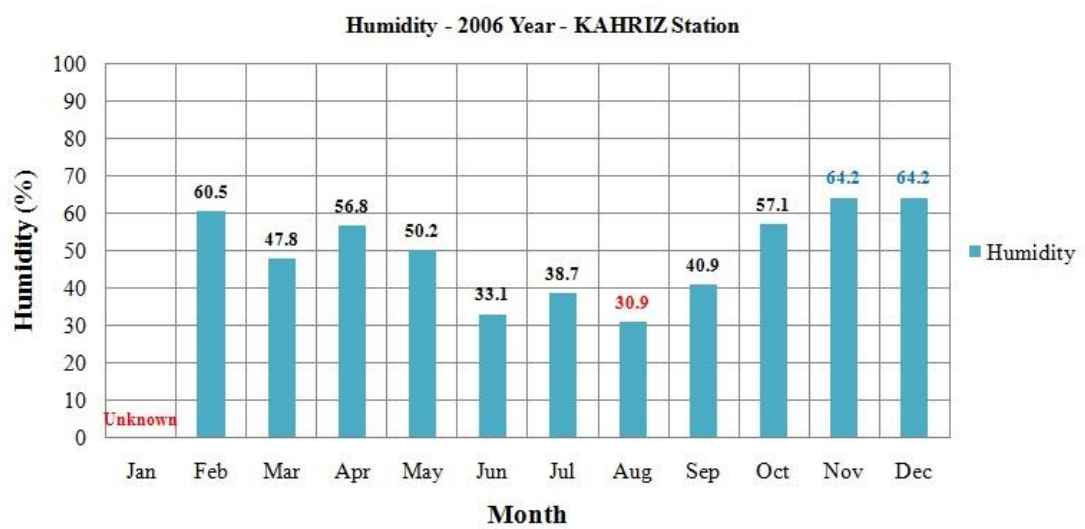


**Figure B.78 :** Humidity of Kahriz station in 2006.

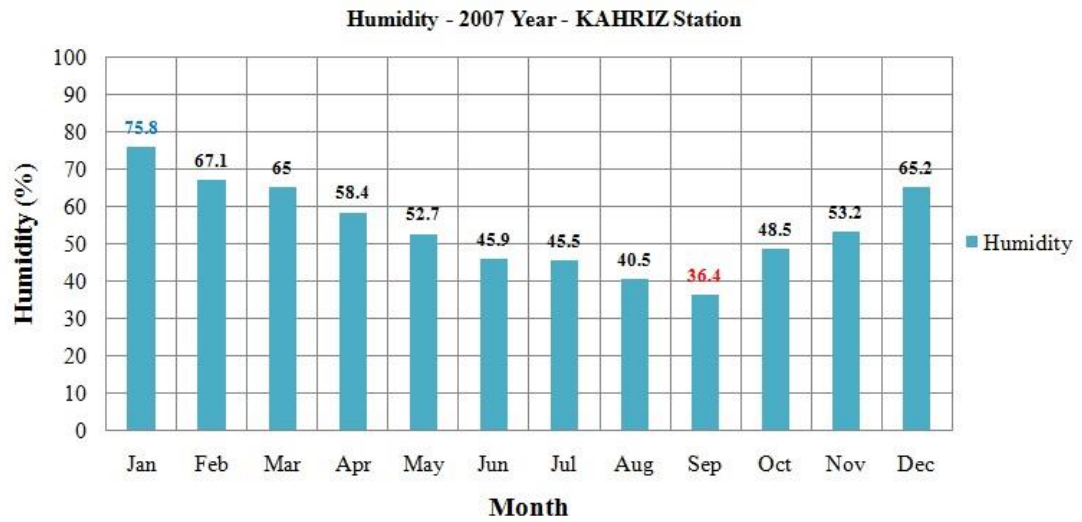


**Figure B.79** : Humidity of Kahriz station in 2007.

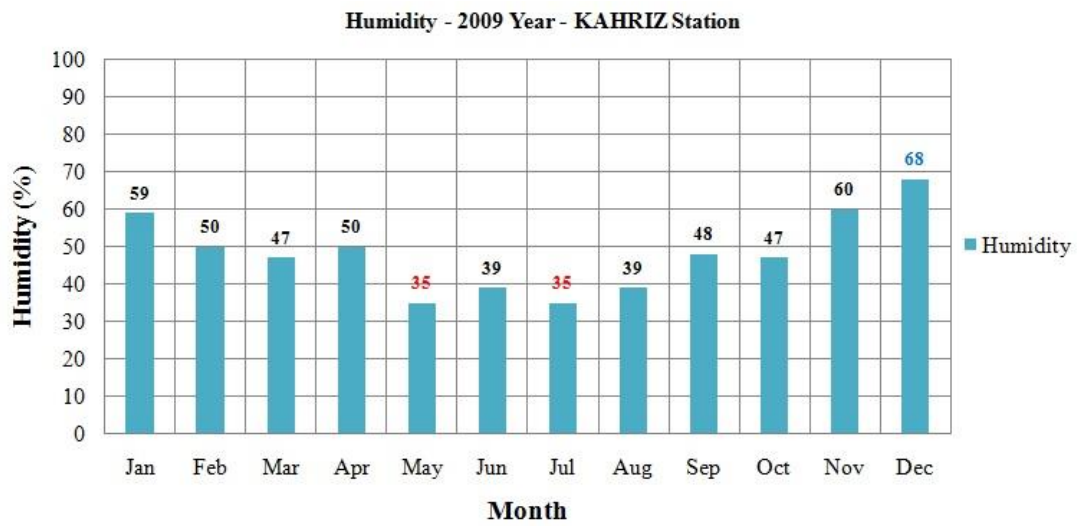


**Figure B.80** : Humidity of Kahriz station in 2009.

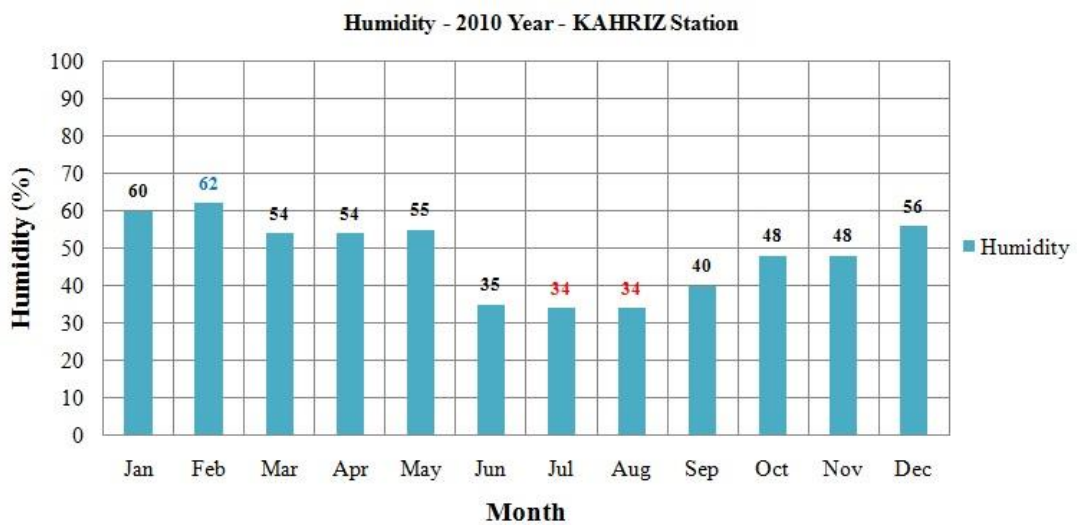


**Figure B.81** : Humidity of Kahriz station in 2010.



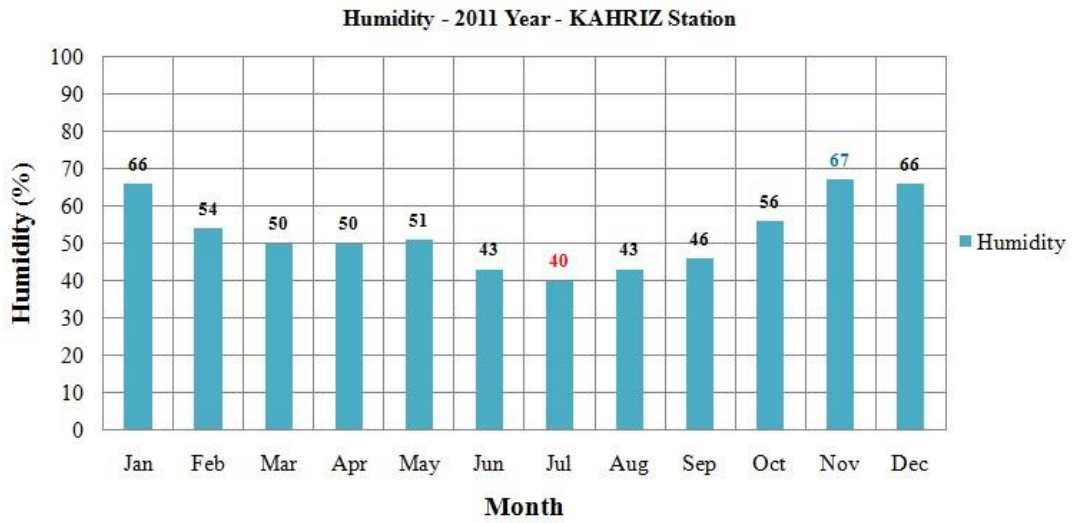


**Figure B.82 : Humidity of Kahriz station in 2011.**

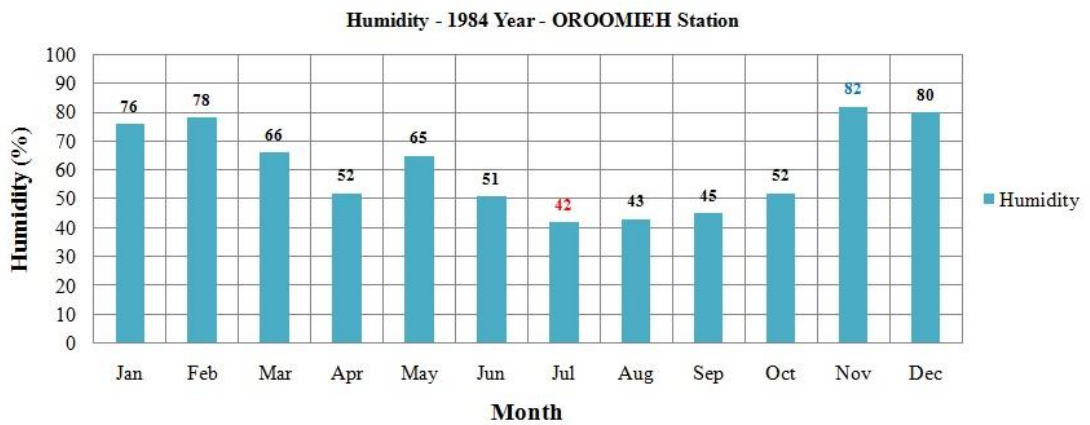


**Figure B.83 : Humidity of Urmia station in 1984.**

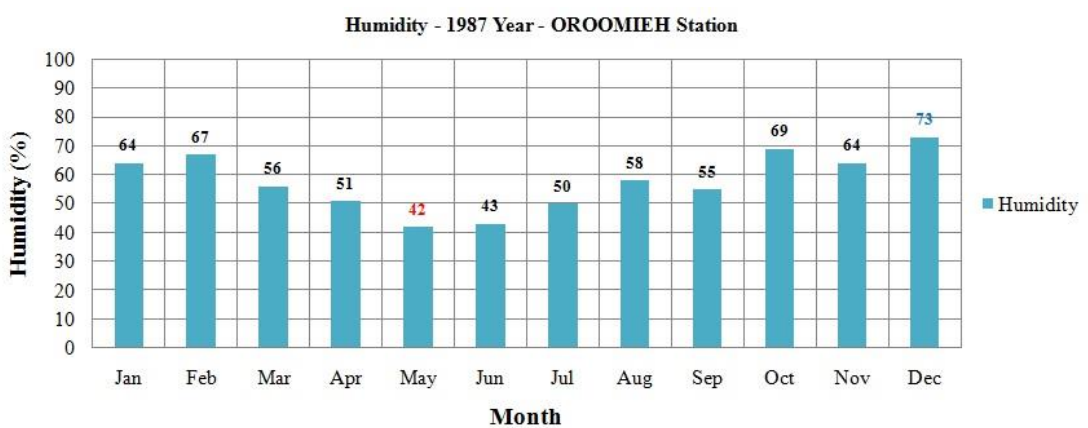


**Figure B.84 : Humidity of Urmia station in 1987.**

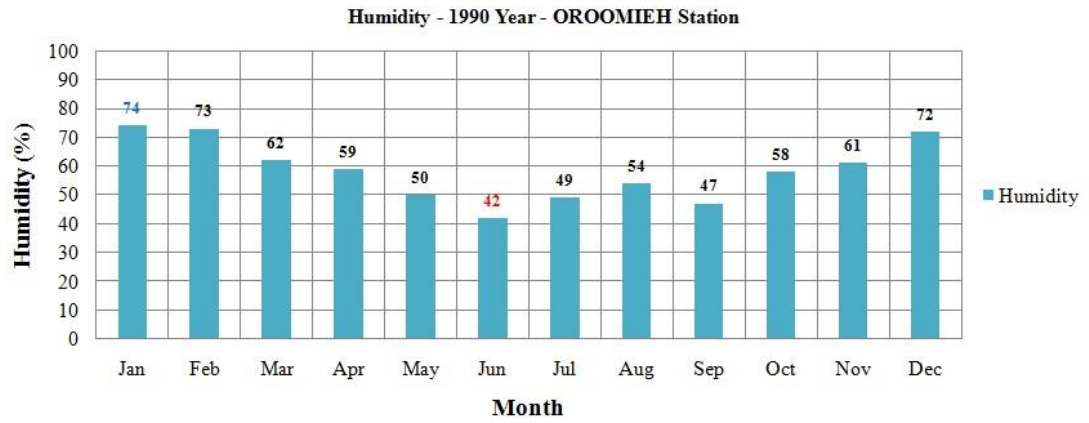


**Figure B.85 : Humidity of Urmia station in 1990.**

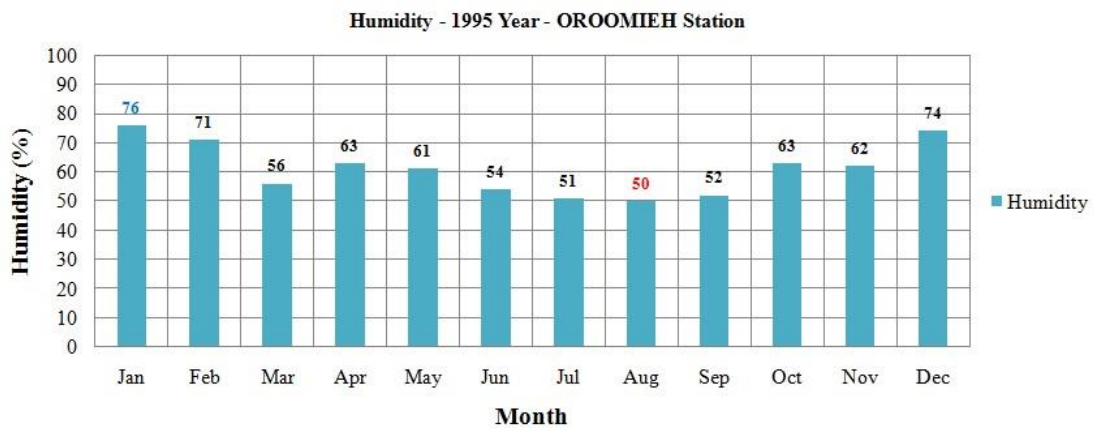


**Figure B.86 : Humidity of Urmia station in 1995.**

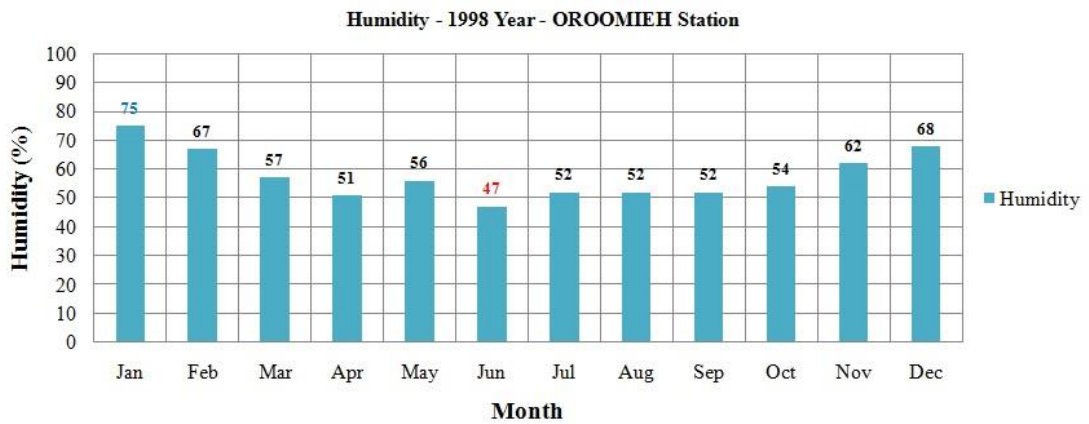


**Figure B.87 : Humidity of Urmia station in 1998.**

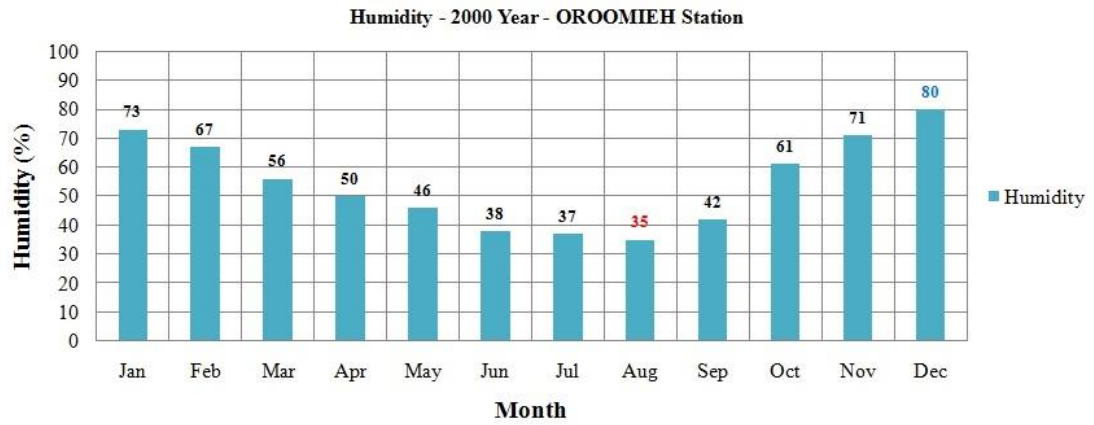


**Figure B.88 : Humidity of Urmia station in 2000**

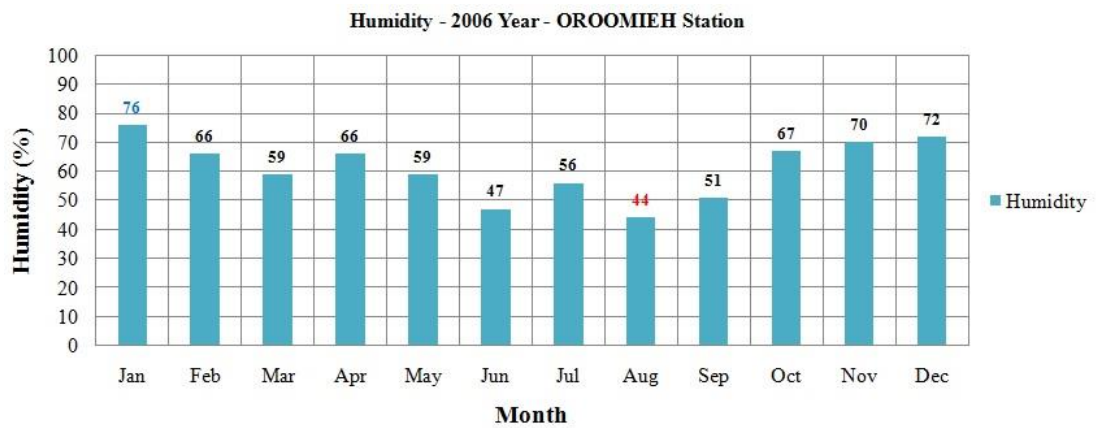


**Figure B.89 : Humidity of Urmia station in 2006.**

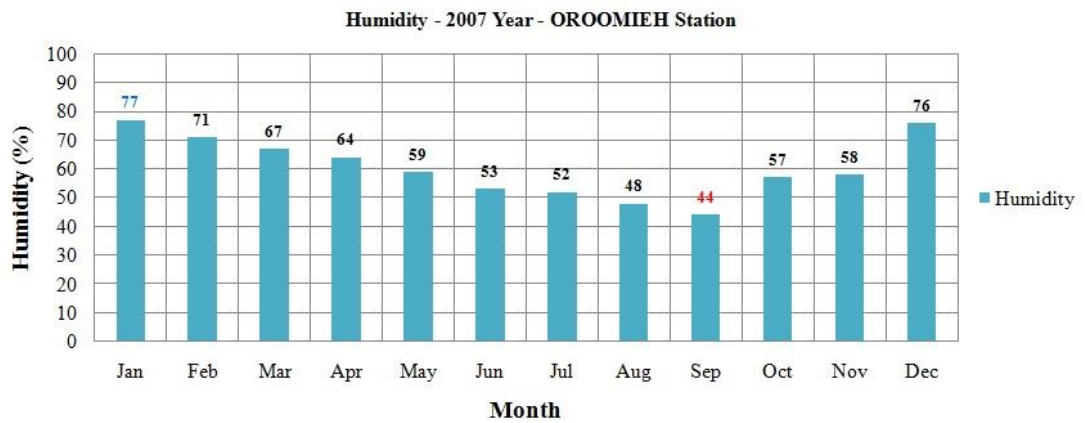


**Figure B.90 : Humidity of Urmia station in 2007.**

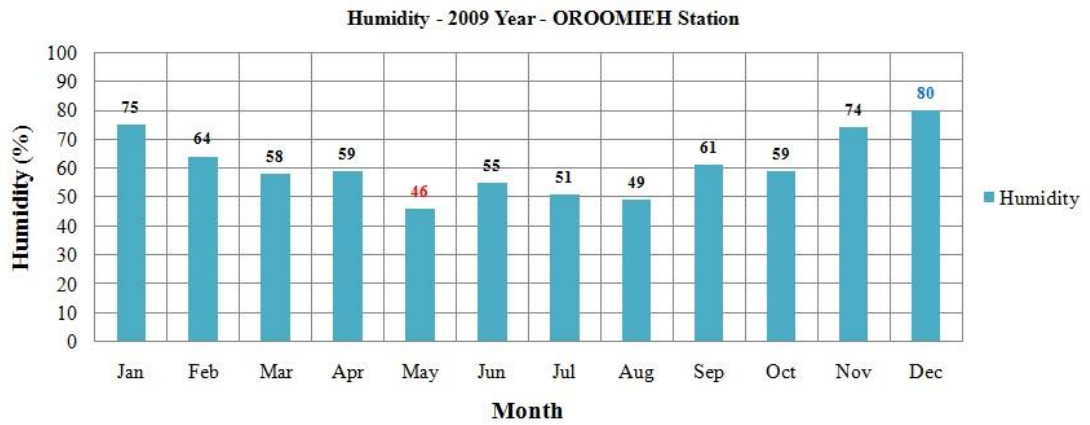


**Figure B.91 : Humidity of Urmia station in 2009.**

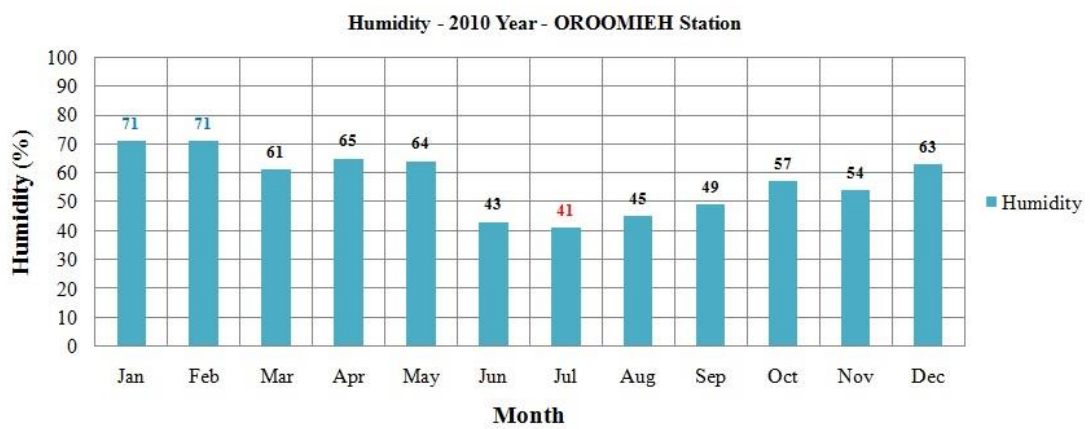


**Figure B.92 : Humidity of Urmia station in 2010.**

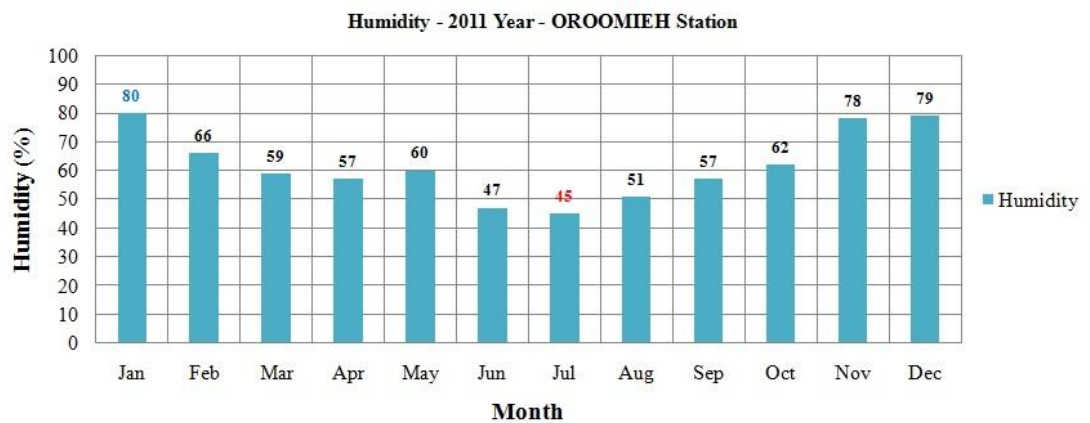


**Figure B.93 : Humidity of Urmia station in 2011.**

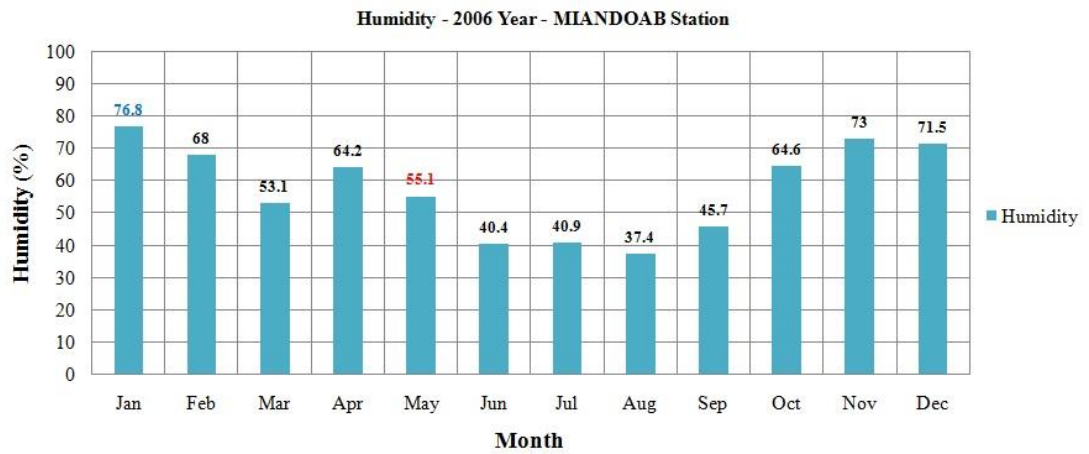


**Figure B.94 :** Humidity of Miandoab station in 2006.

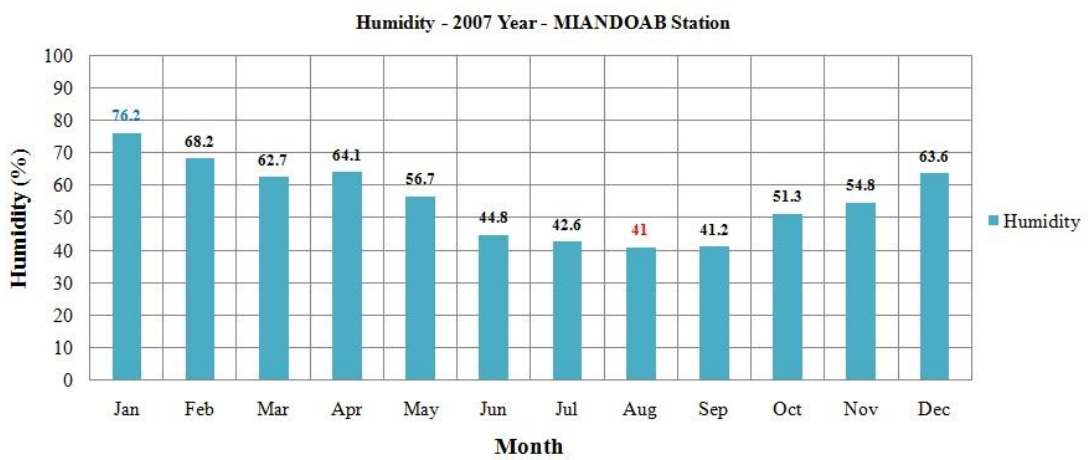


**Figure B.95 :** Humidity of Miandoab station in 2007.

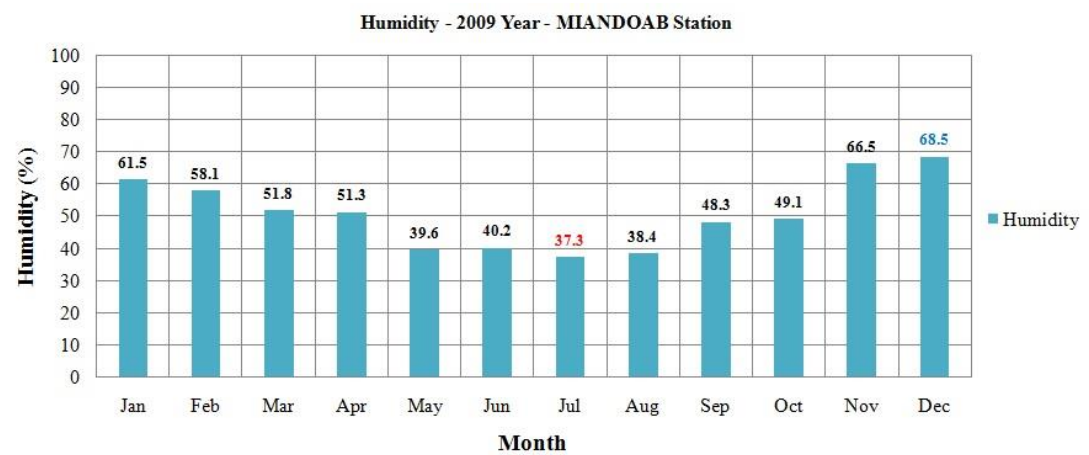


**Figure B.96 :** Humidity of Miandoab station in 2009.

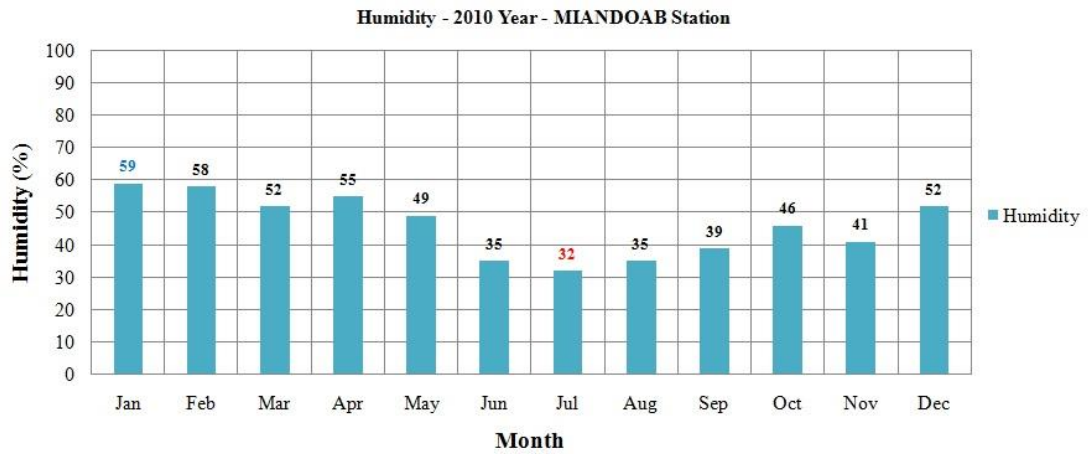


**Figure B.97 :** Humidity of Miandoab station in 2010.

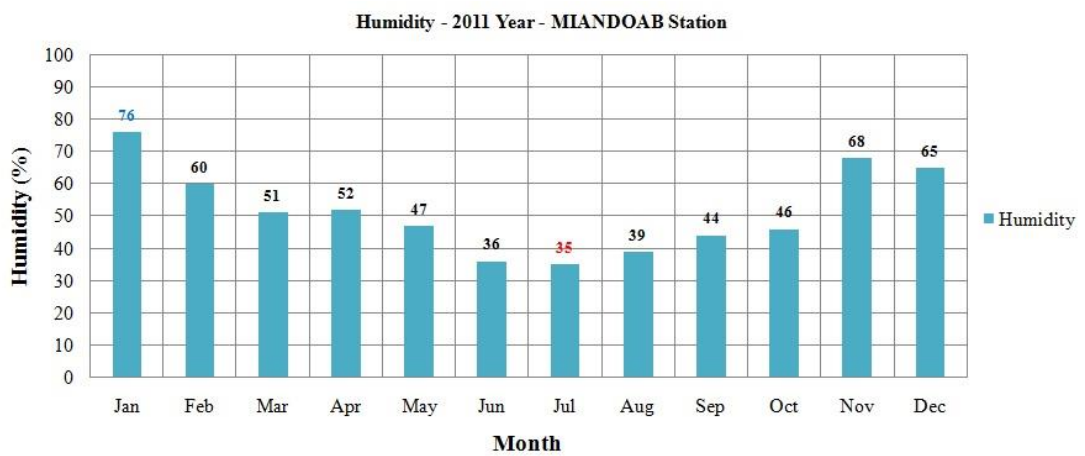


**Figure B.98 :** Humidity of Miandoab station in 2011.

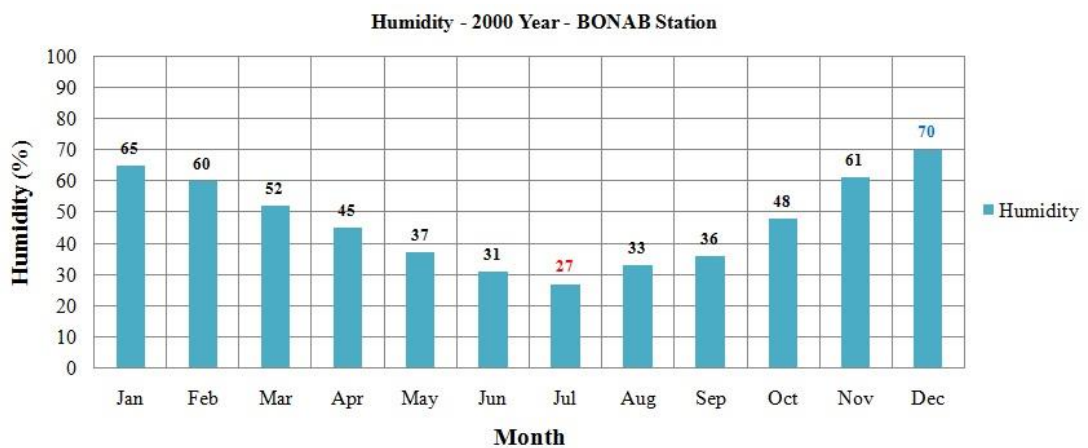


**Figure B.99 :** Humidity of Bonab station in 2000.

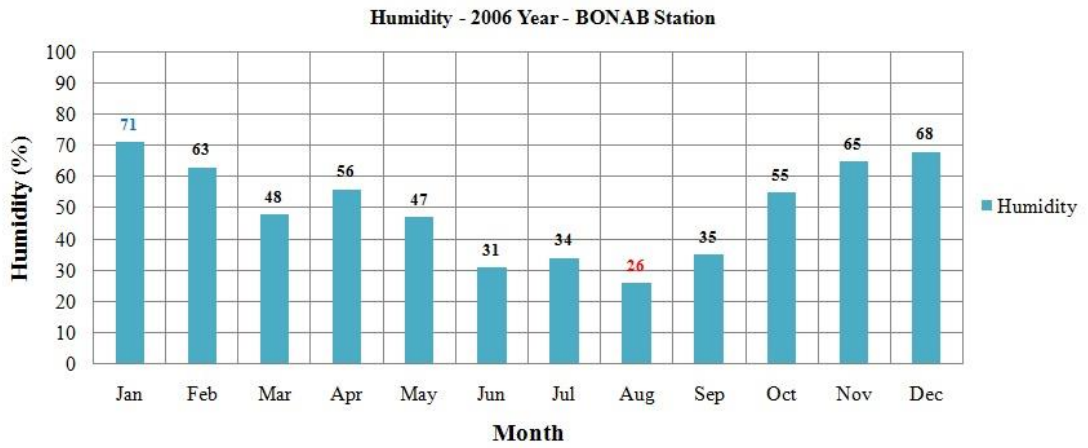


**Figure B.100** : Humidity of Bonab station in 2006.

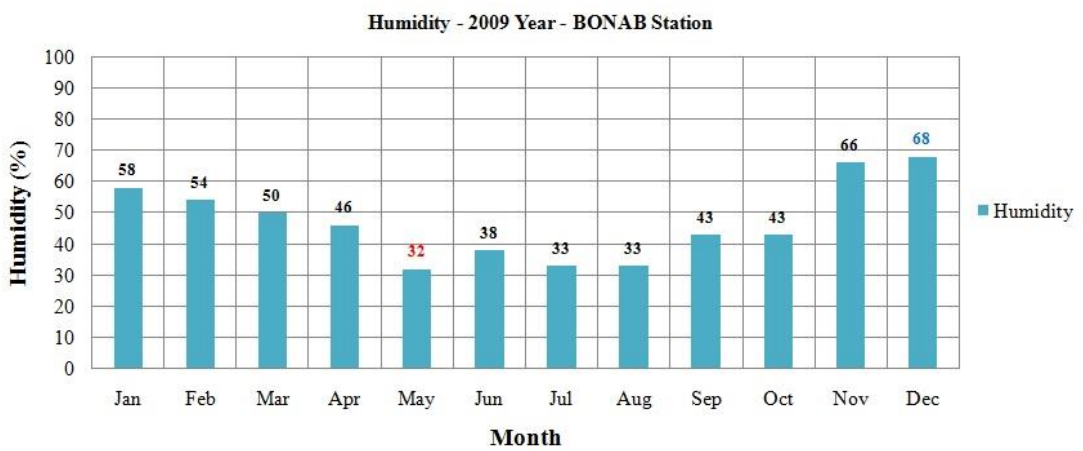


**Figure B.101** : Humidity of Bonab station in 2009.

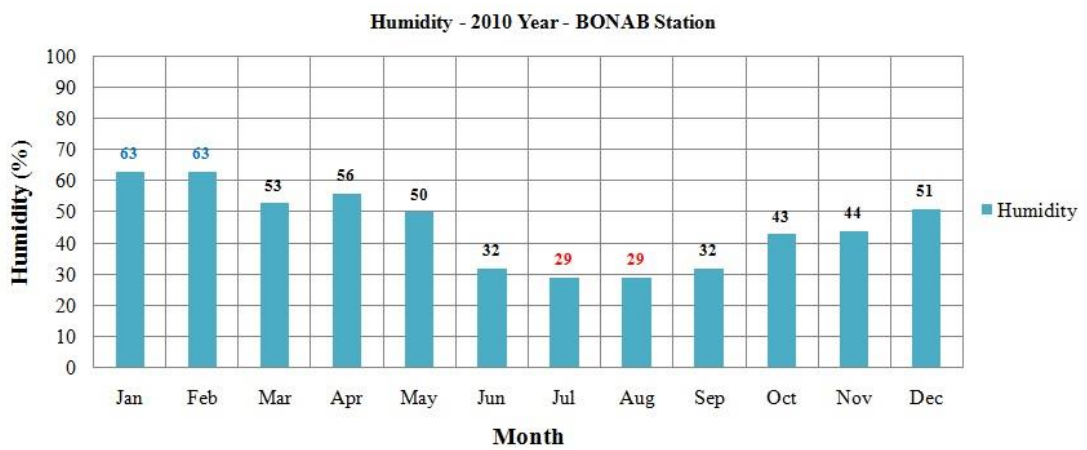


**Figure B.102** : Humidity of Bonab station in 2010.

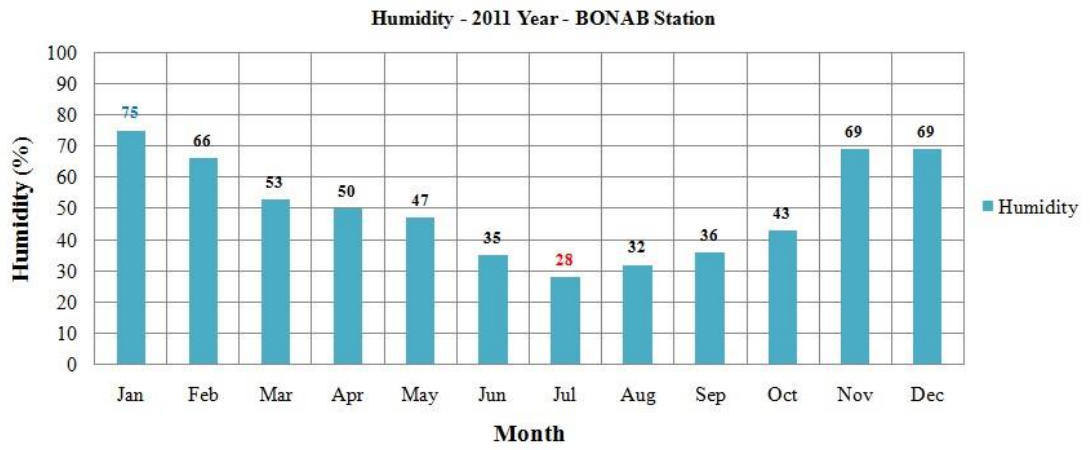


**Figure B.103 : Humidity of Bonab station in 2011.**



## **CURRICULUM VITAE**



**Name Surname: Yusuf Alizade Govarchin Ghale**

**Place and Date of Birth: 09.04.1984/Urmia-West Azerbaijan-Iran**

**Address: Avcilar/Istanbul**

**E-Mail: Yusufalizade2000@gmail.com**

**B.Sc.: Shahid Rajai Teacher Training University-Tehran/Iran**

### **PUBLICATIONS/PRESENTATIONS ON THE THESIS**

- Evaluation of Spatio-Temporal Variations in Urmia Lake Using Remote Sensing and GIS. (2014). International Geosciences Congress, Iran.

